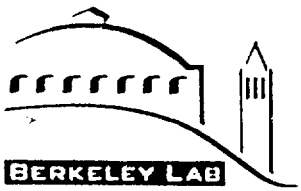

Level 4 Milestone SPC315M4
June 16, 1998
Version 1.0
Yucca Mountain Site Characterization Project

Drift Seepage Test and Niche Moisture Study:

Phase 1 Report on Flux Threshold Determination, Air Permeability Distribution, and Water Potential Measurement

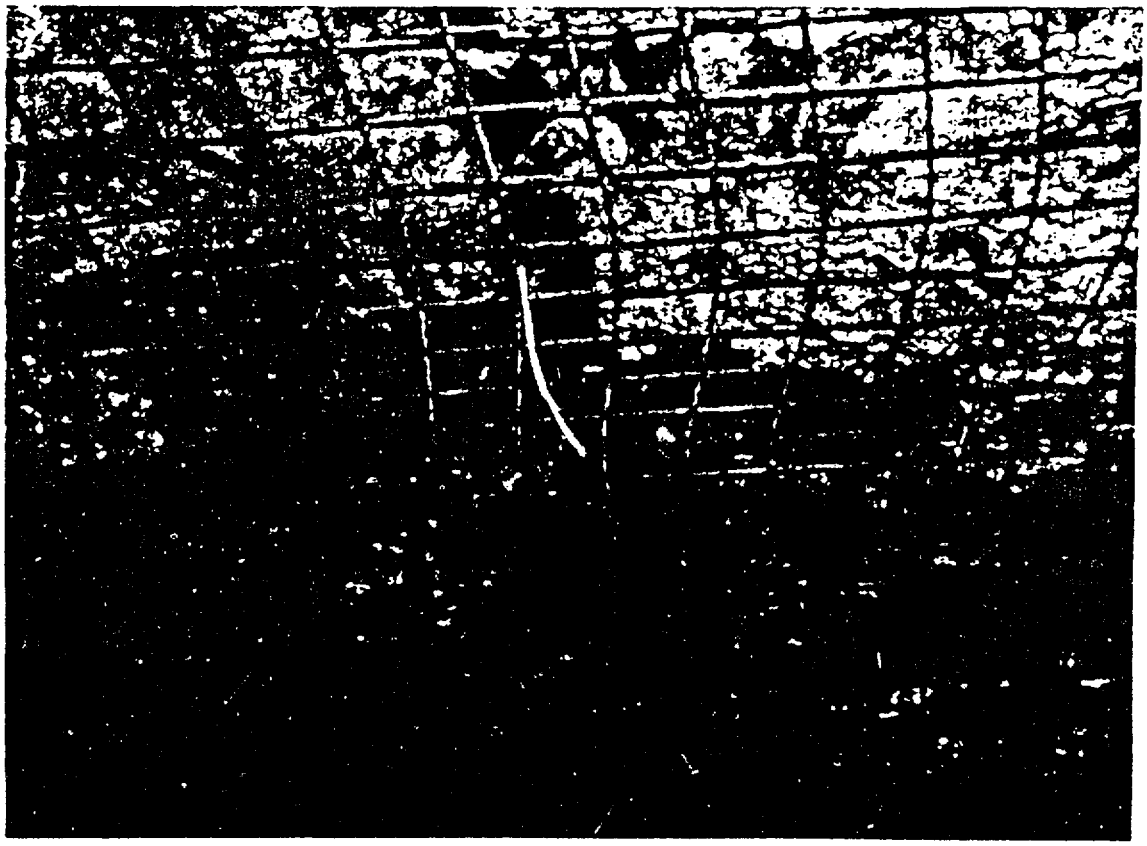

Earth Sciences Division
Lawrence Berkeley National Laboratory
One Cyclotron Road MS 90-1116
Berkeley, CA 94720

Table of Contents

Chapter 1 Introduction to Drift Seepage Test and Niche Moisture Study

J. S. Y. Wang, R. C. Trautz, P. J. Cook, and R. Salve

1.0 Scope and Objectives of the Drift Seepage Test and Niche Moisture Study

The niche seepage threshold and fracture capillarity determination, together with air permeability tests to characterize fracture heterogeneity, and water potential measurements to quantify *in situ* conditions at niches, can lead to drift-scale quantification of fluxes into mined openings and can determine the hydrological and moisture conditions for the waste emplacement drifts. Borehole clusters and niches are used in the drift seepage test and niche moisture study to:

1) measure *in situ* permeability and hydrologic parameters of repository-level rock for use in the unsaturated zone (UZ) drift-scale model, as well as for input to the UZ site-scale model for total system performance assessment (TSPA), viability assessment (VA), and licensing application (LA);

2) evaluate drift-scale seepage processes in order to quantify the extent to which mined openings reduce flow into drifts, and to determine the threshold for flow into the drift with finite liquid-pulse releases (representing the arrival of episodic fast flows to the repository horizon); and

3) monitor and compare moisture conditions in different niches in the Exploratory Study Facility (ESF) within potential fast flow path zones and outside of fast path zones, as well as develop testing and monitoring approaches for the evaluation of waste isolation attributes in the waste emplacement drifts.

Two niches were excavated in the summer of 1997 for the study in Phase 1, with one niche in a known fast-flow-path zone (Niche 3566), and one in a relatively fast-path free zone (Niche 3650). The numeric identification of a niche represents the distance of the niche location from the ESF North Portal in meters. In Phase 1, the known fast-path niche (Niche 3566) in a bomb-pulse location was used for passive monitoring of potential fast-flow pathways under ambient conditions. The fast-path free niche (Niche 3650) was used for active liquid flow testing of seepage processes, aimed to determine the threshold of flow into the drift. After the drift-scale flow testing, the active testing niche will be sealed for long-term monitoring and, conversely, the monitoring niche will be activated for flow testing. Two other niches are

planned for study in 1998: Niche 3107, near the cross-over point where the Cross Drift passes over the ESF Main Drift, and Niche 4788, in an extensively fractured zone. Figure 1.1 illustrates the locations of the niches and other alcoves in the ESF.

This report is the fourth technical report for the drift seepage test and niche moisture study. The milestone reports and topical chapters are listed below to summarize the evolution of field-testing activities and associated modeling analyses:

First Report, SPC31DM4, June 1997 on site selection, test design, and preliminary results before first niche excavation:

> Drift Seepage Test and Niche Moisture Study: Phase 1 Progress Report on Data Interpretation and Model Predictions, J.S.Y. Wang, P.J. Cook, R.C. Trautz, A. James, S. Finsterle, E. Sonnenthal, R. Salve, G. Hesler, and A. L. Flint.

Second Report, SPC314M4, September 1997, on pre-excavation tests and flow path observations during niche excavations, with

> Chapter 1: Field Testing and Observation of Flow Paths in Niches, J.S.Y. Wang, P.J. Cook, R.C. Trautz, and R. Salve;
>
> Chapter 2: Cross-Hole Pneumatic Tests of Fractured Flow Paths, P.J. Cook, R.C. Trautz, and J.S.Y. Wang;
>
> Chapter 3: Liquid Migration along Fracture Flow Paths, R.C. Trautz, P.J. Cook, and J.S.Y. Wang;
>
> Chapter 4: Fracture Flow Models for the Niche Liquid Release Tests, A.L. James and S. Finsterle;
>
> Chapter 5: Niche Moisture Analysis, A.L. Flint and L.E. Flint;
>
> Chapter 6: Hydrologic Monitoring in Unsaturated Fractured Tuff Boreholes: Preliminary Results, R. Salve, T.K. Tokunaga, J.S.Y. Wang, R. Solbau, and J. Clyde.

Third Report, SP33PLM4, January 1998, on the first set of post-excavation seepage testing and predictive modeling, with

Chapter 1: Preliminary Test Results and Model Analyses of Seepage into Drifts, J.S.Y. Wang, R.C. Trautz, P.J. Cook, S. Finsterle, A.L. James, and J. Birkholzer; Chapter 2: Test Results of First Seepage Tests at Niche 3650 in the Exploratory Study Facility, R.C. Trautz and J.S.Y. Wang;

Chapter 3: Sensitivity Analysis of Drift Seepage with Two-Dimensional and Three-Dimensional Models, S. Finsterle and A.L. James;

Chapter 4: Sensitivity Analysis and Predictive Modeling of Infiltration Tests Planned for Alcove 1, C.F. Ahlers, S.A. Finsterle, and J.S.Y. Wang.

This *Fourth Report, SPC315M4*, for Phase 1 of the Drift Seepage Test and Niche Moisture Study contains the following chapters:

Chapter 2: Compilation of Seepage Results from the Pre- and Post-Excavation Liquid-Release Tests, R.C. Trautz, J.S.Y. Wang, and P.J. Cook;

Chapter 3: Compilation of Borehole Permeability Values from the Pre- and Post-Excavation Air Injection Tests, P.J. Cook, R.C. Trautz, and J.S.Y. Wang;

Chapter 4: Compilation of Water Potentials Measured in the Niches, R. Salve and J.S.Y. Wang.

The emphasis of this fourth report is on Chapter 2 for the results of liquid release tests for seepage threshold determination.

1.1 Summary of Liquid Release Tests for Seepage Threshold Determination

The key findings of liquid release tests described in Chapter 2 are as follows:

- The presence of a seepage threshold was demonstrated from liquid-release tests conducted at Niche 3650.
- 40 post-excavation liquid-release tests were conducted on 16 different test intervals located in boreholes above the niche.

- Of the 16 zones tested, water seeped into the niche from 10 intervals, water appeared at the niche ceiling but did not drip in 3 cases, and water did not appear at all when introduced into the 3 remaining zones.
- Based on repeated tests at different time intervals, redistribution of injected water in the fracture system is likely to occur within one day to two weeks.
- The seepage percentage, defined as the amount of water seeped into the niche divided by the amount released into the rock, ranged from 0% to 56%, with the anomalous high value corresponding to a test started within 2 hours of a proceeding test in the same interval.
- As liquid release rate decreases, seepage percentage decreases until reaching a seepage threshold, below which no seepage occurs.
- The relationships between seepage threshold data and saturated hydraulic conductivity values were used to derive two capillary or sorptive related parameters, representing two types of *in situ* fractures: nearly vertical individual fractures and a network of interconnected fractures. Steady downward flow through homogeneous porous medium and other simple assumptions were used to interpret the fitting parameter. The field test results could also substantiate the model interpretations using simple two- and three-dimensional models for transient niche seepage processes.
- Without the mined opening to act as a barrier to divert seepage, the liquid flow was shown to penetrate deeper than the niche ceiling. This was based on direct observations during niche excavation of dye flow paths below the ceiling. Only a percentage or none at all of water released in the post-excavation test, in the same test interval with the same liquid release rate used in the corresponding pre-excavation test, dripped through the ceiling into the niche.
- The saturated hydraulic conductivities for gravity-driven flows associated with the liquid releases could be smaller than the air permeabilities from air-injection tests. The injected air was likely flowing in all directions within fracture planes, and liquid flow was observed to be mainly in the downward direction through a fraction of the fracture planes.
- The aspect ratio of depth to lateral spreading of wetting front movement is a measure of the type of flow that predominates. Large lateral spreading (low aspect ratio) of the wetting front is associated with inter-connected fracture networks containing both high and low-angle fractures, as opposed to large aspect ratios for flow along individual high-angle fractures.
- Mining the rock mass with minimal use of construction water is a successful method for directly observing the flow paths in an unsaturated fractured system, given associated limitations of costs and controls.
- Borehole observations with absorbent materials placed in holes were not effective for capturing the liquid flow paths.

1.2 Summary of Air-Injection Tests to Quantify Fracture Heterogeneity

The key findings of air-injection tests described in Chapter 3 are:

- Roughly 50,000 curves of pressure response and flow rate for Niche 3650 and a smaller number for Niche 3566 were generated in the cross-hole tests to map out the fracture heterogeneity at the niche sites with 0.3 m spatial resolution, under pre- and post-excavation conditions.
- Overall permeability of the known fast-path niche (Niche 3566) is higher than that of the bomb-pulse-fast-path-free niche (Niche 3650).
- At Niche 3566, the radial boreholes through brecciated zones tested inside the niche have significantly higher permeability than the axial boreholes parallel to the niche axis through relatively competent rock mass.
- At Niche 3650, the peak of permeability distribution from pre- to post-excavation increases by about two orders of magnitude.

1.3 Summary of Water Potential Measurements in the Niches

The key findings of water potential tests described in Chapter 4 are as follows:

- Psychrometers were used in either the end zones or along the boreholes at Niche 3566, Niche 3650, and Niche 3107 to measure water-potential distributions.
- The water-potential data suggested that the extent of dry out from ventilation effects was possibly greater than 3 meters.
- At Niche 3566, two zones were measured to have significant high potentials, one at the end of the middle borehole along the niche axis before niche excavation, and one along a radial borehole oriented from the niche toward the Sundance Fault.
- In the zone beyond where ventilation effects of the ESF were felt, Niche 3566 appeared to be wetter than Niche 3650.

1.4 Summary of Niche Sensitivity Analysis and Predictive Modeling

While this report does not focus on modeling, the interpretation of field data is guided by the following findings documented in earlier reports:

- Based on simulations for test design, water released in a borehole would travel through fractures to depths beyond the niche ceiling for volumes on the order of 0.5 liter and fracture parameters consistent with UZ site-scale model.
- Flow velocities were estimated to be fast, and matrix imbibition was predicted to have a small effect on flow if field conditions were wet.
- Sensitivity analyses suggested that seepage at a particular given rate was expected to be large for low fracture porosity, low fracture capillarity, and low permeability. Reducing permeability resulted in slower flow propagation, but higher average saturation. High saturations were required to overcome the capillary barrier at the niche. High permeability does not induce high seepage. The injected fluid can be effectively diverted around the niche with a high fracture permeability in the rock, and reducing the likelihood of local ponding at the niche boundary.
- Seepage in three-dimensional models, representing a fracture network with multiple fracture paths, was shown to be lower than seepage in two-dimensional models, representing flow limited to discrete fracture planes.
- Niche seepage simulations for different conceptual models suggested that the seepage was not very sensitive to local heterogeneity and matrix imbibition, but very sensitive to the niche boundary conditions, with free drainage boundary (without a capillary barrier requiring local ponding conditions to initiate dripping) grossly overestimating the seepage percentage.

1.5 Data Status and Quality Assurance

All the liquid release, air injection, and water-potential measurements and analyses in this study were performed by qualified personnel and equipment calibrated under the Lawrence Berkeley National Laboratory Quality Assurance (LBNL QA) program. All test results and data presented are qualified data. While this report does not present new modeling results, the interpretations of data in this report rely on the modeling results from earlier milestones. The codes TOUGH2 and ITOUGH2 used in UZ site-scale model and UZ drift-scale models are currently unqualified due to a deficiency related to the software qualification process. These codes will be qualified upon issuance of software procedures that meet the QARD. The conclusions of this study are based on Q data. Data are submitted concurrently with this milestone report to the YMP Data Management System, with Data Tracking Numbers assigned as follows: DTN LB980001233124.003 for liquid release and seepage data; DTN LB980001233124.002 for air injection and permeability data; and DTN LB980001233124.001 for psychometric water potential data.

1.6 Acknowledgment

We thank Jens Birkholzer, Christine Doughty, and April James for their technical reviews, and Don Mangold for the EA review of this report and comments for improvement. We thank Alan Mitchell and his colleagues at the ESF Test Coordination Office for the field support at ESF, and for the coordination with the ESF Constructor for drilling and excavation operations. This work was supported by the Director, Office of Civilian Radioactive Waste Management, through a Memorandum Phase Order EA9013MC5X between TRW Environmental Safety Systems, Inc. and Ernest Orlando Lawrence Berkeley National Laboratory for the Yucca Mountain Site Characterization Project through U. S. Department of Energy Contract No. DE-AC03-76SF00098.

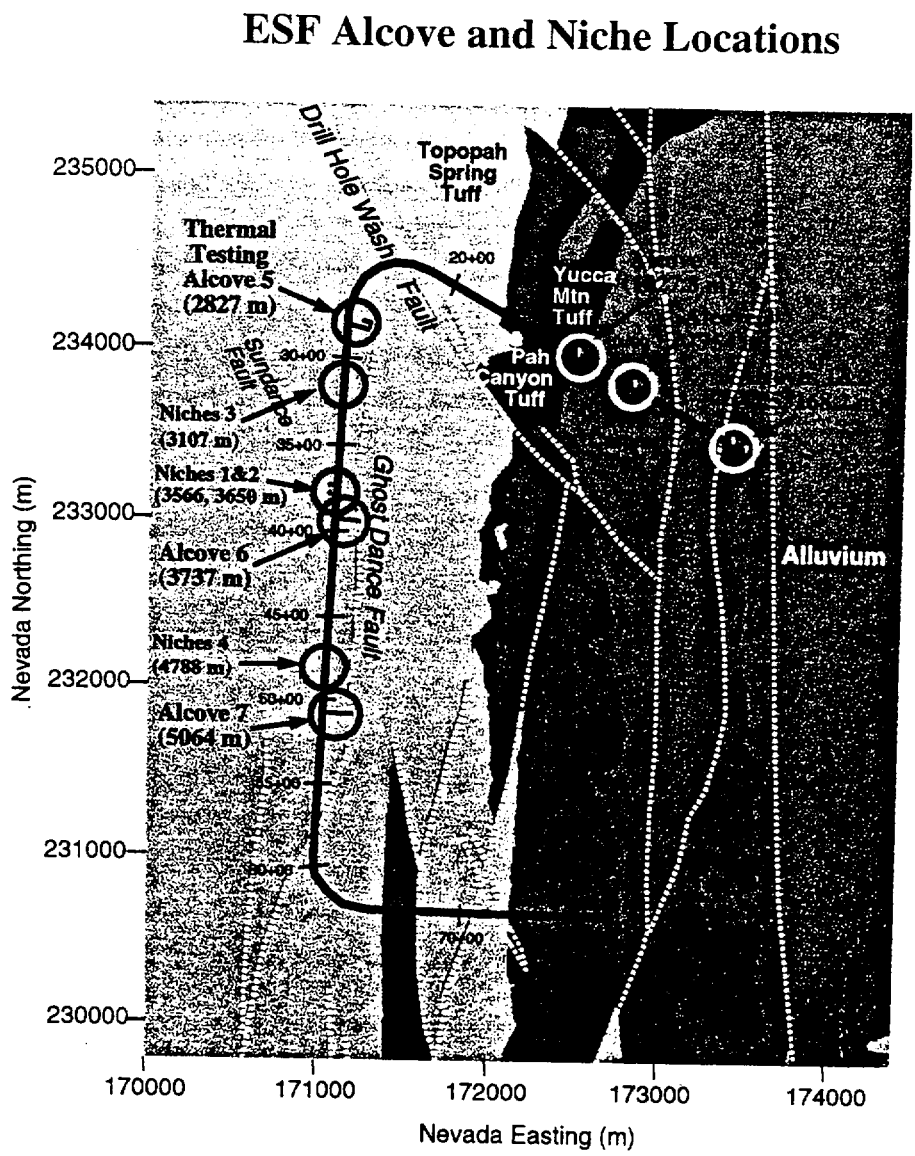

Figure 1.1 Location of the niches and alcoves in the ESF.

Chapter 2 Compilation of Seepage Results from the Pre- and Post-Excavation Liquid-Release Tests

R.C. Trautz, J.S.Y. Wang, and P.J. Cook

2.0 Introduction

This chapter summarizes a series of liquid-release tests that were conducted at Niches 3566 and 3650, located in the Exploratory Study Facility (ESF) shown on Figure 2.1. Each niche consists of an 8.7- to 9.0-meter (m) long drift, or mined opening, constructed on the west side of the ESF main drift within the middle non lithophysal zone of the Topopah Spring welded unit. Liquid-release tests were conducted at both niche sites, and will also be performed at several proposed sites, to characterize the flow of water through fractures and to quantify water seeping into an underground opening from a short artificial localized liquid-release event.

The data and observations compiled in this chapter were collected during the Niche Study, which started in February 1997. The material in Sections 2.2.1 Pre-Excavation Tests, 2.3 Tracer Selection, 2.4.1 Test Equipment, 2.4.2 Pre-Excavation Liquid-Release Tests and 2.5 Pre-Excavation Liquid-Release Tests were included in a previous milestone report, SPC314M4 (Wang et al. 1997) and are reproduced herein to provide a complete record of the liquid-release studies.

All the pneumatic and liquid-release measurements and analyses used and referred to in this chapter were performed by qualified personnel and equipment calibrated under the Lawrence Berkeley National Laboratory Quality Assurance (LBNL QA) program. All the liquid-release data presented are to be considered qualified data. The codes TOUGH2 and ITOUGH2 used in UZ site-scale model and UZ drift-scale models are currently unqualified due to a deficiency related to the software qualification process. These codes will be qualified upon issuance of software procedures that meet the QARD. The data tracking numbers (DTN) of data used in the site description are included in the reference lists. Conclusions produced herein are based on qualified data.

2.0.1 Capillary Barrier Concept

The potential exists for a capillary barrier to form in an unsaturated, layered porous medium at a location where there is a significant contrast in pore sizes and a corresponding contrast in unsaturated hydraulic conductivities between layers. A capillary barrier may form when an

unsaturated hydrogeologic unit containing relatively fine pores or fractures overlies a unit consisting of relatively coarse pores. Coarse-pore soils typically drain at relatively large matric potentials and, like any porous material, will not conduct water at or below their residual saturation. In contrast, a relatively fine-pore soil may still be able to conduct appreciable quantities of water at and below the same matric potential. Since the fine soil can still conduct water and the underlying coarse soil cannot, a capillary barrier is created at the contact between the two layers under unsaturated conditions. Water cannot penetrate into the lower coarse layer until its water content increases, at which point it can conduct sufficient water to overcome the barrier effect; or until the saturation of the fine layer increases to 100 percent (or below 100 percent saturation at a critical value of the matric potential, defined as the air-entry potential, Hillel 1971), causing water to break through from the upper into the lower layer.

Montazer and Wilson (1984) used a simple capillary tube model to estimate the critical matric potential, or critical height to which the water must rise in a small tube (or pore), before water will drain into a larger tube located below. When the radius of a large tube (e.g., coarse soil) is much greater than an overlying small tube (e.g., fine soil), then the critical height to which the water must rise in the small tube is inversely proportional to its diameter and, for all practical purposes, independent of the large tube diameter. This is also true for rock units, which typically exhibit a wide range of pore sizes, including fine pores found in the rock matrix and coarse pores represented by fractures.

2.0.2 Repository Performance

By analogy, the potential exists for a capillary barrier to form when a fine-grained unit, such as the highly fractured Topopah Spring welded unit, overlies a large open space, such as an underground opening. The proposed repository at Yucca Mountain, if constructed, will consist of tens of kilometers of waste emplacement drifts or large pores overlain by the fine-grained Topopah Spring welded unit.

It is important to determine whether a capillary barrier will form above a mined opening because such a barrier can have a direct impact on waste isolation, as shown in Figure 2.2. Water introduced at the land surface during an episodic infiltration event, assuming it migrates to the repository level, may be diverted laterally around the opening if a capillary barrier exists. In contrast, if a capillary barrier does not form, then water may drip into the opening and come in contact with the waste package.

2.0.3 Site Selection

Two sites were selected in early 1997 for the location of the study. The first niche is located at Construction Station (CS) 35+66 (hereafter referred to as Niche 3566) in a brecciated zone between the Sundance Fault and a cooling joint where rock samples containing elevated chlorine-36 ($^{36}Cl/Cl$) ratios were collected. Sweetkind et al. (1997) found that elevated $^{36}Cl/Cl$ ratios indicate a component of bomb-pulse ^{36}Cl introduced as global fallout from above-ground nuclear device testing conducted between 1952 and 1958. Therefore, water containing elevated $^{36}Cl/Cl$ ratios represents young meteoric water introduced to the hydrologic cycle within approximately the last 40 to 50 years. The detection of elevated $^{36}Cl/Cl$ ratios implies that relatively young groundwater is present at Niche 3566 and that a preferential-flow pathway, perhaps associated with the Sundance Fault, may be present.

In contrast, the second niche is located at CS 36+50 (hereafter referred to as Niche 3650) in a competent rock mass with lower fracture density than Niche 3566. The isotopic signature of samples collected in the vicinity of Niche 3650 suggests that bomb-pulse ^{36}Cl is not present and a preferential-flow pathway from the land surface to the repository horizon is not present at this location.

2.1 Test Objectives

Liquid-release tests were conducted as part of the ESF Drift Seepage Test and Niche Moisture Study for the following reasons:

- To determine if water introduced above a mined opening (drift or tunnel) will drip into the opening because of gravity or migrate around the opening due to the formation of a capillary barrier;
- To quantify the amount of seepage that would enter the opening from a short duration release of water above a drift;
- To quantify the interaction between the matrix and fractures; and
- To provide a data set for the calibration of drift-scale numerical models.

Secondary objectives of the study include the characterization and documentation of fluid flow pathways in unsaturated fractured systems and evaluation of hydrologic properties of the rock mass.

2.2 Test Overview

This section provides a general overview of the tests, including activities performed during pre- and post-excavation of the niches. Detailed descriptions of test activities are provided in Sections 2.3 through 2.6.

2.2.1 Pre-Excavation Tests

During early June and early August 1997, a series of low-flow rate, liquid-release tests were conducted in boreholes installed prior to excavating each of the niches. The liquid-release tests were conducted in several boreholes located above and within the footprint of the proposed niche, by pumping water containing colored or fluorescent dyes into short test intervals straddling both high and low air-permeability zones. A finite amount of dye-spiked water was introduced into each test interval, with essentially no pressure buildup, to simulate a transient liquid-release event of short duration.

2.2.2 Niche Excavation Activities

Niche 3566 and Niche 3650 were excavated during late June and mid August 1997, respectively. The niches were excavated without water using an Alpine Miner to observe and photograph the distribution of fractures and dye within the welded tuff. Dye was observed along individual fractures as well as along intersecting fractures to depths ranging from 0 to 2.6 m below the liquid-release points. Flow of water through a relatively undisturbed fracture-matrix system was documented in this manner.

2.2.3 Post-Excavation Seepage Tests

A series of short duration seepage tests was performed starting in mid November 1997, continuing for approximately 4 months, and ending in mid March 1998. The seepage tests were conducted after Niche 3650 was excavated, by pumping water into boreholes located above the niche. The tests were used to quantify the amount of water seeping into the drift from a localized

source of water of known duration and intensity. In addition, the tests were used to establish the threshold rate at which water would no longer seep into the mined opening.

Seepage tests were not performed at Niche 3566. Rather, the bulkhead door at this site was closed and sealed soon after the niche was constructed and instrumented. The U.S. Geological Survey installed sensors within Niche 3566 to measure relative humidity within the confined space and to monitor water potential within the surrounding rock mass.

2.3 Tracer Selection

Various colored and fluorescent tracers were used during the study to document the flow path traveled by the wetting front. This section describes the literature review and laboratory work performed by Lawrence Berkeley National Laboratory (LBNL) to identify and select the tracers that were eventually used during the pre-and post-excavation liquid-release tests.

McLaughlin (1982) recommends that an ideal tracer should have the following general properties:

- It must correctly describe the velocity variations of the liquid being traced without modifying in any way the conductive or storage properties of the porous medium;
- It should not be retained by the porous medium through physical filtration or chemical retardation;
- It must be detected at low concentration;
- It must have a low background level in the environment within which it will be used;
- The tracer must be chemically and biologically stable;
- It should be harmless at the concentration used; and
- It should be inexpensive to purchase, collect, and evaluate.

Many of the colorless inorganic (e.g., Cl, Li, Br, I, etc.) and organic tracers used by hydrologists today exhibit many of these ideal properties, including mobility, lack of adsorption, and detection at very low concentration. Their use as tracers in unsaturated flow studies is limited, however,

because the exact pathway taken by the water through the unsaturated porous medium can be difficult to established through field observations. Instead, samples must be collected and analyzed for the tracer in the field or laboratory, using special extraction procedures and analytical equipment to indirectly locate the associated wetting front. Even then, the exact location of the pathway cannot be resolved unless a large number of samples are collected and processed at considerable effort and expense.

Colored dyes, on the other hand, produce a visible stain showing the location of the fluid's pathway that can be mapped and photographed. Unfortunately, dyes are typically used to stain the material of interest (e.g., clothes, food, biological tissue, porous media, etc.), which requires that they adsorb onto the surface of the material to some degree. Flury and Fluhler (1995) used infiltration experiments to show that the highly soluble food color additive, Brilliant Blue FCF (FD&C Blue No. 1), has a relative retardation of 1.2 compared with the anion I^-. In addition, Flury and Fluhler (1994) reported that the concentration of the dye must be relatively high (3 to 5 grams per liter [g l^{-1}]) to be visible in soils compared to its visibility in water (less than 1 milligram per liter [mg l^{-1}]. Infiltration studies performed by Omoti and Wild (1979a, 1979b) in the laboratory indicated that two fluorescing dyes, pyranine and fluorescein, could not be observed at concentrations less than about 20 mg l^{-1} in soil.

Given the limitation of each type of tracer described above and the added constraint that the mining operation, once started, could not be delayed to collect samples and perform time-consuming, on-site chemical analyses, organic dyes were selected as the tracers of choice. A review of the scientific literature was performed to determine the type of dyes that have been used in unsaturated zone studies. Physical, chemical, and toxicological data and analytical procedures were compiled pertaining to these tracers during late February and early March 1997 to determine whether they were suitable for use in the Exploratory Studies Facility (ESF). The tracers were ordered from the manufacturers by mid March to early April 1997. Material Safety Data Sheets (MSDS) were obtained from the manufacturer and sent to the ESF Test Coordination Office for evaluation by the Waste Isolation and Evaluation group and by Environment, Health, and Safety, as requested.

Table 2.1 lists the tracers selected for the test, including four relatively nontoxic dyes approved for use in foods, drugs, and cosmetics (FD&C) by the U.S. Food and Drug Administration, and seven fluorescent dyes. Although the literature review showed that many of these dyes readily adsorbed onto porous materials, we expected that the dyes would not exhibit significant retardation relative to the wetting front in a highly permeable fracture network during short-duration liquid-release tests. Model simulations of the injection tests showed that the water moves rapidly through the fractures and that advection is the predominate flow and transport mechanism, lending general support for our expectation.

The initial concentration of the injected dye was critical to the success of the study, given that visual observation of the dye stain was to be used to characterize the fluid flow path. Upon purchasing the dyes listed on Table 2.1, we performed a series of simple small-scale experiments in the laboratory to determine the visible limits of various dyes on a sample of the Topopah Spring welded unit. In addition, the laboratory tests were used to confirm whether there was a significant difference between the location of the wetting front and the dye stain. This was accomplished by applying a small volume of dye-spiked water onto an inclined surface (representing a fracture face) of a welded tuff sample producing a wetted area ranging from 0.03 to 0.09-m long by 0.025 to 0.04-m wide. The position of the wetted area was then compared to the dye-stained area that was observed after the sample dried.

The results of the visibility experiments are reported on Table 2.1. These experiments showed that the minimum dye concentration required for it to be visually observed on a dry tuff sample ranged from 0.5 to 5 g l^{-1} for the FD&C dyes and 0.25 to 1 g l^{-1} for the fluorescent compounds. With the exception of fluorescein, the test results also showed that the location of the dye stain corresponded to the position of the wetted area. The wetting front moved slightly beyond the limits of the dye-stained area, when fluorescein was used as the tracer.

Based upon these data, a permit was obtained from the State of Nevada allowing the injection of water containing a maximum concentration of 10 g l^{-1} and 2 g l^{-1} for the FD&C and fluorescent dyes, respectively. The higher permitted concentration accounted for the fact that it might not be possible to observe the dye at its minimum visible concentration when the rock appeared darker in the field because of higher water saturation or natural variation in rock color.

4 Test Configuration

This section contains a brief description of the test configuration, including the location of the boreholes and intervals tested, and equipment used during the tests.

2.4.1 Test Equipment

The test equipment used during the pre-excavation liquid-release tests and the post-excavation seepage tests was identical with the exception of the capture system, which was not used prior to niche construction. A description of the test equipment was included in Wang, et al. (1998) and is repeated here for completeness.

The test equipment included a straddle-packer system, a liquid-delivery system, and a data-acquisition system. A high-flow-rate, peristaltic pump or high-precision, low-flow-rate piston pump, along with two Mettler-Toledo electronic balances and ancillary equipment including graduated cylinders, beakers, and tubing, were used to meter and deliver the liquid to the test interval. A Hitachi 133 megahertz (MHz) notebook personnel computer (PC) and National Instrument's LabVIEW® software were used to acquire and store the data during the test.

Water and tracer were mixed in a graduated cylinder and placed on one of the two Mettler-Toledo electronic scales. The fluid was pumped from this reservoir using the high-flow-rate, peristaltic pump or the high-precision, low-flow-rate piston pump through an injection line to the test interval within the borehole. Test intervals were created using a 0.0635-m-diameter, 3.05-m-long straddle packer system. This system consists of six low-pressure inflatable packers connected in series with a 0.305-m-long test interval between each packer (Figure 2.3). After the straddle-packer system was placed in the borehole and pushed to the target depth, the packers were inflated using compressed air, thus effectively isolating each test interval. Individual injection lines were routed through the interior of the packer assembly, allowing the fluid to be pumped from the surface through the packers to a specific test interval.

A return line was also connected to each test interval, allowing water to flow from the test interval back to the surface where it was collected in a reservoir and weighed using a second Mettler-Toledo balance. The return line remained open during the test, preventing the water level within the interval from exceeding approximately 0.0635-m at all times. When the return line is open, the storage capacity of the test interval is approximately 0.582 liters (*l*) of fluid. The height of the water level that could potentially pond in the test interval was governed by the elevation of the inlet to the return line.

LabVIEW® was used to record the weight of the tracer solution on the Mettler-Toledo balances during injection. In addition, the change in weight with time, or mass rate of injection, was computed, at a user-specified logging interval. Near-real time data were displayed on the PC so the operator could monitor the progress of the test in the field.

A capture system was installed in the niche below the injection boreholes to collect any water dripping from the ceiling. The capture system consists of 44 0.305-m wide by 1.22-m long trays constructed of clear lexan plastic hung from an aluminum frame. In turn, the aluminum frame was suspended on poles so that the top of the capture system was approximately 0.4 to 1.0 m below the ceiling at the walls and centerline of the niche, respectively. The plastic trays are about 0.2 m deep and divided into four separate compartments, each 0.305 m square. Figure 2.4 shows a plan view of the capture system, and its position relative to the overlying boreholes and the boundary of the niche. Photographs of the capture system are provided as Figures 2.5 and 2.6.

\.2. Pre-Excavation Liquid-Release Tests

The pre-excavation liquid-release tests were conducted in boreholes installed at Niches 3566 and 3650 prior to niche construction. The liquid-release tests were performed on June 3, 1997, at Niche 3566, and on August 5, 1997 through August 8, 1997, at Niche 3650. Sections 2.4.2.1 through 2.4.2.4 below provide general descriptions of the liquid-release tests.

2.4.2.1 Borehole Configuration

Three boreholes were installed at Niche 3566 and seven holes were drilled at Niche 3650 to gain access to the rock for air permeability and liquid-release tests prior to mining each niche. A Longyear drill, equipped with drill rod, core-barrel, and diamond impregnated bit, was used to bore each of the 0.0762-m diameter holes to a maximum depth of 10 m. The boreholes were drilled without water, using compressed air to remove the cuttings and to cool the bit.

Figures 2.7 and 2.8 show that the three holes at Niche 3566 were installed along the same vertical plane coincident with the center of the niche. The three boreholes were assigned the designation U, M, and B corresponding to the upper, middle, and bottom borehole, respectively. Boreholes M and B were subsequently excavated after testing when the rock was mined out, creating the niche. Borehole U still remains.

Figures 2.7 and 2.9 show the location of the seven borings installed at Niche 3650. Three of the borings, designated UL, UM, and UR (upper left, upper middle, and upper right), were installed approximately one meter apart above the crown of the niche in the same horizontal plane. The remaining boreholes (ML, MR, BL, and BR) were drilled within the limits of the proposed niche and were subsequently mined out when the niche was constructed.

2.4.2.2 Test Interval Configuration

Water containing a known amount of tracer was injected into five test intervals in Borehole M before Niche 3566 was excavated. Five tracers were selected and used at this location, including three FD&C dyes (Blue No. 1, Red No. 40, and Yellow No. 5) and two fluorescent dyes (sulfo rhodamine B and acid yellow 7). Figure 2.10 is color-coded, showing where each dye was introduced.

Tracer-spiked water was injected into 14 test intervals at Niche 3650, including four intervals in Borehole UL, five in Borehole UM, two in Borehole UR, two in Borehole ML, and one interval in Borehole MR. Figures 2.11 and 2.12 show the locations of each interval tested and are also color-coded, showing where each dye was introduced. When the rock was mined away at Niche 3566, it was determined that FD&C Blue No. 1, Red No. 40 and sulfo rhodamine B were the most

visible of the dyes used. Therefore, FD&C dyes Red No. 40 and Blue No. 1 were used exclusively in the upper set of boreholes (U series) and sulfo rhodamine B was used exclusively in the middle borings (M series) at Niche 3650.

Each of the test intervals was approximately 0.305-m long and 0.0762 m in diameter, and could hold approximately 0.772 *l* of water when full.

2.4.2.3 Test Sequence

The air injection test data described in Wang et al. (1997) were reviewed to determine suitable locations for introducing tracer-spiked water. The zone exhibiting the highest air permeability value was targeted for liquid-release testing. The zone exhibiting the maximum air permeability value was straddled using the packer assembly, and the packers were then inflated, creating five separate intervals. In most cases, the remaining test intervals had air permeability values that were two to three orders of magnitude less than the maximum. This allowed liquid-release tests to be performed on intervals exhibiting a wide range of conductivities.

Upon inflating the packers, the injection line was pumped full of tracer-spiked water before starting the test to minimize storage of water in the line. Water was then pumped at a constant rate into the test interval until approximately 1 *l* of fluid was "pumped" into the interval. The pumping rate and mass of water being pumped into the interval were monitored over time and recorded. The fluid was allowed to remain undisturbed in the borehole for a few minutes before it was pumped back through the injection line or "recovered." The recovery rate and mass of water being recovered were also recorded.

In several instances, fluid was also pumped out the return line during the test where it was captured and weighed on the second balance. This occurred when the test interval was "tight" having low air permeability. Up to five tests were conducted per hole before the packers were deflated and the packer assembly was removed from the boring. The rate of "return" flow and mass of water returned were monitored over time and recorded.

Each test was conducted at a constant pumping rate and the pumping rates for all of the tests ranged from 0.5 to 3.6 grams per second (g/s). However, the test performed in Borehole UM in Niche 3650 at a depth of 4.27 to 4.57 m was an exception. Blue dye was injected into this test interval at a very low pumping rate, equal to 0.0216 g/s, because this interval had a low air permeability.

2.4.2.4 Mass of Water Released

Tables 2.2 and 2.3 summarize the mass of fluid released into each test interval as well as the pumping rate, recovery rate, and other details specific to each test. It should be noted that the pumping time reported on these tables represents the time required to "pump" the fluid into the boring after filling the injection line (i.e., it does not include line storage). In contrast, the "total recovery time" includes line storage. Total recovery time includes both the time required to pump the remaining fluid out of the test interval and to pump the water out of the injection line. "Standby time" is defined as the time period beginning when pumping ceased and ending when recovery of the fluid commenced.

The "recovered mass" presented on Tables 2.2 and 2.3 represents the total mass of water removed during recovery minus line storage. Therefore, these values represent the actual mass of water that was removed from the test interval during the recovery phase of each test. Multiplying the total recovery time by the average recovery rate will not result in the recovered mass shown on Tables 2.2 and 2.3. As noted above, the total recovery time also includes the time required to pump out the water stored in the injection lines.

The mass of water released into the rock formation was determined by mass balance. It was computed by subtracting the mass of fluid recovered plus the return mass (if any), from the mass of water pumped into the test interval:

Released Mass (g)	=	Pumped Mass (g)	-	Recovered Mass (g)	-	Returned Mass (g)

2.4.3 Post-Excavation Seepage Tests

As mentioned earlier in Section 2.2.3, the post-excavation seepage tests were performed at Niche 3650, while Niche 3566 was reserved for long-term monitoring of the ambient rock conditions. Therefore, Sections 2.4.3.1 through 2.4.3.4 below apply to the seepage tests conducted exclusively at Niche 3650 after the niche was constructed. Seepage testing was conducted between November 12, 1997 and March 12, 1998.

2.4.3.1 Borehole Configuration

As noted in Section 2.4.2.1 above, seven boreholes were originally installed at the Niche 3650 site; however, four of the boreholes were intentionally mined away during niche construction. Figures 2.13 and 2.14 show the location of the boreholes that remain. The post-excavation boreholes, designated UL, UM, and UR (upper left, upper middle, and upper right), were installed

approximately one meter apart above the crown of the niche in the same horizontal plane. Borehole UL, UM, and UR are located approximately 0.65 m above the ceiling of the niche.

2.4.3.2 Test Configuration

Water containing a known amount of tracer and/or water was released into 16 separate test intervals located above Niche 3650 at separate points in time. Five test intervals were selected and tested in Borehole UL, five in Borehole UM, and six intervals in Borehole UR. Table 2.4 summarizes the intervals tested, the tracer used (if any) during each liquid-release test, and the tracer concentration.

Figure 2.15 is color-coded, showing where each tracer was introduced relative to the boundaries of the niche. Nine out of the 16 post-excavation zones evaluated are identical to the test intervals investigated during the pre-excavation tests including:

- Four intervals tested in Borehole UL including 5.18 – 5.49 m, 5.79 – 6.10 m, 6.40 – 6.71 m, and 7.01 – 7.32 m; and

- Five intervals tested in Borehole UM including 4.27 – 4.57 m, 4.88 – 5.18 m, 5.49 – 5.79 m, 6.10 – 6.40 m, and 6.71 – 7.01 m.

Here, the measurements refer to the depth from the collar of the borehole to the beginning (e.g., 6.71) - end (e.g., - 7.01 m) of the test zone in meters.

During the pre-excavation liquid-release tests, water was introduced into two zones in Borehole UR (1.52 – 1.83 m and 2.13 – 2.44 m). Unfortunately, repeat measurements could not be made on these zones during the post-excavation seepage tests because the intervals were located directly above the bulkhead (Figure 2.4). The location of the bulkhead made it difficult to collect water seeping from the ceiling and to photograph the wetting front breaking through at the ceiling, so testing was abandoned at these locations. Therefore, six alternative intervals were selected for seepage testing in Borehole UR as follows:

- Six intervals tested in Borehole UR including 4.27 – 4.57 m, 4.88 – 5.18 m, 5.49 – 5.79 m, 6.10 – 6.40 m, 6.71 – 7.01 m, and 7.62 – 7.92 m.

In addition to the 15 test intervals listed in the bulleted paragraphs above, seepage tests were performed on interval 7.62 – 7.92 m in Borehole UL. This interval was not tested during the pre-

excavation liquid-release tests. Each of the test intervals was approximately 0.305-m long, 0.0762 m in diameter, and could hold about 0.772 *l* of water when full.

Color additives FD&C Blue No. 1 and FD&C Red No. 40 were used exclusively during the pre-excavation liquid-release tests in the upper boreholes. An alternating sequence of blue and red colored dyes were employed, starting with FD&C Blue No. 1 in the first test interval 5.18 – 5.49 m in Borehole UL and 4.27 – 4.57 m in Borehole UM.

In comparison, various tracers having contrasting colors to those employed during the pre-excavation tests were utilized in the upper boreholes at Niche 3650 during the post-excavation seepage experiments. Fluorescent dyes, including pyranine (green), sulfo rhodamine B (pinkish purple), amino G acid (blue) and acid yellow 7 (greenish yellow), were used in Borehole UM as shown on Table 2.4. Sulfo rhodamine B was employed exclusively in Borehole UL due to the fact that no seepage was observed from 3 of the 5 zones, thus eliminating the need to differentiate between wetting fronts using different colored dyes. A combination of FD&C dyes and sulfo rhodamine B were introduced into Borehole UR.

It should be noted that dye-spiked water was typically introduced into a given test interval only once at the beginning of the testing sequence. This is because there was some concern that multiple injections containing highly concentrated dyes might eventually clog the pore spaces and change the fluid-flow pathway.

2.4.3.3 Test Sequence

The seepage tests were conducted using the same general test sequence employed during the pre-excavation liquid-release tests, with one major improvement. The storage volume of the injection lines was measured and the same lines were employed throughout the testing sequence. This allowed the lines to be filled nearly to capacity (if desired) prior to each seepage experiment. Prior to this point in time, the test sequence was to pump the water up to the collar of the boring and the remaining line storage was computed using the cross-sectional area of the injection tubing and the known distance back to the test interval. The remaining storage was then filled by continuing to pump water into the injection line up to or near the limit of the computed line storage. This method introduced additional error in the computed mass of water released, which was effectively eliminated when the line storage was measured directly.

Water was pumped into the test interval at a constant pumping rate, with the rates from all forty tests ranging from 0.012 to 2.892 g/s. Any water that flowed out of the return line to the surface during the test was collected, weighed, and recorded. The flow direction was reversed after a predetermined mass (typically 1,000 ± 50 g) of water was pumped and any remaining water was

pumped back out of the borehole or recovered. Every attempt was made to introduce approximately the same mass of water into a given test interval so that tests performed at different pumping rates could be compared with one another. The primary exception to this rule was the final test performed in Borehole UM 4.88 – 5.18 m where 5,597.5 g of water was intentionally released into this zone. The reason for this departure will become apparent in subsequent sections of this chapter.

Any water that dripped into the capture system during the tests was drained off into a container and weighed. In addition, both the absolute time (date and hour (hr):minute (min):second (s)) of arrival of the wetting front at the niche ceiling and the time when water began to drip and stop dripping into the capture system were recorded (if the event was observed). Summaries of the absolute time data are provided on Table 2.5, and the duration of several key events (e.g., pumping time, wetting front arrival time, etc.) are summarized on Table 2.6. Key observations pertinent to each test are summarized in Table 2.7.

Digital photographs were taken during most of the seepage tests to document the arrival of the wetting front (if any), and its location and spreading pattern along the ceiling of the niche. Time-lapse video recordings of the niche ceiling were used to estimate the arrival time of the wetting front when field personnel were not present during overnight tests.

2.4.3.4 Mass of Water Released during the Seepage Tests

Table 2.8 summarizes the mass of fluid recorded at the beginning of the test before pumping water into the injection line ("start of test"), after filling the injection line but before releasing liquid into the interval ("start of release"), after pumping ended but before recovery started ("end of release"), after recovery ended at the end of the test ("end of recovery"), and the mass of fluid which flowed out the return line ("return mass"). The amount of fluid pumped during the test is also summarized on Table 2.8 and computed as follows.

The total mass of water pumped during the test includes water required to fill the injection line before injection as well as the water released into the test interval, and is equal to:

"Pumped Mass from Start Test & End Release data (g)"	=	"Start of Test" Mass (g)	-	"End of Release" Mass (g)

The mass of water pumped into the test interval can be estimated using the mass of water remaining on the injection balance after the injection line was filled (i.e., "start of release" mass) and from the mass of water remaining after release ended (i.e., "end of release" mass). Referring

to Table 2.8, the amount of water that was pumped into the test interval after nearly filling the injection line is approximately equal to the following:

"Pumped Mass from Start & End Release Data (g)"	=	"Start of Release" Mass (g)	-	"End of Release" Mass (g)

It is important to note, however, that the amount of water that was pumped (either total or that which reportedly went into the interval) is not equal to the water released to the formation. Both masses need to be corrected for the amount of water that flowed back through the return line during the test ("return mass" from Table 2.8), any pre- or post-test "line storage deficit(-)/surplus(+)," and/or "recovered mass" computed for the pre-test and recovery processes, respectively.

Columns (l) and (m) on Table 2.9 summarize the mass of water released to the formation as computed using the "start of test" and "end of recovery" data and the "start of release" and "end of release" data, respectively. For the sake of brevity, the reader should refer to Table 2.9 and its endnotes for a complete description of the terms used in the table and the algorithms used to compute the amount of water that was released. It suffices to say that the mass of liquid released to the formation was determined through mass balance, but with greater accuracy than the pre-excavation liquid-release tests, using the measured injection line storage.

Examination of Table 2.9 shows that mass of water released to the rock formation for the 40 seepage tests ranged from 274.5 to 5,597.5 g. Table 2.10 summarizes the rate of pumping, the rate of release into the formation, and the rate of recovery during pump back of the water. The duration of pumping (calculated using start & end of release data), release, and recovery are also recorded on this table. The rates were computed by simply dividing the pumped mass, released mass, and recovered mass by the respective duration of each event; therefore, these values represent time averaged rates.

It is important to point out that for a limited number of tests (e.g., Test #1 12-10-97) the release time may be greater than the pumping time. Although this would at first appear to be physically impossible, the injecting times were corrected for pre-release injection line storage. That is, it was very difficult to fill the injection line so that the amount of water in the line was exactly equal to the measured line storage shown on Table 2.9. Sometimes too little water was pumped into the injection line creating a storage deficit, meaning that a small volume of tubing had to be filled with water during the early stages of the test before water actually entered the test zone. Likewise, a line storage surplus occurred when the injection line was overfilled slightly prior to the test, and thus water entered the zone before the test officially began. In the former case, the

injection times will be less than the pumping times; in the latter case, the injection times will be slightly greater than the pumping times.

2.5 Results of Pre-Excavation Liquid-Release Tests

2.5.1 Tracer Distribution

After the liquid-release tests were completed, each niche was excavated using a mechanical Alpine Miner to observe and photograph the distribution of dyes injected into the rock mass. With the exception of the first two meters of Niche 3566, both niches were mined dry without the use of water. Minor amounts of water were introduced, however, at the bottom of the working face during mining operations because of leaking seals on the cutter head of the Alpine Miner. It is our understanding that the water is circulated through the cutter head to cool it during its operation, and that water leaking past the seals cannot be avoided. Mining operations took place from June 23 through June 25, 1997 at Niche 3566 and from August 14 through August 20, 1997 at Niche 3650.

Each niche was constructed by mining away 0.3 to 0.6 m of rock during each cut. The depth of the cut and speed in which the rock was mined away was dependent upon the hardness of the rock. In areas were the dye was injected, smaller cuts ranging from 0.15 to 0.3 m in depth were requested so that the distribution of the dye could be observed. Numerous digital photographs were taken using a Minolta camera, model RD-175, and field sketches were drawn of the distribution of dyes observed during mining operations. These records were used to generate the dye distribution maps and photographic cross sections presented as Figures 2.16 through 2.23, described below.

2.5.1.1 Niche 3566

Referring to Figure 2.16 and Table 2.11 for Niche 3566, the red and blue dyes, which were released into zones having high air permeability, migrated primarily south and/or west of their respective test intervals along low-angle fractures. The maximum observed lateral extent of the red dye is about 0.8 m, and the blue dye is approximately 0.3 m (as determined from these drawings). The asymmetrical horizontal distribution of the dyes is clearly evident from Figure 2.16.

Photographic Cross Sections A-A' and B-B' (Figures 2.19 and 2.20) show the vertical distribution of dyes observed on the working face of the niche at a depth of 2.85 and 4.98 m,

respectively, measured along the center line of the opening. The photographic section represented by Figure 2.19 shows that the red dye migrated through a series of interconnected vertical and horizontal fractures. The maximum depth of red dye migration was about 1.5 m (Table 2.11). The blue dye migrated primarily through two vertical fractures as shown in Figure 2.20. The maximum observed depth for the blue dye was 1.3 m as recorded on Table 2.11. Surprisingly, 50% less water was released during the blue dye test than the red dye test, yet the observed depth of penetration was nearly the same for both tests.

This observation demonstrates the important role that low-angle fractures may play in retarding downward migration of water through unsaturated, fractured media. Intuitively, low-angle fractures that are highly connected to their high angle counterparts should divert water laterally and slow the advancing wetting front.

2.5.1.2 Niche 3650

Referring to Figure 2.17 and Table 2.12 for Niche 3650, the red and blue dyes released into the upper boreholes did not exhibit a consistent direction of fluid migration. Dyes observed in Zones 1 and 5 migrated with their associated wetting fronts primarily to the west from the test intervals, while dyes observed in Zones 2 and 4 migrated primarily to the southeast. The red dye observed in Zone 3 was distributed primarily along one or two large vertical fractures found at this location, which contained calcite fracture coatings and fill material. Zone 3 also exhibited one of the highest air permeabilities measured at Niche 3650.

Photographic Cross-Sections C-C' and D-D' (Figures 2.21 and 2.22) show the vertical distribution of blue and red dyes observed on the working face of the niche at a depth of 4.34 and 5.74 m, respectively, measured along the center line of the opening. Photographic section C-C' was observed directly beneath the test interval of Zone 2 (Figure 2.17), where the wetting front had advanced to a depth of 1.32 m. The maximum depth of dye penetration for the wetting front was observed to the southeast of this location, where it reached 1.68 meters (Table 2.12). Approximately 0.68 *l* of water containing the blue dye was released at this location at a very low flow rate or about 0.0216 g/s.

Photographic Cross-Section D-D' (Figure 2.22) shows red dye at a depth of 0.82 m below the upper boreholes. It is not certain whether the dye observed at this location migrated from the test interval in Zone 3 or Zone 5. In either case, the dye appears to have migrated along several vertical fractures to this location. The fracture that is present along the left-hand side of the photograph appears to be filled with calcite, and the red dye does not penetrate deeper into the profile down this fracture surface at this location. In this case, the fracture fill material has closed the fracture and terminated the flow path.

Photographic Cross Section E-E' (Figure 2.23) shows the distribution of sulfo rhodamine B (pink/purple fluorescent dye) at a mined depth of 6.01 m. As shown on Table 2.12 the dye clearly migrated to a depth of 1.02 m through a single vertical fracture intersecting the injection interval in Borehole ML. Rhodamine stained the absorbant sock placed in Borehole BL located 1 m directly beneath Borehole ML, confirming that the wetting front had migrated to this depth. The lower boreholes (i.e., Boreholes ML, MR, BL, and BR when the upper boreholes were tested, and Boreholes BL and BR when the middle boreholes were tested) were filled with an absorbant boom or sock during all of the infiltration tests. It was hoped that the tracer would then stain the absorbant material when the wetting front came in contact with one or more of the observation boreholes.

2.5.2 Characterization of Pre-Excavation Flow Paths

Two primary types of flow paths were observed in the field during the mining operation, including:

1) Flow through one or two individual vertical fractures. Examples of predominately individual fracture flow were observed at Niche 3566 in Borehole M at 4.98 m (blue dye shown on Figure 2.20). Likewise, vertical fracture flow was observed at Niche 3650 in Borehole UR at 3.59 m (blue dye – not illustrated), UM at 5.01 m (red dye – not illustrated) and ML at 6.01 m (rhodamine shown on Figure 2.23); and

2) Flow through several interconnected horizontal and vertical fractures (i.e., flow through a fracture network). Examples of network-dominated flow were observed at Niche 3566 in Borehole M at 2.85 m (red dye on Figure 2.19) and in M at 3.1 m (Acid Yellow 7 – not shown). Examples of network flow were observed at Niche 3650 at five mined depths, of which photographic examples are provided on Figure 2.21 (blue dye from Borehole UM at 4.34 m) and Figure 2.22 (red dye); the remaining examples are not shown.

The mass of water released into each interval where dye was observed is plotted versus the maximum depth of dye penetration, lateral distance traveled by the wetting front, total distance traveled by the wetting front, and ratio of depth to lateral distance (hereafter defined as the aspect ratio) in Figures 2.24 through 2.27, respectively. Data are presented on these plots using two different symbols, with diamonds representing flow through individual vertical fractures and squares representing predominately network flow.

Examination of Figure 2.24 shows, as one would expect, that there is a general trend for the wetting front to move deeper into the profile as the mass of water released increases.

Surprisingly, the data do not indicate that the wetting front moves deeper into the profile when water is introduced into individual vertical fractures as opposed to fracture networks. This apparent anomaly may be an artifact of sampling and observation bias rather than that of fracture flow mechanics. Any vertical fractures that contribute to flow and that are oriented parallel to the mined face of the niche will not be observed as frequently as low-angle fractures. This is because these vertical fractures will be mined away during a single cut of the working face before the dye can be observed and the depth of the dye mapped. At least one vertical set of fractures was mined away in this manner at Niche 3650 in Borehole UM at 5.01 m (Zone 3, Figure 2.17). The red dye at this location was observed on the surface of two large fractures exposed only in the ceiling of the niche after the working face had been mined beyond 5.01 m. Therefore, the maximum depth of the dye was recorded as being 0.86 m below the injection point, i.e., from Borehole UM to a point just below the ceiling of the niche where the dye was observed. The dye may have migrated much deeper than this depth, but it could not be determined based on observation alone.

Figure 2.25 indicates that there is no direct correlation between the mass of liquid releases and the maximum observed lateral (horizontal direction from the injection point) distance traveled by the wetting front. However, the data show that liquid spreads laterally over larger distances in the interconnected network of fractures than in individual vertical fractures, as one would expect. This is because the low-angle fractures in a well-connected fracture network will divert water laterally, causing the wetting front to spread horizontally.

In general, (referring to Figure 2.26), the maximum distance that the dye traveled from the point of release to the furthest point of observation, increases with the mass of water released. As was the case with depth of penetration, the data do not show that the type of flow (i.e., network or individual fracture flow) has any significant influence on the maximum travel distance. Data from both types of flow, when plotted together on Figure 2.26, do not show any significant trend or grouping by type of flow. However, examination of Figure 2.27, which shows the ratio of depth to lateral distance traveled (aspect ratio) versus mass of water released, shows a significant trend. Although the data are sparse, the aspect ratio is consistently higher for the individual fracture flow data than for the fracture network data. In addition, the aspect ratio appears to increase with the mass of water released within each flow-type group.

2.6 Results of Post-Excavation Seepage Tests

2.6.1 Seepage Tests

As mentioned earlier, 40 individual seepage tests were performed during the 4-month testing period. When water appeared at the niche ceiling during a test and dripped into the capture system, it was collected and the mass of water was weighed on an electronic scale. Table 2.13 provides a summary of the mass captured in grams and the seepage percentage, defined below:

$$\text{Seepage Percentage} = 100 \times \text{Seepage Mass (Outflow)} / \text{Released Mass (Inflow)}$$

$$= 100 \times \frac{\text{"Mass Captured (g)"}}{\text{"Mass Released (g)"}}$$

The seepage percentage ranged from 0% for very low permeability zones to 56.2% for predominately gravity driven flow through highly saturated fractures. As mentioned earlier, every attempt was made to pump approximately the same mass of liquid during each test so that the results could be compared.

2.6.2 Distribution of Seepage

Appendix A contains a series of figures that show the distribution of seepage into the underlying capture system for each test. The figures provide a graphical summary of the test zone location and the distribution of liquid captured in each 0.305 by 0.305-m cell. Table 2.14 provides a tabular summary of the same data.

Depending upon the liquid-release rate, the wetting front typically arrived at the niche ceiling within a few minutes to a couple of hours after the test started (Table 2.15). Where liquid was observed seeping into the capture system it was from one or more fractures intersecting the ceiling of the niche. Close examination of the seepage process in several cases showed that when the wetting front arrived through large fractures, the entire fracture did not necessarily conduct water. Instead, water migrated along the edges of large breakouts (voids) in the fracture plane, forming wedges of water. Once the wetting front arrived, liquid spread laterally by capillary action across the niche ceiling. However, lateral spreading was usually confined to within 0.05 to 0.06 m of the conducting fracture. The wetting front rarely moved more than 0.08 or 0.09 m from the fracture before encountering an asperity or low point on the ceiling where the liquid eventually accumulated and dripped.

Seepage into the capture system occurred for 10 out of 16 zones tested. Of the remaining six test zones that did not seep, liquid appeared at the niche ceiling, but did not drip at three of these

locations, including UM 6.10 – 6.40 m, UM 6.71 – 7.01 m, and UR 7.62 – 7.92 m. Zone UR 7.62 – 7.92 m was only tested once, so further investigation might have revealed that this interval seeped. Interval UM 6.10 – 6.40 m is fairly unique in that water appeared at the ceiling regardless of the liquid-release rate, but water never accumulated and dripped into the capture system. Fluid was initially pumped into interval UM 6.71 – 7.01 m at a high rate, exceeding the saturated hydraulic conductivity of the interval, resulting in the release of only 274.5 g of water into the rock mass. The wetting front did not migrate to the niche ceiling in this case. When the liquid-release rate was lowered from 0.555 to 0.202 g/s, however, 988.3 g of water entered interval UM 6.71 – 7.01 m and the wetting front eventually appeared at the niche ceiling, but dripping did not occur.

Water was introduced into three test intervals in Borehole UL, including 5.18 – 5.49 m, 5.79 – 6.10 m, and 6.40 – 6.71 m, but the wetting front never migrated to the niche ceiling. The intervals only imbibed 379.2 to 420.3 g of liquid when the tests were conducted at relatively high pumping rates ranging from 0.19 to 0.528 g/s. When the pumping rate was reduced from 0.19 to 0.014 g/s for interval UL 5.18 – 5.49 m, the amount of liquid that entered the rock mass only increased by 131.9 g from 405.4 to 537.3 g, and the wetting front still did not appear at the niche ceiling. The rock exposed in the niche ceiling beneath these intervals appears to be more massive (with less fracturing) than other areas of the niche.

In general, the largest number of zones that seeped were observed near the back of Borehole UL, near the front of Borehole UM and along nearly the entire length of the zones tested in Borehole UR. The front section of Borehole UL exhibited the fewest number of zones that seeped.

It is interesting to note that in most cases the majority of the liquid that seeped was captured in one or two compartments or cells of the capture system, as can be seen by examining the figures in Appendix A. Rarely was liquid captured in more than three compartments during any given test. When this did occur, one cell typically captured a large percentage of the seepage volume with much smaller volumes distributed among the remaining cells. In most cases, the liquid that seeped was captured directly beneath the test zone or in capture cells immediately adjacent to the interval. Exceptions were noted in the case of intervals UR 6.10 – 6.40 m and UR 6.71 – 7.01 m, where large amounts of water seeped into cells located 0.3 to 0.6 m to the southeast of the test intervals.

2.6.3 Fracture Hysteresis

During the early stages of the post-excavation seepage tests, it was observed that the fracture system exhibited hysteresis; that is, there was a memory effect or wetting history. Figures 2.28 and 2.29 show the sequence of tests performed on intervals UM 4.27 – 4.57 m and UM 4.88 –

5.18 m, respectively. Referring to Figure 2.28, the first and second test were conducted approximately 2 weeks apart, and about the same seepage percentage was obtained even though the first test was conducted at a much greater liquid-release rate (2.019 versus 0.503 g/s). It was determined by examining the air-permeability results for this interval that the first test was conducted at a flow rate probably exceeding the saturated hydraulic conductivity of the interval, thus, the liquid release process was *profile-controlled* (Hillel, 1971), i.e., controlled by the saturated hydraulic conductivity of the rock.

On the other hand, the second test was probably conducted at a rate that was slightly less than the hydraulic conductivity, but not significantly less to make a difference in the measured seepage percentages (22.6 versus 23.7%). The third test was conducted at a liquid-release rate nearly equal to the second test (0.506 g/s), yet it had a much higher seepage percentage (56.2%). In addition, the wetting front arrived in approximately half the amount of time during the third test (8:34 min:s) than it did for the second test (16:48 min:s). Since the second and third tests were only separated in time by 2 hours, it can be concluded that the fracture system exhibits a memory effect, or hysteresis. That is, the water saturation of the fractures remained high over the 2 hour time period separating the tests, and affected the seepage outflow and travel time of the wetting front during the third test. Subsequent tests were performed at lower liquid-release rates at 4-week intervals and did not exhibit significant hysteresis.

A second series of tests performed on UM 4.88 – 5.18 m also exhibited fracture hysteresis as shown in Figure 2.29. Again, Tests 1 and 2 were conducted approximately 2 weeks apart, but this time the results were sigificantly different. The seepage percentage was roughly 50 percent less for the second test (4.2% seepage) than for the first test (9.6%). However, this can be explained by the fact that both tests were conducted at a rate that did not exceed the saturated hydraulic conductivity of the interval and, thus, the liquid-release process was *flux-controlled* (Hillel 1971), i.e., controlled by the water supply rate.

The third test in this sequence was separated in time from the second by about one day and was performed at a lower liquid-release rate (0.144 vs. 0.507 g/s). Even though the system had a day to recover and the liquid-release rate was lower, more liquid seeped during the third test (7.1%) than during the second test (4.2%). The wetting front, however, was slower to arrive during the third test, probably because of the lower liquid-release rate. Subsequent tests conducted at still lower rates, but separated in time by one to two months of inactivity, did not exhibit a memory effect.

In conclusion, it was determined that the memory effect or wetting history had a profound impact on seepage. Therefore, it was decided soon after these tests were conducted in early December

1997 that a minimum of two weeks of inactivity should separate seepage experiments so that each interval would have an opportunity to recover before testing resumed.

2.6.4 Determination of Seepage Threshold Flux From Test Results

Many of the seepage tests were initially conducted at liquid-release rates that exceeded the equivalent saturated hydraulic conductivity of the test interval determined from air-permeability data. Subsequent tests were performed at lower liquid-release rates to determine whether a threshold could be defined where seepage would no longer occur.

The liquid-release rate at which seepage no longer occurred, defined hereafter as the seepage threshold rate, was established for 7 out of the 10 test zones that seeped. Appendix B contains a series of bar charts that summarize the liquid-release rate versus seepage percentage, the mass of water released, and dates of each test. Figure 2.30 provides a concise graphical summary of all the data. Seepage threshold rates were almost obtained for two of the three remaining test intervals, including UL 7.62 – 7.92 and UR 6.71 – 7.01 m. We are confident that the threshold rate could have been obtained for the remaining intervals had additional time been available to complete the work.

The liquid-release flux (q_s, m/s) was computed using the liquid-release rate (Q_s, g/s), the density of water (ρ_w, g/cm^3, assumed value of 1.0E+06 g/m^3), and the cross-sectional area (A, m^2) of flow as follows:

$$q_s = \frac{Q_s}{A\,\rho_w}$$

The cross-sectional area (A) was determined by assuming that the liquid level could rise 6.35 cm to the inlet of the return line before it would flow back to the surface. If the entire test interval filled with liquid, then the cross-sectional area of flow would be equal to the curved surface area of a right circular cylinder, or approximately 729.7 cm^2 ($2\pi rh$, where r = 3.81 cm and h = 30.48 cm). If fluid rises to the level of the return port, then the cross-sectional area of flow is assumed to be less than the surface area of the test interval and equal to that portion of the curved surface area of a right circular cylinder lying below the water line as follows (CRC 1975):

$$A = [2\pi - (2\,\text{Arccosine}(d/r))]\, r\, h,$$

where d is equal to the vertical distance from the center of the cylinder to the water line (2.54 cm), r is equal to radius of the borehole (3.81 cm), and h is equal to the test interval length (30.48 cm). Using the equation and parameters specified above, the estimated surface area is equal to 534.3 cm^2.

It should be noted that water would most certainly move up the borehole wall above the water level established in the test interval because of capillary forces, thus increasing the cross-sectional area available to flow. However, without knowing how far the wetted area would spread, the cross-sectional area cannot be determined *a priori*; therefore, using the smaller area (i.e., 534.3 versus 729.7 cm^2) would be a more conservative approach. That is, the liquid-release flux at which seepage will begin will be greater than the true flux (i.e., over-estimated) if a smaller area is used in the calculation.

Table 2.16 provides a summary of the net downward liquid-release flux (K_o) computed using this approach, and Figure 2.31 provides a concise graphical summary of all the flux data. Appendix C contains data plots showing the logarithm of the liquid-release flux versus the seepage percentage for the 10 zones that seeped. The graphs were created using Microsoft® Excel '97, which was also used to compute the equation for the trendline and the R–squared value (R^2) shown on the graph and reported on Table 2.17. The symbol "—Log (all data)" in the legend on the graphs refers to the logarithmic transform that was conducted on the data before the regression. The R-squared values were computed and are listed for those intervals where three or more data points are available; otherwise, a perfect correlation of $R^2 = 1$ would be obtained with only two data points.

Table 2.17 also summarizes the seepage threshold flux (K_{o*}) defined as the liquid-release rate below which water will not seep into the drift (i.e., seepage equals 0). The K_{o*} values were determined using the regression equations provided on Table 2.17 and by changing the value of K_o in the regression formula until the seepage percentage was less than 1E-12, or nearly zero. The seepage threshold flux may be interpreted as follows:

- If the liquid-release flux exceeds the seepage threshold flux ($K_o > K_{o*}$) for the given interval, then water will seep into the drift.

- If the liquid-release flux is less than the seepage threshold flux ($K_o < K_{o*}$), then water will not enter the drift and it will presumably migrate around the opening.

Figure 2.32 shows a log-log plot of seepage threshold flux versus the saturated hydraulic conductivity (K_l) for each test zone. The air permeabilities obtained from the post-excavation gas-injection tests were converted into equivalent saturated hydraulic conductivities to produce the values recorded on Table 2.17 and plotted on Figure 2.32.

2.6.5 Interpretation of Seepage Results Using Seepage Exclusion Theory

Philip et al. (1989) recognized that buried cavities are obstacles to flow causing the water pressure on parts of the cavity surface to increase resulting in the formation of a capillary barrier. However, when downward seepage is fast enough and/or the cavity is large enough, then water will seep into the opening. Philip et al. (1989) provides an analytical solution to this problem. This solution is used below, along with the liquid-release fluxes from Section 2.6.4 and air permeability data, to explain the seepage data collected during the study and to show theoretically that a capillary barrier formed at Niche 3650.

Inherent in any analysis is the underlying assumptions, which were provided in Philip et al. (1989) as follows:

- Steady-downward flow of water through a homogeneous, isotropic unsaturated porous media (Philip, p. 17, section 1.4). However, Philip notes that the requirement for homogeneity is relatively weak;
- The flow velocity is spatially uniform and continuous (Philip, p. 17, section 1.4);
- The flow domain is infinite in extent (Philip, p.17, section 1.5); and
- There exists a functional relation between unsaturated hydraulic conductivity, $K(\psi)$, and moisture potential, ψ, that is exponential in nature (Philip, p. 18, equation 12);

In addition, we supplement these assumptions with a few of our own that are pertinent to our particular case as follows:

- The measured air permeability of the test interval adequately represents the saturated liquid permeability of the test domain;
- Imbibition from the fracture into the adjoining matrix is negligible over the time period in which seepage observations are made;
- There is no dead-end storage in the fracture system being tested; and
- The relative humidity at the intersection of the niche ceiling and the conducting fractures is assumed to be at or near 100 percent. However, this localized condition may not necessarily be met everywhere within the niche and/or the ESF main drift.

Philip et al. (1989) developed the theory of water exclusion from, or entry into, cavities from steady uniform downward seepage through an unsaturated porous medium. Using a quasi-linear formulation of the equation of steady unsaturated flow, Philip et al. (1989, p. 19) developed the following theoretical relation between seepage threshold rate and the saturated hydraulic conductivity:

$$K_{o*} = K_1 [\vartheta_{max}(s)]^{-1} \qquad (1),$$

where the nomenclature used herein are the same as Philip's, namely ϑ is the dimensionless potential, s is the value of the dimensionless cavity length, and ϑ_{max} is the maximum value of the dimensionless potential at the boundary of the cavity. Philip et al. (1989) shows that ϑ_{max} occurs at the centerline of the crown or ceiling of a cylindrical cavity. The dimensionless cavity length, s, is a measure of the relative importance of gravity and capillarity in determining flow. As $s \rightarrow 0$, capillarity dominates, whereas gravity dominates as $s \rightarrow \infty$. In turn, s is related to α, the sorptive number ([length]$^{-1}$), which enters into the exponential representation of the dimensional unsaturated hydraulic conductivity (K, [length/time]) as a function of water potential (ψ, [length]). The reader is encouraged to review Philip et al. (1989) for a detailed understanding of the assumptions and analyses pertinent to this discussion.

When s is large, Philip et al., (1989) demonstrate that a boundary layer adjoining the ceiling of the cavity surface will develop. This allows the steady flow equation to be replaced by a boundary layer equation that is readily solved. The asymptotic expansion of ϑ_{max} for large values of s yields:

$$\vartheta_{max} = 2s + 2 - \frac{1}{s} + \frac{2}{s^2} - \ldots \qquad (2)$$

Philip et al., (1989) note that the first three terms on the right hand side of Equation (2) produce an adequate engineering estimate that is within 10 percent or better of the exact value of ϑ_{max}, when $s \geq 1$. Therefore, Equation (1) and the first three terms in the series of Equation (2) were used to generate the data found in Appendix D, which in turn are plotted as two lines on Figure 2.32. The s values were selected so the lines produced the best-fit possible by eye to the data set.

Two lines were used instead of one because the data appear to be grouped into two distinct sets. The first line was produced using an s value of 100, which fits four data points that exhibit a very nice linear trend (red triangles on Figure 2.32). The second line was created using an s value of 20. Although the data for the second line show greater variability (i.e., blue diamonds on Figure 2.32), a weak linear trend in the data is still apparent. One possible explanation for the fact that the data appear to fit two lines with different s values may be that the data are derived from two distinct fracture populations. As noted earlier for the pre-excavation liquid-release tests, fracture

flow paths appear to be grouped into two general populations, including flow through individual fractures and flow through an interconnected network of fractures.

Indisputable physical evidence of flow through individual vertical fractures is available for two of four points (red triangles) fitted to the s = 100 line. One or two large vertical fractures were observed conducting water during the post-excavation seepage tests performed at each of the UL 7.62 – 7.92 m and UM 4.88 – 5.18 m locations. Indirect evidence of individual fracture flow is also available for the remaining zones (UR 6.10 – 6.40 and UR 6.71—7.01 m). The evidence is based on the observation that the bulk of the water seeped into capture cells located 0.6 to 0.9 m from the end of the test interval–the furthest distance traveled for any of the tests. This suggests that lateral diversion of the wetting front may have occurred through one or two high-angle fractures dipping to the southwest away from the test intervals. Otherwise, the center of the seepage mass would have arrived directly below the test interval.

Additional indirect evidence of individual fracture flow for Zones UR 6.10 – 6.40 m and UR 6.71—7.01 m includes the fact that the wetting front arrived relatively fast in each case. In fact, this is a common characteristic of all the data that trend along the s = 100 line; that is, the arrival times for these data are typically much faster than the remaining data grouped along the s = 20 line. In contrast, field observations and indirect evidence demonstrate that data trending along the s = 20 line indicate that flow is through interconnected fracture networks. Zones UM 4.27 – 4.57 m, UM 5.49 – 5.79 m, and UR 4.27 – 4.57 m showed obvious signs of multiple conducting fractures. However, interval UR 5.49 – 5.79 m appears to be the only exception to this rule; the wetting front arrived quickly and the data point for this interval is far removed from both lines.

Another indication that the two data sets represent distinct populations of fractures is derived from the values of s. As stated earlier, s is a measure of the driving forces behind unsaturated flow, namely as $s \rightarrow 0$, capillarity dominates, whereas gravity dominates as $s \rightarrow \infty$. Therefore, highly conductive individual fractures that are free draining because of gravity-dominated flow should exhibit a greater value of s than a network of interconnected fractures influenced to a greater extent by lateral spreading of the wetting front and capillary driven flow. Based on this information and the observations presented in the previous paragraph, we hypothesize that the data trending along the s = 100 line are characteristic of individual vertical fractures, and the data trending along the s = 20 line are characteristic of interconnected fracture networks.

Philip et al., (1989) notes that the dimensionless cavity length s is related to the exponential fitting parameter α (length^{-1}) and a characteristic length of the cavity l (length) by the following expression:

$$s = 0.5\,\alpha\,l \qquad (3)$$

Using Equation (2), and assuming a value of 2 m for cavity length, which is approximately equal to the equivalent radius of the niche, α is equal to the following values for the different fracture populations:

$$\alpha_{\text{Individual Fractures}} = \alpha_{s=100} = 100\ \text{m}^{-1}$$
$$\alpha_{\text{Fracture Networks}} = \alpha_{s=20} = 20\ \text{m}^{-1} \qquad (4).$$

The quantity $2\alpha^{-1}$ defined by Philip (1986) is a moisture potential characteristic of the unsaturated flow process and is designated the sorptive length. Therefore, for s = 100 and s = 20 the following values of the sorptive length can be determined from (4) as follows:

$$2\alpha_{(s=100)}^{-1} = 0.02\ \text{m} = 0.02\ \text{m} \times (101{,}325\ \text{Pa} / 10.33\ \text{m of } H_20) = 196\ \text{Pa};\ \text{and}$$

$$2\alpha_{(s=20)}^{-1} = 0.10\ \text{m} = 981\ \text{Pa}.$$

We believe this provides additional evidence that the data were collected from two different populations, indicative of different flow pathways. Field tests that are characteristic of flow through interconnected fracture networks ($2\alpha_{(s=20)}^{-1}$ = 981 Pa) should exhibit stronger capillary forces (i.e., larger sorptive lengths) than zones exhibiting flow through individual fractures ($2\alpha_{(s=100)}^{-1}$ = 196 Pa). Finsterle and James (in Wang et al., 1998) came to a similar conclusion by performing a sensitivity analysis of drift-scale seepage using two-dimensional and three-dimensional models designed to evaluate the capillary barrier concept. They concluded that strong capillary forces cause the wetted area to spread, resulting in lower overall saturations and less seepage. The seepage data shown on Table 2.18 support the modeling conclusion. Namely, that for a given liquid-release rate, the zones that exhibit flow characteristics of a fracture network have a much lower seepage percentage than the data for corresponding individual fractures.

Close examination of Table 2.18, however, indicates that Zone UM 4.88 – 5.18 m appears to be an anomaly, even though direct observation indicated that a large vertical fracture was present and conducting water at this location. That is, the seepage percentage data from this zone are much lower than the values from the individual fracture flow data, and similar in value to the network fracture flow data set for a given liquid-release rate. Contrarily, we believe these data do support the concept that Zone UM 4.88 – 5.18 m is representative of individual fracture flow. The fact that this zone exhibits low saturations at high rates is because the zone also has the highest air permeability of any of the zones tested, approximately two orders of magnitude greater than the geometric mean for the data collected from this borehole. Finsterle and James'

(in Wang et al., 1998) sensitivity study also showed that reducing the permeability results in slower wetting front propagation, but higher average plume saturation. High saturations are required to eventually overcome the capillary barrier and for water to seep into the drift. Therefore, the amount of water seeping into the niche is much lower for high permeabilities than for low permeabilities at a given liquid-release rate when a capillary barrier forms. This is because the water percolates at a much lower saturation in the high-permeability case. We believe that the field observations and seepage data from Test Interval UM 4.88 – 5.18 m provide definitive support for this conclusion. In addition, we conclude that the data and field observations support the hypothesis that two general types of flow predominate at Niche 3650 at a scale of 0.65 m: namely, flow through individual fractures and interconnected fracture networks.

2.6.6 Physical Evidence of a Capillary Barrier

We have shown so far that the seepage threshold flux can be measured, analyzed successfully using a theoretical capillary barrier model, and explained, but we have not demonstrated conclusively that a capillary barrier actually formed. Two sources of evidence will be presented below lending support to the conclusion that a barrier formed during the tests.

2.6.6.1 Weak Evidence Demonstrating the Formation of a Capillary Barrier

Figures 2.33 and 2.34 are digital photographs of the Niche 3650 ceiling that were taken during a liquid-release test conducted on Zone UR 4.27 – 4.57 m on February 5, 1998. The photograph comprising Figure 2.33 was shot shortly after the wetting front arrived at the ceiling during Test #1 2-5-98. At the end of the test, another photograph of the ceiling was taken, as shown on Figure 2.34. The blue stain appearing near the left-hand side of both photographs represents the final wetted area of a previous test (Test #1 1-14-98) performed on the same test interval three weeks earlier on January 14, 1998. Test #1 1-14-98 and Test #1 2-5-98 were conducted at liquid-release rates equal to 0.198 and 0.055 g/s, respectively. Water seeped into the capture system during the first test and did not drip into the capture system during the second test.

The green line that appears in both photographs was painted onto the ceiling of the niche to show the position (i.e., axis) of Borehole UR located approximately 0.65 m above the ceiling. Another short line was added to the photograph in order to show the position of the test interval relative to the wetting fronts.

Close examination of the photographs clearly shows that the wetted area produced during Test #1 1-14-98 (blue dye stain) lies directly beneath the test interval. Water was introduced in the test interval and exited out a number of fine fractures within the blue stained area. In contrast, the

wetting front (wetted area on ceiling) arrived at a different location during the second test performed at a lower liquid-release rate. Eventually, the wetting front for Test #1 2-5-98 also arrived near the bottom of the original wetted area at the end of the test, as can be seen in Figure 2.34.

It is important to note that the spread of the wetted area is greater as indicated by the arrows on Figure 2.34 for the low rate test (Test #1 2-5-98) when seepage did not occur. One would expect lateral spreading of the plume across the ceiling of the niche as shown in the photograph if a capillary barrier formed. In general, lateral spreading of the wetted area was observed for several zones that seeped as the liquid-release rate was lowered toward the seepage threshold value. It is important not to over interpret the data since an equally plausible explanation for this observation can be formulated. The lateral spreading may simply be due to the fact that certain pores within the fracture plane may not conduct water at lower rates corresponding to lower saturations. Under unsaturated conditions, the water must follow a more tortuous route through smaller pores resulting in greater spreading of the plume. Therefore, lateral spreading of the wetted area should be considered "weak" evidence demonstrating that a capillary barrier was present.

Another piece of weak evidence leading one to believe a capillary barrier formed was collected during the last two tests conducted on interval UM 4.88 – 5.18 m. Test #1 1-8-98 and Test #1 3-6-98 were conducted almost two months apart, and both tests were performed at liquid-release rates (0.047 and 0.013 g/s, respectively) below the seepage threshold level. The most significant difference between the tests involved the amount of water released and length of the test. Test #1 1-8-98 was run for approximately 6.25 hours, and 1044.2 g of water was injected into the test zone. In contrast, dye-spiked water was released during Test #1 3-6-98 for approximately 5 days resulting in 5,597.5 g of fluid entering the rock mass. The introduction of a much larger volume of water (i.e., approximately 5 times greater) during the second test without seepage, coupled with the observation that the wetted area also spread further than its previous limits, provides weak evidence of the formation of a capillary barrier. An alternative hypothesis explaining the fact that water did not drip even though five times more water was introduced can be provided. Perhaps the flow rate was low enough and the flow path was tortuous enough that the water was simply imbibed into the matrix during the test.

2.6.6.2 Strong Evidence Demonstrating the Formation of a Capillary Barrier

The most compelling evidence of the formation of a capillary barrier was observed when a small breakout in the ceiling is present. A breakout can best be described as a location were a chunk of rock breaks out of the ceiling during the mining process, producing a void that extends upward beyond the relatively flat section of the niche ceiling. The cartoon provided as Figure 2.35 attempts to clarify this explanation.

Typically, the block of rock drops from the ceiling exposing high angle fractures extending upward into the rock mass above the niche. When the near-vertical surfaces are exposed directly beneath a test interval, it provides an important opportunity to observe the arrival of the wetting front in 3-dimensions. In general, only a 2-dimensional plan view of the wetted area is possible at the niche ceiling when a breakout is not present.

Figures 2.36 and 2.37 provide examples of a 3-dimensional observation point and the wetted area that resulted from liquid-release test performed on interval UM 5.49 – 5.79 m during Test 1 Niche 3650 (11/12/97). Although it is difficult to conceptualize using a flat 2-dimensional photograph, a breakout zone is present near the top center of Figures 2.36 and 2.37. The photographs were taken looking up at the ceiling, with the breakout zone extending beyond the limit of the photograph toward the top of the page. The axis of the borehole was painted on the niche ceiling and appears on the photograph, along with the location of the test interval. A dotted line is used to outline the breakout zone. Within the breakout zone are several fractures, including a high-angle fracture whose face is part of the niche ceiling within the breakout. Two small, yellow arrows with the labels "v" and "h" are drawn at the intersection of the high-angle vertical fracture and near horizontal ceiling of the niche. The vertical arrow (v) is drawn parallel to the dip of the high-angle fracture point up into the breakout zone, and the horizontal arrow (h) is drawn parallel to the horizontal plane forming the niche ceiling as shown on Figure 2.35.

Referring to Figure 2.36, the wetting front arrived at the niche ceiling beneath Zone UM 5.49 – 5.79 m in approximately 3.5 minutes. The wetting front arrived at the location noted on the figure near the intersection of the high angle fracture with the niche ceiling. Surprisingly, within a few seconds the wetting front was observed moving **up** several small fractures that terminated at the face of the high-angle fracture. Approximately 20 seconds after the wetting front arrived, the wetting front reached the position shown in Figure 2.36. The light-blue arrows show the direction that the wetting front traveled. Figure 2.37 shows the position of the wetting front about 2 minutes after the wetting front arrived when water began dripping into the capture system. The wetting front moved an additional 8 cm **up** the fine fracture from Location 1 to Location 2, shown next to the blue arrow on Figure 2.37 in 1.33 minutes.

It is important to note that the wetting front arrived first at the ceiling of the niche and then was observed migrating up several fine fractures exposed in the sidewall of the breakout. This demonstrates that the water saturation was building up within the fracture network for approximately 2 minutes before water began dripping into the capture system. We believe these observations provide strong evidence that a capillary barrier formed for a brief time and then collapsed once saturated conditions were reached within the fracture system.

2.6.7 Hydromechanical Effects of Niche Construction

In Level 4 Milestone report SP33PLM (Wang et al. 1998), it was noted that the pre- and post-excavation air permeability results were dramatically different. The geometric mean air permeability for the data collected from Borehole UM increased after niche construction by roughly two orders of magnitude.

Additional evidence is available from the liquid-release tests, which also reflect the hydromechanical effect of mining out the niche. For example, return flow occurred when the pumping rate exceeded the saturated hydraulic conductivities of Test Intervals UM 4.27 – 4.57 m, UM 5.49 – 5.79 m, and UM 6.10 – 6.40 m during the pre-excavation tests. In other words, the pumping rate was too high and the liquid-release process was *profile-controlled.* In contrast, the same intervals were tested after excavating the niche at a liquid-release rate that was greater than or equal to pre-excavation rate. In each case, return flow did not occur and the mass of water that entered the rock was significantly greater than the pre-excavation tests. Although there are certainly exceptions to these general observations, this would imply that the hydromechanical effects of mining increased both the air permeability and the saturated hydraulic conductivity of the fracture system.

Another hydromechanical effect of mining that was observed in the field can be deduced from comparing differences in pre- and post-excavation flow pathways. That is, the wetting front was observed migrating along different sets of fractures during the post-excavation tests when compared to the dye-stained areas produced by testing the same interval during the pre-excavation tests. This comparison assumes, of course, that the dye-stained area accurately depicts the original position of the wetting front in the undisturbed fracture system prior to niche construction. The laboratory results from the dye-evaluation studies reported in Section 2.3 supports this assumption, since the location of the stained area was typically in close agreement with the final position of the wetting front.

During the first series of post-excavation tests, water was pumped into the same intervals and at the same pumping rate as the pre-excavation tests. Of the six zones (UL 7.01 – 7.32 m and all zones in UM) that were tested in common and where seepage (dye) was observed at the ceiling of the niche, water was observed following the same flow path from only two of these zones (UL 7.01 – 7.32 and UM 5.49 – 5.79 m). The most dramatic example of the pre- and post-excavation wetting fronts arriving along different flow paths occurred from Zone UM 6.10 – 6.40 m. The red dye from the pre-niche test was not present on the ceiling of the niche after excavation. However, the wetting front from a post-excavation test conducted on this same interval arrived at two separate locations. A less dramatic, yet more typical example of the difference in pre- and post-excavation flow paths is pictured in Figure 2.38. Here, the red stain shown on the photograph in the large fracture resulted from the wetting front moving through this area during

the pre-niche construction test. In contrast, the pink stain was created when sulfo rhodamine B-spiked water was introduced into the same interval at about the same rate (pre = 3.0 vs. post = 2.892 g/s). Although the stains created by the wetting fronts are located adjacent to one another (which commonly occurs), it is clear that the hydromechanical effects of mining caused the flow path to change even though water was introduced from a common source.

2.6.8 Air permeability vs. Hydraulic Conductivity

Although it was not the original intent of this study to provide a comprehensive evaluation of the relation between air permeability measured using air-injection tests, and the hydraulic conductivity measured using liquid-release tests, several key observations have direct bearing on the use of these results by project scientists. Under slightly ponded conditions in the borehole (i.e., saturated conditions), the liquid-release flux (K_o) may initially exceed the saturated hydraulic conductivity of the test interval during the early stages of the test when capillary forces predominate. During the later stages of the test, gravity-driven flow will dominate, and the liquid-release flux measured at the borehole should eventually approach the saturated hydraulic conductivity of the interval being tested. Based on the small sorptive length ($2\alpha^{-1}$) values computed in Section 2.6.5, it can be safely assumed that gravity-driven flow is the primary flow mechanism operating in fracture systems tested at Niche 3650. One would expect capillarity effects to be short lived, and for all practical purposes the maximum liquid-release rate ($K_{o\text{-}max}$) for a given interval should be less than the equivalent saturated hydraulic conductivity determined using the air permeability results ($K_{air\text{-}sat}$), if unsaturated conditions prevail. Theoretically, $K_{o\text{-}max}$ could exceed $K_{air\text{-}max}$ if water ponds within the borehole during the test under saturated conditions; however, the packer system was designed so that water could not pond by more than 0.0635 m, otherwise return flow to the surface would occur.

Table 2.19 contains a summary of the air permeabilities converted to equivalent saturated hydraulic conductivies ($K_{air\text{-}max}$) and the maximum observed liquid-release flux ($K_{o\text{-}max}$) that was measured for each zone. A cross-sectional area of 729.7 cm^2 was used to compute the hydraulic conductivities from the air permeability values because gravitational effects on air are negligible and, thus, the entire cross-sectional area of the borehole is typically available for airflow. An area equal to 534.4 cm^2 was used to compute the liquid-release fluxes as explained in Section 2.6.4.

Comparing the $K_{air\text{-}max}$ results to the $K_{o\text{-}max}$ values on Table 2.19, indicates that saturated flow should have occurred for only two tests. The second-to-last column in Table 2.19 indicates that "yes" saturated flow conditions should have prevailed for intervals UM 4.27 – 4.57 m and UM 5.49 – 5.79 m. If a "no" is recorded in this column, then $K_{air\text{-}max} > K_{o\text{-}max}$ and unsaturated flow should have prevailed.

It should be noted that return flow was observed during five of the liquid-release tests, corresponding to five different intervals (marked with a "yes" in the last column of Table 2.19). Return flow provides direct evidence, regardless of the air permeability results, that the liquid pumping rate exceeded the saturated hydraulic conductivity of the test interval. This implies that the liquid-release rates marked with a "yes" in the last column equaled or exceeded the actual hydraulic conductivity of the test interval. Examination of Table 2.19 shows that the equivalent saturated hydraulic conductivity, which was determined using the air-permeability results, overestimates the liquid hydraulic conductivity approximately 30 % of the time (5 out of 16 intervals). Interval UL 5.79-6.10 m exhibits the most severe difference, with $K_{air\text{-}max}$ (3.82E-04 m/s) overestimating the saturated hydraulic conductivity (3.78E-06 m/s) by about two orders of magnitude.

2.7 Summary

2.7.1 Pre-Excavation Liquid-Release Testing in Niche 3566 and 3650

The maximum depth and maximum travel distance that the wetting front moves during a short duration liquid-release test performed in unsaturated, fractured rock increases with increasing mass of fluid injected. It appears that maximum depth and travel distance data cannot be used to determine the type of flow (i.e., individual fracture versus network flow) that controls water movement during the test. Lateral spreading and the aspect ratio (i.e., ratio of depth to lateral spreading) may be stronger measures of the type of flow that predominates. Increased lateral spreading of the wetting front appears to be typical of well-connected fracture networks containing both high and low-angle fractures, whereas larger aspect ratios appear to be typical of flow in individual vertical fractures.

The data collected and used in this analysis may be biased by the mining method, preventing the accurate measurement of liquid migration depth in vertical fractures oriented perpendicular to the axis of the niche. One method of overcoming this bias would be to install future niches at various angles to the ESF tunnel so that different sets of vertical fractures are intersected and sampled/observed during the mining operation.

There was limited success using absorbant materials placed in holes located beneath the test interval to determine if the wetting front/dye had migrated to that depth. Only one out of six observation boreholes containing absorbant material showed visible signs of staining by the dye. It appears that the wetting front either did not migrate to the depth of the observation boring or

that the flow path was too tortuous, so that the wetting front simply did not come in contact with the material in the hole.

Mining away the rock mass to directly observe the dye was very successful and is a much better method of characterizing flow paths in fractured-unsaturated systems. However, this method also has its limitations, including high costs and the limited ability to control the depth of mining during each advance of the working face. Too large a cut in the rock face during the mining operation will remove the fractures that contain the dye and prevent the flow path from being adequately characterized. Too small a cut, on the other hand, will drive up the cost of the mining operation. A delicate balance between mining costs and having sufficient data to evaluate the flow path must, therefore, be considered when proposing a study of this type.

2.7.2 Post-Excavation Seepage Testing of Niche 3650

Forty post-excavation liquid-release tests were conducted on 16 different test intervals located in boreholes above the niche (Section 2.6.1). The purpose of the seepage tests was to investigate the amount of water that would drip into a mined opening from a transient liquid-release event of short duration. Of the 16 zones tested, water seeped into the capture system from 10 test intervals, water appeared at the niche ceiling but did not drip in 3 cases, and water did not appear at all when introduced into the 3 remaining zones. The seepage percentage, defined as the amount water captured in the niche divided by the amount released into the rock, ranged from 0 to 56.2%.

It was determined during the early stages of testing that the memory effect or wetting history had a profound impact on seepage, as described in Section 2.6.3. If the liquid-release tests were performed too close together in time, then it was found that the seepage percentage increased dramatically, as one would expect. This is because the fractures contain residual moisture, and their unsaturated hydraulic conductivity will be higher during subsequent tests. In addition, imbibition into the matrix will not be as quick during subsequent tests because the capillary gradient near the fracture-matrix interface will not be as steep. Based on the results of this study, it appears that redistribution of moisture in the fracture system occurs within a one-day to two-week period after the test. The process of moisture redistribution to its original state is unknown; however, one can surmise that water is either imbibed into the matrix, moves around the niche due to capillarity, or is removed from the fractures by the near-field drying potential of the ESF ventilation system between the tests. In any event, it was decided during the early stages of the testing program that a minimum period of two weeks should separate seepage tests performed on a given interval in order to allow the fracture system to recover.

The seepage threshold flux, defined as the flux of water that when introduced into the test interval would first begin to result in observable seepage from the niche ceiling, was computed and evaluated in Section 2.6.4 and 2.6.5 of this report. Surprisingly, the saturated hydraulic conductivities and seepage threshold data can be evaluated and interpreted with reasonable success using analytical techniques derived for a homogenous, unsaturated porous media derived by Philip et al. (1989) subject to the limiting assumptions listed in section 2.6.5. The analysis resulted in realistic values of the sorptive length ($2\alpha^{-1}$), an exponential fitting parameter characteristic of the unsaturated flow process. Values for $2\alpha^{-1}$ equal to 196 and 981 Pa were derived from the test data and are believed to represent flow through two types of *in situ* fractures, including individual high-angle fractures and a network of interconnected fractures.

The data evaluated in Section 2.6.5 also support several important conclusions drawn by Finsterle and James (in Wang et al. 1998) who performed a sensitivity analysis using 2- and 3-dimensional models to evaluate the effect of permeability, and capillarity on the formation of a capillary barrier. What they concluded and the data from this study support the following observations:

- A reduction in permeability results in slower wetting front propagation, but higher average plume saturation. High saturations are required to eventually overcome the capillary barrier and for water to seep into the drift. Therefore, the amount of water seeping into the niche is much lower for high permeabilities than for low permeabilities when the injected water flows at lower saturation levels at a given rate of liquid release.

- Strong capillary forces cause the wetted area to spread, resulting in lower overall saturations and less seepage for a given flux.

Direct evidence of the formation of a capillary barrier during a liquid-release test was photographed in the field and documented in Section 2.6.6 of this report. The wetting front arrived at the ceiling of the niche and then migrated up several fine fractures exposed in the sidewall of a breakout. The movement of water up the fractures instead of downwards with gravity demonstrates that the water saturation was building up within the fracture network for approximately 2 minutes before water began dripping into the capture system. We believe these observations provide strong evidence that a capillary barrier formed for a brief time and then collapsed once saturated conditions were reached. Indirect field evidence which also demonstrates that a capillary barrier formed includes: 1) increased lateral spreading of the wetting front as the liquid-release rate is lowered; and 2) the ability of the rock mass to divert a relatively large mass of water (approximately 5,600 g) with zero seepage when the water was applied at a rate below the seepage threshold flux.

In general, the hydromechanical effects of mining were found to increase the air and water permeability and liquid conductive capacity of the fracture system above a mined opening. In addition, the results from the Finsterle and James (in Wang et al. 1998) sensitivity study using 2- and 3-dimensional drift-scale models show that an increase in the permeability results in a decrease in seepage percentage. The data presented in Section 2.6.5 support their conclusion. The observations and results from both studies have important ramifications as to the potential design of a geologic repository. The hydromechanical effects of mining result in favorable conditions, assuming they typically result in increased fracture-system permeability above the opening, as was found at Niche 3650. This is because the hydromechanical effects should decrease the amount of water entering the drift and coming in contact with the waste package. Furthermore, backfilling the opening around the waste canisters with a fined-grained material such as sand or even coarse aggregate may actually prevent the capillary barrier from forming and allow more water to contact the waste package.

The air permeability data collected during the niche study were compared to the liquid-release data in Section 2.6.8 of this report. It was found that the air-permeability data, when they are converted to equivalent saturated hydraulic conductivities, overestimate the true hydraulic conductivity approximately 30% of the time. The air-permeability data were found to overestimate the true conductivities by a factor of 1.5 to two-orders of magnitude. The gross difference in values may be caused by dead-end fractures that prevent the downward gravity-driven migration of water through the fracture system during a liquid-release test and constrain the resulting measured liquid hydraulic conductivity. Three of the zones that did not seep, including UL 5.18 – 5.49 m, UL 5.79 – 6.10 m, and UL 6.40 – 6.71 m, exhibited this type of behavior. Air injected into the fracture system during an air permeability test does not have the same constraints. Air can move up, down, or sideways within the fracture plane to find the path of least resistance, and the resulting equivalent air conductivity is not constrained greatly by gravitation forces.

The disturbing aspect of this result stems from the fact that the air-permeability results are often used to calibrate unsaturated zone models. If unsaturated zone models are calibrated using air-permeability data (or fracture apertures derived from air k results), which overstate the true liquid permeability of the fracture system, then the models may be conservative at high saturation by overestimating the true liquid flux and underestimating the travel time through the mountain. In contrast, however, the model may not be conservative at low saturation. This is because the models are conditioned upon air data which produce higher permeabilities, as shown in this report, than the true liquid permeability. At low saturation, the model will predict that the higher permeability fractures have drained, when in reality the true distribution of fractures have not. In this case, the model will underestimate the true flux and overestimate the travel time through the unsaturated zone at Yucca Mountain. Innovative methods, such as those described in this report,

should be used to measure *in situ* hydraulic parameters directly or to confirm the results of indirect measurements, including air permeability test results.

References

CRC Standard Mathematical Tables, 1975. Edited by S.M. Selby, 23rd Ed., CRC Press, Inc. Cleveland, OH, 756.

Flury, M. and Fluhler, H. 1994. "Brilliant Blue FCF as a Dye Tracer for Solute Transport Studies: A Toxicological Overview." *Journal of Environmental Quality, 23* (5), 1108-1112.

Flury, M. and Fluhler, H. 1995. "Tracer Characteristics of Brilliant Blue FCF." *Soil Sci. Soc. Am. J., 59* (1), 22-27.

Freeze, R.A. and Cherry, J.A. 1979. *Groundwater*, Prentice-Hall, Inc. Englewood Cliffs, N.J., 604p.

Hillel, D. 1971. *Soil and Water: Physical Principles and Processes*. New York: Academic Press.

McLaughlin, M.J. 1982. "A Review of the Use of Dyes as Soil Water Tracers." *Water SA, 8* , 4, 196-201.

Montazer, P. and Wilson, W.E. 1984. *Conceptual Hydrologic Model of Flow in the Unsaturated Zone, Yucca Mountain, Nevada.* U.S. Geol. Surv. Water Resour. Invest. Rep. 84-4345. Denver, Colorado: U.S. Geological Survey. NNA.19870519.0109, GS930408312291.001 (Non-Q).

Omoti, U. and Wild, A. 1979a. "Use of Fluorescent Dyes to Mark the Pathways of Solute Movement through Soils under Leaching Conditions: 1. Laboratory Experiments, 2. Field Experiments." *Soil Science, 128* (1), 28-33.

Omoti, U. and Wild, A. 1979a. "Use of Fluorescent Dyes to Mark the Pathways of Solute Movement through Soils under Leaching Conditions: 1. Laboratory Experiments, 2. Field Experiments." *Soil Science, 128* (1), 98-104.

Philip, J.R., 1986. "Linearized Unsteady Multidimensional Infiltration." *Water Resour. Res.*, 22 (12), 1717-1727.

Philip, J.R.; Knight, J.H.; and Waechter, R.T. 1989a. NNA.19900403.0006. "Unsaturated Seepage and Subterranean Holes: Conspectus, and Exclusion Problem for Cylindrical Cavities." *Water Resour. Res., 25* (1), 16-28.

Sweetkind, D.S.; Fabryka-Martin, J.T; Flint, A.L.; Potter, C.J.; and Levy, S.S. 1997. *Evaluation of the Structural Significance of Bomb-pulse ^{36}Cl at Sample Locations in the Exploratory Studies Facility, Yucca Mountain, Nevada.* USGS Level 4 Milestone SPG33M4. Denver, Colorado: U.S. Geological Survey.

Wang, J.S.Y., Cook, P.J.; Trautz, R.C.; Salve, R.; James, A.L.; Finsterle, S.; Tokunaga, T.K.; Solbau, R.; and Clyde, J. 1997. *Field Testing and Observation of Flow Paths in Niches, Phase 1 Status*

Report of the Drift Seepage Test and Niche Moisture Study. Yucca Mountain Project Level 4 Milestone SPC314M4. Berkeley, California: Lawrence Berkeley National Laboratory. LB970601233124.001 (Q).

Wang, J.S.Y; Trautz, R.C.; Cook, P.J.; Finsterle, S.; James, A.L.; Birkholzer J.; and Ahlers, C.F. 1998. *Testing and Modeling of Seepage into Drift: Input of Exploratory Study of Facility Seepage Test Results to Unsaturated Zone Models*, Yucca Mountain Project Level 4 Milestone SP33PLM4. Berkeley, California: Lawrence Berkeley National Laboratory.

Chapter 2

Tables

Table 2.1 List of Tracers

Food Coloring Dyes	Color on Tuff Sample	Minimum Visible Concentration (g/l)
FD&C Blue No.1	Brilliant blue	0.5
FD&C Red No. 40	Red	5
FD&C Yellow No. 5	Yellow	5
FD&C Yellow No. 6	Sunrise Orange	5
Fluorescent Dyes*		
Amino G Acid	Clear (invisible) - light Blue (UV)	0.5
Fluorescein	Fluorescent yellowish green (UV)	1
Pyranine	Fluorescent greenish yellow (UV)	1
Acid Yellow 7	Yellow (invisible) - Bright Yellow (UV)	1
Rhodamine B	Pink/purple (visible) - Orange (UV)	0.25
Rhodamine WT	Pink/purple (visible) - Orange (UV)	0.25
Sulfo Rhodamine	Pink/purple (visible) - Orange (UV)	0.25

FD&C = color additives certified for use by the FDA in Food, Drugs & Cosmetics

* Color and minimum visible concentration for fluorescent dyes were determined using visible observation and long-wave UV lamp

Table 2.2

PRE-EXCAVATION LIQUID RELEASE SUMMARY: NICHE 3566

Yucca Mountain Project
Exploratory Study Facility

Lawrence Berkeley National Laboratory

Borehole Location	Test Date	Depth of [1] Release (m)	Tracer	Concentration (g-dye per kg-water)	Average Rate of Pumping (g/s)	Average Rate of Recovery (g/s)	Pumping Time (min)	Standby Time (min)	Total [2] Recovery Time (min)	Pumped Mass (g)	Returned Mass (g)	Recovered [3] Mass (g)	Released Mass (g)
Middle	6/4/97	2.13 - 2.44	FD&C Red No. 40	7.9	-3.6	3.2	4.42	8.83	0.75	947.3	0.0	5.6	941.7
	6/4/97	2.77 - 3.05	Acid Yellow 7	1.9	-3.4	3.2	4.25	3.17	2.92	837	263.4	453.3	120.3
	6/3/97	3.35 - 3.66	FD&C Yellow No. 6	8.3	-3.5	3.3	4.50	2.00	2.67	932.6	358.2	433.9	140.5
	6/3/97	3.96 - 4.27	Sulfo Rhodamine B	2.0	-3.3	3.6	4.17	4.77	3.00	819.4	198.7	476.5	144.2
	6/3/97	4.57 - 4.88	FD&C Blue No. 1	8.4	-3.4	3.2	4.42	2.25	6.67	899.7	0.0	425.7	474

[1] Depth measurement is from the collar of the boring to the test interval.
[2] Total recovery time includes the time needed to evacuate the injection interval and the injection line (i.e., includes line storage).
[3] The recovered mass does not include line storage. It represents the mass of fluid pumped out of the test interval during recovery.

Table 2.3

PRE-EXCAVATION LIQUID-RELEASE SUMMARY: NICHE 3650

Yucca Mountain Project

Exploratory Study Facility

Lawrence Berkeley National Laboratory

Borehole Location	Test Date	Depth of [1] Release (m)	Tracer	Concentration (g-dye per Kg-water)	Average Rate of Pumping (g/s)	Average Rate of Recovery (g/s)	Pumping Time (min)	Standby Time (min)	Total [2] Recovery Time (min)	Pumped Mass (g)	Returned Mass (g)	Recovered Mass [3] (g)	Released Mass (g)
Upper Left	8/7/97	5.18 - 5.49	FD&C Blue No. 1	8.4	-2.0	2.0	8.31	3.17	6.92	1013.3	319.3	590.8	103.2
	8/7/97	5.79 - 6.10	FD&C Red No. 40	8.7	-2.0	1.9	8.43	3.00	6.67	1003.1	0.0	735.5	267.6
	8/7/97	6.40 - 6.71	FD&C Blue No. 1	8.4	-2.9	2.8	5.67	3.25	5.83	1001.1	394.7	559.6	46.8
	8/7/97	7.01 - 7.32	FD&C Red No. 40	8.7	-2.0	1.4	8.47	2.83	4.90	997.7	0.0	303.2	694.5
Upper Middle	8/7/97	4.27 - 4.57	FD&C Blue No. 1	8.8	-0.0216	1.8	771.38	10.50	3.00	999.5	156.9	158.3	675.8 **
	8/6/87	4.88 - 5.18	FD&C Red No. 40	7.7	-3.0	2.6	5.48	3.92	1.08	994.2	0.0	56.8	937.4
	8/7/97	5.49 - 5.79	FD&C Blue No. 1	8.4	-2.1	2.0	8.06	2.83	5.00	1002.2	486.5	400.0	115.7
	8/7/97	6.10 - 6.40	FD&C Red No. 40	8.7	-0.5	1.7	36.58	3.83	8.25	1000.2	210.2	683.2	106.8
	8/6/97	6.71 - 7.01	FD&C Blue No. 1	7.7	-1.9	1.6	8.20	2.25	6.67	959.0	0.0	520.3	438.7
Upper Right	8/7/97	1.52 - 1.83	FD&C Red No. 40	7.8	-2.0	2.0	7.63	3.42	2.33	897.5	394.8	132.8	369.9
	8/7/97	2.13 - 2.44	FD&C Blue No. 1	8.4	-2.0	1.9	8.50	2.83	1.75	1000.0	0.0	0.2	999.8
Middle Left	8/8/97	4.88 - 5.18	Sulfo Rhodamine B	2.0	-1.9	2.0	6.73	2.50	6.17	784.3	112.2	520.5	151.6
	8/8/97	6.71 - 7.01	Sulfo Rhodamine B	2.0	-2.0	2.0	8.22	2.67	6.00	999.9	351.7	477.3	170.9
Middle Right	8/8/97	5.18 - 5.49	Sulfo Rhodamine B	2.0	-1.9	2.0	8.07	3.08	4.42	1001.9	379.3	314.3	308.3

[1] Depth measurement is from the collar of the boring to the test interval.

[2] Total recovery time includes the time needed to evacuate the test interval and the injection line (i.e., includes line storage).

[3] The recovered mass does not include line storage. It represents the mass of fluid pumped out of the test interval during recovery.

** This value was adjusted for evaporation of water out of the injection reservoir during 771 minutes of testing.

Table 2.4 - 1 of 2

Post-Niche Excavation Tracer Use Summary

Niche 3650

Exploratory Study Facility

Lawrence Berkeley National Laboratory

Borehole	Test Name	Date	Depth (m)	Tracer	Tracer Concentration g/l
UL	Test #1 12-11-97	12/11/97	5.18-5.49	S. Rhodamine B	1.4
	Test #2 2-12-98	2/12/98	5.18-5.49	S. Rhodamine B	1.4
	Test #2 12-11-97	12/11/97	5.79-6.10	S. Rhodamine B	1.1
	Test #3 12-11-97	12/11/97	6.40-6.71	None	0.0
	Test #1 12-10-97	12/10/97	7.01-7.32	S. Rhodamine B	2.0
	Test #1 1-6-B1198	1/6/98	7.01-7.32	None	0.0
	Test #2 1-6-98	1/6/98	7.62-7.92	None	0.0
	Test #1 2-12-98	2/12/98	7.62-7.92	None	0.0
	Test #1 3-4-98	3/4/98	7.62-7.92	S. Rhodamine B	0.6
UM					
	Test 5 Niche 3650	11/13/97	4.27-4.57	Pyranine	3.1
	Test #1 12-3-97	12/3/97	4.27-4.57	None	0.0
	Test #2 12-3-97	12/3/97	4.27-4.57	None	0.0
	Test #1 1-7-98	1/7/98	4.27-4.57	None	0.0
	Test #2 2-10-98	2/10/98	4.27-4.57	None	0.0
	Test 1 Niche 3650	11/12/97	4.88-5.18	S. Rhodamine B	2.0
	Test #1 12-4-97	12/4/97	4.88-5.18	None	0.0
	Test #2 12-5-97	12/5/97	4.88-5.18	None	0.0
	Test #1 1-8-98	1/8/98	4.88-5.18	None	0.0
	Test #1 3-6-98	3/6/98	4.88-5.18	FD&C Yellow No. 6 & FD&C Blue No. 1	3.4
	Test 4 Niche 3650	11/13/97	5.49-5.79	Amino G Acid	3.1
	Test #2 12-4-97	12/4/97	5.49-5.79	None	0.0
	Test #1 1-9-98	1/9/98	5.49-5.79	None	0.0
	Test #1 2-11-98	2/11/98	5.49-5.79	None	0.0
	Test 3 Niche 3650	11/13/97	6.10-6.40	Acid Yellow 7	1.6
	Test #3 12-4-97	12/4/97	6.10-6.40	None	0.0
	Test #1 1-12-98	1/12/98	6.10-6.40	None	0.0

Table 2.4 - 2 of 2

Post-Niche Excavation Tracer Use Summary

Niche 3650

Exploratory Study Facility

Lawrence Berkeley National Laboratory

Borehole	Test Name	Date	Depth (m)	Tracer	Tracer Concentration g/l
UM	Test 2 Niche 3650	11/12/97	6.71-7.01	S. Rhodamine B	2.0
	Test #1 12-5-97	12/5/97	6.71-7.01	None	0.0
UR	Test #1 1-14-98	1/14/98	4.27-4.57	FD&C Blue No. 1	4.1
	Test #1 2-5-98	2/5/98	4.27-4.57	None	0.0
	Test #1 1-15-98	1/15/98	4.88-5.18	FD&C Blue No. 1	1.6
	Test #1 2-6-98	2/6/98	4.88-5.18	None	0.0
	Test #2 1-13-98	1/13/98	5.49-5.79	None	0.0
	Test #2 2-10-98	2/10/98	5.49-5.79	None	0.0
	Test #2 1-14-98	1/14/98	6.10-6.40	FD&C Blue No. 1	3.8
	Test #1 2-4-98	2/4/98	6.10-6.40	None	0.0
	Test #1 1-13-98	1/13/98	6.71-7.01	None	0.0
	Test #1 2-3-98	2/3/98	6.71-7.01	None	0.0
	Test #1 3-5-98	3/5/98	6.71-7.01	S. Rhodamine B	0.5
	Test #1 3-12-98	3/12/98	7.62-7.92	FD&C Yellow No. 6 & FD&C Blue No. 1	3.4

Table 2.5 - 1 of 3

Absolute Times for Post-Excavation Seepage-Test Events

Niche 3650: Borehole UL

Exploratory Study Facility

Lawrence Berkeley National Laboratory

Borehole	Test Name	Date	Depth (m)	Pumping Begins	Pumping Ends	Recovery Begins	Recovery Ends	Return begins	Wetting Front Arrives	Dripping Begins	Dripping Ends
UL	Test #1 12-11-97	12/11/97	5.18-5.49	10:06:00	11:33:38	11:36:10	11:38:38	11:32:30	--	--	--
	Test #1 2-12-98	2/12/98	5.18-5.49	2/12/98 14:58	2/13/98 11:25	2/13/98 11:29	2/13/98 11:45	--	--	--	--
	Test #2 12-11-97	12/11/97	5.79-6.10	12:25:00	12:56:43	12:58:49	13:01:32	12:55:45	--	--	--
	Test #3 12-11-97	12/11/97	6.40-6.71	13:49:07	14:22:20	14:24:20	14:29:30	14:18:44	--	--	--
	Test #1 12-10-97	12/10/97	7.01-7.32	18:24:00	18:32:35	18:34:35	18:37:45	--	18:28:00	18:33:07	18:38:50
	Test #1 1-6-98	1/6/98	7.01-7.32	11:07:40	12:35:44	12:37:45	12:43:33	--	12:02:30	--	--
	Test #2 1-6-98	1/6/98	7.62-7.92	14:17:00	14:50:45	14:52:00	14:54:15	--	14:28:30	14:35:20	15:26
	Test #1 2-12-98	2/12/98	7.62-7.92	11:11:00	14:02:06	14:03:00	14:10:03	--	11:20:30	11:46:10	14:07
	Test #1 3-4-98	3/4/98	7.62-7.92	3/4/98 12:04	3/5/98 11:10	3/5/98 11:15	3/5/98 11:21	--	3/4/98 12:47	NO	NR

-- The event did not occur.

NO - Not Observed. The event occurred when field personnel were not present to observe and record the time of the event.

NR - Not Recorded. The time that the event occurred was not recorded.

Absolute Times for Post-Excavation Seepage-Test Events

Niche 3650: Borehole UM

Exploratory Study Facility

Lawrence Berkeley National Laboratory

Borehole	Test Name	Date	Depth (m)	Pumping Begins	Pumping Ends	Recovery Begins	Recovery Ends	Return begins	Wetting Front Arrives	Dripping Begins	Dripping Ends
UM	Test 5 Niche 3650	11/13/97	4.27-4.57	14:05:00	14:13:27	14:16:27	14:19:30	--	14:11:56	14:12:10	14:46:00
	Test #1 12-3-97	12/3/97	4.27-4.57	12:00:04	12:33:56	12:37:07	12:39:52	--	12:16:52	12:21:51	13:04:56
	Test #2 12-3-97	12/3/97	4.27-4.57	14:30:08	15:03:55	15:06:00	15:08:26	--	14:38:42	14:39:50	15:25
	Test #1 1-7-98	1/7/98	4.27-4.57	12:43:09	18:42:15	18:46:25	18:51:50	--	15:10:00	17:18:48	19:08:40
	Test #2 2-10-98	2/10/98	4.27-4.57	2/10/98 14:15	2/11/98 9:51	2/11/98 9:55	2/11/98 10:02	--	2/10/98 17:57	--	--
	Test 1 Niche 3650	11/12/97	4.88-5.18	12:02:00	12:08:04	12:11:54	12:14:59	--	12:05	12:05	NR
	Test #1 12-4-97	12/4/97	4.88-5.18	9:47:40	10:22:15	10:24:15	10:27:00	--	9:52:38	10:04:00	10:25:42
	Test #2 12-5-97	12/5/97	4.88-5.18	11:43:08	13:45:46	13:47:46	13:50:27	--	11:59:00	12:24:45	13:58
	Test #1 1-8-98	1/8/98	4.88-5.18	10:45:00	17:00:30	17:03:30	17:12:24	--	12:26	--	--
	Test #1 3-6-98	3/6/98	4.88-5.18	3/6/98 13:16	3/11/98 10:50	3/11/98 10:54	3/11/98 11:01	--	3/6/98 19:17	--	--
	Test 4 Niche 3650	11/13/97	5.49-5.79	12:38:52	12:47:05	12:49:50	12:52:45	--	12:42:20	12:44:22	13:02:00
	Test #2 12-4-97	12/4/97	5.49-5.79	11:50:20	12:24:49	12:26:49	12:29:28	--	11:57:20	12:01:26	12:34:38
	Test #1 1-9-98	1/9/98	5.49-5.79	9:27:00	14:26:40	14:29:48	14:34:31	--	10:12:50	12:28:26	14:35
	Test #1 2-11-98	2/11/98	5.49-5.79	2/11/98 11:50	2/12/98 9:06	2/12/98 9:10	2/12/98 9:18	--	2/11/98 14:38	--	--
	Test 3 Niche 3650	11/13/97	6.10-6.40	10:21:00	10:53:25	10:57:30	11:02:01	--	10:55:30	--	--
	Test #3 12-4-97	12/4/97	6.10-6.40	13:25:02	14:51:57	15:00:20	15:02:00	--	14:30:14	--	--
	Test #1 1-12-98	1/12/98	6.10-6.40	13:44:00	14:05:09	14:15:08	14:20:15	--	14:06:30	--	--
	Test 2 Niche 3650	11/12/97	6.71-7.01	14:22:01	14:30:20	14:33:02	14:37:30	14:30:10	--	--	--
	Test #1 12-5-97	12/5/97	6.71-7.01	9:37:00	10:59:35	11:01:35	11:04:21	--	10:30:00	--	--

-- The event did not occur.

NO - Not Observed. The event occurred when field personnel were not present to observe and record the time of the event.

NR - Not Recorded. The time that the event occurred was not recorded.

Table 2.5 - 3 of 3

Absolute Times for Post-Excavation Seepage-Test Events

Niche 3650: Borehole UR

Exploratory Study Facility

Lawrence Berkeley National Laboratory

Borehole	Test Name	Date	Depth (m)	Pumping Begins	Pumping Ends	Recovery Begins	Recovery Ends	Return begins	Wetting Front Arrives	Dripping Begins	Dripping Ends
UR	Test #1 1-14-98	1/14/98	4.27-4.57	10:31:12	11:56:05	11:58:00	12:07:35	--	11:27:20	11:47:00	12:10:08
	Test #1 2-5-98	2/5/98	4.27-4.57	9:20:00	14:24:46	14:28:03	14:35:00	--	12:05:10	--	--
	Test #1 1-15-98	1/15/98	4.88-5.18	10:10:00	11:39:40	11:41:40	11:49:00	--	10:39:50	11:32:10	11:54:30
	Test #1 2-6-98	2/6/98	4.88-5.18	9:30:00	14:50:42	14:53:00	14:56:40	--	10:43:15	--	--
	Test #2 1-13-98	1/13/98	5.49-5.79	13:05:00	14:12:45	14:17:45	14:28:45	--	13:14	--	--
	Test #2 2-10-98	2/10/98	5.49-5.79	10:05:00	10:22:20	10:22:40	10:30:39	10:22:05	10:08:50	10:16:12	10:22:45
	Test #2 1-14-98	1/14/98	6.10-6.40	13:10:00	14:38:19	14:40:00	14:49:00	--	13:26:00	13:48:00	15:00:52
	Test #1 2-4-98	2/4/98	6.10-6.40	9:21:00	14:18:00	14:21:00	14:30:15	--	10:23:35	11:13:04	14:39:36
	Test #1 1-13-98	1/13/98	6.71-7.01	10:35:04	12:01:32	12:03:18	12:10:00	--	10:42:00	10:50:56	12:05:13
	Test #1 2-3-98	2/3/98	6.71-7.01	11:39:00	14:26:56	14:28:00	14:33:38	--	11:49:26	12:20:15	14:33:58
	Test #1 3-5-98	3/5/98	6.71-7.01	3/5/98 13:03	3/6/98 10:23	3/6/98 10:28	3/6/98 10:36	--	3/5/98 14:17	NO	3/6/98 11:01
	Test #1 3-12-98	3/12/98	7.62-7.92	3/12/98 12:55	3/13/98 10:11	3/13/98 10:16	3/13/98 10:28	--	NO	--	--

-- The event did not occur.

NO - Not Observed. The event occurred when field personnel were not present to observe and record the time of the event.

NR - Not Recorded. The time that the event occurred was not recorded.

Table 2.6 - 1 of 2

Duration of Post-Excavation Seepage-Test Events

Niche 3650

Exploratory Study Facility

Lawrence Berkeley National Laboratory

Borehole	Test Name	Date	Depth (m)	Pumping Time (hr:min:s)	Standby Time (hr:min:s)	Recovery Time (hr:min:s)	Dripping Duration (hr:min:s)
UL	Test #1 12-11-97	12/11/97	5.18-5.49	1:27:38	0:02:32	0:02:28	–
	Test #1 2-12-98	2/12/98	5.18-5.49	20:27:00	0:04:30	0:15:30	–
	Test #2 12-11-97	12/11/97	5.79-6.10	0:31:43	0:02:06	0:02:43	–
	Test #3 12-11-97	12/11/97	6.40-6.71	0:33:13	0:02:00	0:05:10	–
	Test #1 12-10-97	12/10/97	7.01-7.32	0:08:35	0:02:00	0:03:10	0:05:43
	Test #1 1/6/98	1/6/98	7.01-7.32	1:28:04	0:02:01	0:05:48	–
	Test #2 1-6-98	1/6/98	7.62-7.92	0:33:45	0:01:15	0:02:15	0:50:40
	Test #1 2-12-98	2/12/98	7.62-7.92	2:51:06	0:00:54	0:07:03	2:20:55
	Test #1 3-4-98	3/4/98	7.62-7.92	23:06:00	0:05:00	0:06:40	NO
UM	Test 5 Niche 3650	11/13/97	4.27-4.57	0:08:27	0:03:00	0:03:03	0:33:50
	Test #1 12-3-97	12/3/97	4.27-4.57	0:33:52	0:03:11	0:02:45	0:43:05
	Test #2 12-3-97	12/3/97	4.27-4.57	0:33:47	0:02:05	0:02:26	0:45:10
	Test #1 1-7-98	1/7/98	4.27-4.57	5:59:06	0:04:10	0:05:25	1:49:52
	Test #2 2-10-98	2/10/98	4.27-4.57	19:36:00	0:04:00	0:07:56	–
	Test 1 Niche 3650	11/12/97	4.88-5.18	0:06:04	0:03:50	0:03:05	NR
	Test #1 12-4-97	12/4/97	4.88-5.18	0:34:35	0:02:00	0:02:45	0:21:42
	Test #2 12-5-97	12/5/97	4.88-5.18	2:02:38	0:02:00	0:02:41	1:33:15
	Test #1 1-8-98	1/8/98	4.88-5.18	6:15:30	0:03:00	0:08:54	–
	Test #1 3-6-98	3/6/98	4.88-5.18	117:34:00	0:04:00	0:07:30	–
	Test 4 Niche 3650	11/13/97	5.49-5.79	0:08:13	0:02:45	0:02:55	0:17:38
	Test #2 12-4-97	12/4/97	5.49-5.79	0:34:29	0:02:00	0:02:39	0:33:12
	Test #1 1-9-98	1/9/98	5.49-5.79	4:59:40	0:03:08	0:04:43	2:06:34
	Test #1 2-11-98	2/11/98	5.49-5.79	21:16:18	0:03:42	0:08:05	–
	Test 3 Niche 3650	11/13/97	6.10-6.40	0:32:25	0:04:05	0:04:31	–
	Test #3 12-4-97	12/4/97	6.10-6.40	1:26:55	0:08:23	0:01:40	–
	Test #1 1-12-98	1/12/98	6.10-6.40	0:21:09	0:09:59	0:05:07	–
	Test 2 Niche 3650	11/12/97	6.71-7.01	0:08:19	0:02:42	0:04:28	–
	Test #1 12-5-97	12/5/97	6.71-7.01	1:22:35	0:02:00	0:02:46	–

– The event did not occur.

NO - Not Observed. The event occurred when field personnel were not present to observe/record the time of the event.

NR - Not Recorded. The time that the event occurred was not recorded.

Table 2.6 - 2 of 2

Duration of Post-Excavation Seepage-Test Events

Niche 3650

Exploratory Study Facility

Lawrence Berkeley National Laboratory

Borehole	Test Name	Date	Depth (m)	Pumping Time (hr:min:s)	Standby Time (hr:min:s)	Recovery Time (hr:min:s)	Dripping Duration (hr:min:s)
UR	Test #1 1-14-98	1/14/98	4.27-4.57	1:24:53	0:01:55	0:09:35	0:23:08
	Test #1 2-5-98	2/5/98	4.27-4.57	5:04:46	0:03:17	0:06:57	--
	Test #1 1-15-98	1/15/98	4.88-5.18	1:29:40	0:02:00	0:07:20	0:22:20
	Test #1 2-6-98	2/6/98	4.88-5.18	5:20:42	0:02:18	0:03:40	--
	Test #2 1-13-98	1/13/98	5.49-5.79	1:07:45	0:05:00	0:11:00	--
	Test #2 2-10-98	2/10/98	5.49-5.79	0:17:20	0:00:20	0:07:59	0:06:33
	Test #2 1-14-98	1/14/98	6.10-6.40	1:28:19	0:01:41	0:09:00	1:12:52
	Test #1 2-4-98	2/4/98	6.10-6.40	4:57:00	0:03:00	0:09:15	3:26:32
	Test #1 1-13-98	1/13/98	6.71-7.01	1:26:28	0:01:46	0:06:42	1:14:17
	Test #1 2-3-98	2/3/98	6.71-7.01	2:47:56	0:01:04	0:05:38	2:13:43
	Test #1 3-5-98	3/5/98	6.71-7.01	21:20:37	0:04:20	0:08:30	--
	Test #1 3-12-98	3/12/98	7.62-7.92	21:16:45	0:04:15	0:12:20	--

-- The event did not occur.

NO - Not Observed. The event occurred when field personnel were not present to observe/record the time of the event.

NR - Not Recorded. The time that the event occurred was not recorded.

Summary of Seepage Test Observations

Niche 3650

Exploratory Study Facility

Lawrence Berkeley National Laboratory

Borehole	Test Name	Date	Depth (m)	Water Appeared?	Water Dripped?	Comments
UL	Test #1 12-11-97	12/11/97	5.18-5.49	No	No	
	Test #1 2-12-98	2/12/98	5.18-5.49	No	No	
	Test #2 12-11-97	12/11/97	5.79-6.10	No	No	
	Test #3 12-11-97	12/11/97	6.40-6.71	No	No	
	Test #1 12-10-97	12/10/97	7.01-7.32	Yes	Yes	
	Test #1 1-6-98	1/6/98	7.01-7.32	Yes	No	Water appeared at different location than previous test.
	Test #2 1-6-98	1/6/98	7.62-7.92	Yes	Yes	Water still dripping at 15:26 when field personnel had to leave during shift change.
	Test #1 2-12-98	2/12/98	7.62-7.92	Yes	Yes	
	Test #1 3-4-98	3/4/98	7.62-7.92	Yes	Yes	

Summary of Seepage Test Observations

Niche 3650

Exploratory Study Facility

Lawrence Berkeley National Laboratory

Borehole	Test Name	Date	Depth (m)	Water Appeared?	Water Dripped?	Comments
UM	Test 5 Niche 3650	11/13/97	4.27-4.57	Yes	Yes	
	Test #1 12-3-97	12/3/97	4.27-4.57	Yes	Yes	
	Test #2 12-3-97	12/3/97	4.27-4.57	Yes	Yes	This test was conducted 2 hrs. after ending Test #1 12-3-97 and showed a memory effect.
	Test #1 1-7-98	1/7/98	4.27-4.57	Yes	Yes	
	Test #2 2-10-98	2/10/98	4.27-4.57	Yes	No	Arrival time determined from video log (+/- 5 min.)
	Test 1 Niche 3650	11/12/97	4.88-5.18	Yes	Yes	
	Test #1 12-4-97	12/4/97	4.88-5.18	Yes	Yes	
	Test #2 12-5-97	12/5/97	4.88-5.18	Yes	Yes	Time of last drip estimated. This test showed a memory effect from Test #1 12-4-97.
	Test #1 1-8-98	1/8/98	4.88-5.18	Yes	No	
	Test #1 3-6-98	3/6/98	4.88-5.18	Yes	No	Arrival time determined from video log (+/- 4 min.5 sec.)
	Test 4 Niche 3650	11/13/97	5.49-5.79	Yes	Yes	Water observed moving up fracture intersecting breakout
	Test #2 12-4-97	12/4/97	5.49-5.79	Yes	Yes	Water observed moving up fracture intersecting breakout
	Test #1 1-9-98	1/9/98	5.49-5.79	Yes	Yes	
	Test #1 2-11-98	2/11/98	5.49-5.79	Yes	No	
	Test 3 Niche 3650	11/13/97	6.10-6.40	Yes	No	
	Test #3 12-4-97	12/4/97	6.10-6.40	Yes	No	Extra 331.2 g of water accidentally pumped into hole during recovery.
	Test #1 1-12-98	1/12/98	6.10-6.40	Yes	No	Evaporation cover was resting on draw pipe causing erroneous weight readings in output file toward end of test. Problem was corrected and end test mass is correct in scientific notebook.
	Test 2 Niche 3650	11/12/97	6.71-7.01	No	No	
	Test #1 12-5-97	12/5/97	6.71-7.01	Yes	No	

Summary of Seepage Test Observations

Niche 3650

Exploratory Study Facility

Lawrence Berkeley National Laboratory

Borehole	Test Name	Date	Depth (m)	Water Appeared?	Water Dripped?	Comments
UR	Test #1 1-14-98	1/14/98	4.27-4.57	Yes	Yes	
	Test #1 2-5-98	2/5/98	4.27-4.57	Yes	No	Wetting front showed up at two separate locations.
	Test #1 1-15-98	1/15/98	4.88-5.18	Yes	Yes	Several fine fractures conducting water
	Test #1 2-6-98	2/6/98	4.88-5.18	Yes	No	Wetting front difficult to see (low saturation) when it first arrived at niche ceiling.
	Test #2 1-13-98	1/13/98	5.49-5.79	Yes	No	Electronic balance acting strange during initial stage of test, but problem corrected.
	Test #2 2-10-98	2/10/98	5.49-5.79	Yes	Yes	Water washed dust and small rock chips into capture system when front arrvied.
	Test #2 1-14-98	1/14/98	6.10-6.40	Yes	Yes	Wetting front moved up small fracture intersecting breakout.
	Test #1 2-4-98	2/4/98	6.10-6.40	Yes	Yes	
	Test #1 1-13-98	1/13/98	6.71-7.01	Yes	Yes	Collected water/seepage samples.
	Test #1 2-3-98	2/3/98	6.71-7.01	Yes	Yes	
	Test #1 3-5-98	3/5/98	6.71-7.01	Yes	Yes	
	Test #1 3-12-98	3/12/98	7.62-7.92	Yes	No	

Computation of Pumped Mass: Post-Excavation Seepage Tests

Niche 3650

Exploratory Study Facility

Lawrence Berkeley National Laboratory

Borehole	Test Name	Date	Depth (m)	Mass of Water At: Start of Test (g)	Start of Release (g)	End of Release (g)	End of Recovery (g)	Return Mass (g)	Pumped Mass from Start Test & End Release Data (g)	Pumped Mass From Start & End Release Data (g)
UL	Test #1 12-11-97	12/11/97	5.18-5.49	1463.6	1213.2	213.4	456.4	586.1	1250.2	999.8
	Test #1 2-12-98	2/12/98	5.18-5.49	1437.5	1178.7	177.7	900.2	0.0	1259.8	1001.0
	Test #2 12-11-97	12/11/97	5.79-6.10	1307.8	1054.5	50.5	303.8	611.7	1257.3	1004.0
	Test #3 12-11-97	12/11/97	6.40-6.71	1368.8	1100.0	100.2	364.5	578.7	1268.6	999.8
	Test #1 12-10-97	12/10/97	7.01-7.32	2030.0	1754.9	751.3	1012.5	0.0	1278.7	1003.6
	Test #1 1-6-98	1/6/98	7.01-7.32	1997.8	1726.8	723.6	991.6	0.0	1274.2	1003.2
	Test #2 1-6-98	1/6/98	7.62-7.92	1997.9	1716.3	689.4	958.0	0.0	1308.5	1026.9
	Test #1 2-12-98	2/12/98	7.62-7.92	2118.9	1835.6	800.7	1081.8	0.0	1318.2	1034.9
	Test #1 3-4-98	3/4/98	7.62-7.92	2046.9	1761.4	726.5	1003.4	0.0	1320.4	1034.9
UM	Test 5 Niche 3650	11/13/97	4.27-4.57	1313.7	1070.1	46.3	299.6	0.0	1267.4	1023.8
	Test #1 12-3-97	12/3/97	4.27-4.57	2072.4	1821.0	798.0	1045.2	0.0	1274.4	1023.0
	Test #2 12-3-97	12/3/97	4.27-4.57	2003.1	1757.0	731.9	978.1	0.0	1271.2	1025.1
	Test #1 1-7-98	1/7/98	4.27-4.57	1972.6	1725.6	709.7	964.4	0.0	1262.9	1015.9
	Test #2 2-10-98	2/10/98	4.27-4.57	1929.0	1670.4	507.0	761.1	0.0	1422.0	1163.4
Column				(a)	(b)	(c)	(d)	(e)	(f) = (a) - (c)	(g) = (b) - (c)

Refer to the end of table for footnotes.

Computation of Pumped Mass: Post-Excavation Seepage Tests

Niche 3650

Exploratory Study Facility

Lawrence Berkeley National Laboratory

Borehole	Test Name	Date	Depth (m)	Mass of Water At: Start of Test (g)	Start of Release (g)	End of Release (g)	End of Recovery (g)	Return Mass (g)	Pumped Mass from Start Test & End Release Data (g)	Pumped Mass From Start & End Release Data (g)
UM	Test 1 Niche 3650	11/12/97	4.88-5.18	1997.5	1750.7	698.0	945.7	0.0	1299.5	1052.7
	Test #1 12-4-97	12/4/97	4.88-5.18	2002.7	1743.6	691.7	943.9	0.0	1311.0	1051.9
	Test #2 12-5-97	12/5/97	4.88-5.18	2001.9	1746.8	686.2	940.1	0.0	1315.7	1060.6
	Test #1 1-8-98	1/8/98	4.88-5.18	2034.1	1776.7	721.7	989.9	0.0	1312.4	1055.0
	Test #1 3-6-98	3/6/98	4.88-5.18	7380.0	7113.3	1516.1	1776.7	0.0	5863.9	5597.2
	Test 4 Niche 3650	11/13/97	5.49-5.79	1288.0	1024.8	5.0	243.7	0.0	1283.0	1019.8
	Test #2 12-4-97	12/4/97	5.49-5.79	2004.7	1744.2	701.4	962.2	0.0	1303.3	1042.8
	Test #1 1-9-98	1/9/98	5.49-5.79	2016.4	1747.0	704.2	977.7	0.0	1312.2	1042.8
	Test #1 2-11-98	2/11/98	5.49-5.79	1993.0	1723.7	681.7	949.3	0.0	1311.3	1042.0
	Test 3 Niche 3650	11/13/97	6.10-6.40	1278.8	1005.1	5.3	274.4	0.0	1273.5	999.8
	Test #3 12-4-97	12/4/97	6.10-6.40	2012.2	1750.0	749.6	590.3	0.0	1262.6	1000.4
	Test #1 1-12-98	1/12/98	6.10-6.40	2020.6	1740.0	735.3	664.8	0.0	1285.3	1004.7
	Test 2 Niche 3650	11/12/97	6.71-7.01	1312.5	1038.3	78.0	350.5	676.9	1234.5	960.3
	Test #1 12-5-97	12/5/97	6.71-7.01	2000.6	1729.7	729.2	997.6	0.0	1271.4	1000.5
Column				(a)	(b)	(c)	(d)	(e)	(f) = (a) - (c)	(g) = (b) - (c)

Refer to the end of table for footnotes.

Computation of Pumped Mass: Post-Excavation Seepage Tests

Niche 3650

Exploratory Study Facility

Lawrence Berkeley National Laboratory

Borehole	Test Name	Date	Depth (m)	Mass of Water At: Start of Test (g)	Start of Release (g)	End of Release (g)	End of Recovery (g)	Return Mass (g)	Pumped Mass from Start Test & End Release Data (g)	Pumped Mass From Start & End Release Data (g)
UR	Test #1 1-14-98	1/14/98	4.27-4.57	2188.8	1944.6	934.4	1190.1	0.0	1254.4	1010.2
	Test #1 2-5-98	2/5/98	4.27-4.57	2005.7	1753.2	743.2	1002.7	0.0	1262.5	1010.0
	Test #1 1-15-98	1/15/98	4.88-5.18	1302.7	1040.3	19.9	285.8	0.0	1282.8	1020.4
	Test #1 2-6-98	2/6/98	4.88-5.18	2066.9	1807.3	787.0	1047.8	0.0	1279.9	1020.3
	Test #2 1-13-98	1/13/98	5.49-5.79	2003.9	1769.5	751.1	1099.6	0.0	1252.8	1018.4
	Test #2 2-10-98	2/10/98	5.49-5.79	2016.0	1754.2	733.8	1007.2	631.0	1282.2	1020.4
	Test #2 1-14-98	1/14/98	6.10-6.40	1300.8	1025.4	10.6	287.2	0.0	1290.2	1014.8
	Test #1 2-4-98	2/4/98	6.10-6.40	2011.5	1736.6	719.3	992.8	0.0	1292.2	1017.3
	Test #1 1-13-98	1/13/98	6.71-7.01	1993.6	1719.4	700.2	983.4	0.0	1293.4	1019.2
	Test #1 2-3-98	2/3/98	6.71-7.01	2009.9	1728.0	699.9	979.5	0.0	1310.0	1028.1
	Test #1 3-5-98	3/5/98	6.71-7.01	1312.5	1029.4	9.4	291.4	0.0	1303.1	1020.0
	Test #1 3-12-98	3/12/98	7.62-7.92	1779.8	1238.6	218.0	1110.5	0.0	1561.8	1020.6
Column				(a)	(b)	(c)	(d)	(e)	(f) = (a) - (c)	(g) = (b) - (c)

Refer to end of table for footnotes

Computation of Pumped Mass: Post-Excavation Seepage Tests

Niche 3650

Exploratory Study Facility

Lawrence Berkeley National Laboratory

Borehole	Test Name	Date	Depth (m)	Mass of Water At: Start of Test (g) [1]	Start of Release (g) [2]	End of Release (g) [3]	End of Recovery (g) [4]	Return Mass (g) [5]	Pumped Mass from Start Test & End Release Data (g) [6]	Pumped Mass From Start & End Release Data (g) [7]
Column No.				(a)	(b)	(c)	(d)	(e)	(f) = (a) - (c)	(g) = (b) - (c)

Footnotes:

[1] Mass of water on injection scale prior to pumping.

[2] Mass of water after filling injection line and prior to injection into the test interval.

[3] Mass of water remaining after liquid release ended but before recovery began.

[4] Mass of water remaining after recovery ended.

[5] Return mass is the amount of water that flowed out of the return line back to the surface during the test.

[6] This value represents the mass of water pumped into the injection line and test interval and, therefore, includes injection line storage.

[7] This value represents the mass of water pumped into the test interval plus it may contain a small component of injection line storage.

Computation of Released Mass: Post-Excavation Seepage Tests

Niche 3650

Exploratory Study Facility

Lawrence Berkeley National Laboratory

Borehole	Test Name	Date	Depth (m)	Pre-Test Line Storage from Start Test/ Start Release Data (g)	Pre-Test Line Storage Deficit (-)/ Surplus (+) (g)	Recovered Mass, End Release/ End Recovery Data (g)	Post-Test Line Storage Deficit (-)/ Surplus (+) (g)	Mass Released From Start Test & End Recovery Data (g)	Mass Released from Start & End Release Data (g)	Actual Line Storage (g)
UL	Test #1 12-11-97	12/11/97	5.18-5.49	250.4	-8.3	243	-15.7	405.4	405.4	
	Test #1 2-12-98	2/12/98	5.18-5.49	258.8	0.1	722.5	463.8	537.3	537.3	258.7
	Test #2 12-11-97	12/11/97	5.79-6.10	253.3	-13.1	253.3	-13.1	379.2	379.2	266.4
	Test #3 12-11-97	12/11/97	6.40-6.71	268.8	-0.8	264.3	-5.3	420.3	420.3	269.6
	Test #1 12-10-97	12/10/97	7.01-7.32	275.1	1.9	261.2	-12	1005.5	1005.5	
	Test #1 1-6-98	1/6/98	7.01-7.32	271	-2.2	268	-5.2	1001	1001	273.2
	Test #2 1-6-98	1/6/98	7.62-7.92	281.6	-1.5	268.6	-14.5	1025.4	1025.4	
	Test #1 2-12-98	2/12/98	7.62-7.92	283.3	0.2	281.1	-2	1035.1	1035.1	283.1
	Test #1 3-4-98	3/4/98	7.62-7.92	285.5	2.4	276.9	-6.2	1037.3	1037.3	
UM	Test 5 Niche 3650	11/13/97	4.27-4.57	243.6	-15.1	253.3	-5.4	1008.7	1008.7	
	Test #1 12-3-97	12/3/97	4.27-4.57	251.4	-7.3	247.2	-11.5	1015.7	1015.7	
	Test #2 12-3-97	12/3/97	4.27-4.57	246.1	-12.6	246.2	-12.5	1012.5	1012.5	
	Test #1 1-7-98	1/7/98	4.27-4.57	247	-11.7	254.7	-4	1004.2	1004.2	
	Test #2 2-10-98	2/10/98	4.27-4.57	258.6	-0.1	254.1	-4.6	1163.3	1163.3	258.7
Column				(h) = (a) - (b)	(i) = (h) - (n)	(j) = (d) - (c)	(k) = (j) - (n)	(l)	(m)	(n)

Refer to the end of the table for footnotes.

Computation of Released Mass: Post-Excavation Seepage Tests

Niche 3650

Exploratory Study Facility

Lawrence Berkeley National Laboratory

Borehole	Test Name	Date	Depth (m)	Pre-Test Line Storage from Start Test/ Start Release Data (g)	Pre-Test Line Storage Deficit (-)/ Surplus (+) (g)	Recovered Mass, End Release/ End Recovery Data (g)	Post-Test Line Storage Deficit (-)/ Surplus (+) (g)	Mass Released From Start Test & End Recovery Data (g)	Mass Released from Start & End Release Data (g)	Actual Line Storage (g)
UM	Test 1 Niche 3650	11/12/97	4.88-5.18	246.8	-19.6	247.7	-18.7	1033.1	1033.1	
	Test #1 12-4-97	12/4/97	4.88-5.18	259.1	-7.3	252.2	-14.2	1044.6	1044.6	
	Test #2 12-5-97	12/5/97	4.88-5.18	255.1	-11.3	253.9	-12.5	1049.3	1049.3	
	Test #1 1-8-98	1/8/98	4.88-5.18	257.4	-9	268.2	1.8	1044.2	1044.2	266.4
	Test #1 3-6-98	3/6/98	4.88-5.18	266.7	0.3	260.6	-5.8	5597.5	5597.5	
	Test 4 Niche 3650	11/13/97	5.49-5.79	263.2	-6.4	238.7	-30.9	1013.4	1013.4	
	Test #2 12-4-97	12/4/97	5.49-5.79	260.5	-9.1	260.8	-8.8	1033.7	1033.7	
	Test #1 1-9-98	1/9/98	5.49-5.79	269.4	-0.2	273.5	3.9	1038.7	1038.7	
	Test #1 2-11-98	2/11/98	5.49-5.79	269.3	-0.3	267.6	-2	1041.7	1041.7	269.6
	Test 3 Niche 3650	11/13/97	6.10-6.40	273.7	0.5	269.1	-4.1	1000.3	1000.3	
	Test #3 12-4-97	12/4/97	6.10-6.40	262.2	-11	-159.3	-101.3	989.4 *	989.4	
	Test #1 1-12-98	1/12/98	6.10-6.40	280.6	7.4	-70.5	-343.7	1012.1	1012.1	273.2
	Test 2 Niche 3650	11/12/97	6.71-7.01	274.2	-8.9	272.5	-10.6	274.5	274.5	
	Test #1 12-5-97	12/5/97	6.71-7.01	270.9	-12.2	268.4	-14.7	988.3	988.3	283.1
Column				(h) = (a) - (b)	(i) = (h) - (n)	(j) = (d) - (c)	(k) = (j) - (n)	(l)	(m)	(n)

Refer to the end of the table for footnotes.

* 331.2 g of water was accidentally injected into the test interval during the recovery stage of Test #3 12-4-97. The injected mass reported here represents the amount of water introduced during injection and does not include the 331.2 g of water introduced during recovery.

Computation of Released Mass: Post-Excavation Seepage Tests

Niche 3650

Exploratory Study Facility

Lawrence Berkeley National Laboratory

Borehole	Test Name	Date	Depth (m)	Pre-Test Line Storage from Start Test/ Start Release Data (g)	Pre-Test Line Storage Deficit (-)/ Surplus (+) (g)	Recovered Mass, End Release/ End Recovery Data (g)	Post-Test Line Storage Deficit (-)/ Surplus (+) (g)	Mass Released From Start Test & End Recovery Data (g)	Mass Released from Start & End Release Data (g)	Actual Line Storage (g)
UR	Test #1 1-14-98	1/14/98	4.27-4.57	244.2	-14.5	255.7	-3	995.7	995.7	
	Test #1 2-5-98	2/5/98	4.27-4.57	252.5	-6.2	259.5	0.8	1003	1003	258.7
	Test #1 1-15-98	1/15/98	4.88-5.18	262.4	-4	265.9	-0.5	1016.4	1016.4	
	Test #1 2-6-98	35832	4.88-5.18	259.6	-6.8	260.8	-5.6	1013.5	1013.5	266.4
	Test #2 1-13-98	35808	5.49-5.79	234.4	-35.2	348.5	78.9	904.3	904.3	
	Test #2 2-10-98	2/10/98	5.49-5.79	261.8	-7.8	273.4	3.8	377.8	377.8	269.6
	Test #2 1-14-98	35809	6.10-6.40	275.4	2.2	276.6	3.4	1013.6	1013.6	
	Test #1 2-4-98	2/4/98	6.10-6.40	274.9	1.7	273.5	0.3	1018.7	1018.7	273.2
	Test #1 1-13-98	1/13/98	6.71-7.01	274.2	-8.9	283.2	0.1	1010.2	1010.2	
	Test #1 2-3-98	2/3/98	6.71-7.01	281.9	-1.2	279.6	-3.5	1026.9	1026.9	283.1
	Test #1 3-5-98	3/5/98	6.71-7.01	283.1	0	282	-1.1	1020	1020	
	Test #1 3-12-98	3/12/98	7.62-7.92	541.2	1.8	892.5	353.1	669.3	669.3	539.4
Column				(h) = (a) - (b)	(i) = (h) - (n)	(j) = (d) - (c)	(k) = (j) - (n)	(l)	(m)	(n)

Refer to the end of the table for footnotes.

Computation of Released Mass: Post-Excavation Seepage Tests

Niche 3650

Exploratory Study Facility

Lawrence Berkeley National Laboratory

Borehole	Test Name	Date	Depth (m)	Pre-Test Line Storage from Start Test/ Start Release Data (g) [1]	Pre-Test Line Storage Deficit (-)/ Surplus (+) (g) [2]	Recovered Mass, End Release/ End Recovery Data (g) [3]	Post-Test Line Storage Deficit (-)/ Surplus (+) (g) [4]	Mass Released From Start Test & End Recovery Data (g) [5]	Mass Released from Start & End Release Data (g) [6]	Actual Line Storage (g) [7]
Column				(h) = (a) - (b)	(i) = (h) - (n)	(j) = (d) - (c)	(k) = (j) - (n)	(l)	(m)	(n)

Columns (a) through (g) refer to items listed on Table 2.8. Columns (h) through (n) are summarized in this table.

[1] Pre-test line storage is the amount of liquid pumped into the injection line prior to releasing liquid into the test interval.

[2] Pre-Test Line Storage Deficit (-)/Surplus(+) = A negative (-) value or deficit indicates that the injection line was underfilled by the stated amount prior to release and a surplus (+) indicates the injection line was overfilled slightly prior to release.

[3] The recovered mass represents the amount of liquid pumped back from the injection line and the test interval after the release ended.

[4] Post-Test Line Storage Deficit (-)/Surplus(+) = A negative (-) value or deficit indicates that the injection line still contained a small amount of residual fluid after being purged at the end of the test. A positive (+) value or surplus indicates that the amount of liquid recovered exceeded the storage capacity of the injection line and, therefore, additional liquid must have been recovered from the test interval (i.e., test interval storage).

The mass of liquid injected into the rock (columns (l) and (m)) may be computed using the start test/end recovery data or the start/end release data as follows:

[5] - If there is a Post-Test Line Storage deficit (-), then the amount of liquid recovered is less than the actual line storage (n) indicating that residual liquid could not be completely removed from the injection line. The amount of liquid released into the rock is calculated as follows: (l) = pumped mass (f) minus the returned mass (e) - (j) + (k), where (j) - (k) is equal to the actual line storage (n).

- If there is a Post-Test Line Storage surplus (+), then the amount of liquid recovered exceeded the actual line storage and the excess liquid must have been recovered from the test interval. The amount of liquid released into the rock is calculated as follows: (l) = (f) - (e) - (j).

[6] - If there is a Post-Test Line Storage deficit (-), then it is assumed that all the liquid pumped back after injecting was recovered from line storage. The mass of liquid released into the rock equals (m) = (g) - (e) + (I) and is not effected by the post-test line storage.

- If there is a Post-Test Line Storage surplus (+), then fluid was pumped back from the test interval during recovery. The surplus must be subtracted from the pumped mass to compute the released mass as follows: (m) = (g) - (e) + (I) - (h).

[7] The Actual Line Storage was measured independently of the tests by measuring the mass of water required to fill the injection line.

Table 2.10 - 1 of 3

Rate and Time Summary: Post-Excavation Seepage Tests

Niche 3650

Exploratory Study Facility

Lawrence Berkeley National Laboratory

Borehole	Test Name	Date	Depth (m)	Pumping Rate g/s	Pumping Time (min)	Liquid Release Rate g/s	Release Time (min)	Standby Time (min)	Recovery Rate g/s	Recovery Time (min)
UL	Test #1 12-11-97	12/11/97	5.18-5.49	0.190	87.63	0.078	86.91	2.53	1.642	2.47
	Test #2 2-12-98	2/12/98	5.18-5.49	0.014	1227.00	0.007	1227.12	4.50	0.777	15.50
	Test #2 12-11-97	12/11/97	5.79-6.10	0.528	31.72	0.202	31.30	2.10	1.554	2.72
	Test #3 12-11-97	12/11/97	6.40-6.71	0.502	33.22	0.211	33.19	2.00	0.853	5.17
	Test #1 12-10-97	12/10/97	7.01-7.32	1.949	8.58	1.949	8.60	2.00	1.375	3.17
	Test #1 1-6-98	1/6/98	7.01-7.32	0.190	88.07	0.190	87.87	2.02	0.770	5.80
	Test #2 1-6-98	1/6/98	7.62-7.92	0.507	33.75	0.507	33.70	1.25	1.990	2.25
	Test #1 2-12-98	2/12/98	7.62-7.92	0.101	171.10	0.101	171.13	0.90	0.665	7.05
	Test #1 3-4-98	3/4/98	7.62-7.92	0.012	1386.00	0.012	1389.21	5.00	0.692	6.67

Rate and Time Summary: Post-Excavation Seepage Tests

Niche 3650
Exploratory Study Facility

Lawrence Berkeley National Laboratory

Borehole	Test Name	Date	Depth (m)	Pumping Rate g/s	Pumping Time (min)	Liquid Release Rate g/s	Release Time (min)	Standby Time (min)	Recovery Rate g/s	Recovery Time (min)
UM	Test 5 Niche 3650	11/13/97	4.27-4.57	2.019	8.45	2.019	8.33	3.00	1.384	3.05
	Test #1 12-3-97	12/3/97	4.27-4.57	0.503	33.87	0.503	33.62	3.18	1.498	2.75
	Test #2 12-3-97	12/3/97	4.27-4.57	0.506	33.78	0.506	33.37	2.08	1.686	2.43
	Test #1 1-7-98	1/7/98	4.27-4.57	0.047	359.1	0.047	354.96	4.17	0.784	5.42
	Test #2 2-10-98	2/10/98	4.27-4.57	0.016	1176.0	0.016	1175.9	4.00	0.534	7.93
	Test 1 Niche 3650	11/12/97	4.88-5.18	2.892	6.07	2.892	5.95	3.83	1.339	3.08
	Test #1 12-4-97	12/4/97	4.88-5.18	0.507	34.58	0.507	34.34	2.00	1.528	2.75
	Test #2 12-5-97	12/5/97	4.88-5.18	0.144	122.63	0.144	121.33	2.00	1.577	2.68
	Test #1 1-8-98	1/8/98	4.88-5.18	0.047	375.50	0.047	372.30	3.00	0.502	8.90
	Test #1 3-6-98	3/6/98	4.88-5.18	0.013	7054.0	0.013	7054.38	4.00	0.579	7.50
	Test 4 Niche 3650	11/13/97	5.49-5.79	2.069	8.22	2.069	8.17	2.75	1.364	2.92
	Test #2 12-4-97	12/4/97	5.49-5.79	0.504	34.48	0.504	34.18	2.00	1.640	2.65
	Test #1 1-9-98	1/9/98	5.49-5.79	0.058	299.67	0.058	299.61	3.13	0.966	4.72
	Test #1 2-11-98	2/11/98	5.49-5.79	0.014	1276.3	0.014	1275.93	3.70	0.552	8.08
	Test 3 Niche 3650	11/13/97	6.10-6.40	0.514	32.42	0.514	32.43	4.08	0.993	4.52
	Test #3 12-4-97	12/4/97	6.10-6.40	0.192	86.92	0.192	85.96	8.38	-1.593	1.67
	Test #1 1-12-98	1/12/98	6.10-6.40	0.792	21.15	0.792	21.31	9.98	-0.230	5.12
	Test 2 Niche 3650	11/12/97	6.71-7.01	1.924	8.32	0.555	8.24	2.70	1.017	4.47
	Test #1 12-5-97	12/5/97	6.71-7.01	0.202	82.58	0.202	81.58	2.00	1.617	2.77

Rate and Time Summary: Post-Excavation Seepage Tests

Niche 3650

Exploratory Study Facility

Lawrence Berkeley National Laboratory

Borehole	Test Name	Date	Depth (m)	Pumping Rate g/s	Pumping Time (min)	Liquid Release Rate g/s	Release Time (min)	Standby Time (min)	Recovery Rate g/s	Recovery Time (min)
UR	Test #1 1-14-98	1/14/98	4.27-4.57	0.198	84.88	0.198	83.66	1.92	0.445	9.58
	Test #1 2-5-98	2/5/98	4.27-4.57	0.055	304.77	0.055	302.90	3.28	0.622	6.95
	Test #1 1-15-98	1/15/98	4.88-5.18	0.190	89.67	0.190	89.32	2.00	0.604	7.33
	Test #1 2-6-98	2/6/98	4.88-5.18	0.053	320.70	0.053	318.56	2.30	1.185	3.67
	Test #2 1-13-98	1/13/98	5.49-5.79	0.251	67.75	0.230	65.41	5.00	0.528	11.00
	Test #2 2-10-98	2/10/98	5.49-5.79	0.981	17.33	0.366	17.20	0.33	0.571	7.98
	Test #2 1-14-98	1/14/98	6.10-6.40	0.192	88.32	0.191	88.51	1.68	0.512	9.00
	Test #1 2-4-98	2/4/98	6.10-6.40	0.057	297.00	0.057	297.50	3.00	0.493	9.25
	Test #1 1-13-98	1/13/98	6.71-7.01	0.196	86.47	0.196	85.71	1.77	0.704	6.70
	Test #1 2-3-98	2/3/98	6.71-7.01	0.102	167.93	0.102	167.74	1.07	0.827	5.63
	Test #1 3-5-98	3/5/98	6.71-7.01	0.013	1280.62	0.013	1280.62	4.33	0.553	8.50
	Test #1 3-12-98	3/12/98	7.62-7.92	0.013	1276.75	0.009	1274.50	4.25	1.206	12.33

Table 2.11

Observed Extent of Dyes at Niche 3566 During Excavation

Yucca Mountain Project

Exploratory Study Facility

Lawrence Berkeley National Laboratory

Observed Dye	Borehole	Date	Start Time Release	Test[1] Interval (m)	Mass Released (g)	Release[2] Time (min)	Date of Mine Out	Time of Mine Out	Mined[3] Depth (m)	Maximum Observed Distribution of Dye		
										Penetration Depth (m)[4]	Lateral Extent[5]	
											South (m)	North (m)
FD&C Red No. 40	M	6/4/97	17:59	2.13 - 2.44	941.7	13.25	6/23/97	17:11	2.24	1.52	0.33	0.15
							6/23/97	21:26	2.85	1.35	0.5	0.24
							6/23/97	23:14	3.1	0.47	0.23	0.31
Acid Yellow 7	M	6/4/97	17:10	2.77 - 3.05	120.3	9.57	6/23/97	23:14	3.1	0.3	0.13	0.15
FD&C Blue No. 1	M	6/3/97	21:01	4.57 - 4.88	474	11.48	6/24/97	NA	4.65	1.3	0.3	0.05
							6/24/97	12:00	4.98	1.27	0.23	0.23

[1] Depth measurement is from the collar of the boring to the test interval.

[2] Release time represents the total time it took to inject, standby, and recover the fluid (excluding line storage).

[3] Depth in meters measured along the center line of the Niche from the niche opening to the working face.

[4] Penetration Depth equals the vertical distance in meters from the test interval to the observed dye location.

[5] The reference point for this measurement is the center line of the niche. Lateral distances were measured along the working face north and south of the center line.

NA = data Not Available

Table 2.12 - 1 of 2

Observed Extent of Dyes at Niche 3650 During Excavation

Yucca Mountain Project
Exploratory Study Facility

Lawrence Berkeley National Laboratory

Observed Dye	Borehole	Date	Start Time Release	Test[1] Interval (m)	Mass Released (g)	Release[2] Time (minutes)	Date of Mine Out	Time of Mine Out	Mined[3] Depth (m)	Maximum Observed Distribution of Dye		
										Penetration Depth (m)[4]	Lateral Extent[5]	
											South (m)	North (m)
FD&C Red No. 40	UL	8/7/97	14:14	7.01 - 7.32	694.5	13.41	8/19/97	19:30	6.14	0.66	1.27	N.O.
							8/19/97	23:16	7.17	1.42	1.22 - 1.52	N.O.
FD&C Blue No. 1	UM	8/7/97	20:18	4.27 - 4.57	647	783.17	8/16/97	17:00	3.79	1.68	0.23	0.25
							8/16/97	18:05	4.08	1.63	0.23	0.53
							8/19/97	8:45	4.34	1.32	0.29	0.58
							8/19/97	10:30	4.6	0.86	0.0	0.25
FD&C Red No. 40	UM	8/6/87	14:05	4.88 - 5.18	937.4	9.72	8/19/97	NA	4.85	NA	NA	NA
							8/19/97	12:30	5.01	0.86	0.28	0.09
							8/19/97	NA	5.31	0.66	NA	NA
FD&C Blue No. 1	UM	8/6/97	14:49	6.71 - 7.01	438.7	15.73	8/19/97	16:51	5.74	0.82	0.42	N.O.
							8/19/97	18:36	6.01	1.25	0.48	N.O.
							8/19/97	20:37	6.3	1.82	0.11	0.14
							8/19/97	21:30	6.74	1.42	0.35	0.33
							8/19/97	23:16	7.17	1.04	0.53	0.28
							8/20/97	13:30	7.24	0.63	0.0	0.08

[1] Depth measurement is from the collar of the boring to the test interval.
[2] Released time represents the total time it took to inject, standby, and recover the fluid (excluding line storage).
[3] Depth in meters measured along the center line of the Niche from the niche opening to the working face.
[4] Penetration Depth equals the vertical distance in meters from the test interval to the observed dye location.
[5] The reference point for this measurement is the center line of the niche. Lateral distances were measured along the working face north and south of the center line.
NA = data Not Available, N.O. = dye Not Observed north or south of niche center line

Table 2.12 - 1 of 2

Observed Extent of Dyes at Niche 3650 During Excavation

Yucca Mountain Project
Exploratory Study Facility

Lawrence Berkeley National Laboratory

Observed Dye	Borehole	Date	Start Time Release	Test[1] Interval (m)	Mass Released (g)	Release[2] Time (minutes)	Date of Mine Out	Time of Mine Out	Mined[3] Depth (m)	Maximum Observed Distribution of Dye		
										Penetration Depth (m)[4]	Lateral Extent[5]	
											South (m)	North (m)
FD&C Red No. 40	UL	8/7/97	14:14	7.01 - 7.32	694.5	13.41	8/19/97	19:30	6.14	0.66	1.27	N.O.
							8/19/97	23:16	7.17	1.42	1.22 - 1.52	N.O.
FD&C Blue No. 1	UM	8/7/97	20:18	4.27 - 4.57	647	783.17	8/16/97	17:00	3.79	1.68	0.23	0.25
							8/16/97	18:05	4.08	1.63	0.23	0.53
							8/19/97	8:45	4.34	1.32	0.29	0.58
							8/19/97	10:30	4.6	0.86	0.0	0.25
FD&C Red No. 40	UM	8/6/87	14:05	4.88 - 5.18	937.4	9.72	8/19/97	NA	4.85	NA	NA	NA
							8/19/97	12:30	5.01	0.86	0.28	0.09
							8/19/97	NA	5.31	0.66	NA	NA
FD&C Blue No. 1	UM	8/6/97	14:49	6.71 - 7.01	438.7	15.73	8/19/97	16:51	5.74	0.82	0.42	N.O.
							8/19/97	18:36	6.01	1.25	0.48	N.O.
							8/19/97	20:37	6.3	1.82	0.11	0.14
							8/19/97	21:30	6.74	1.42	0.35	0.33
							8/19/97	23:16	7.17	1.04	0.53	0.28
							8/20/97	13:30	7.24	0.63	0.0	0.08

[1] Depth measurement is from the collar of the boring to the test interval.
[2] Released time represents the total time it took to inject, standby, and recover the fluid (excluding line storage).
[3] Depth in meters measured along the center line of the Niche from the niche opening to the working face.
[4] Penetration Depth equals the vertical distance in meters from the test interval to the observed dye location.
[5] The reference point for this measurement is the center line of the niche. Lateral distances were measured along the working face north and south of the center line.
NA = data Not Available, N.O. = dye Not Observed north or south of niche center line

Table 2.13 - 1 of 2

Captured Mass and Seepage Percentage

Niche 3650

Exploratory Study Facility

Lawrence Berkeley National Laboratory

Borehole	Test Name	Date	Depth (m)	Liquid Release Rate g/s	Mass Released g	Mass Captured g	Seepage Percentage (%)
UL	Test #1 12-11-97	12/11/97	5.18-5.49	0.078	405.4	0.0	0.0
	Test #1 2-12-98	2/12/98	5.18-5.49	0.007	537.3	0.0	0.0
	Test #2 12-11-97	12/11/97	5.79-6.10	0.202	379.2	0.0	0.0
	Test #3 12-11-97	12/11/97	6.40-6.71	0.211	420.3	0.0	0.0
	Test #1 12-10-97	12/10/97	7.01-7.32	1.949	1005.5	16.0	1.6
	Test #1 1-6-98	1/6/98	7.01-7.32	0.190	1001.0	0.0	0.0
	Test #2 1-6-98	1/6/98	7.62-7.92	0.507	1025.4	279.7	27.3
	Test #1 2-12-98	2/12/98	7.62-7.92	0.101	1035.1	156.9	15.2
	Test #1 3-4-98	3/4/98	7.62-7.92	0.012	1037.3	59.8	5.8
UM	Test 5 Niche 3650	11/13/97	4.27-4.57	2.019	1008.7	228.0	22.6
	Test #1 12-3-97	12/3/97	4.27-4.57	0.503	1015.7	235.4	23.2
	Test #2 12-3-97	12/3/97	4.27-4.57	0.506	1012.5	568.6	56.2
	Test #1 1-7-98	1/7/98	4.27-4.57	0.047	1004.2	46.0	4.6
	Test #2 2-10-98	2/10/98	4.27-4.57	0.016	1163.3	0.0	0.0
	Test 1 Niche 3650	11/12/97	4.88-5.18	2.892	1033.1	99.6	9.6
	Test #1 12-4-97	12/4/97	4.88-5.18	0.507	1044.6	44.3	4.2
	Test #2 12-5-97	12/5/97	4.88-5.18	0.144	1049.3	74.7	7.1
	Test #1 1-8-98	1/8/98	4.88-5.18	0.047	1044.2	0.0	0.0
	Test #1 3-6-98	3/6/98	4.88-5.18	0.013	5597.5	0.0	0.0
	Test 4 Niche 3650	11/13/97	5.49-5.79	2.069	1013.4	275.7	27.2
	Test #2 12-4-97	12/4/97	5.49-5.79	0.504	1033.7	222.1	21.5
	Test #1 1-9-98	1/9/98	5.49-5.79	0.058	1038.7	33.3	3.2
	Test #1 2-11-98	2/11/98	5.49-5.79	0.014	1041.7	0.0	0.0
	Test 3 Niche 3650	11/13/97	6.10-6.40	0.514	1000.3	0.0	0.0
	Test #3 12-4-97	12/4/97	6.10-6.40	0.192	989.4	0.0	0.0
	Test #1 1-12-98	1/12/98	6.10-6.40	0.792	1012.1	0.0	0.0

Table 2.13 - 2 of 2

Captured Mass and Seepage Percentage

Niche 3650

Exploratory Study Facility

Lawrence Berkeley National Laboratory

Borehole	Test Name	Date	Depth (m)	Liquid Release Rate g/s	Mass Injected g	Mass Captured g	Seepage Percentage (%)
UM	Test 2 Niche 3650	11/12/97	6.71-7.01	0.555	274.5	0.0	0.0
	Test #1 12-5-97	12/5/97	6.71-7.01	0.202	988.3	0.0	0.0
UR	Test #1 1-14-98	1/14/98	4.27-4.57	0.198	995.7	4.0	0.4
	Test #1 2-5-98	2/5/98	4.27-4.57	0.055	1003.0	0.0	0.0
	Test #1 1-15-98	1/15/98	4.88-5.18	0.190	1016.4	4.1	0.4
	Test #1 2-6-98	2/6/98	4.88-5.18	0.053	1013.5	0.0	0.0
	Test #2 1-13-98	1/13/98	5.49-5.79	0.230	904.3	0.0	0.0
	Test #2 2-10-98	2/10/98	5.49-5.79	0.366	377.8	49.7	13.2
	Test #2 1-14-98	1/14/98	6.10-6.40	0.191	1013.6	270.7	26.7
	Test #1 2-4-98	2/4/98	6.10-6.40	0.057	1018.7	220.2	21.6
	Test #1 1-13-98	1/13/98	6.71-7.01	0.196	1010.2	312.4	30.9
	Test #1 2-3-98	2/3/98	6.71-7.01	0.102	1026.9	294.9	28.7
	Test #1 3-5-98	3/5/98	6.71-7.01	0.013	1020.0	38.9	3.8
	Test #1 3-12-98	3/12/98	7.62-7.92	0.009	669.3	0.0	0.0

Table 2.14 - 1 of 3

Distribution of Captured Water

Niche 3650 - Borehole UL
Exploratory Study Facility

Lawrence Berkeley National Laboratory

Test Name	Depth (m)	Liquid Release Rate, g/s	Cell	Captured Mass, g	Cell	Captured Mass, g	Cell	Captured Mass, g	Cell	Captured Mass, g	Cell	Captured Mass, g	Total Mass, g
Test #1 12-11-97	5.18-5.49	0.078	--	--	--	--	--	--	--	--	--	--	--
Test #1 2-12-98	5.18-5.49	0.007	--	--	--	--	--	--	--	--	--	--	--
Test #2 12-11-97	5.79-6.10	0.202	--	--	--	--	--	--	--	--	--	--	--
Test #3 12-11-97	6.40-6.71	0.211	--	--	--	--	--	--	--	--	--	--	--
Test #1 12-10-97	7.01-7.32	1.949	10s, 11w	16.0									16.0
Test #1 1-6-98	7.01-7.32	0.190	--	--	--	--	--	--	--	--	--	--	--
Test #2 1-6-98	7.62-7.92	0.507	8s, 12w	0.4			9s, 12w	279.3					279.7
Test #1 2-12-98	7.62-7.92	0.101	8s, 12w	3.4	8s, 13w	0.2	9s, 12 w	13.0	10s, 12w	140.3			156.9
Test #1 3-4-98	7.62-7.92	0.012							10s, 12w	59.7	11s, 12w	0.1	59.8

-- No water seeped

Table 2.14 - 2 of 3

Distribution of Captured Water

Niche 3650 - Borehole UM

Exploratory Study Facility

Lawrence Berkeley National Laboratory

Test Name	Depth (m)	Liquid Release Rate, g/s	Cell	Captured Mass, g	Cell	Captured Mass, g	Cell	Captured Mass, g	Cell	Captured Mass, g	Cell	Captured Mass, g	Total Mass, g
Test 5 Niche 3650	4.27-4.57	2.019	6s, 5w	228.0									
Test #1 12-3-97	4.27-4.57	0.503	6s, 5w	235.4									228.0
Test #2 12-3-97	4.27-4.57	0.506	6s, 5w	568.6									235.4
Test #1 1-7-98	4.27-4.57	0.047	6s, 5w	46.0									568.6
Test #2 2-10-98	4.27-4.57	0.016	--	--	--	--	--	--	--	--	--	--	46.0
													--
Test 1 Niche 3650	4.88-5.18	2.892	5s, 7w	16.4	6s, 7w	82.5	6s, 8w	0.4	7s, 6w	0.1	7s, 7w	0.2	99.6
Test #1 12-4-97	4.88-5.18	0.507	5s, 8w	44.3									44.3
Test #2 12-5-97	4.88-5.18	0.144	5s, 8w	74.5			6s, 8w	0.2					74.7
Test #1 1-8-98	4.88-5.18	0.047	--	--	--	--	--	--	--	--	--	--	--
Test #1 3-6-98	4.88-5.18	0.013	--	--	--	--	--	--	--	--	--	--	--
Test 4 Niche 3650	5.49-5.79	2.069	6s, 8w	15.0	6s, 9w	98.4	7s, 8w	26.4	7s, 9w	135.9			275.7
Test #2 12-4-97	5.49-5.79	0.504	6s, 8w	20.7	6s, 9w	135.7	7s, 8w	2.5	7s, 9w	63.2			222.1
Test #1 1-9-98	5.49-5.79	0.058	6s, 8w	11.8	6s, 9w	18.2	7s, 8w	3.3					33.3
Test #1 2-11-98	5.49-5.79	0.014	--	--	--	--	--	--	--	--	--	--	--
Test 3 Niche 3650	6.10-6.40	0.514	--	--	--	--	--	--	--	--	--	--	--
Test #3 12-4-97	6.10-6.40	0.192	--	--	--	--	--	--	--	--	--	--	--
Test #1 1-12-98	6.10-6.40	0.792	--	--	--	--	--	--	--	--	--	--	--
Test 2 Niche 3650	6.71-7.01	0.555	--	--	--	--	--	--	--	--	--	--	--
Test #1 12-5-97	6.71-7.01	0.202	--	--	--	--	--	--	--	--	--	--	--

-- No water seeped

Table 2.14 - 3 of 3

Distribution of Captured Water

Niche 3650 - Borehole UR
Exploratory Study Facility

Lawrence Berkeley National Laboratory

Test Name	Depth (m)	Liquid Release Rate, g/s	Cell	Captured Mass, g	Cell	Captured Mass, g	Cell	Captured Mass, g	Cell	Captured Mass, g	Cell	Captured Mass, g	Total Mass, g
Test #1 1-14-98	4.27-4.57	0.198	3s, 9w	4.0									4.0
Test #1 2-5-98	4.27-4.57	0.055	--	--	--	--	--	--	--	--	--	--	--
Test #1 1-15-98	4.88-5.18	0.190	4s, 10w	4.1									4.1
Test #1 2-6-98	4.88-5.18	0.053	--	--	--	--	--	--	--	--	--	--	--
Test #2 1-13-98	5.49-5.79	0.230	--	--	--	--	--	--	--	--	--	--	--
Test #2 2-10-98	5.49-5.79	0.366	3s, 12w	25.9	3s, 13w	23.8							49.7
Test #2 1-14-98	6.10-6.40	0.191	3s, 13w	202.6	4s, 13w	44.7	4s, 14w	23.4					270.7
Test #1 2-4-98	6.10-6.40	0.057	3s, 13w	220.2									220.2
Test #1 1-13-98	6.71-7.01	0.196	3s, 14w	45.4	3s, 15w	264.3	3s, 16w	2.7					312.4
Test #1 2-3-98	6.71-7.01	0.102	3s, 14w	11.4	3s, 15w	283.5							294.9
Test #1 3-5-98	6.71-7.01	0.013	3s, 14w	4.5	3s, 15w	34.3			4s, 15w	0.1			38.9
Test #1 3-12-98	7.62-7.92	0.009	--	--	--	--	--	--	--	--	--	--	--

-- No water seeped

Arrival Times for Liquid-Release Test Events: Post-Excavation Seepage Tests

Niche 3650
Exploratory Study Facility

Lawrence Berkeley National Laboratory

Borehole	Test Name	Date	Depth (m)	Wetting Front Arrives Relative to: [1]		Dripping Begins Relative to: [1]			Dripping Ends Relative to: [1]		
				Start of Pumping (hr:min:s)	End of Pumping (hr:min:s)	Start of Pumping (hr:min:s)	End of Pumping (hr:min:s)	Front Arrival (hr:min:s)	Start of Pumping (hr:min:s)	End of Pumping (hr:min:s)	Front Arrival (hr:min:s)
UL	Test #1 12-11-97	12/11/97	5.18-5.49	--	--	--	--	--	--	--	--
	Test #1 2-12-98	2/12/98	5.18-5.49	--	--	--	--	--	--	--	--
	Test #2 12-11-97	12/11/97	5.79-6.10	--	--	--	--	--	--	--	--
	Test #3 12-11-97	12/11/97	6.40-6.71	--	--	--	--	--	--	--	--
	Test #1 12-10-97	12/10/97	7.01-7.32	0:04:00	- 0:04:35	0:09:07	+ 0:00:32	0:05:07	0:14:50	0:06:15	0:10:50
	Test #1 1-6-98	1/6/98	7.01-7.32	0:54:50	- 0:33:14	--	--	--	--	--	--
	Test #2 1-6-98	1/6/98	7.62-7.92	0:11:30	- 0:22:15	0:18:20	- 0:15:25	0:06:50	1:09:00	0:35:15	0:57:30
	Test #1 2-12-98	2/12/98	7.62-7.92	0:09:30	- 2:41:36	0:35:10	- 2:15:56	0:25:40	2:56:05	0:04:59	2:46:35
	Test #1 3-4-98	3/4/98	7.62-7.92	0:43:30	- 22:22:30	NO	NR	NO	NO	NO	NO

-- The event did not occur.
NO - Not Observed. The event occurred when field personnel were not present to observe/record the time of the event.
NR - Not Recorded. The time that the event occurred was not recorded.
[1] Negative value (-) indicates event occurred hr:min:sec prior to the specified event. Positive value (+) indicates event occurred hr:min:s after the specified event ended.

Arrival Times for Liquid-Release Test Events: Post-Excavation Seepage Tests

Niche 3650

Exploratory Study Facility

Lawrence Berkeley National Laboratory

Borehole	Test Name	Date	Depth (m)	Wetting Front Arrives Relative to: [1]		Dripping Begins Relative to: [1]			Dripping Ends Relative to: [1]		
				Start of Pumping (hr:min:s)	End of Pumping (hr:min:s)	Start of Pumping (hr:min:s)	End of Pumping (hr:min:s)	Front Arrival (hr:min:s)	Start of Pumping (hr:min:s)	End of Pumping (hr:min:s)	Front Arrival (hr:min:s)
UM	Test 5 Niche 3650	11/13/97	4.27-4.57	0:06:56	- 0:01:31	0:07:10	- 0:01:17	0:00:14	0:41:00	0:32:33	0:34:04
	Test #1 12-3-97	12/3/97	4.27-4.57	0:16:48	- 0:17:04	0:21:47	- 0:12:05	0:04:59	1:04:52	0:31:00	0:48:04
	Test #2 12-3-97	12/3/97	4.27-4.57	0:08:34	- 0:25:13	0:09:42	- 0:24:05	0:01:08	0:54:52	0:21:05	0:46:18
	Test #1 1-7-98	1/7/98	4.27-4.57	2:26:51	- 3:32:15	4:35:39	- 1:23:27	2:08:48	6:25:31	0:26:25	3:58:40
	Test #2 2-10-98	2/10/98	4.27-4.57	3:42:55	- 15:53:05	--	--	--	--	--	--
	Test 1 Niche 3650	11/12/97	4.88-5.18	0:03:00	- 0:03:04	0:03:15	- 0:02:49	0:00:15	NR	NR	NR
	Test #1 12-4-97	12/4/97	4.88-5.18	0:04:58	- 0:29:37	0:16:20	- 0:18:15	0:11:22	0:38:02	0:03:27	0:33:04
	Test #2 12-5-97	12/5/97	4.88-5.18	0:15:52	- 1:46:46	0:41:37	- 1:21:01	0:25:45	2:14:52	0:12:14	1:59:00
	Test #1 1-8-98	1/8/98	4.88-5.18	1:41:00	- 4:34:30	--	--	--	--	--	--
	Test #1 3-6-98	3/6/98	4.88-5.18	6:01:30	- 111:32:30	--	--	--	--	--	--
	Test 4 Niche 3650	11/13/97	5.49-5.79	0:03:28	- 0:04:45	0:05:30	- 0:02:43	0:02:02	0:23:08	0:14:55	0:19:40
	Test #2 12-4-97	12/4/97	5.49-5.79	0:07:00	- 0:27:29	0:11:06	- 0:23:23	0:04:06	0:44:18	0:09:49	0:37:18
	Test #1 1-9-98	1/9/98	5.49-5.79	0:45:50	- 4:13:50	3:01:26	- 1:58:14	2:15:36	5:08:00	0:08:20	4:22:10
	Test #1 2-11-98	2/11/98	5.49-5.79	2:48:50	- 18:27:28	--	--	--	--	--	--
	Test 3 Niche 3650	11/13/97	6.10-6.40	0:34:30	+ 0:02:05	--	--	--	--	--	--
	Test #3 12-4-97	12/4/97	6.10-6.40	1:05:12	- 0:21:43	--	--	--	--	--	--
	Test #1 1-12-98	1/12/98	6.10-6.40	0:22:30	+ 0:01:21	--	--	--	--	--	--
	Test 2 Niche 3650	11/12/97	6.71-7.01	--	--	--	--	--	--	--	--
	Test #1 12-5-97	12/5/97	6.71-7.01	0:53:00	- 0:29:35	--	--	--	--	--	--

-- The event did not occur.

NO - Not Observed. The event occurred when field personnel were not present to observe/record the time of the event.

NR - Not Recorded. The time that the event occurred was not recorded.

[1] Negative value (-) indicates event occurred hr:min:s prior to the specified event. Positive value (+) indicates event occurred hr:min:sec after the specified event ended.

Table 2.15 - 3 of 3

Arrival Times for Liquid-Release Test Events: Post-Excavation Seepage Tests

Niche 3650

Exploratory Study Facility

Lawrence Berkeley National Laboratory

Borehole	Test Name	Date	Depth (m)	Wetting Front Arrives Relative to: [1]		Dripping Begins Relative to: [1]			Dripping Ends Relative to: [1]		
				Start of Pumping (hr:min:s)	End of Pumping (hr:min:s)	Start of Pumping (hr:min:s)	End of Pumping (hr:min:s)	Front Arrival (hr:min:s)	Start of Pumping (hr:min:s)	End of Pumping (hr:min:s)	Front Arrival (hr:min:s)
UR	Test #1 1-14-98	1/14/98	4.27-4.57	0:56:08	- 0:28:45	1:15:48	- 0:09:05	0:19:40	1:38:56	0:14:03	0:42:48
	Test #1 2-5-98	2/5/98	4.27-4.57	2:45:10	- 2:19:36	--	--	--	--	--	--
	Test #1 1-15-98	1/15/98	4.88-5.18	0:29:50	- 0:59:50	1:22:10	- 0:07:30	0:52:20	1:44:30	0:14:50	1:14:40
	Test #1 2-6-98	2/6/98	4.88-5.18	1:13:15	- 4:07:27	--	--	--	--	--	--
	Test #2 1-13-98	1/13/98	5.49-5.79	0:09:00	- 0:58:45	--	--	--	--	--	--
	Test #2 2-10-98	2/10/98	5.49-5.79	0:03:50	- 0:13:30	0:11:12	- 0:06:08	0:07:22	0:17:45	0:00:25	0:13:55
	Test #2 1-14-98	1/14/98	6.10-6.40	0:16:00	- 1:12:19	0:38:00	- 0:50:19	0:22:00	1:50:52	0:22:33	1:34:52
	Test #1 2-4-98	2/4/98	6.10-6.40	1:02:35	- 3:54:25	1:52:04	- 3:04:56	0:49:29	5:18:36	0:21:36	4:16:01
	Test #1 1-13-98	1/13/98	6.71-7.01	0:06:56	- 1:19:32	0:15:52	- 1:10:36	0:08:56	1:30:09	0:03:41	1:23:13
	Test #1 2-3-98	2/3/98	6.71-7.01	0:10:26	- 2:37:30	0:41:15	- 2:06:41	0:30:49	2:54:58	0:07:02	2:44:32
	Test #1 3-5-98	3/5/98	6.71-7.01	1:14:17	- 20:06:20	NO	NO	NO	21:57:57	0:37:20	20:43:40
	Test #1 3-12-98	3/12/98	7.62-7.92	NO	NO	--	--	--	--	--	--

-- The event did not occur.

NO - Not Observed. The event occurred when field personnel were not present to observe/record the time of the event.

NR - Not Recorded. The time that the event occurred was not recorded.

[1] Negative value (-) indicates event occurred hr:min:sec prior to the specified event. Positive value (+) indicates event occurred hr:min:s after the specified event ended.

Table 2.16

Liquid-Release Flux for Test Intervals Exhibiting Seepage

Niche 3650

Exploratory Study Facility

Lawrence Berkeley National Laboratory

Borehole	Test Name	Date	Depth (ft)	Liquid Release Rate g/s	Liquid Release Flux (m/s)	Seepage Percentage (%)
UL	Test #1 12-10-97	12/10/97	7.01-7.32	1.949	3.65E-05	1.6
	Test #1 1-6-98	01/06/98	7.01-7.32	0.190	3.55E-06	0.0
	Test #2 1-6-98	01/06/98	7.62-7.92	0.507	9.49E-06	27.3
	Test #1 2-12-98	02/12/98	7.62-7.92	0.101	1.89E-06	15.2
	Test #1 3-4-98	03/04/98	7.62-7.92	0.012	2.33E-07	5.8
UM	Test 5 Niche 3650	11/13/97	4.27-4.57	2.019	3.78E-05	22.6
	Test #1 12-3-97	12/03/97	4.27-4.57	0.503	9.42E-06	23.2
	Test #2 12-3-97	12/03/97	4.27-4.57	0.506	9.46E-06	56.2
	Test #1 1-7-98	01/07/98	4.27-4.57	0.047	8.82E-07	4.6
	Test #2 2-10-98	02/10/98	4.27-4.57	0.016	3.09E-07	0.0
	Test 1 Niche 3650	11/12/97	4.88-5.18	2.892	5.41E-05	9.6
	Test #1 12-4-97	12/04/97	4.88-5.18	0.507	9.49E-06	4.2
	Test #2 12-5-97	12/05/97	4.88-5.18	0.144	2.70E-06	7.1
	Test #1 1-8-98	01/08/98	4.88-5.18	0.047	8.75E-07	0.0
	Test #1 3-6-98	03/06/98	4.88-5.18	0.013	2.48E-07	0.0
	Test 4 Niche 3650	11/13/97	5.49-5.79	2.069	3.87E-05	27.2
	Test #2 12-4-97	12/04/97	5.49-5.79	0.504	9.43E-06	21.5
	Test #1 1-9-98	01/09/98	5.49-5.79	0.058	1.08E-06	3.2
	Test #1 2-11-98	02/11/98	5.49-5.79	0.014	2.55E-07	0.0
UR	Test #1 1-14-98	01/14/98	4.27-4.57	0.198	3.71E-06	0.4
	Test #1 2-5-98	02/05/98	4.27-4.57	0.055	1.03E-06	0.0
	Test #1 1-15-98	01/15/98	4.88-5.18	0.190	3.55E-06	0.4
	Test #1 2-6-98	02/06/98	4.88-5.18	0.053	9.92E-07	0.0
	Test #2 1-13-98	01/13/98	5.49-5.79	0.230	4.31E-06	0.0
	Test #2 2-10-98	02/10/98	5.49-5.79	0.366	6.85E-06	13.2
	Test #2 1-14-98	01/14/98	6.10-6.40	0.191	3.57E-06	26.7
	Test #1 2-4-98	02/04/98	6.10-6.40	0.057	1.07E-06	21.6
	Test #1 1-13-98	01/13/98	6.71-7.01	0.196	3.68E-06	30.9
	Test #1 2-3-98	02/03/98	6.71-7.01	0.102	1.91E-06	28.7
	Test #1 3-5-98	03/05/98	6.71-7.01	0.013	2.48E-07	3.8

Table 2.17

Seepage Threshold Flux

Niche 3650

Exploratory Study Faciltiy

Lawrence Berkeley National Laboratory

Borehole	Depth (m)	Regression Equation	Data Points (n)	R^2 - Value	Seepage Threshold Flux (m/s) (K_{so})	Predicted Seepage Percentage (%)	Air [1] Permeability k, (m^2)	Saturated [2] Hydraulic Conductivity (m/s) (K_s)
UL	7.01-7.32	$y = 0.6833Ln(K_o) + 8.5742$	2	NA	3.55E-06	-2.84E-14	9.17E-12	8.98E-05
	7.62-7.92	$y = 5.7394Ln(K_o) + 92.627$	3	0.979	9.80E-08	0.00E+00	1.54E-11	1.51E-04
UM	4.27-4.57	$y = 5.2757Ln(K_o) + 79.443$	4	0.921	2.89E-07	-8.67E-13	2.67E-12	2.62E-05
	4.88-5.18	$y = 2.304Ln(K_o) + 31.767$	3	0.975	1.03E-06	-9.59E-14	2.57E-10	2.52E-03
	5.49-5.79	$y = 5.8876Ln(K_o) + 87.528$	4	0.963	3.50E-07	0.00E+00	2.20E-12	2.16E-05
UR	4.27-4.57	$y = 0.314Ln(K_o) + 4.3283$	2	NA	1.03E-06	0.00E+00	4.17E-12	4.08E-05
	4.88-5.18	$y = 0.3165Ln(K_o) + 4.3751$	2	NA	9.92E-07	-2.47E-13	1.01E-11	9.87E-05
	5.49-5.79	$y = 28.419Ln(K_o) + 351.09$	2	NA	4.31E-06	0.00E+00	1.75E-12	1.71E-05
	6.10-6.40	$y = 4.2169Ln(K_o) + 79.596$	2	NA	6.35E-09	-2.27E-13	3.08E-12	3.01E-05
	6.71-7.01	$y = 10.574Ln(K_o) + 165.28$	3	0.974	1.63E-07	-3.69E-13	2.33E-11	2.28E-04
All Data	Various	$y = 3.7696Ln(K_o) + 59.976$	30	0.187	1.23E-07	-5.68E-14		

NA - not applicable

y = predicted seepage percentage

K_o = net downward liquid-release flux

[1] k was computed using the distance from the test interval to the niche ceiling (0.65 m) in this table in place of the test interval length (0.3048 m) used to compute the k values in Chapter 3.

[2] K_s = k (m^2) x (100 cm)^2 / m^2 x 980 (m/s)/cm^2 where the conversion factor 980 was obtained from *Freeze and Cherry* (1979, p. 29, Table 2.2).

Table 2.18

Seepage Summary for Different Types of Flow

Niche 3650

Exploratory Study Facility

Lawrence Berkeley National Laboratory

Flow Type:	**Network of Fractures**						**Individual Fractures**			
Borehole:	UL	UM	UM	UR	UR	UR	UL	UM	UR	UR
Depth (m):	7.01-7.32	4.27-4.57	5.49-5.79	4.27-4.57	4.88-5.18	5.49-5.79	7.62-7.92	4.88-5.18	6.10-6.40	6.71-7.01
Equivalent Sat. Hydraulic Cond. K_f , (m/s)	8.98E-05	2.62E-05	2.16E-05	4.08E-05	9.87E-05	1.71E-05	1.51E-04	2.52E-03	3.01E-05	2.28E-04
Liquid-Release Rate (g/s)	Seepage Percentage (%)						Seepage Percentage (%)			
1.949 - 2.892	1.6	22.6	27.2	--	--	--	--	9.6	--	--
0.366 - 0.507	--	23.2	21.5	--	--	13.2	27.3	4.2	--	--
0.101 - 0.230	0.0	--	--	0.4	0.4	0.0	15.2	--	26.7	28.7
0.047 - 0.058	--	4.6	3.2	0.0	0.0	--	--	0.0	21.6	--
0.012 - 0.016	--	0.0	0.0	--	--	--	5.8	--	--	3.8

-- Seepage test was not performed at this liquid-release rate.

Table 2.19

Comparison of Saturated Hydraulic Conductivity to Maximum Observed Flux

Niche 3650

Exploratory Study Facility

Lawrence Berkeley National Laboratory

Borehole	Test Name	Depth (m)	Air [1] Permeability (m^2)	Saturated [2] Hydraulic Conductivity $K_{air\text{-}sat}$ (m/s)	Maximum Liq.-Release Flux ($K_{e\text{-}max}$) (m/s)	Saturated Flow Occurred Base On:	
						$K_{air\text{-}sat}$ and $K_{e\text{-}max}$ Comparison Yes/No?	Observed Return Flow Yes/No?
UL	Test #1 12/11/97	5.18-5.49	1.20E-12	1.18E-05	1.46E-06	No	Yes
	Test #2 12/11/97	5.79-6.10	3.89E-11	3.82E-04	3.78E-06	No	Yes
	Test #3 12/11/97	6.40-6.71	5.16E-12	5.05E-05	3.95E-06	No	Yes
	Test #1 12/10/97	7.01-7.32	9.17E-12	8.98E-05	3.65E-05	No	No
	Test #2 1-6-98	7.62-7.92	1.54E-11	1.51E-04	9.49E-06	No	No
UM	Test 5 Niche 3650	4.27-4.57	2.67E-12	2.62E-05	3.78E-05	Yes	No
	Test 1 Niche 3650	4.88-5.18	2.57E-10	2.52E-03	5.41E-05	No	No
	Test 4 Niche 3650	5.49-5.79	2.20E-12	2.16E-05	3.87E-05	Yes	No
	Test #1 1-12-98	6.10-6.40	9.60E-12	9.41E-05	1.48E-05	No	No
	Test 2 Niche 3650	6.71-7.01	1.56E-12	1.53E-05	1.04E-05	No	Yes
UR	Test #1 1-14-98	4.27-4.57	4.17E-12	4.08E-05	3.71E-06	No	No
	Test #1 1-15-98	4.88-5.18	1.01E-11	9.87E-05	3.55E-06	No	No
	Test #2 2-10-98	5.49-5.79	1.75E-12	1.71E-05	4.31E-06	No	Yes
	Test #2 1-14-98	6.10-6.40	3.08E-12	3.01E-05	3.57E-06	No	No
	Test #1 1-13-98	6.71-7.01	2.33E-11	2.28E-04	3.68E-06	No	No

[1] k was computed using the distance from the test interval to the niche ceiling (0.65 m) in this table in place of the test interval length (0.3048 m) used to compute the k values in Chapter 3.

[2] $K_{air\text{-}sat}$ = k (m^2) x (100 cm)^2 / m^2 x 980 (m/s)/cm^2 where the conversion factor 980 was obtained from *Freeze and Cherry* (1979, p 29, Table 2.2).

Chapter 2

Figures

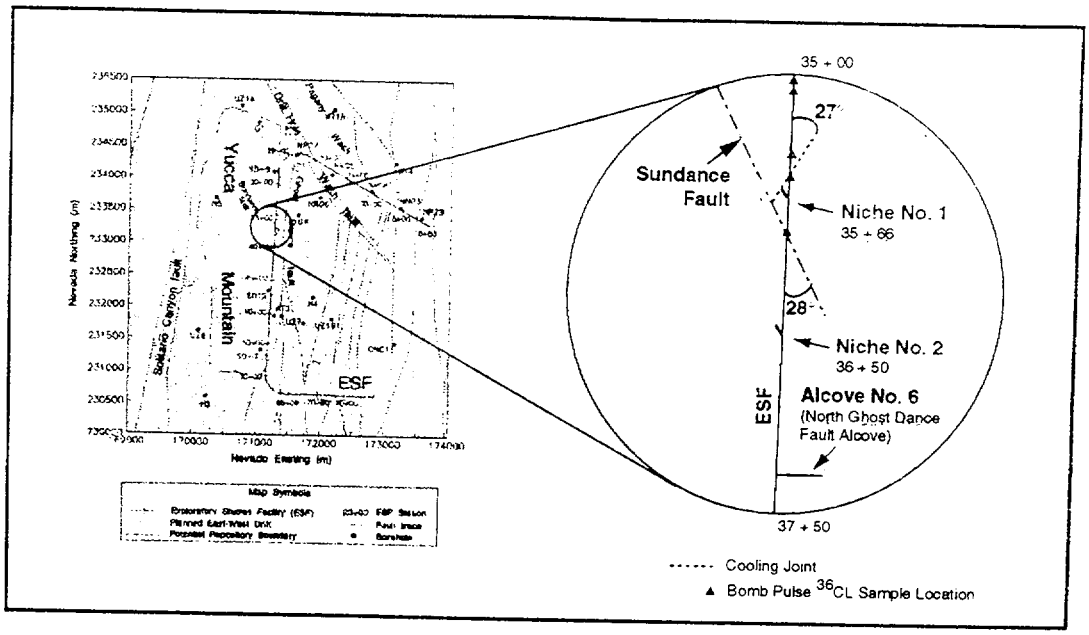

Figure 2.1 Location map of the niche at CA 3566 site near the Sundance Fault and niche at CS 3650 site between Sundance Fault and Alcove 6.

Figure 2.2

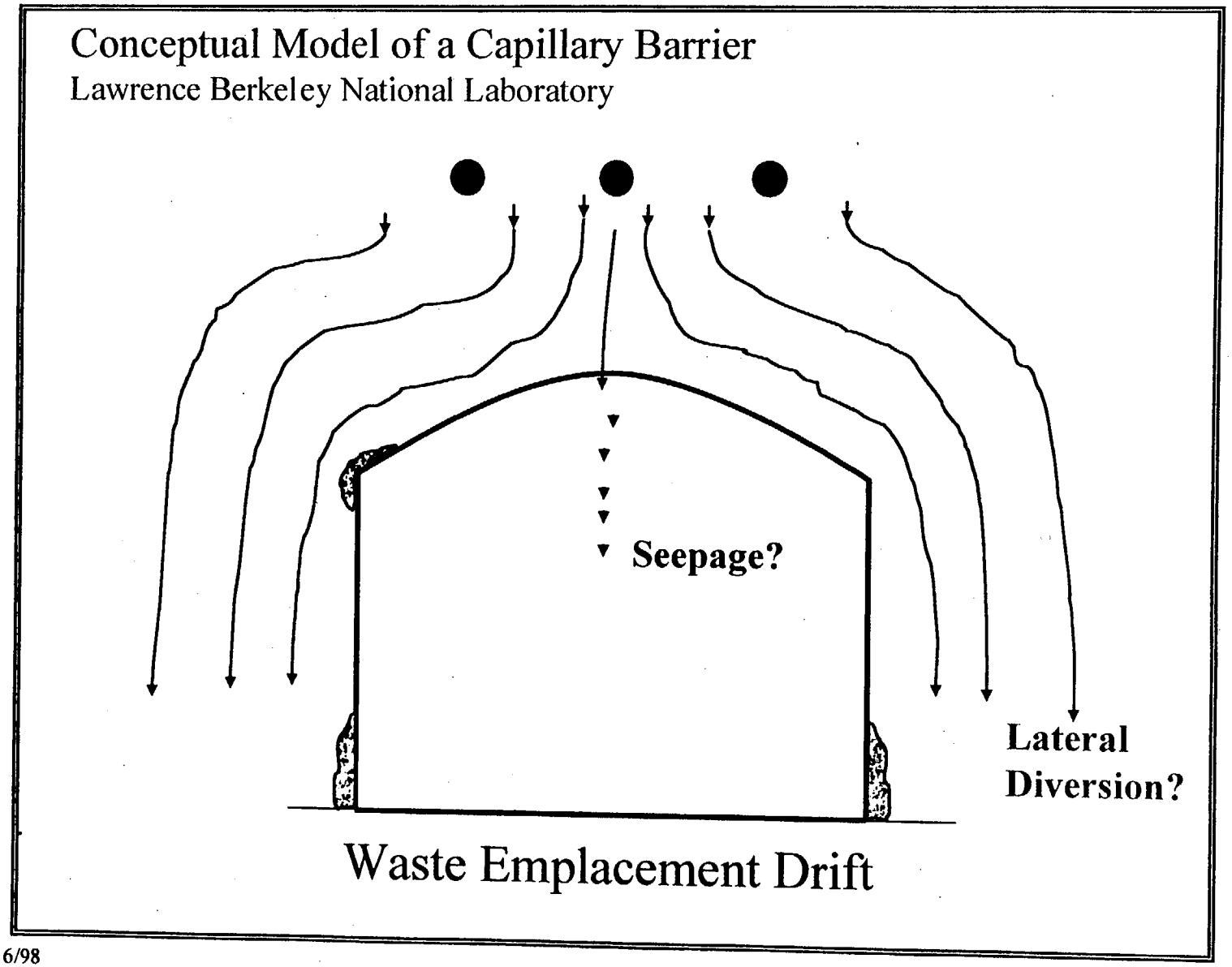
Conceptual Model of a Capillary Barrier
Lawrence Berkeley National Laboratory
Seepage?
Lateral Diversion?
Waste Emplacement Drift

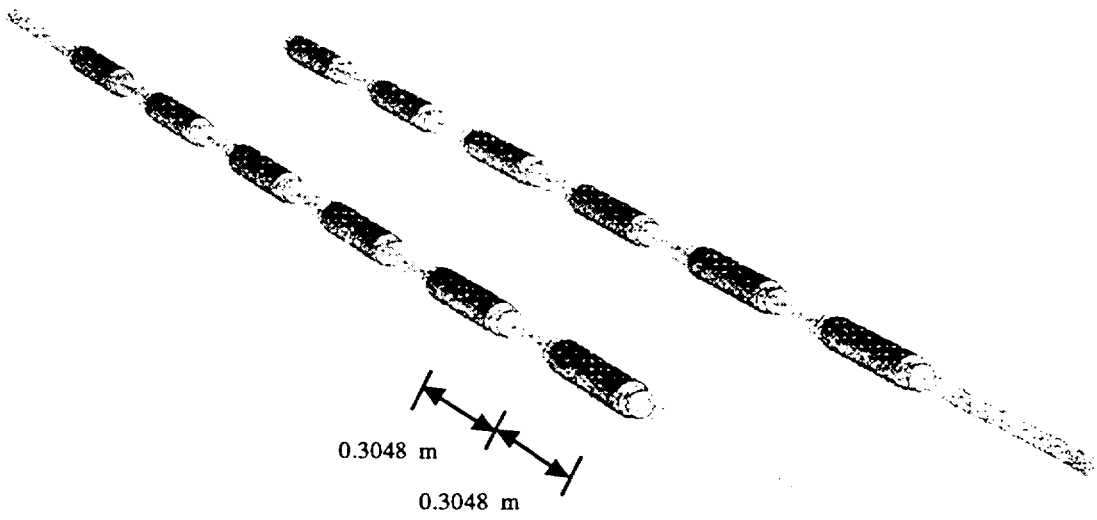

Figure 2.3 Packer design.

Figure 2.4

PLAN VIEW LIQUID CAPTURE SYSTEM - NICHE 3650

Lawrence Berkeley National Laboratory
Exploratory Study Facility
Yucca Mountain, Nevada

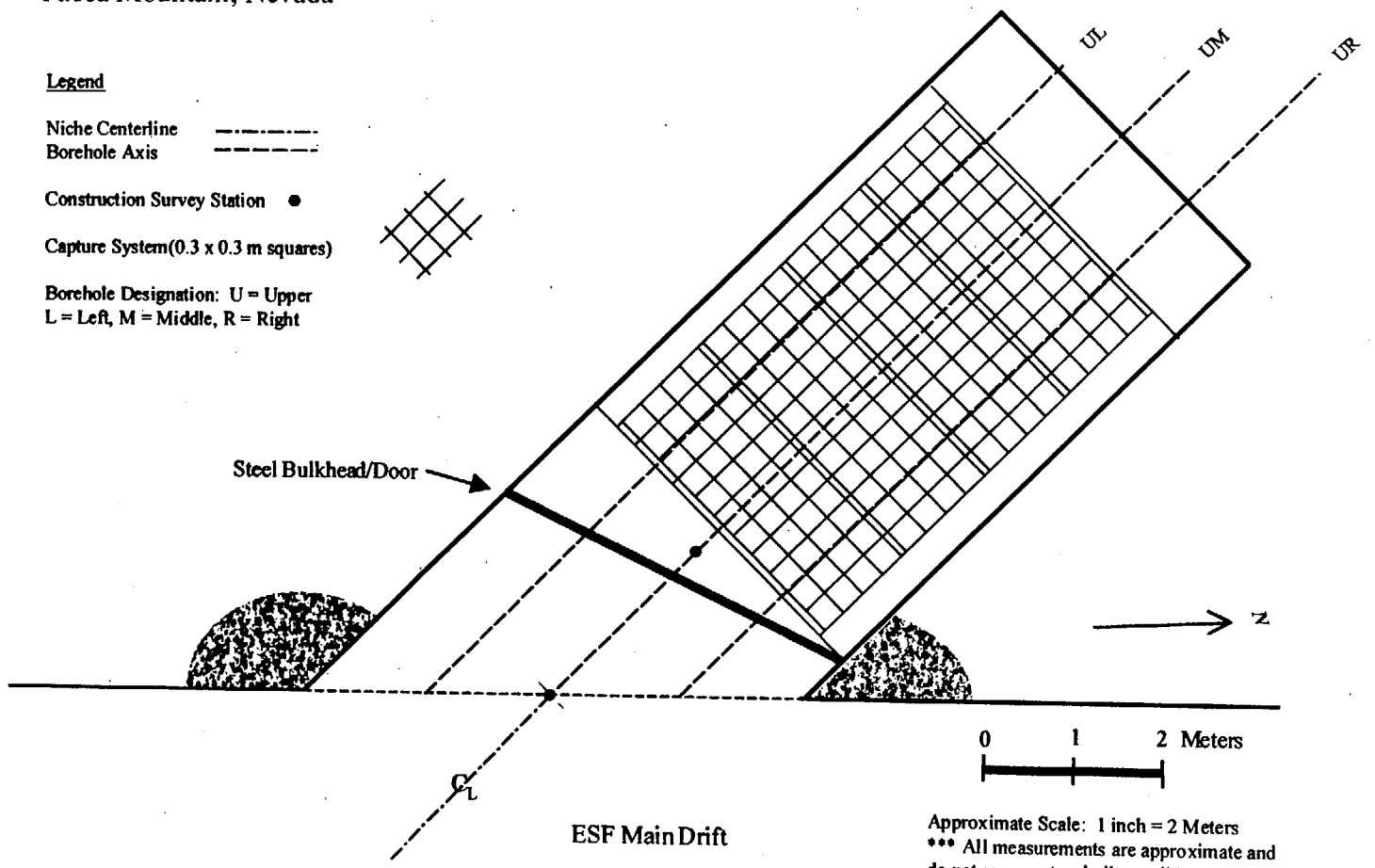

Capture System Top View

Lawrence Berkeley National Laboratory

Figure 2.5

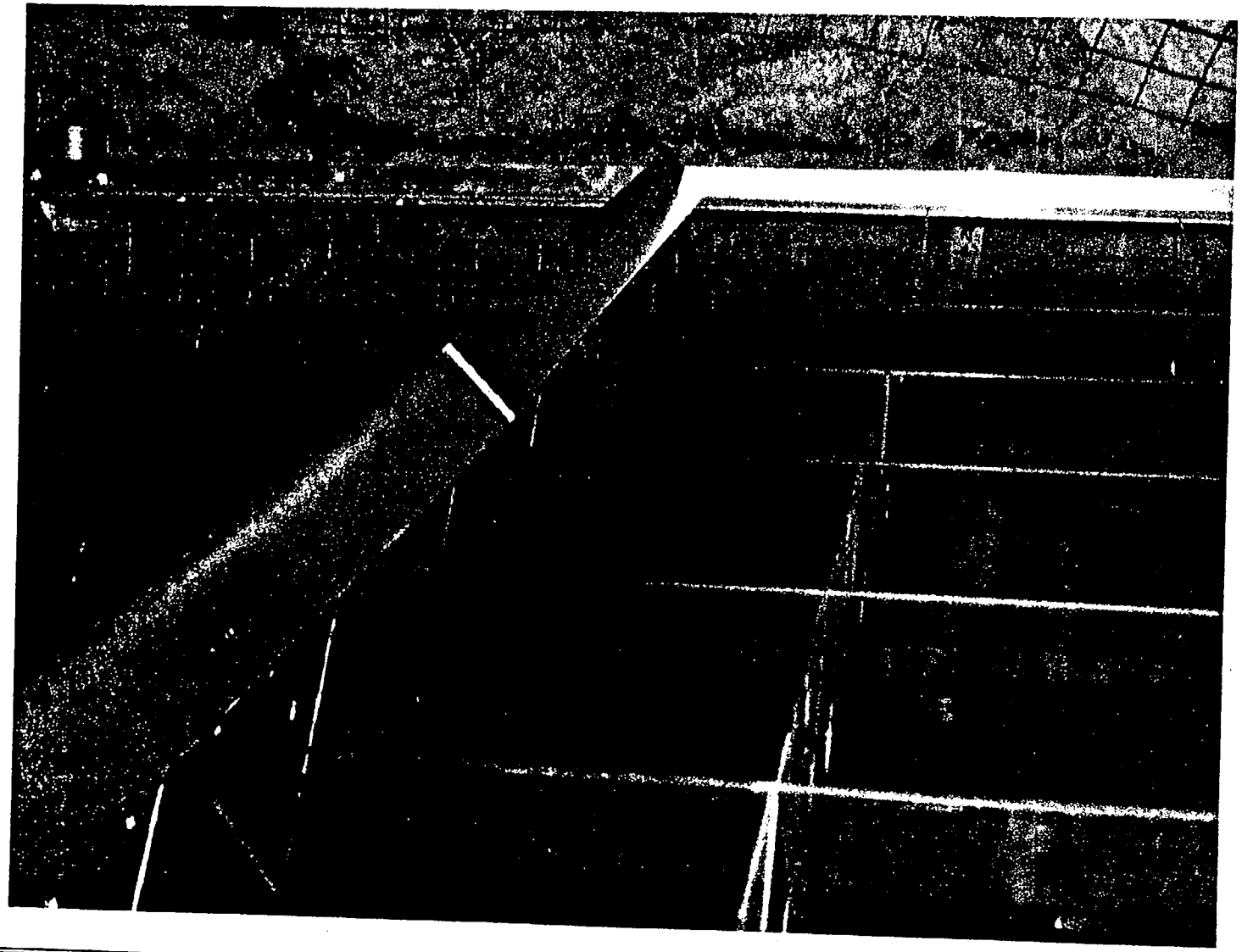

Capture System and Seepage Collection

Lawrence Berkeley National Laboratory

Figure 2.6

FIGURE 2.7

NICHE 3566 & 3650 END VIEWS

Lawrence Berkeley National Laboratory
Exploratory Study Facility
Yucca Mountain, Nevada

Legend

ML Borehole designation
B = Bottom, M = Middle, U=Upper
L = Left, R = Right
*** All measurements are approximate and do not represent as-built conditions

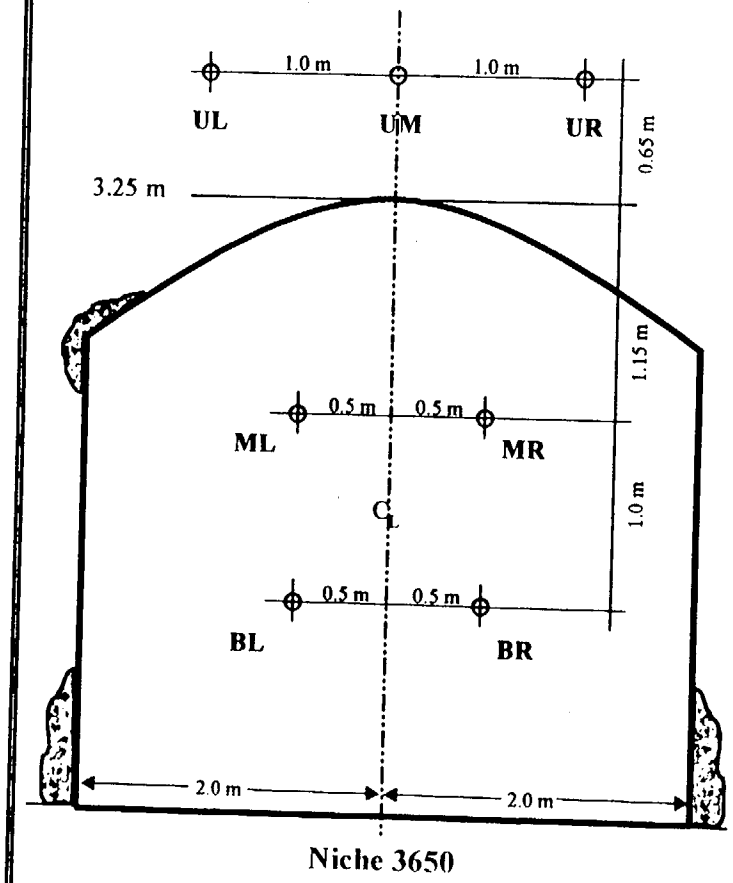

Niche 3650

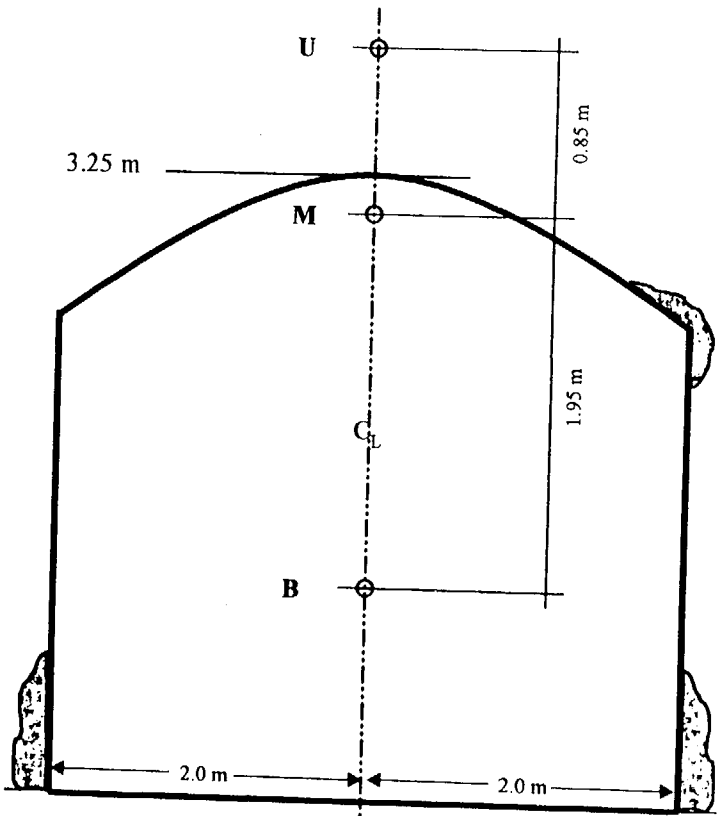

Niche 3566

6/16/98
Version 1.0

Figure 2.8

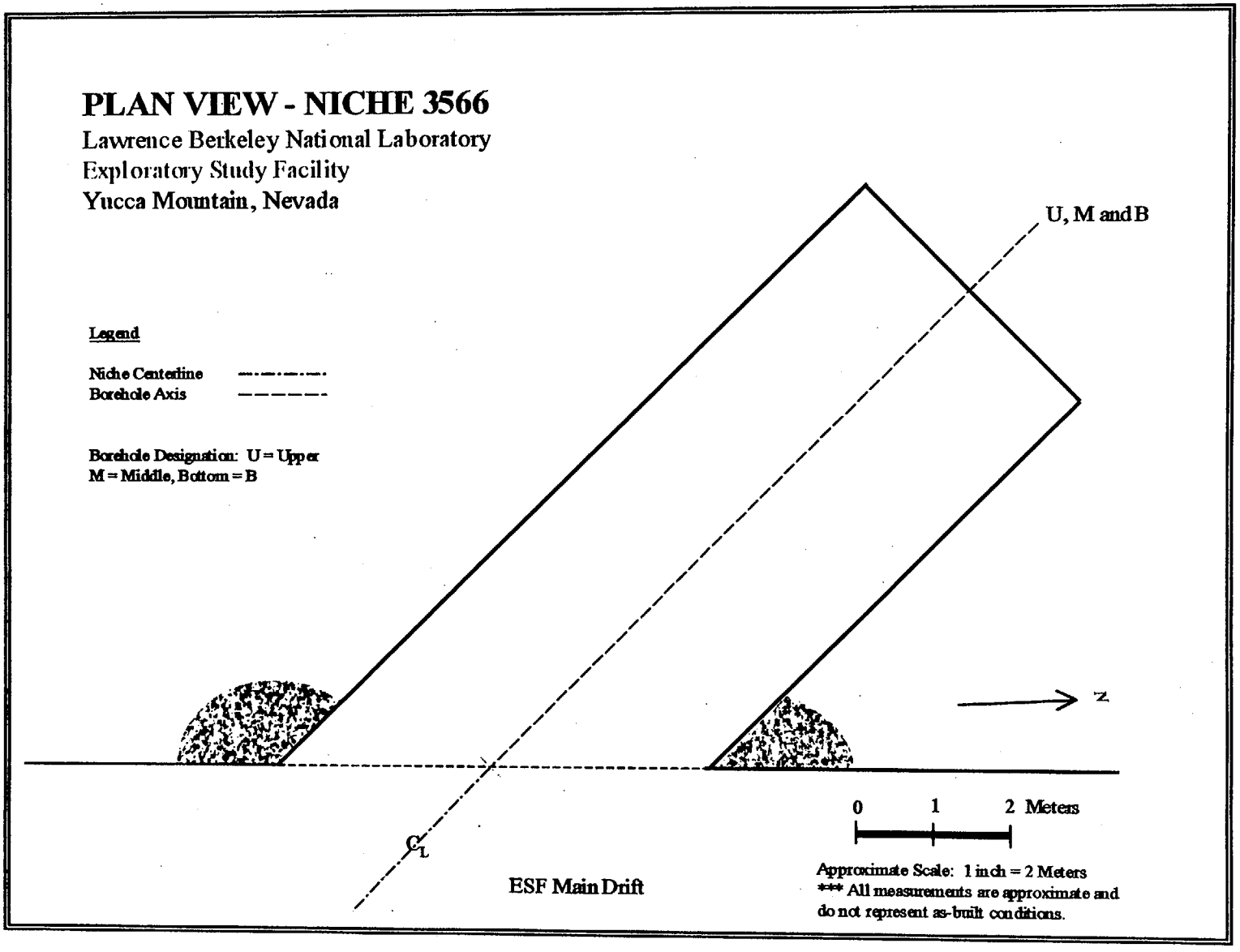
PLAN VIEW - NICHE 3566
Lawrence Berkeley National Laboratory
Exploratory Study Facility
Yucca Mountain, Nevada
U, M and B
Legend
Niche Centerline
Borehole Axis
Borehole Designation: U = Upper
M = Middle, Bottom = B
N
0 1 2 Meters
C_L
ESF Main Drift
Approximate Scale: 1 inch = 2 Meters
*** All measurements are approximate and do not represent as-built conditions.

Figure 2.9

PLAN VIEW - NICHE 3650

Lawrence Berkeley National Laboratory
Exploratory Study Facility
Yucca Mountain, Nevada

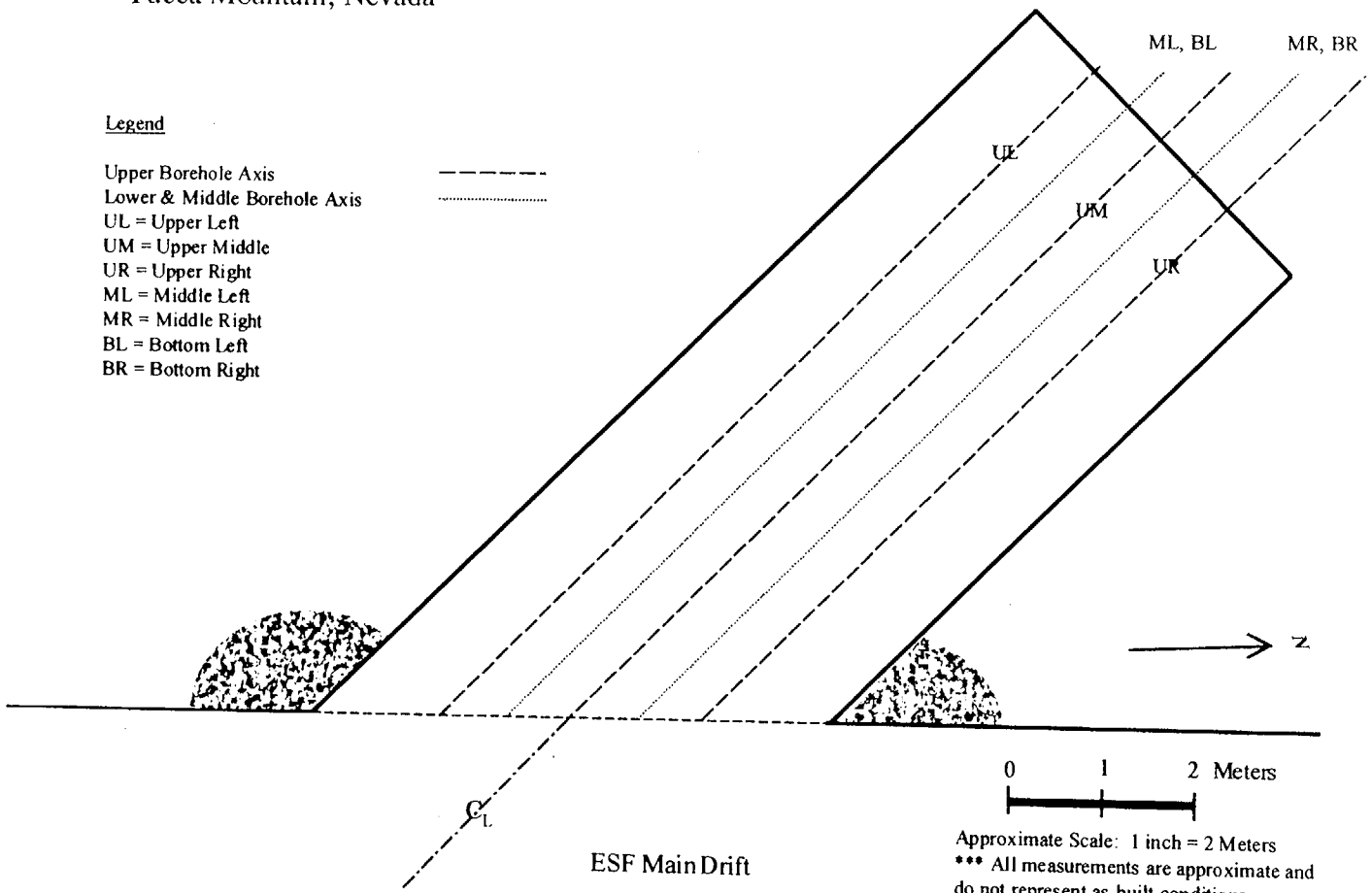

FIGURE 2.10

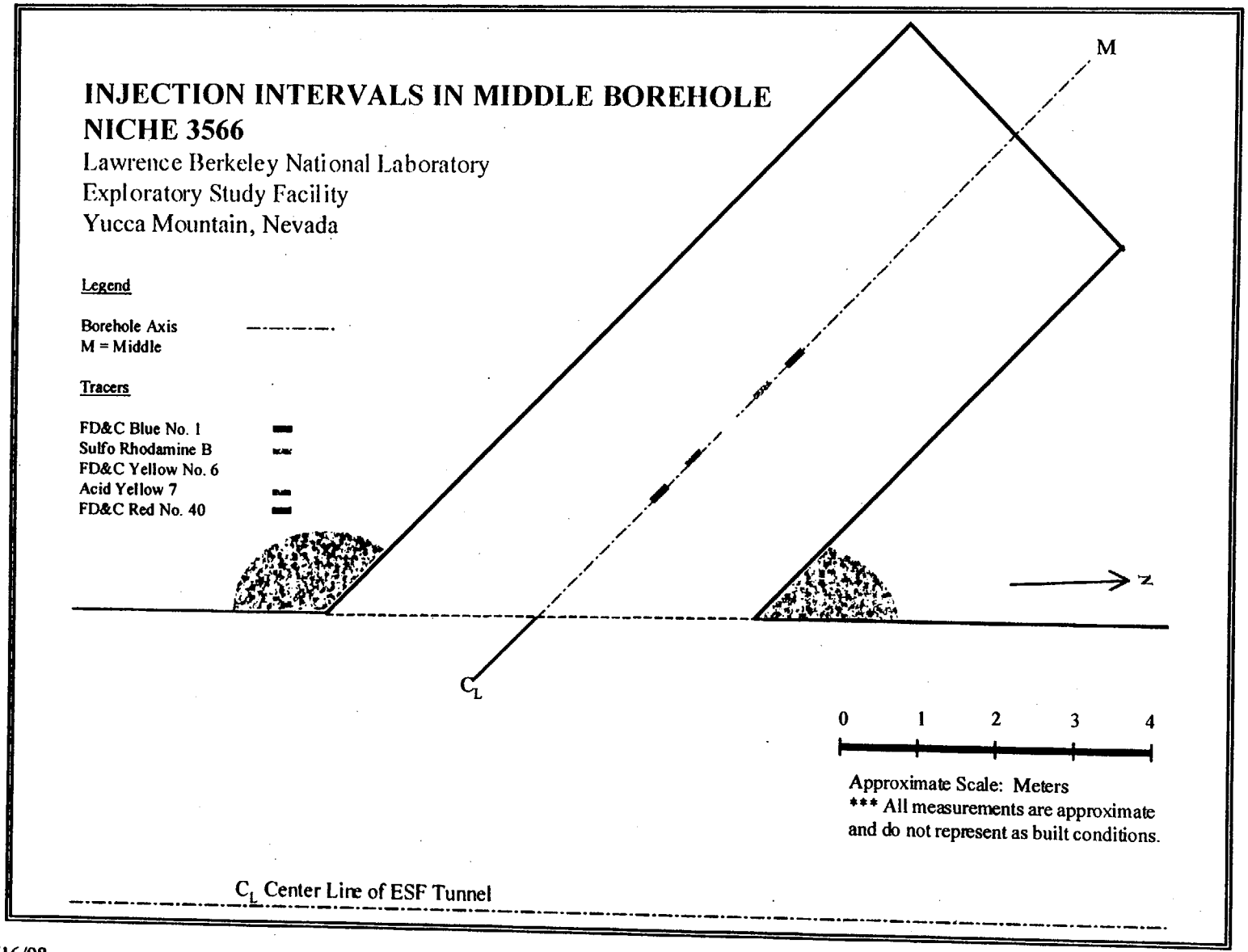
INJECTION INTERVALS IN MIDDLE BOREHOLE
NICHE 3566
Lawrence Berkeley National Laboratory
Exploratory Study Facility
Yucca Mountain, Nevada
Legend
Borehole Axis
M = Middle
Tracers
FD&C Blue No. 1
Sulfo Rhodamine B
FD&C Yellow No. 6
Acid Yellow 7
FD&C Red No. 40
M
N
C_L
0 1 2 3 4
Approximate Scale: Meters
*** All measurements are approximate and do not represent as built conditions.
C_L Center Line of ESF Tunnel

FIGURE 2.11

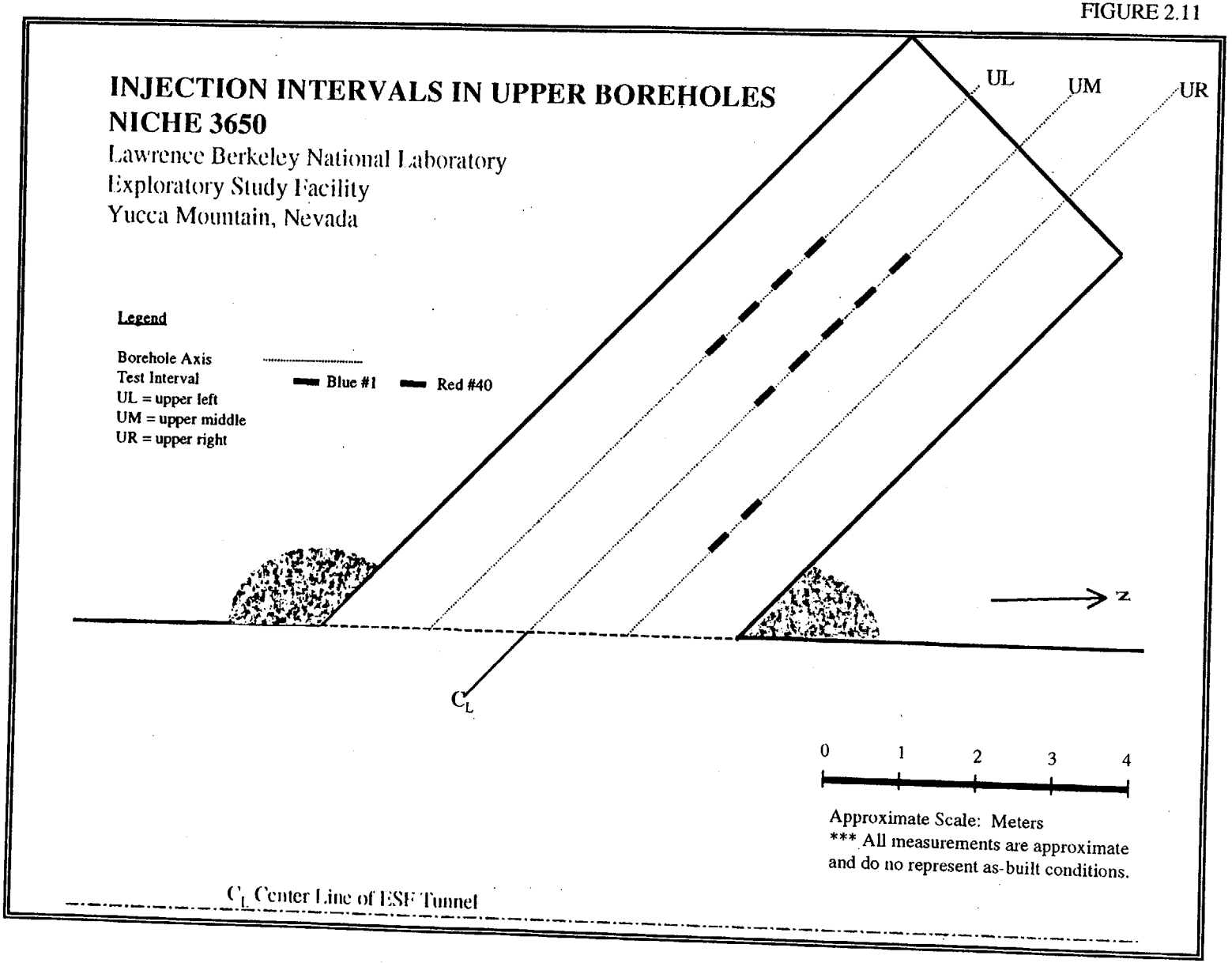

6/16/98
Version 2.0

FIGURE 2.12

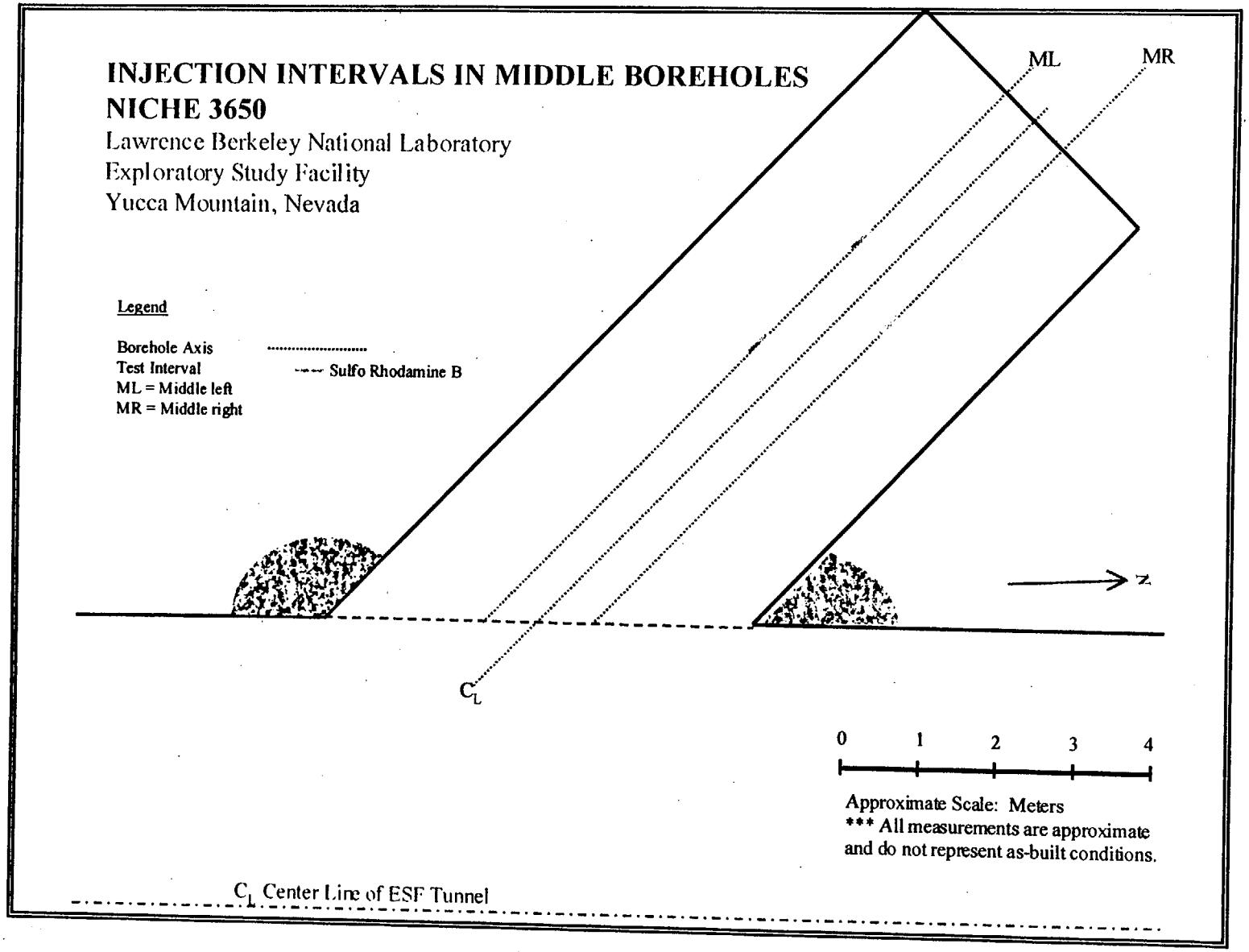
INJECTION INTERVALS IN MIDDLE BOREHOLES
NICHE 3650
Lawrence Berkeley National Laboratory
Exploratory Study Facility
Yucca Mountain, Nevada
Legend
Borehole Axis
Test Interval
ML = Middle left
MR = Middle right
Sulfo Rhodamine B
ML
MR
N
C_L
0 1 2 3 4
Approximate Scale: Meters
*** All measurements are approximate and do not represent as-built conditions.
C_L Center Line of ESF Tunnel

NICHE 3650 END VIEWS - POST EXCAVATION

Lawrence Berkeley National Laboratory
Exploratory Study Facility
Yucca Mountain, Nevada

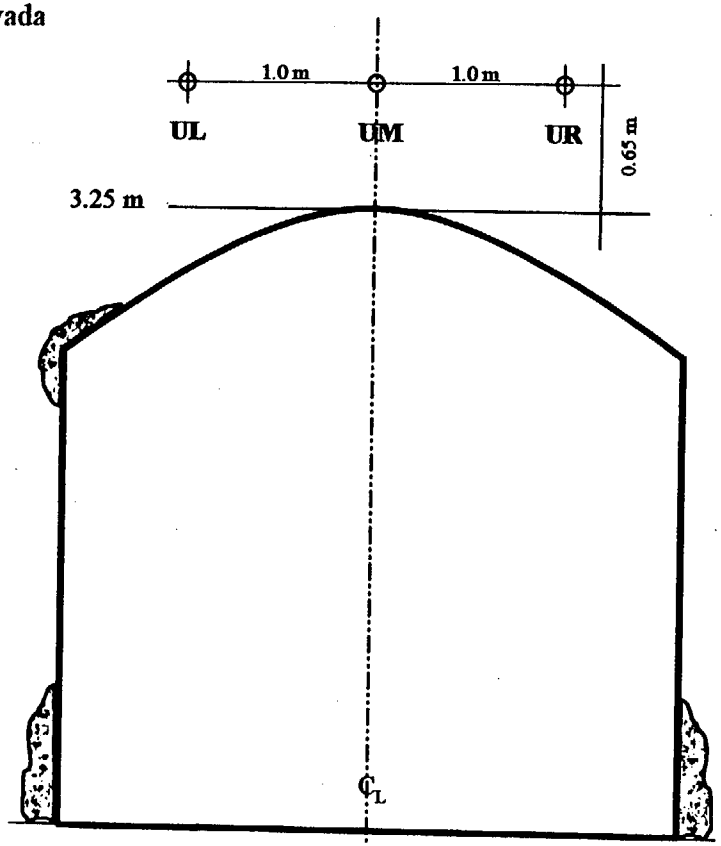

Niche 3650

Legend

UL Borehole designation
U=Upper, L = Left, R = Right

*** All measurements are approximate and do not represent as-built conditions

Figure 2.14

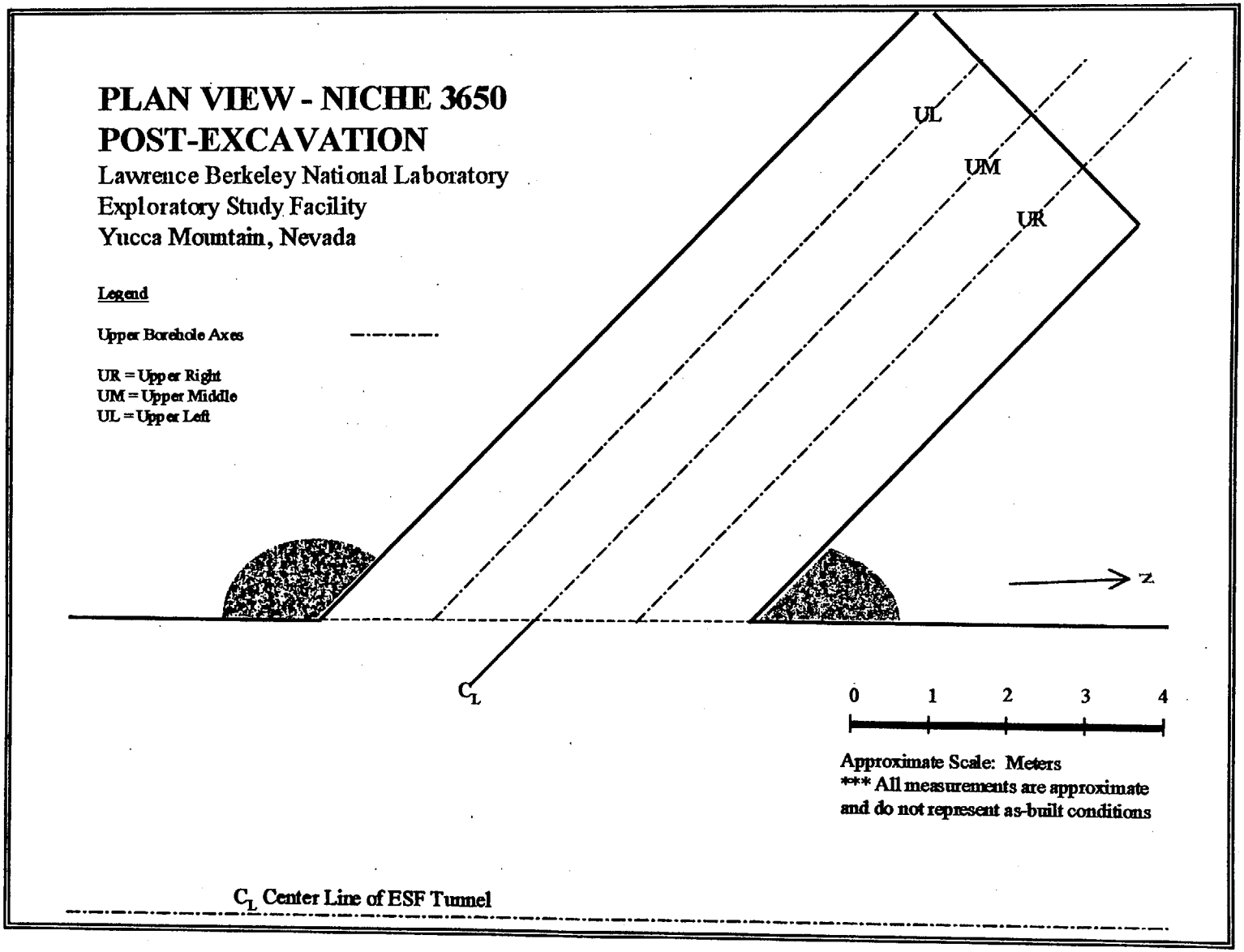
PLAN VIEW - NICHE 3650
POST-EXCAVATION
Lawrence Berkeley National Laboratory
Exploratory Study Facility
Yucca Mountain, Nevada
Legend
Upper Borehole Axes
UR = Upper Right
UM = Upper Middle
UL = Upper Left
UL
UM
UR
N
C_L
0 1 2 3 4
Approximate Scale: Meters
*** All measurements are approximate and do not represent as-built conditions
C_L Center Line of ESF Tunnel

Figure 2.15

LIQUID CAPTURE SYSTEM - NICHE 3650

Lawrence Berkeley National Laboratory
Exploratory Study Facility
Yucca Mountain, Nevada

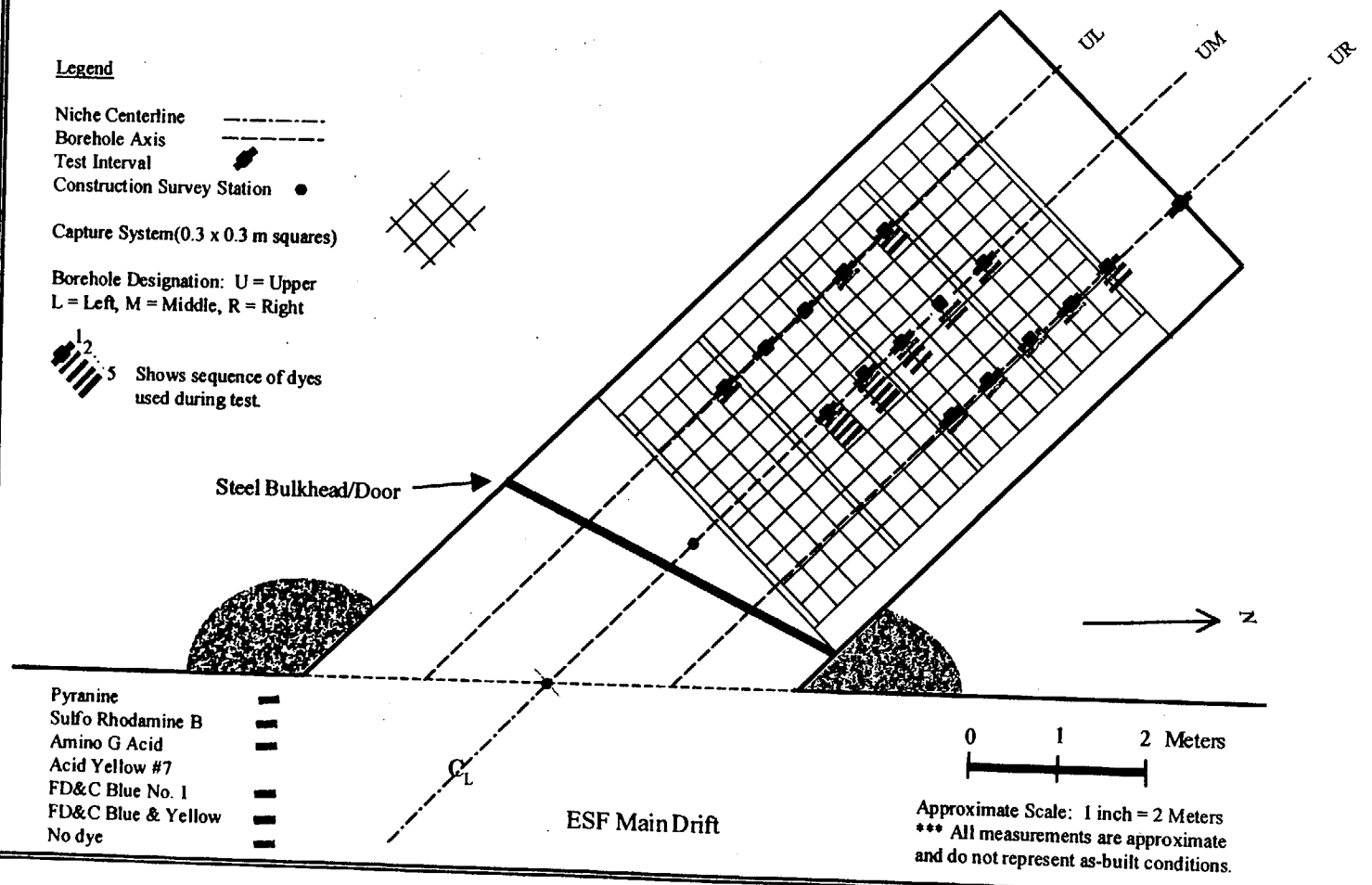

6/16/98
Version 1.0

FIGURE 2.16

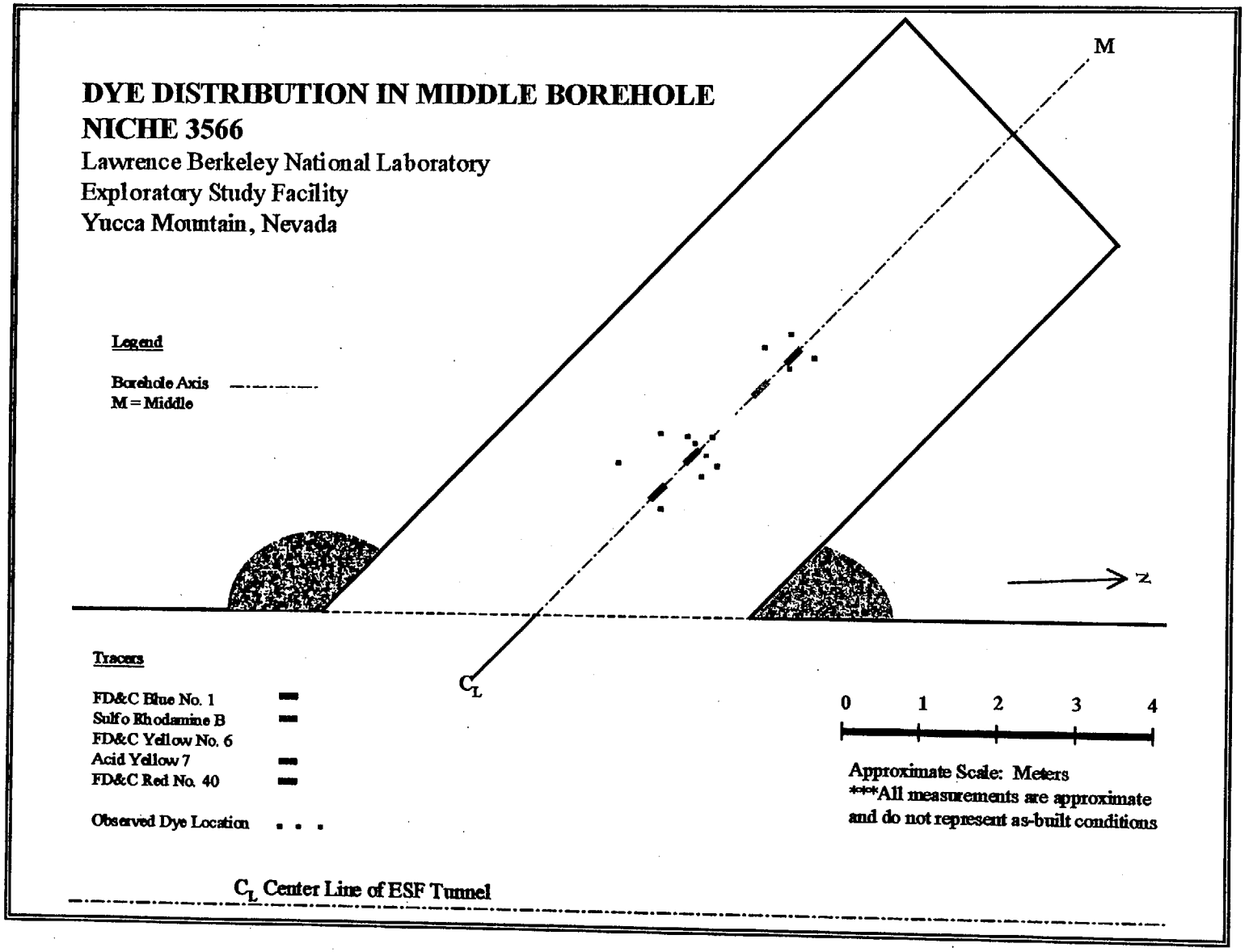
DYE DISTRIBUTION IN MIDDLE BOREHOLE
NICHE 3566
Lawrence Berkeley National Laboratory
Exploratory Study Facility
Yucca Mountain, Nevada
Legend
Borehole Axis
M = Middle
M
N
Tracers
FD&C Blue No. 1
Sulfo Rhodamine B
FD&C Yellow No. 6
Acid Yellow 7
FD&C Red No. 40
Observed Dye Location
C_L
0 1 2 3 4
Approximate Scale: Meters
***All measurements are approximate and do not represent as-built conditions
C_L Center Line of ESF Tunnel

FIGURE 2.17

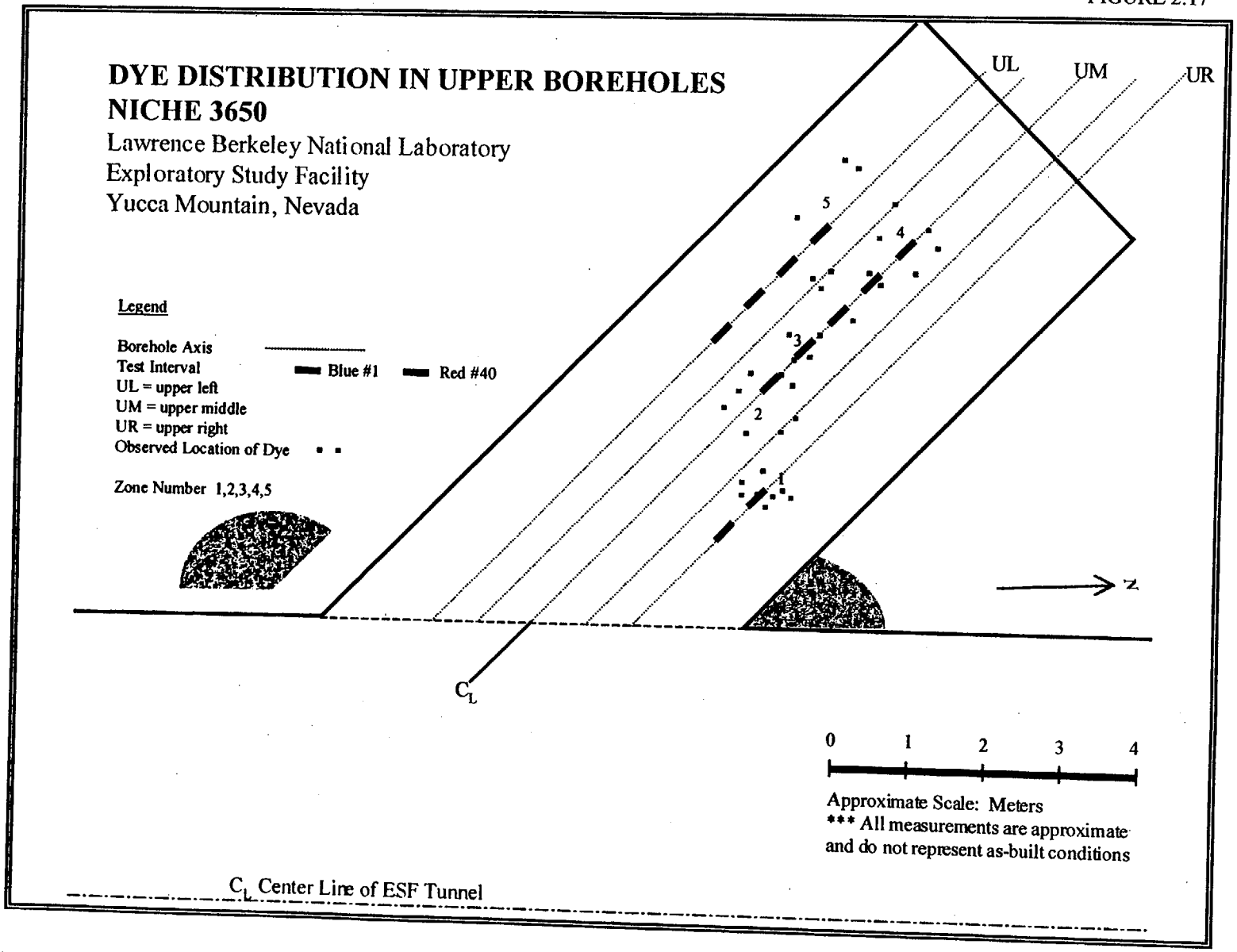
DYE DISTRIBUTION IN UPPER BOREHOLES
NICHE 3650
Lawrence Berkeley National Laboratory
Exploratory Study Facility
Yucca Mountain, Nevada
Legend
Borehole Axis
Test Interval
Blue #1
Red #40
UL = upper left
UM = upper middle
UR = upper right
Observed Location of Dye
Zone Number 1,2,3,4,5
UL
UM
UR
5
4
3
2
1
N
C_L
0
1
2
3
4
Approximate Scale: Meters
*** All measurements are approximate and do not represent as-built conditions
C_L Center Line of ESF Tunnel

FIGURE 2.18

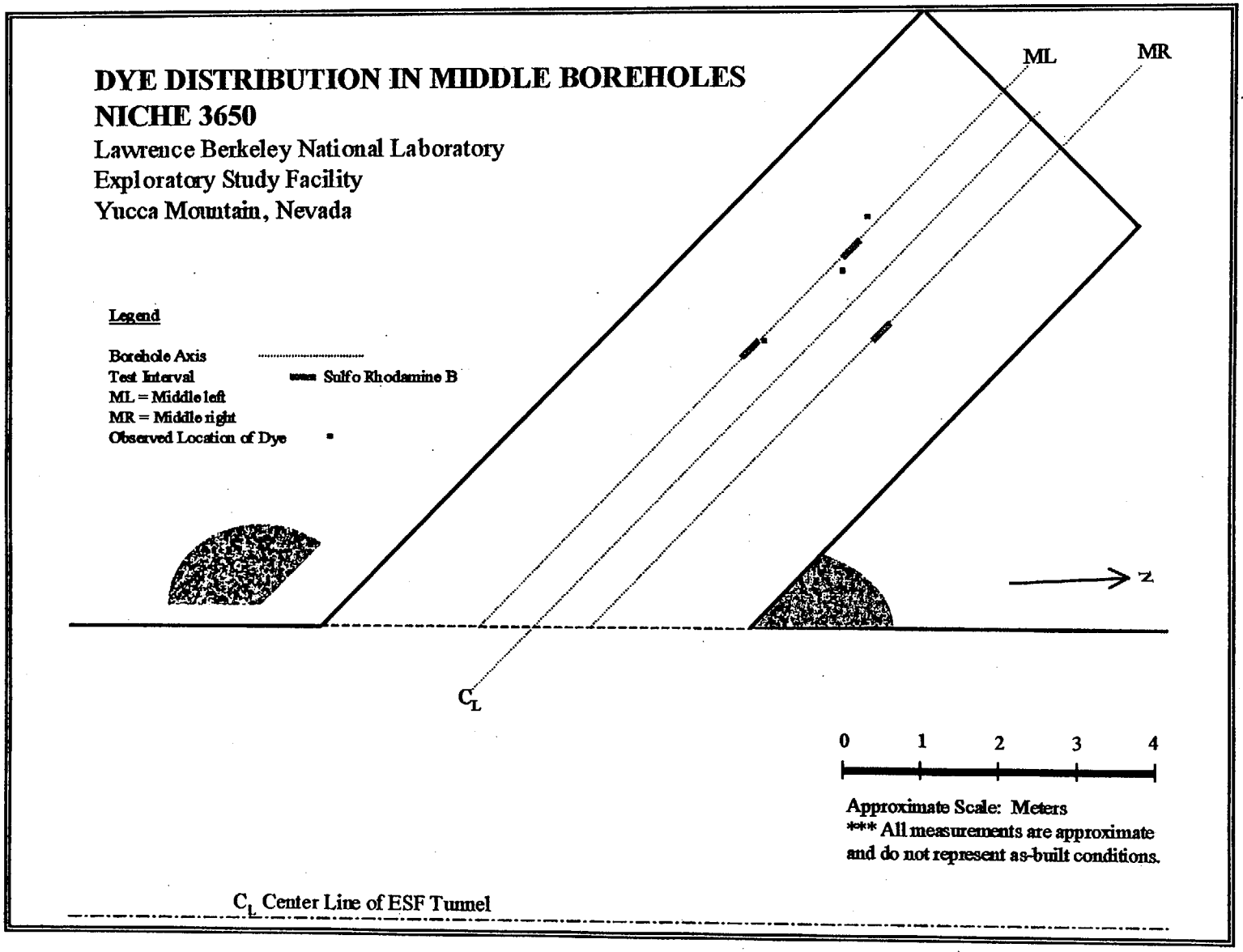
DYE DISTRIBUTION IN MIDDLE BOREHOLES
NICHE 3650
Lawrence Berkeley National Laboratory
Exploratory Study Facility
Yucca Mountain, Nevada
Legend
Borehole Axis
Test Interval
Sulfo Rhodamine B
ML = Middle left
MR = Middle right
Observed Location of Dye
ML
MR
N
C_L
0 1 2 3 4
Approximate Scale: Meters
*** All measurements are approximate and do not represent as-built conditions.
C_L Center Line of ESF Tunnel

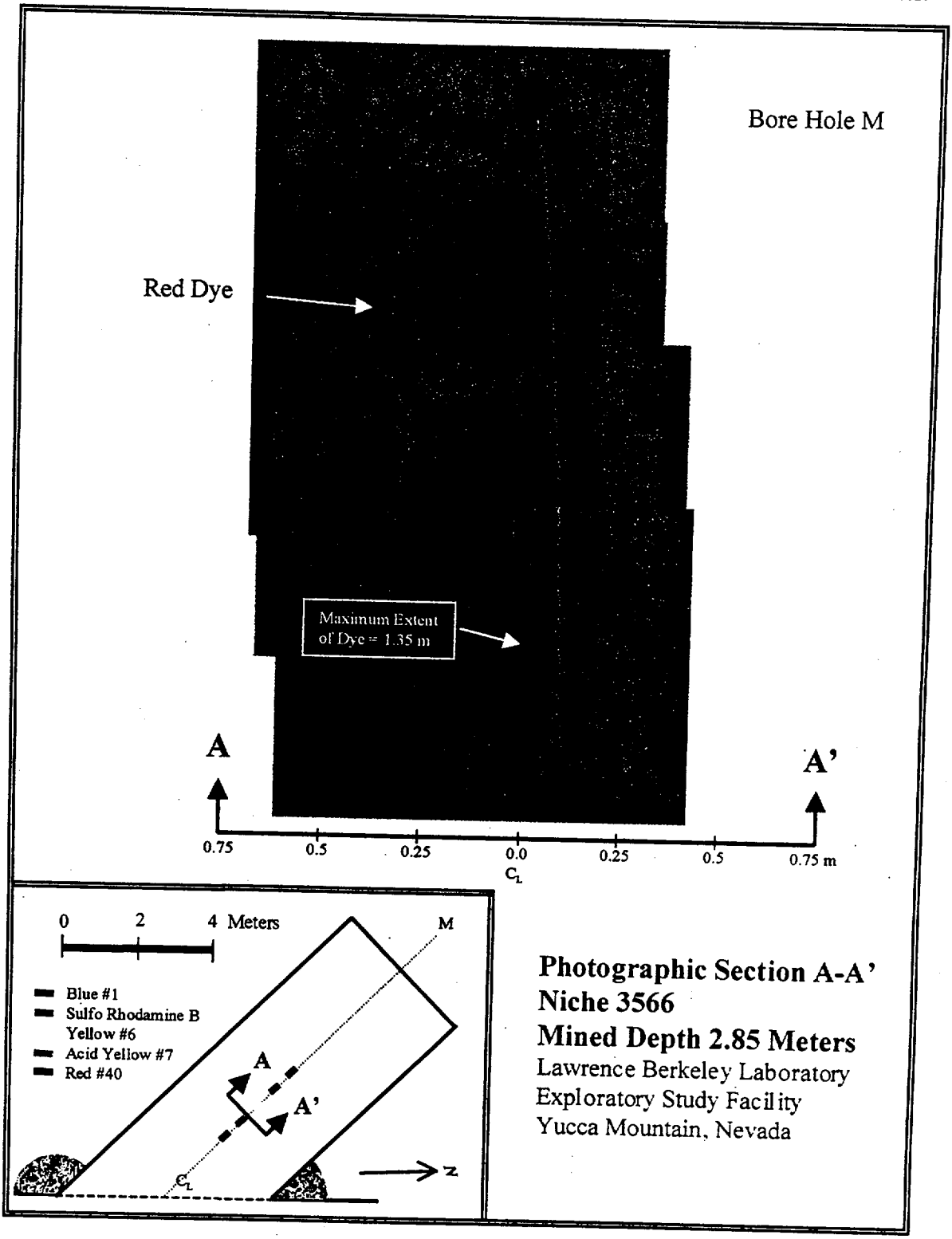

Photographic Section A-A'
Niche 3566
Mined Depth 2.85 Meters
Lawrence Berkeley Laboratory
Exploratory Study Facility
Yucca Mountain, Nevada

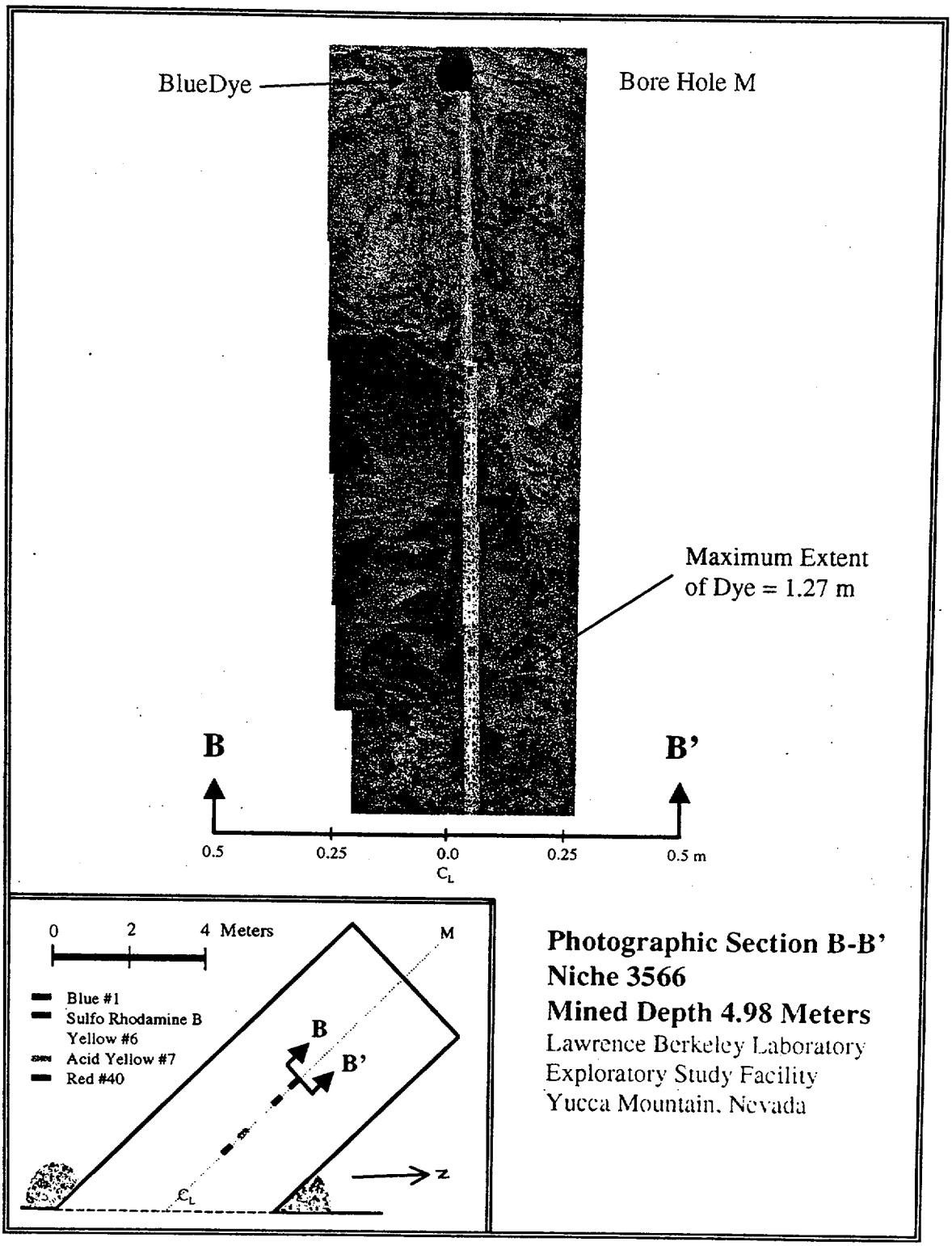

Photographic Section B-B'
Niche 3566
Mined Depth 4.98 Meters
Lawrence Berkeley Laboratory
Exploratory Study Facility
Yucca Mountain, Nevada

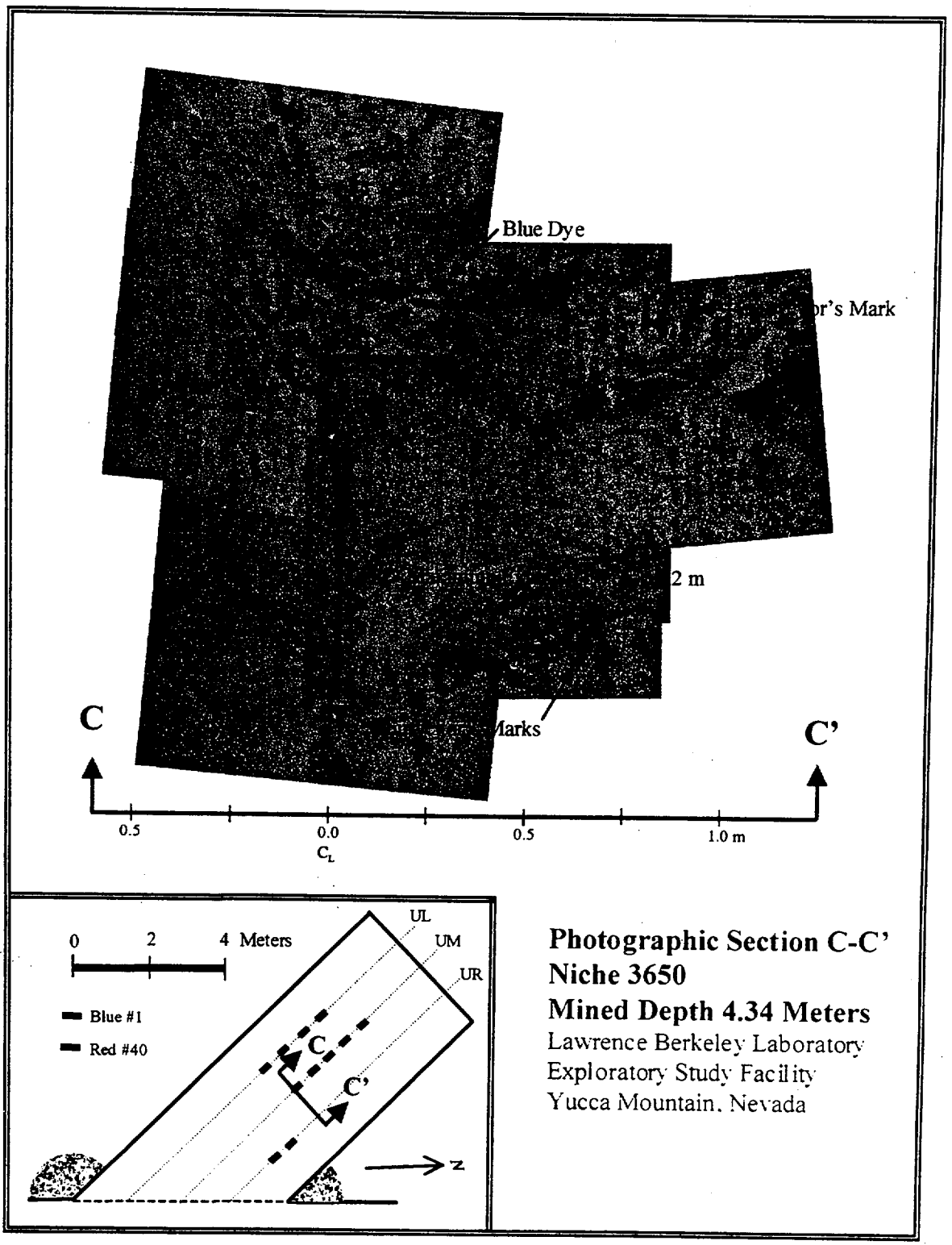

Photographic Section C-C'
Niche 3650
Mined Depth 4.34 Meters
Lawrence Berkeley Laboratory
Exploratory Study Facility
Yucca Mountain, Nevada

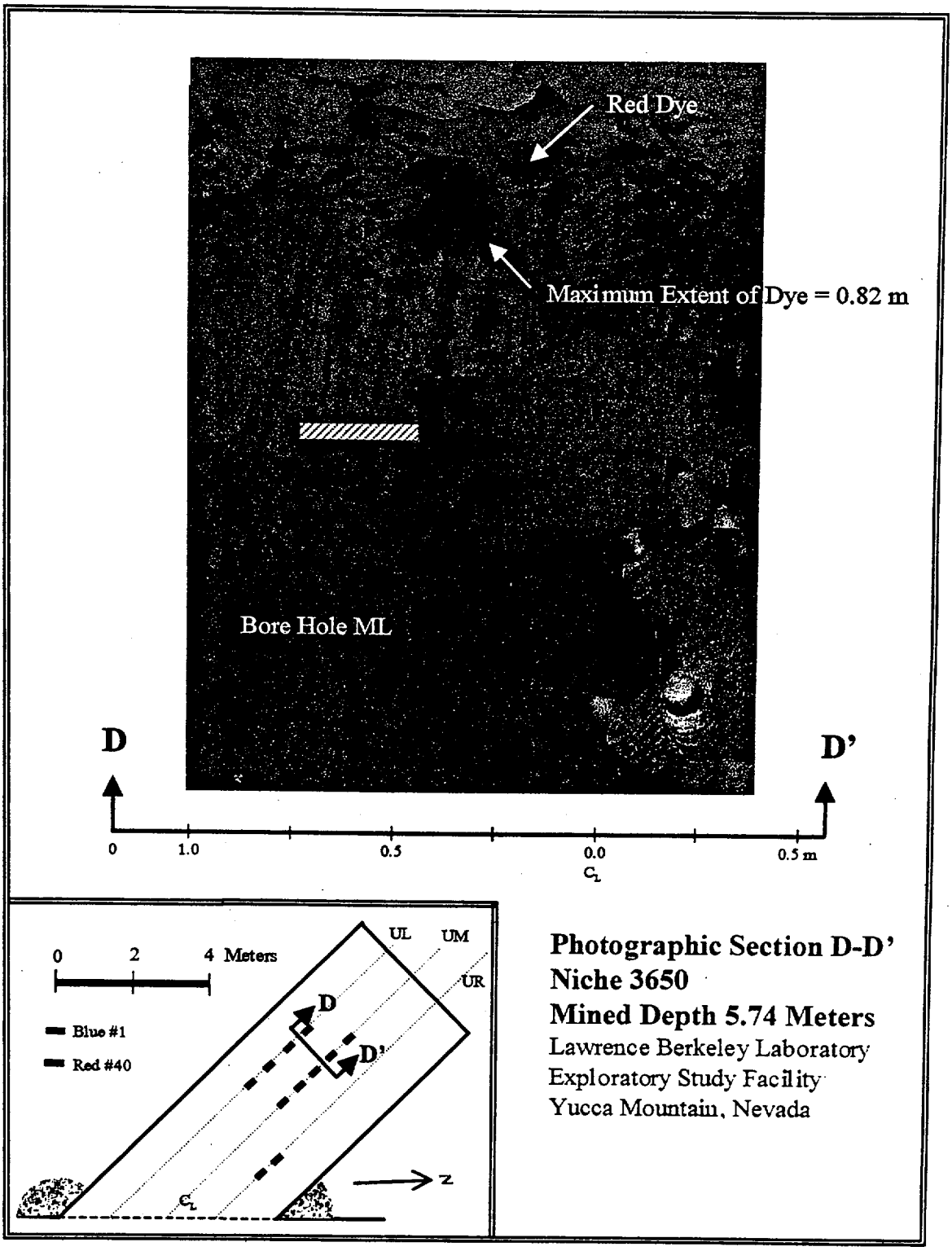

Photographic Section D-D'
Niche 3650
Mined Depth 5.74 Meters
Lawrence Berkeley Laboratory
Exploratory Study Facility
Yucca Mountain, Nevada

FIGURE 2.23

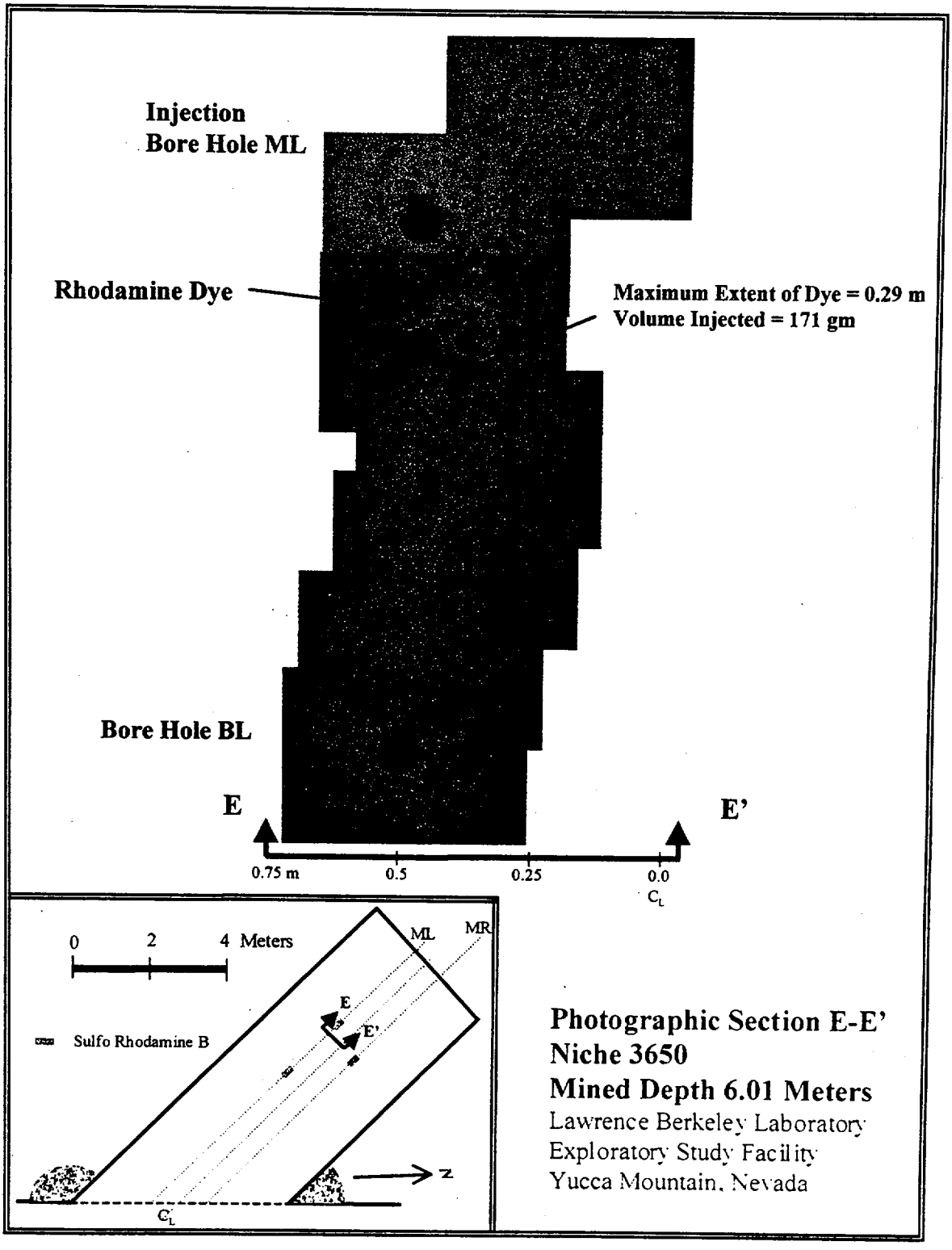
Injection
Bore Hole ML
Rhodamine Dye
Maximum Extent of Dye = 0.29 m
Volume Injected = 171 gm
Bore Hole BL
E
E'
0.75 m
0.5
0.25
0.0
C_L
0
2
4 Meters
ML
MR
E
E'
Sulfo Rhodamine B
z
C_L
Photographic Section E-E'
Niche 3650
Mined Depth 6.01 Meters
Lawrence Berkeley Laboratory
Exploratory Study Facility
Yucca Mountain, Nevada

Figure 2.24 - Mass of Water Released vs. Maximum Depth of Dye Penetration

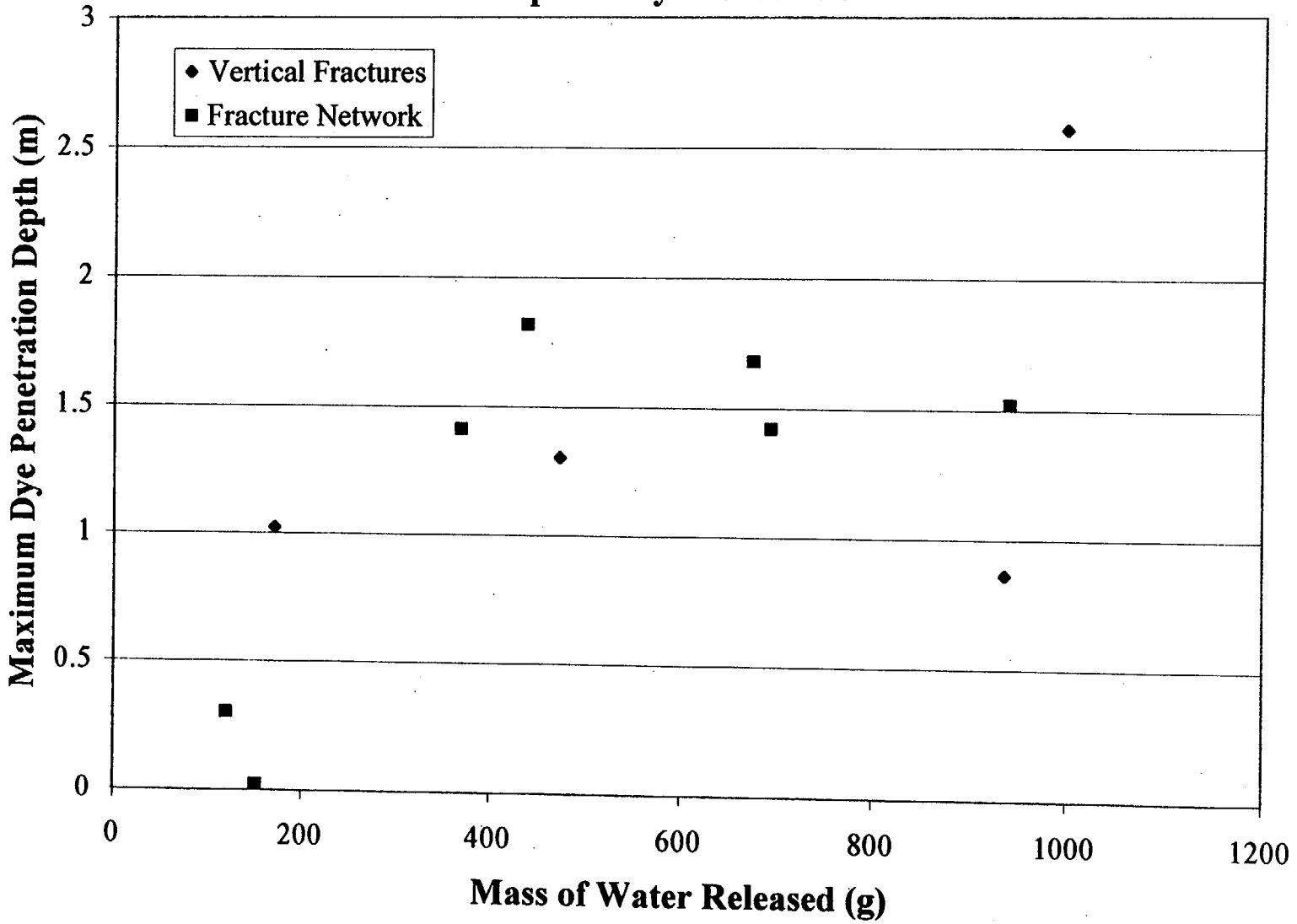

Figure 2.25 - Mass Water Released vs. Maximum Lateral DistanceTraveled by Dye

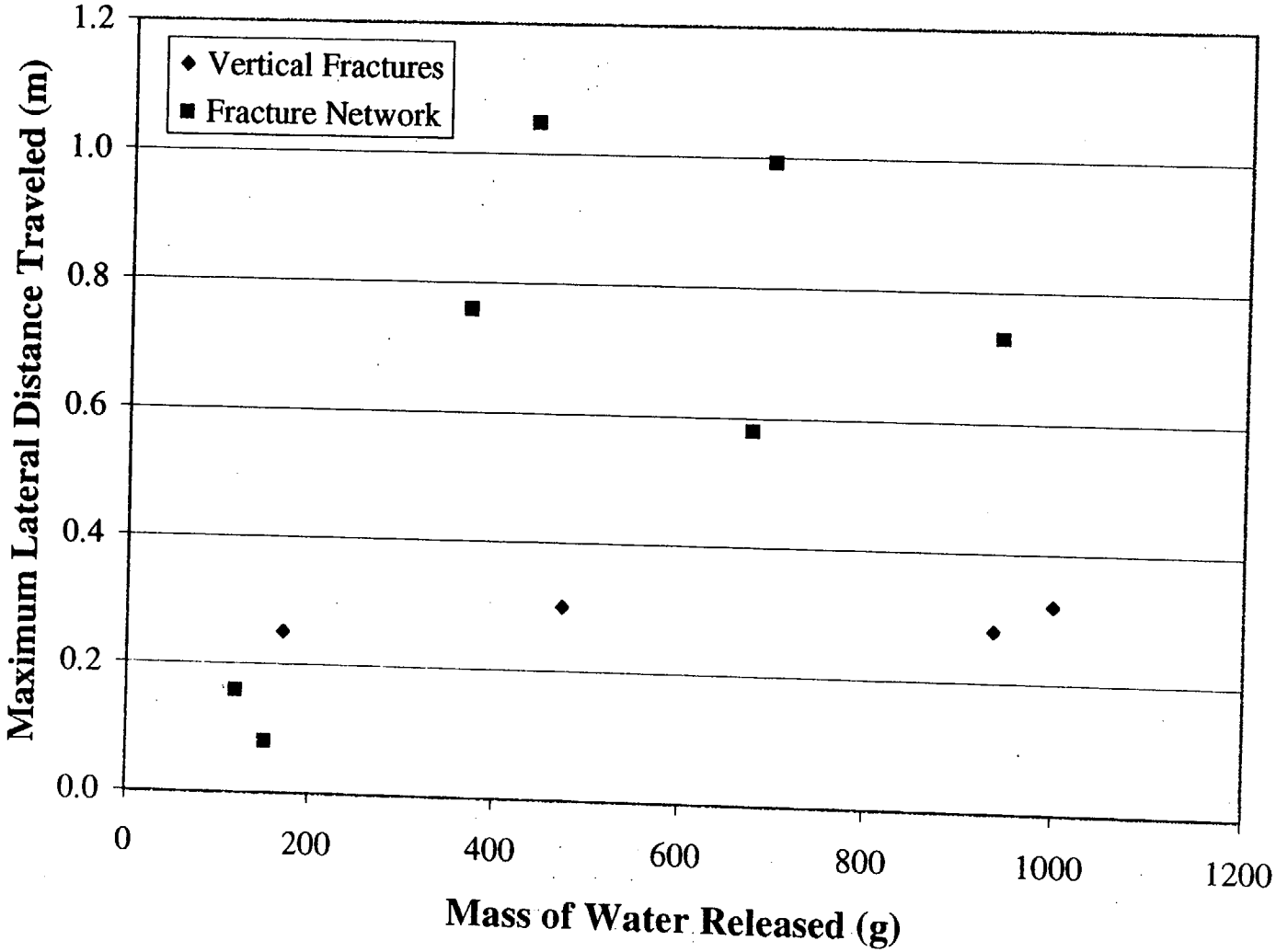

Figure 2.26 - Mass of Water Released vs. Maximum Distance Dye Traveled

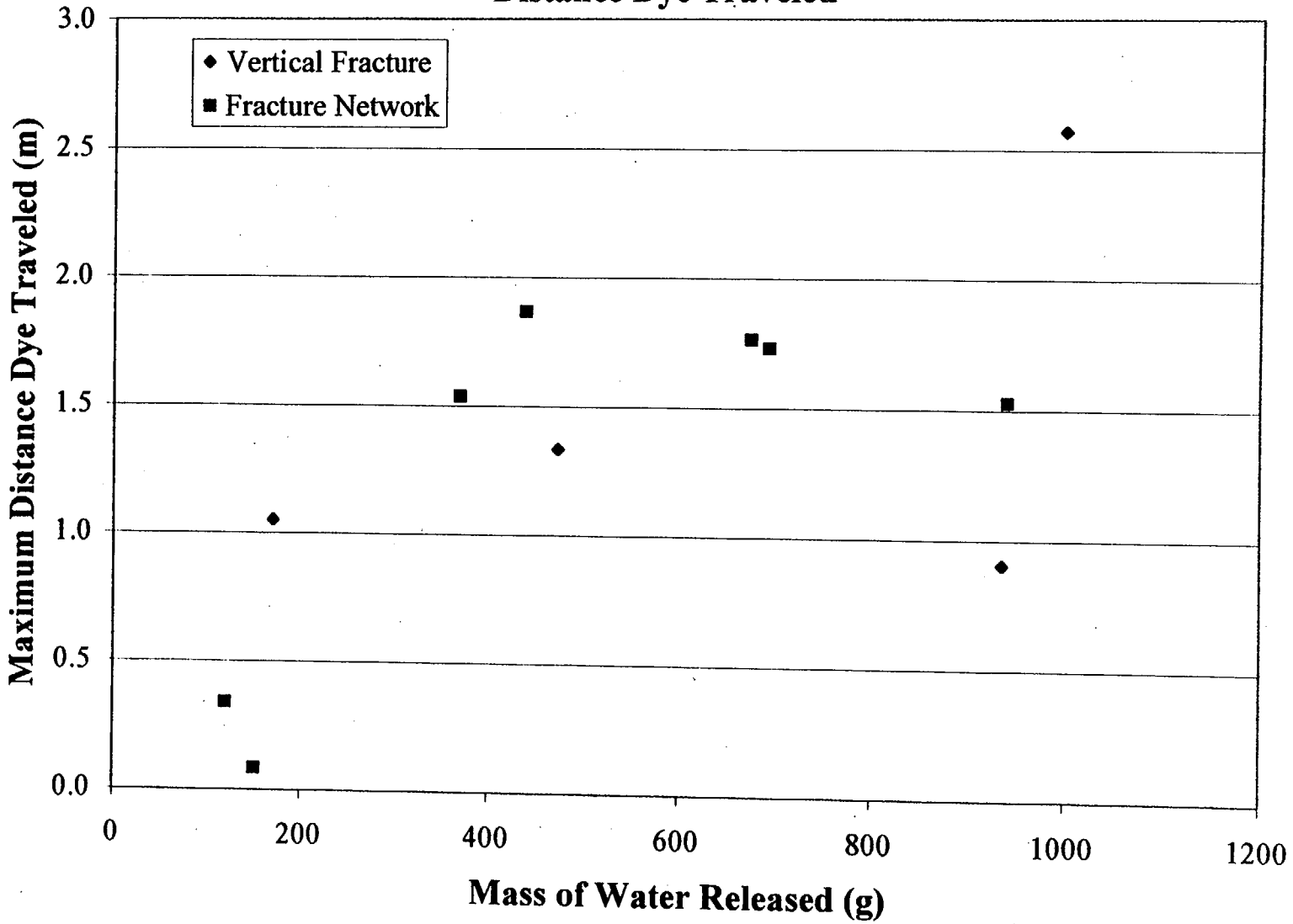

Figrue 2.27 - Mass Water Released vs. Aspect Ratio

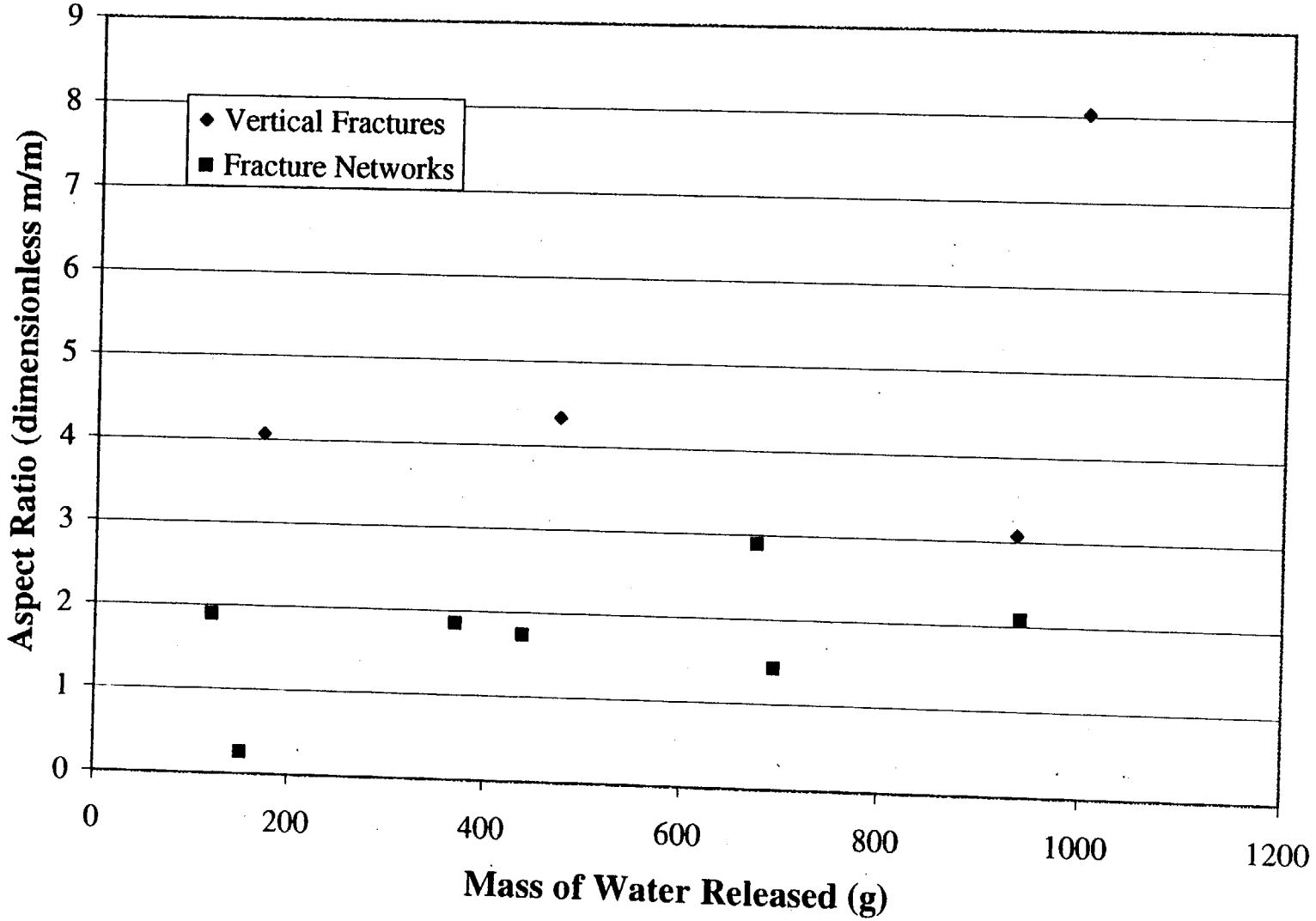

Liquid-Release Rate vs. Seepage Percentage
Niche 3650 Borehole UM: 4.27-4.57 m

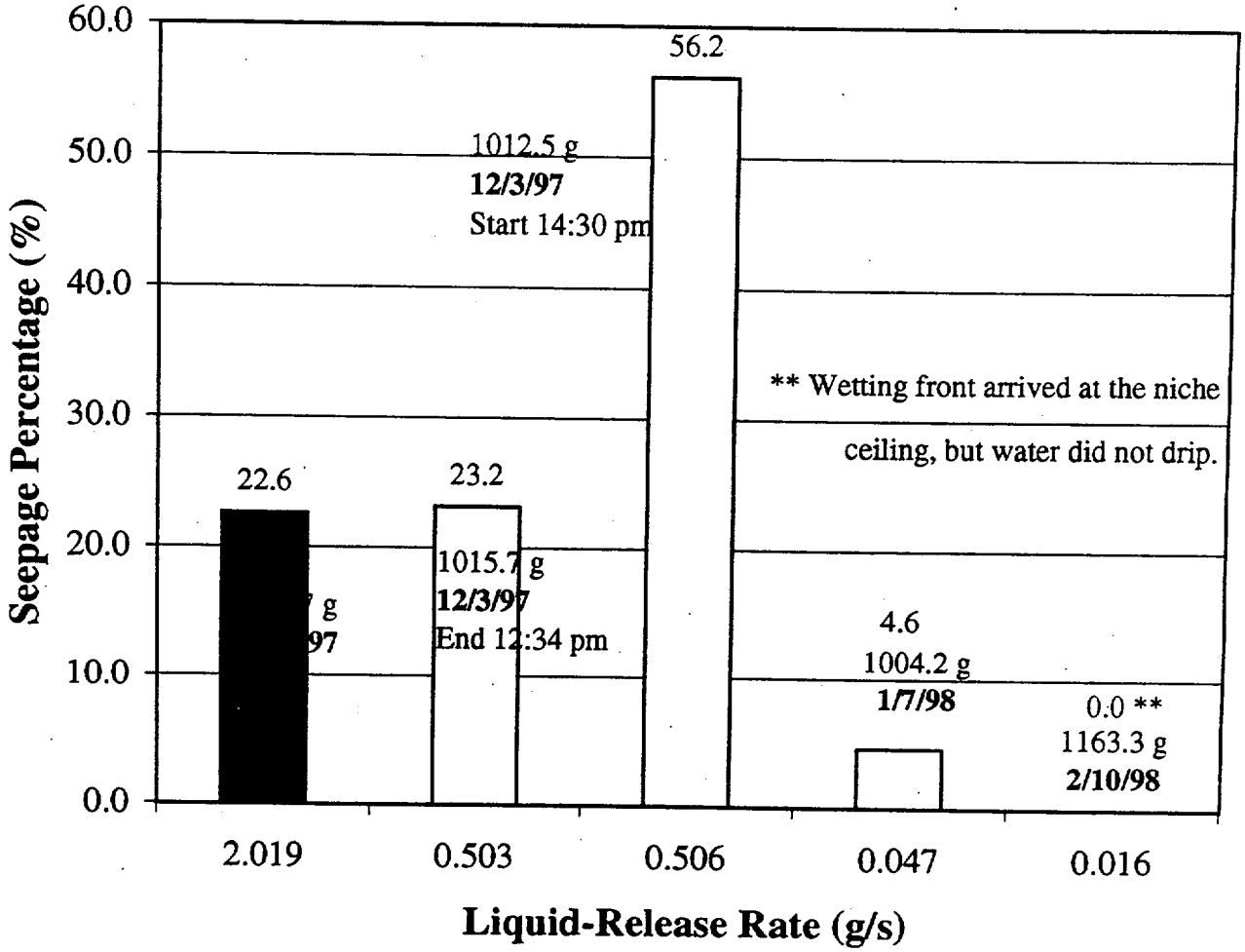

Liquid-Release Rate vs. Seepage Percentage
Niche 3650 Borehole UM: 4.88 - 5.18 m

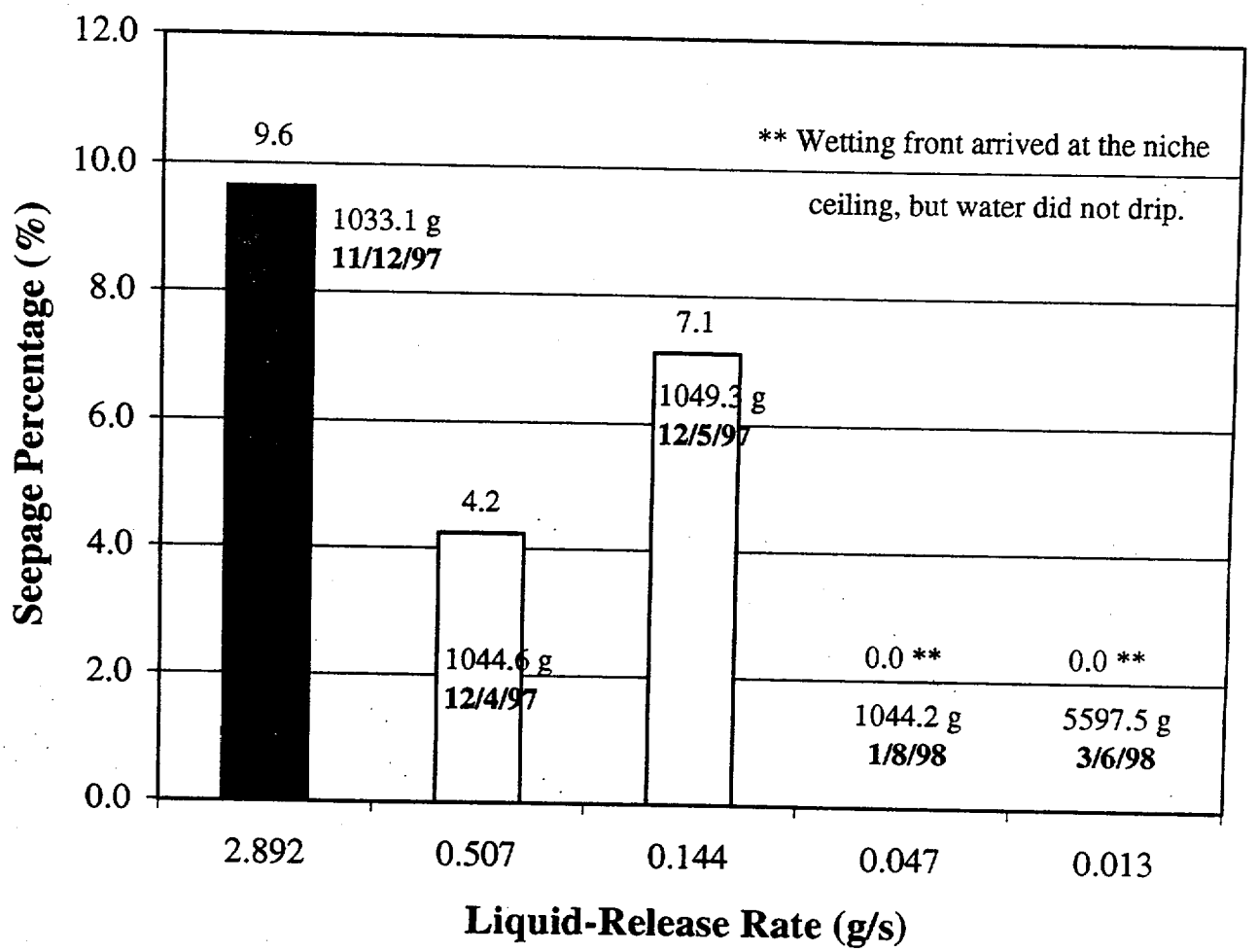

Liquid-Release Rate versus Seepage Percentage
Niche 3650 - All Data

Figure 2.30

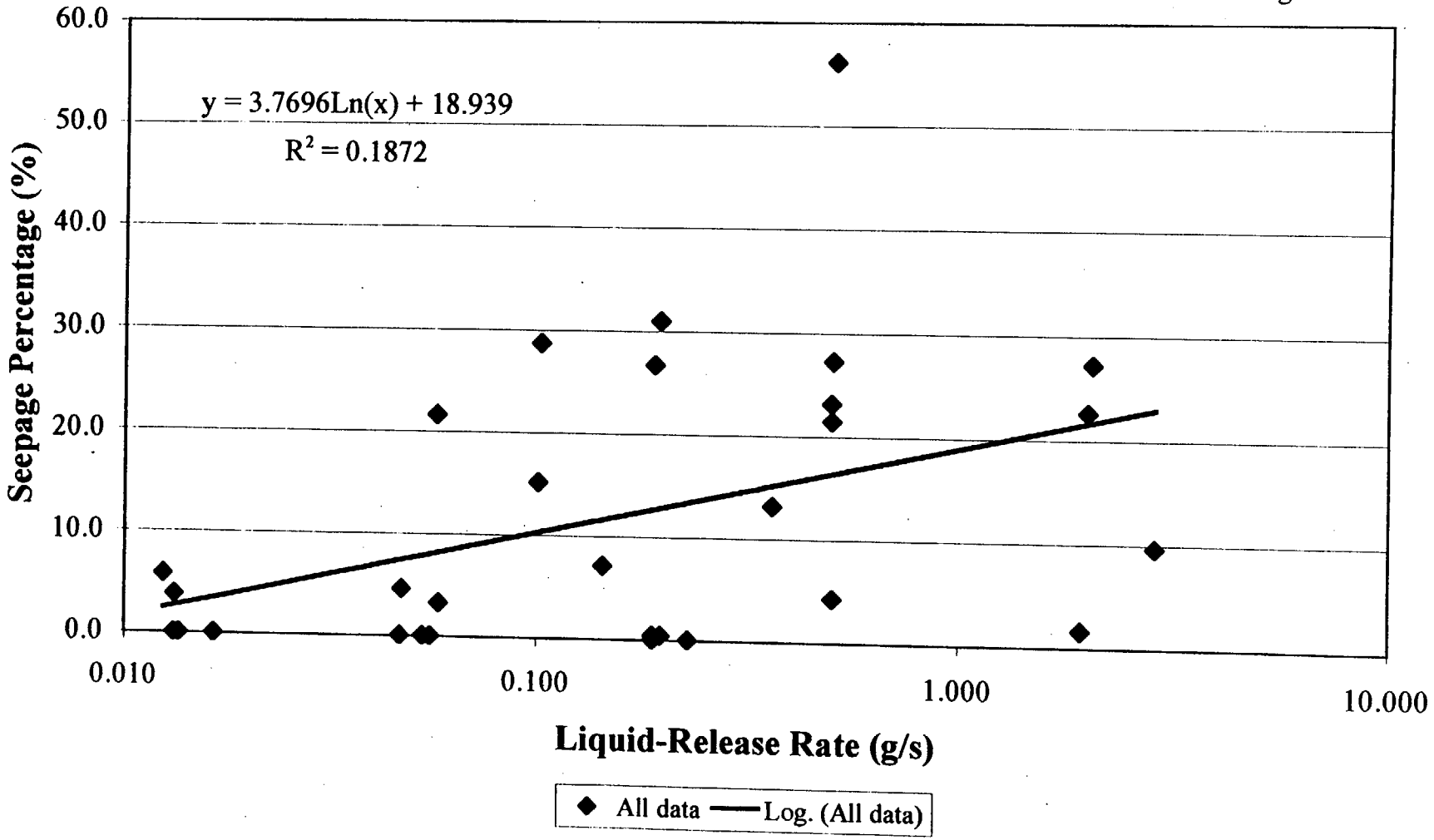

Liquid-Release Flux versus Seepage Percentage
Niche 3650 - All Data

Figure 2.31

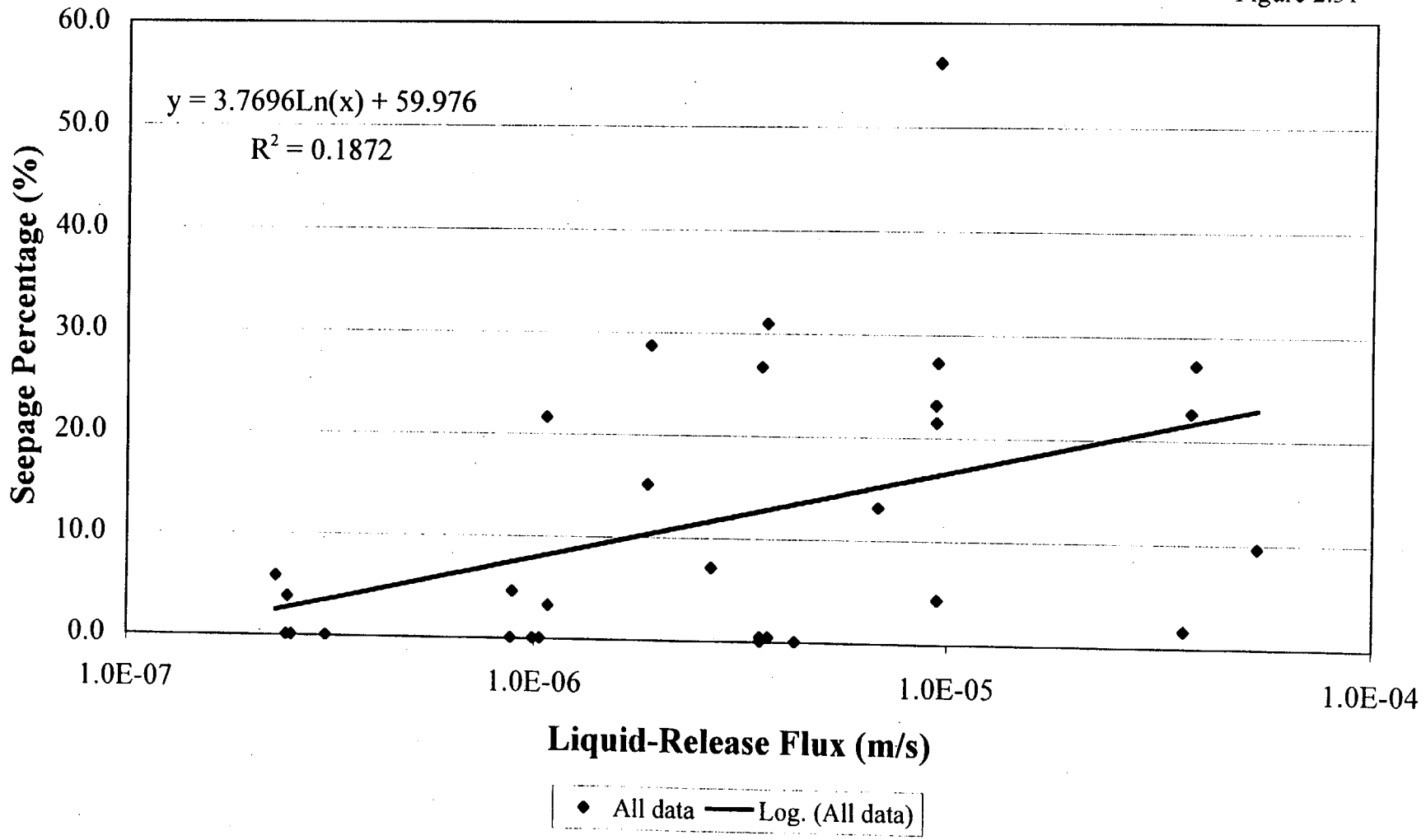

Seepage Threshold Flux

Figure 2.32

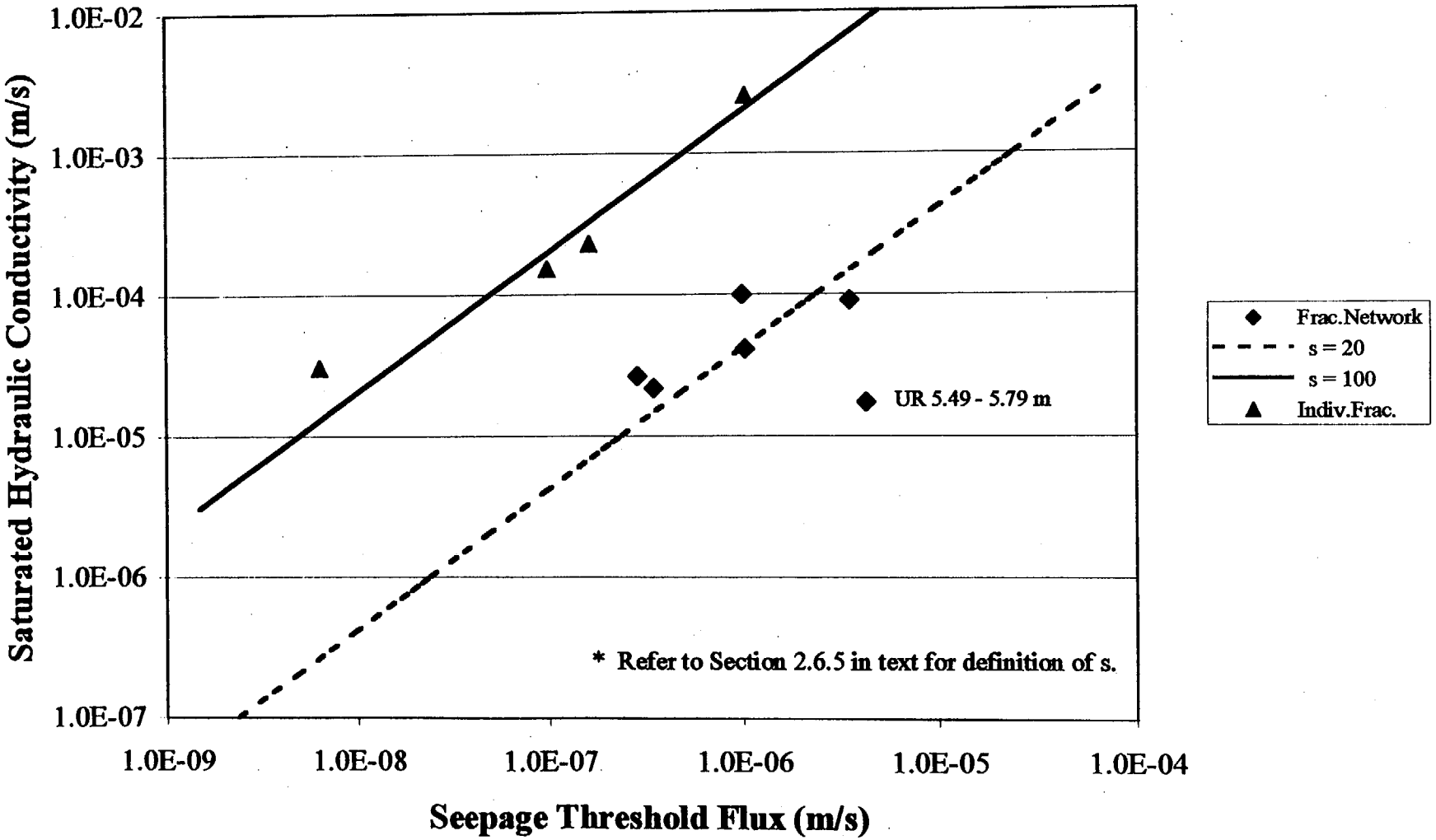

First Arrival Locations for Two Liquid Release Tests

Niche 3650 Borehole UR: 4.27-4.57 m

Lawrence Berkeley National Laboratory

Figure 2.33

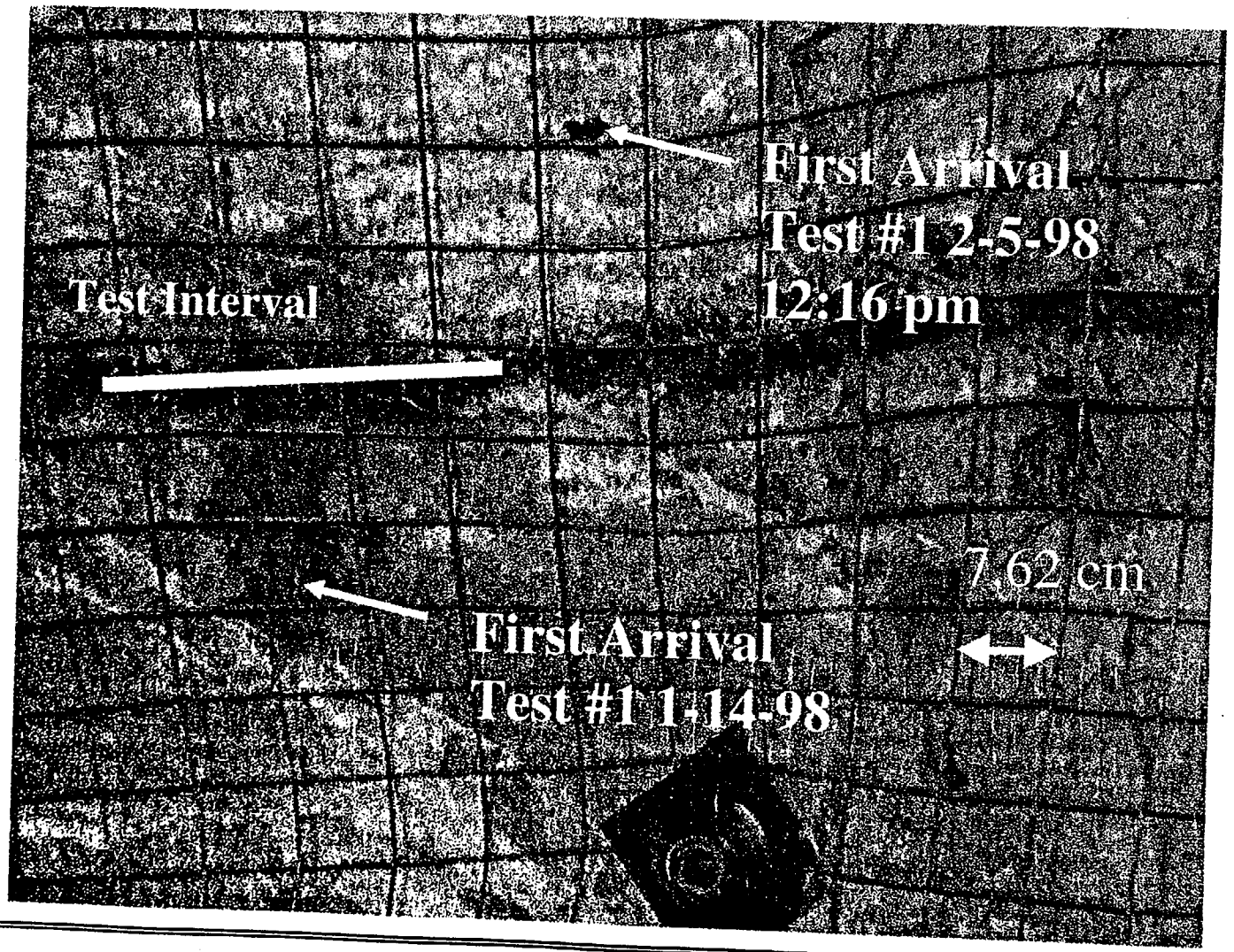

Wetting Front Spreading Caused by Capillary Barrier

Niche 3650 Borehole UR: 4.27-4.57 m

Lawrence Berkeley National Laboratory

Figure 2.34

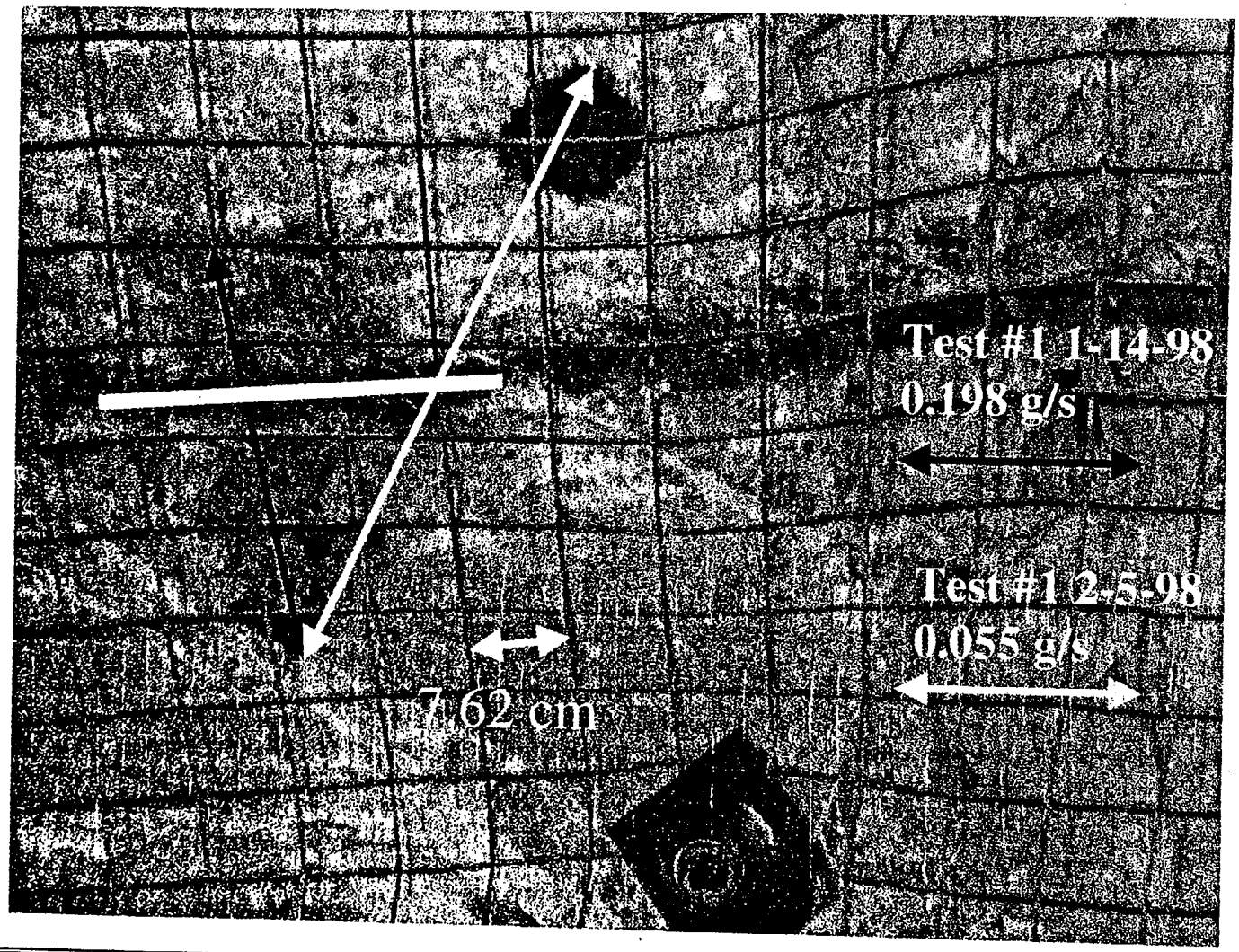

Figure 2.35

END VIEW SHOWING BREAKOUT

Lawrence Berkeley National Laboratory
Exploratory Study Facility
Yucca Mountain, Nevada

Legend

ML Borehole designation
B = Bottom, M = Middle, U=Upper
L = Left, R = Right

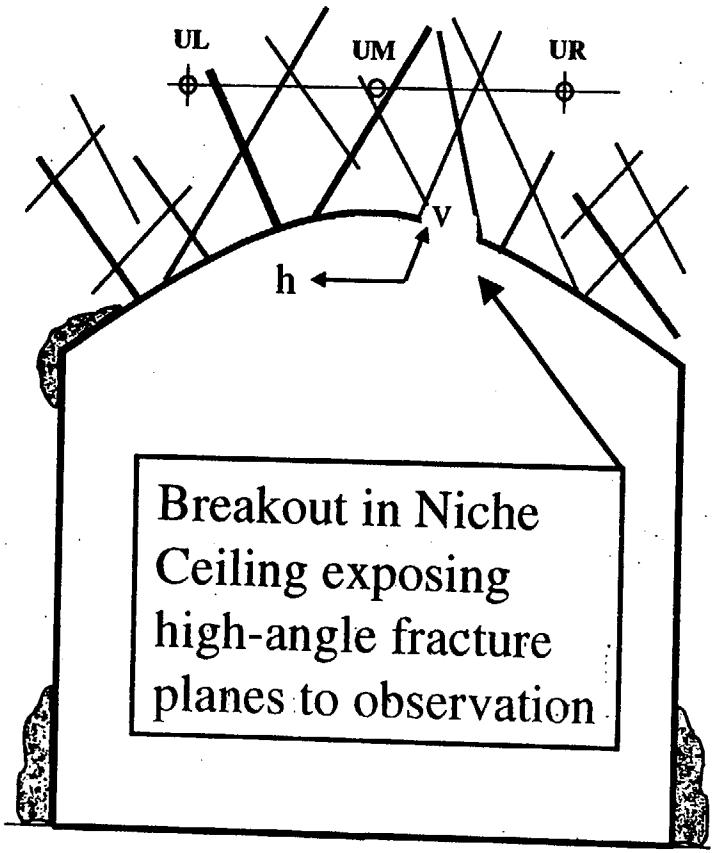

} Fractures

Niche 3650

Saturation Increases as Capillary Barrier Forms

Figure 2.36

Niche 3650 Borehole UM: 5.49-5.79 m, Time = 12:42:40 p.m.

Lawrence Berkeley National Laboratory

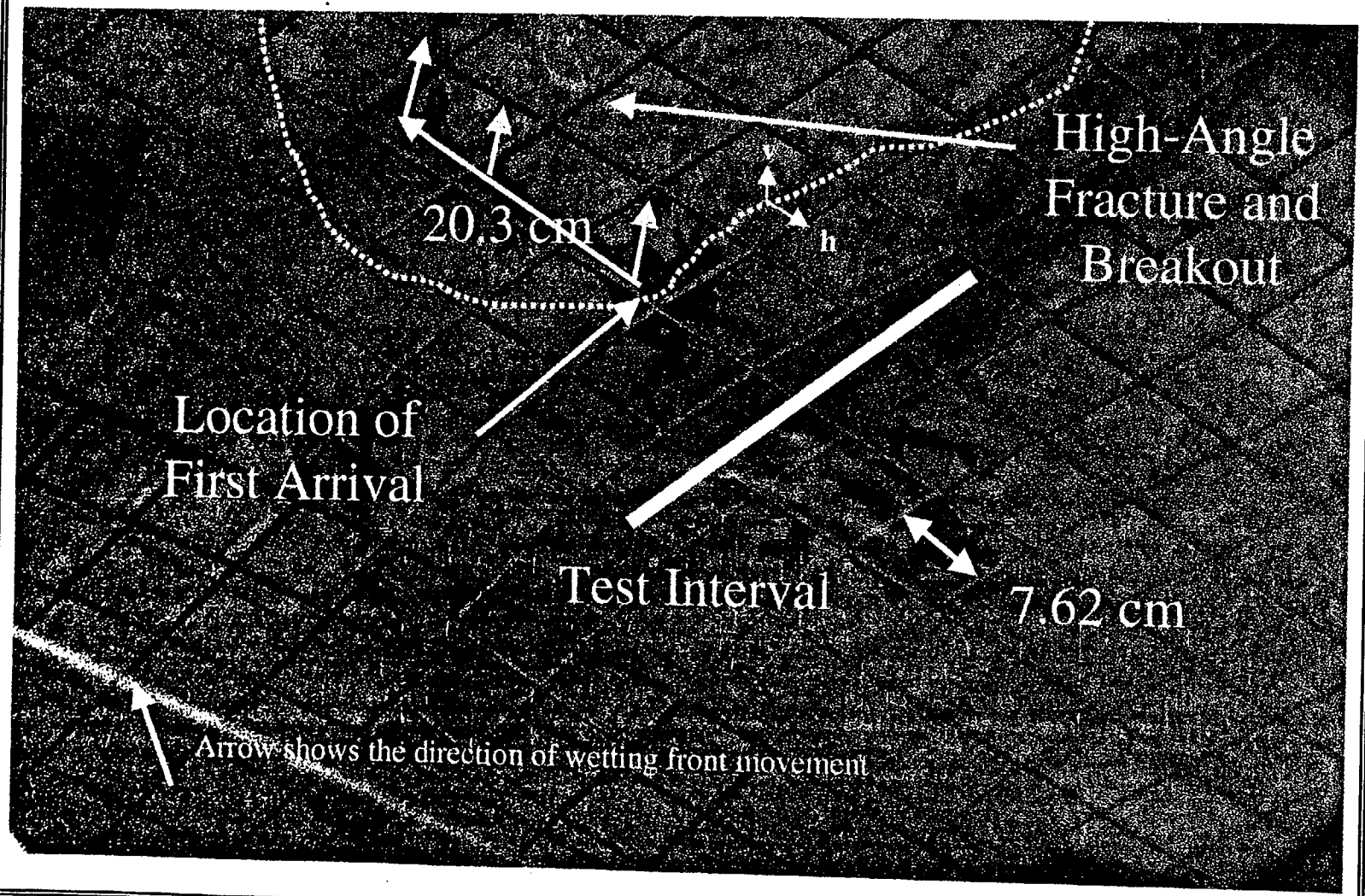

6/16/98
Version 1.0

Capillary Barrier Collapses and Dripping Begins

Niche 3650 Borehole UM: 5.49-5.79 m, Time = 12:44:22 p.m.

Lawrence Berkeley National Laboratory

Figure 2.37

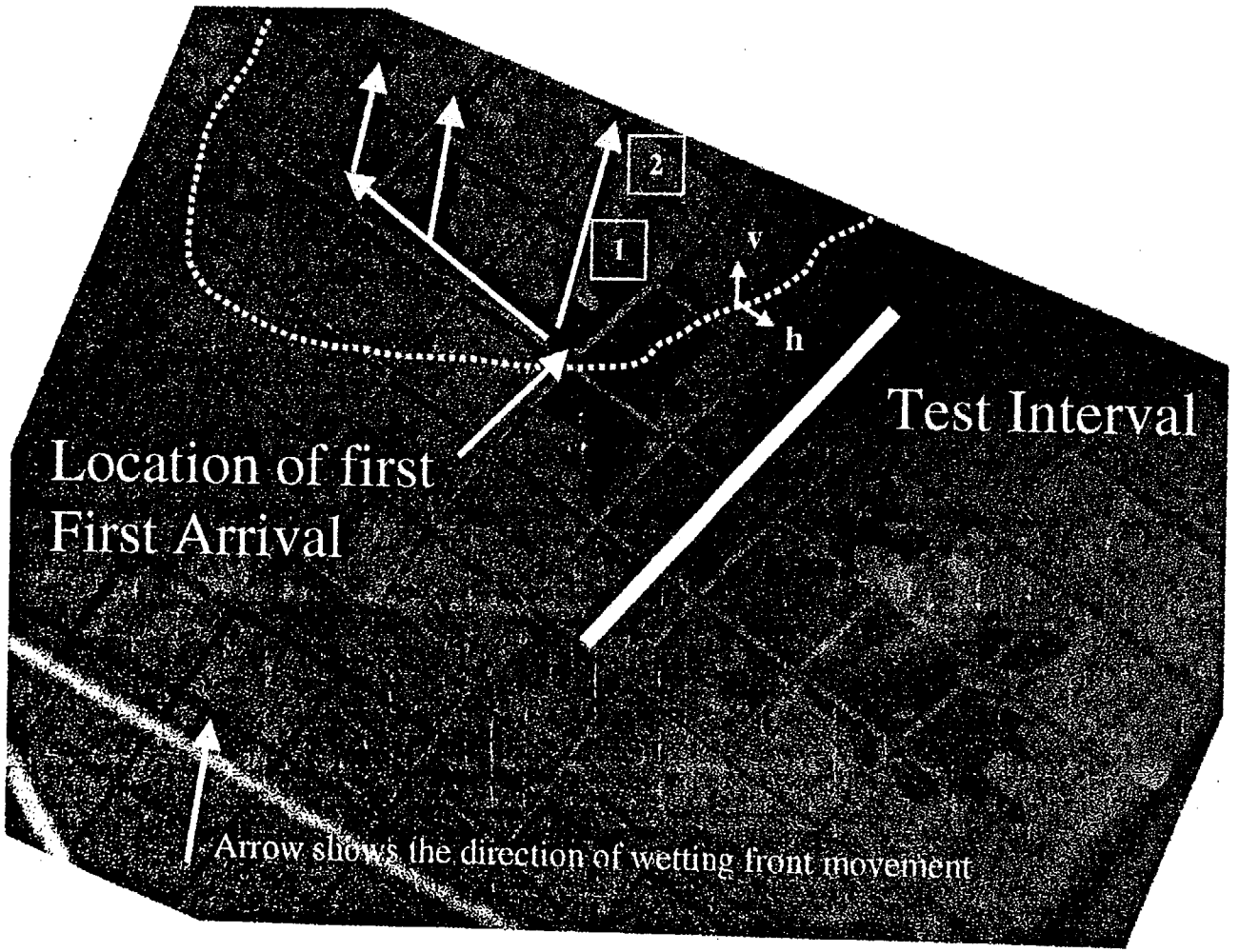

Appendix A

Seepage Distribution in Capture System

Figure A.1

LIQUID OUTFLOW DISTRIBUTION 12/11/97 - NICHE 3650
BOREHOLE UL: TEST INTERVAL 5.18 - 5.49 METERS

Lawrence Berkeley National Laboratory
Exploratory Study Facility
Yucca Mountain, Nevada

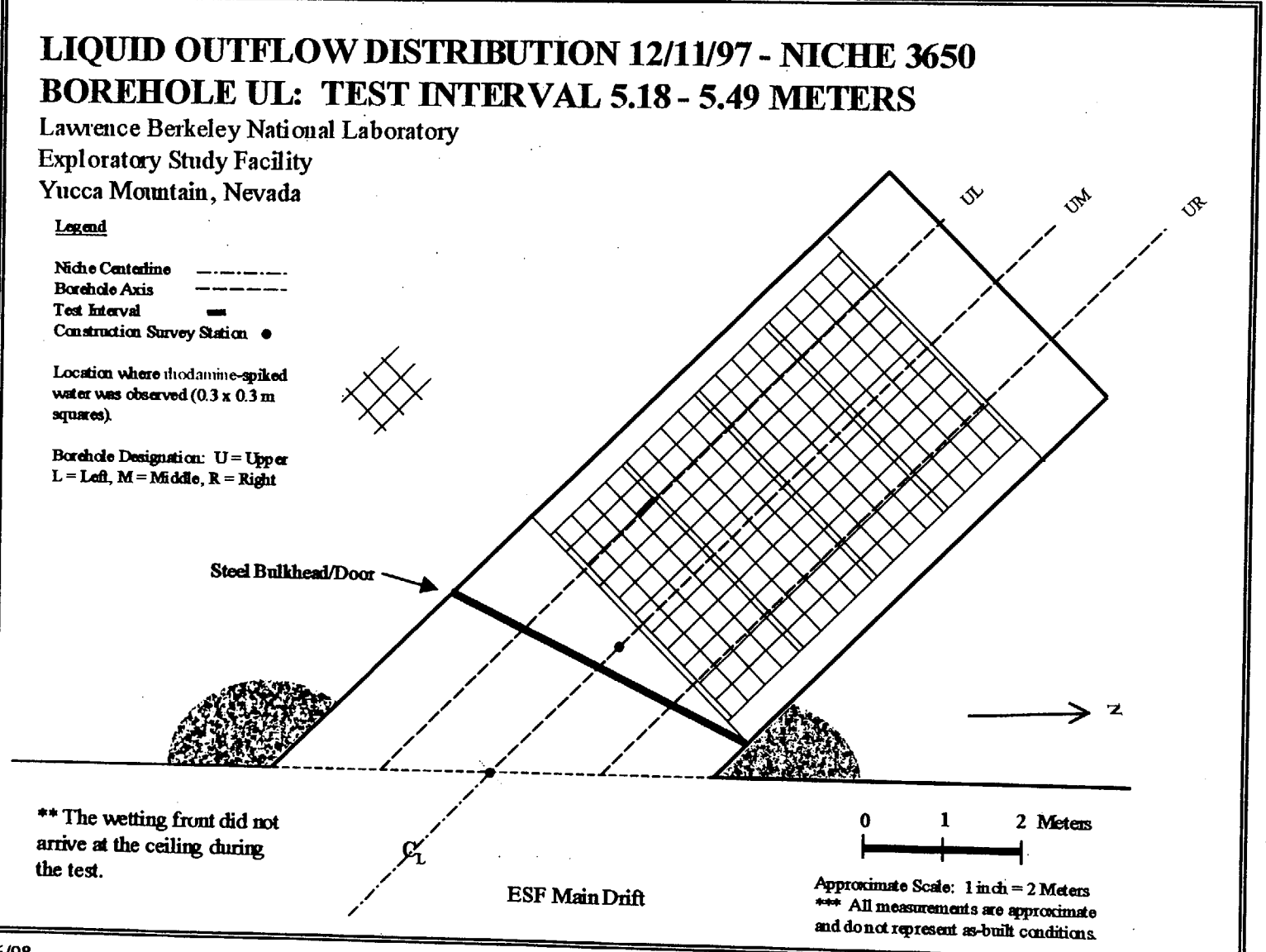

6/16/98
Version 1.0

Figure A.2

LIQUID OUTFLOW DISTRIBUTION 2/12/98 - NICHE 3650
BOREHOLE UL: TEST INTERVAL 5.18 - 5.49 METERS

Lawrence Berkeley National Laboratory
Exploratory Study Facility
Yucca Mountain, Nevada

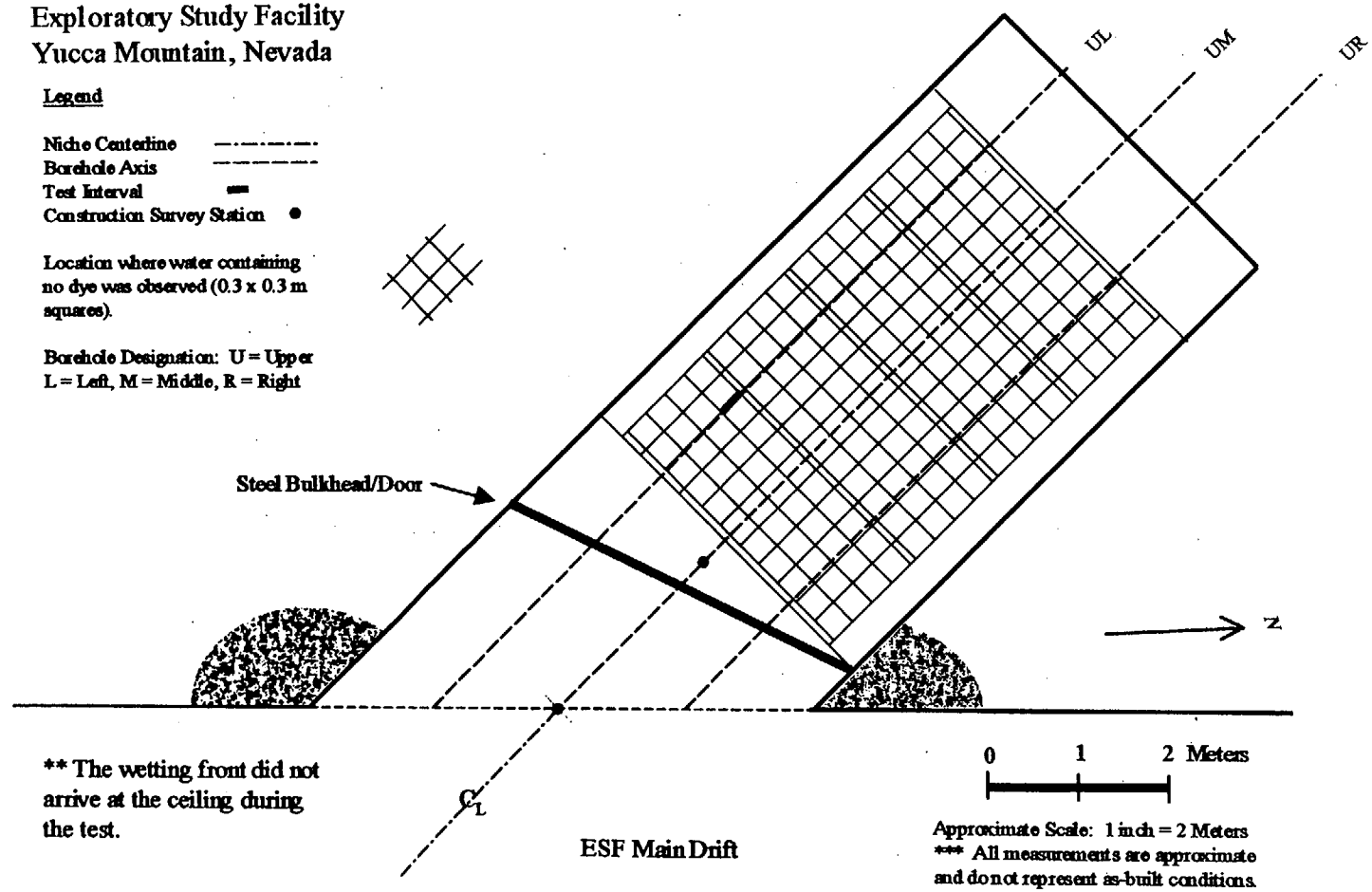

Figure A.3

LIQUID OUTFLOW DISTRIBUTION 12/11/97 - NICHE 3650
BOREHOLE UL: TEST INTERVAL 5.79 - 6.10 METERS

Lawrence Berkeley National Laboratory
Exploratory Study Facility
Yucca Mountain, Nevada

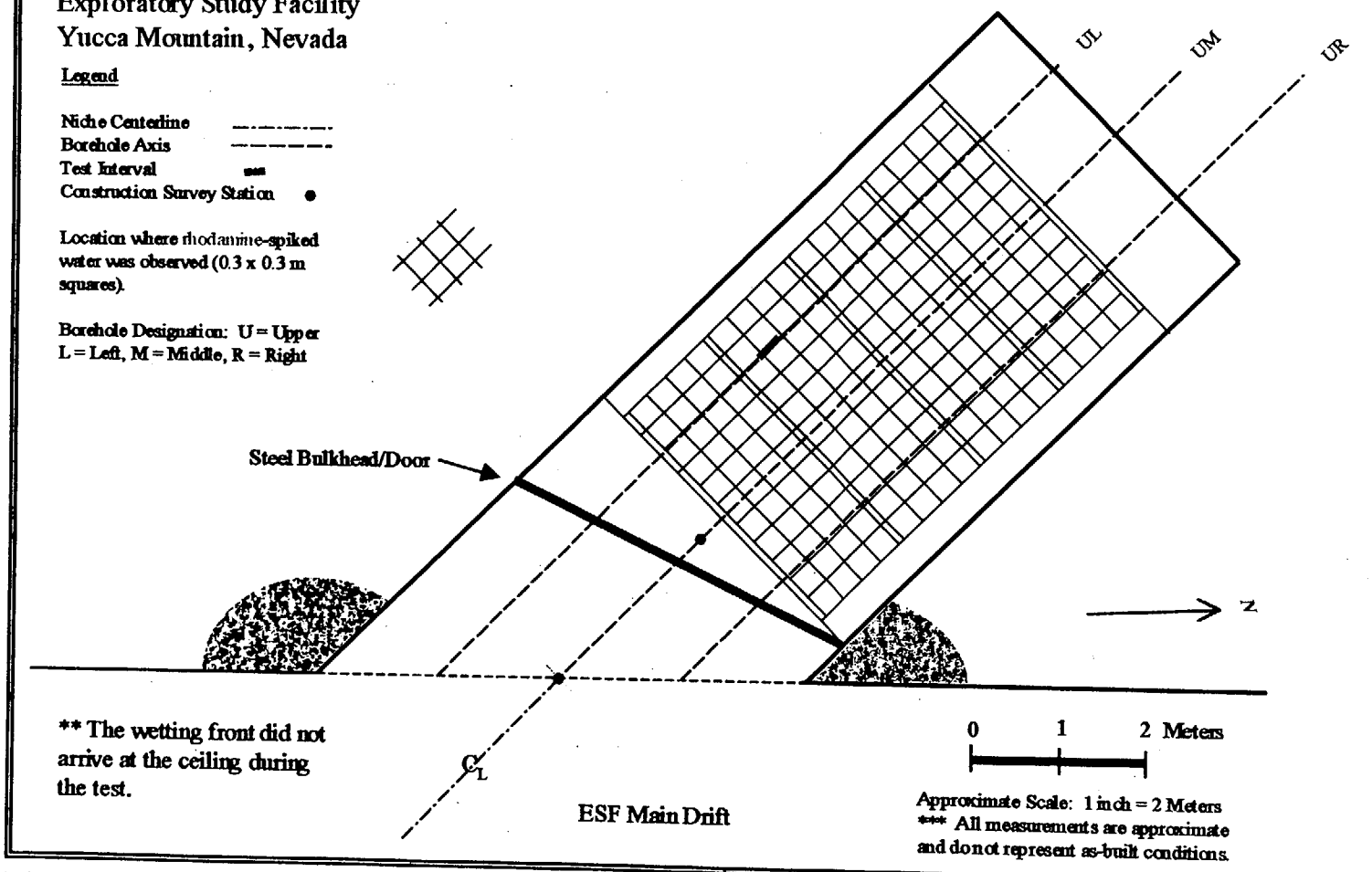

Figure A.4

LIQUID OUTFLOW DISTRIBUTION 12/11/97 - NICHE 3650
BOREHOLE UL: TEST INTERVAL 6.40 - 6.71 METERS

Lawrence Berkeley National Laboratory
Exploratory Study Facility
Yucca Mountain, Nevada

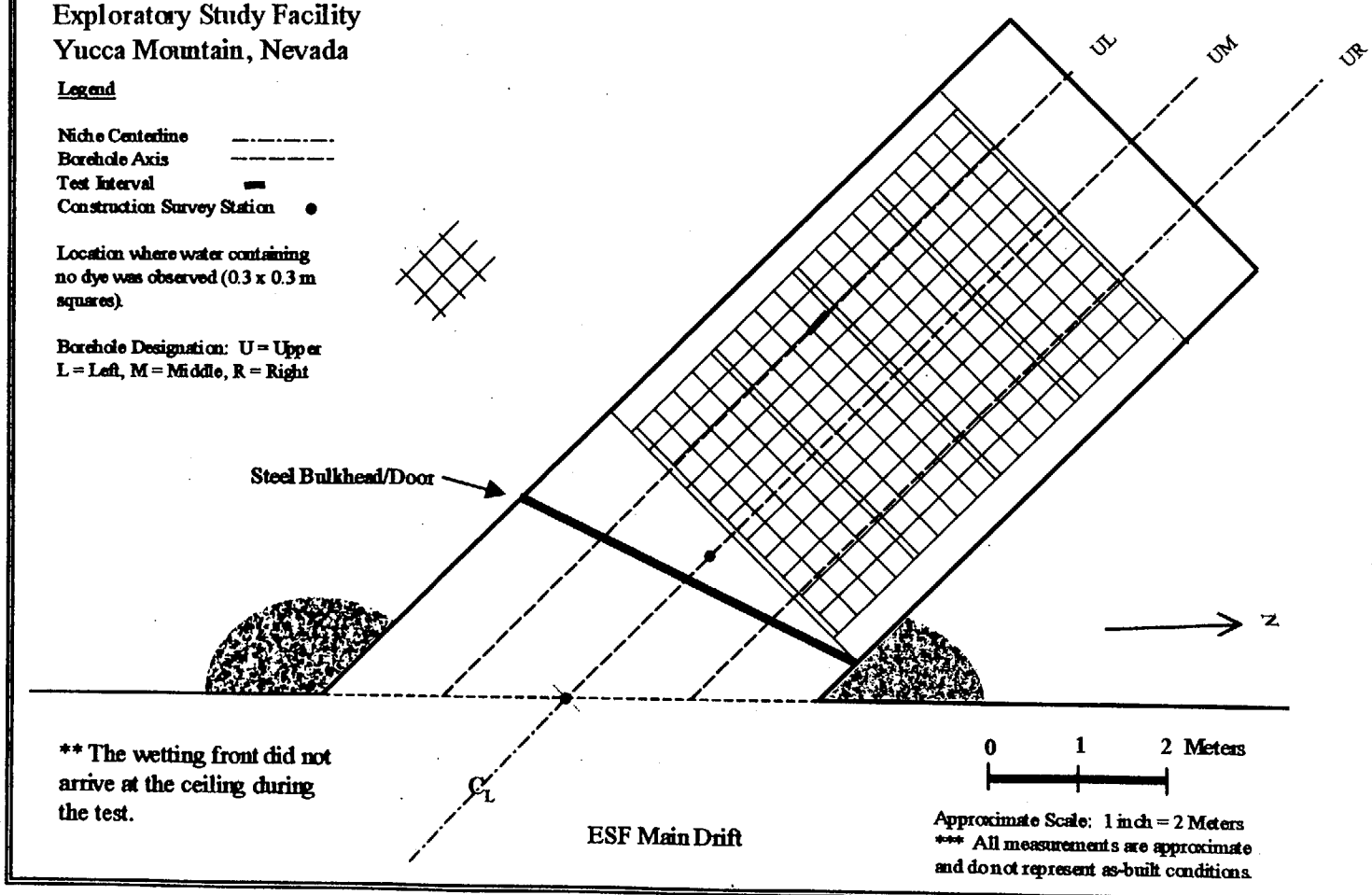

Figure A.5

LIQUID OUTFLOW DISTRIBUTION 12/10/97 - NICHE 3650
BOREHOLE UL: TEST INTERVAL 7.01 - 7.32 METERS

Lawrence Berkeley National Laboratory
Exploratory Study Facility
Yucca Mountain, Nevada

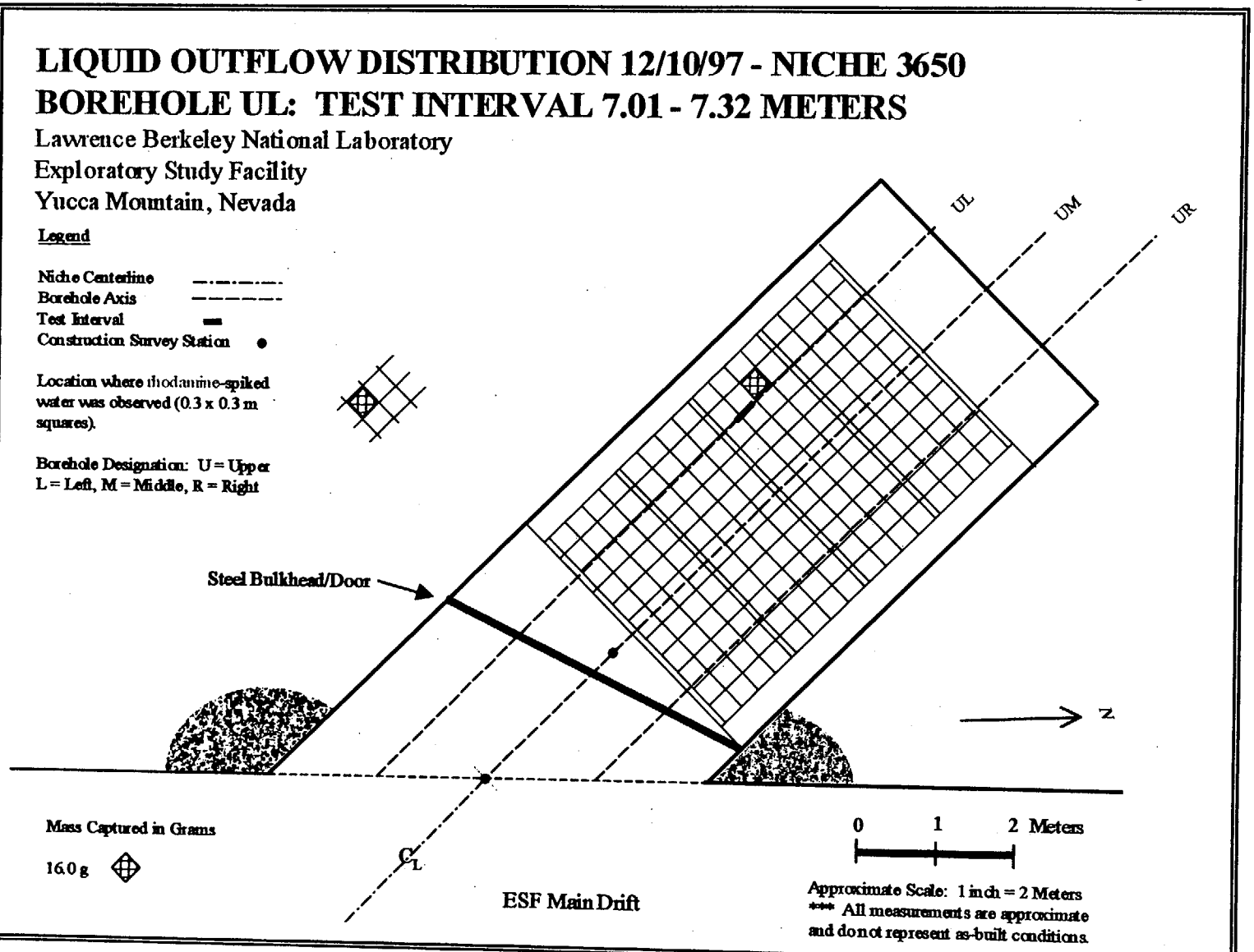

Figure A.6

LIQUID OUTFLOW DISTRIBUTION 1/6/98 - NICHE 3650
BOREHOLE UL: TEST INTERVAL 7.01 - 7.32 METERS

Lawrence Berkeley National Laboratory
Exploratory Study Facility
Yucca Mountain, Nevada

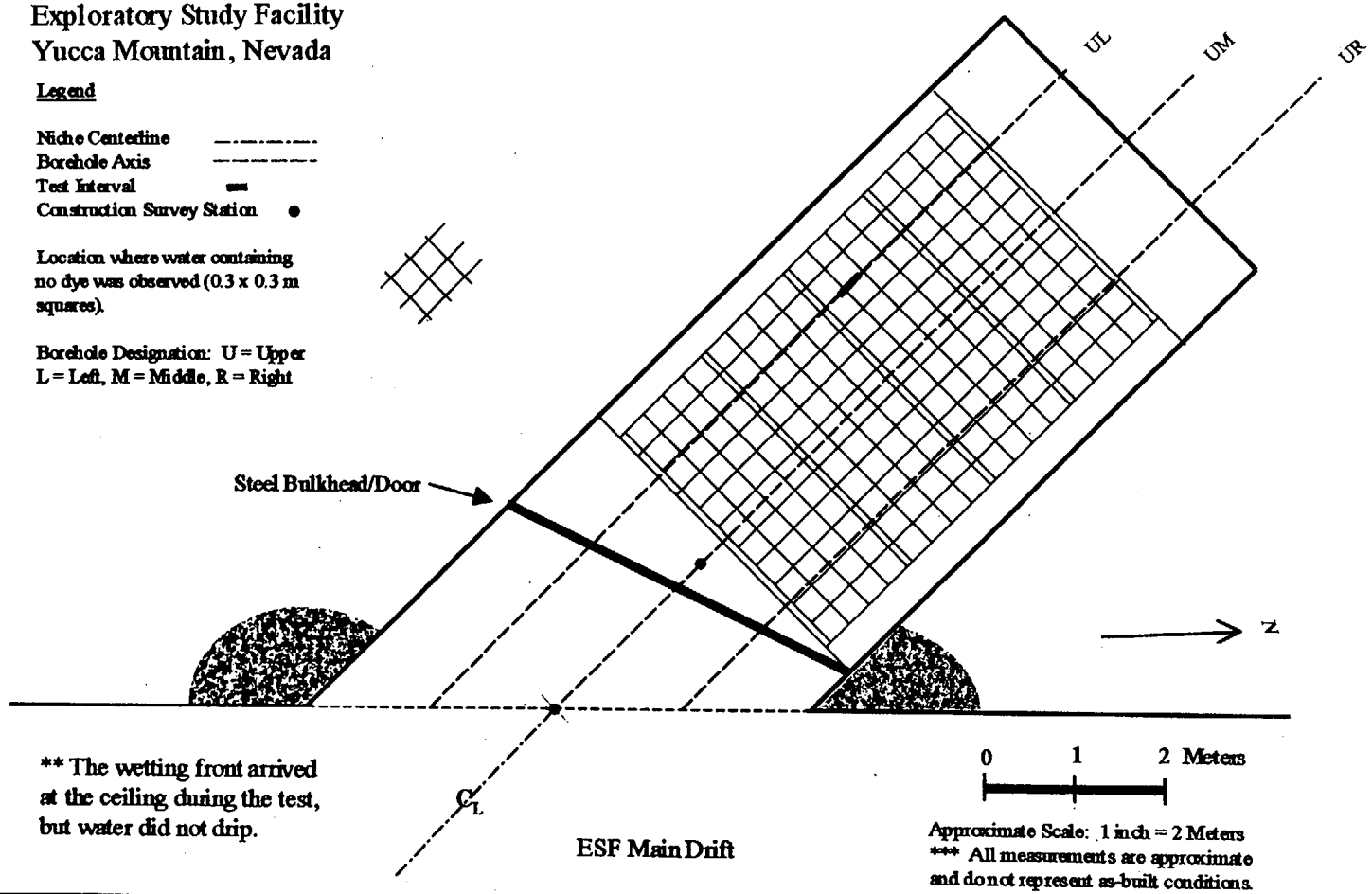

Figure A.7

LIQUID OUTFLOW DISTRIBUTION 1/6/98 - NICHE 3650
BOREHOLE UL: TEST INTERVAL 7.62 - 7.92 METERS

Lawrence Berkeley National Laboratory
Exploratory Study Facility
Yucca Mountain, Nevada

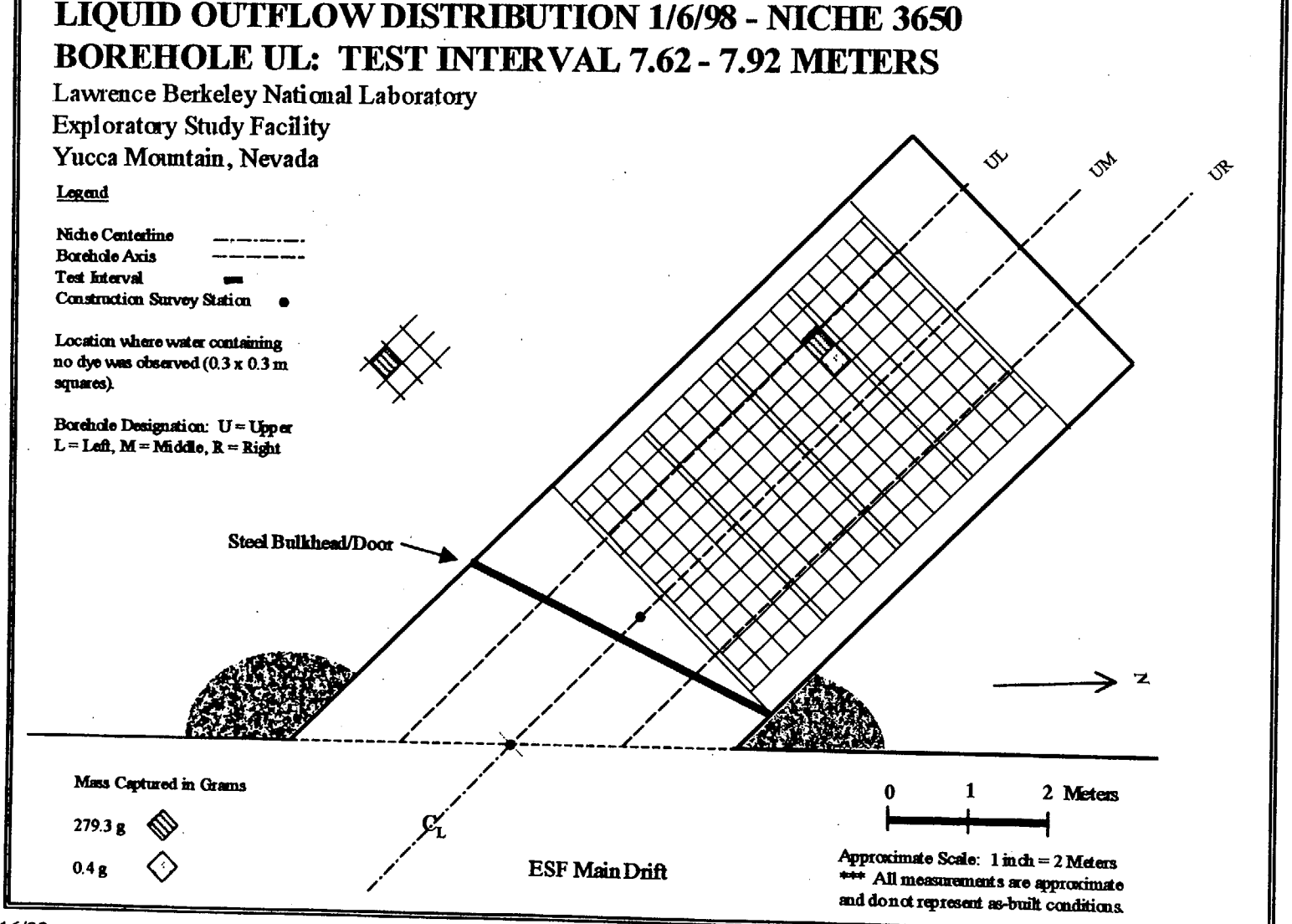

6/16/98
Version 1.0

Figure A.8

LIQUID OUTFLOW DISTRIBUTION 2/12/98 - NICHE 3650
BOREHOLE UL: TEST INTERVAL 7.62 - 7.92 METERS

Lawrence Berkeley National Laboratory
Exploratory Study Facility
Yucca Mountain, Nevada

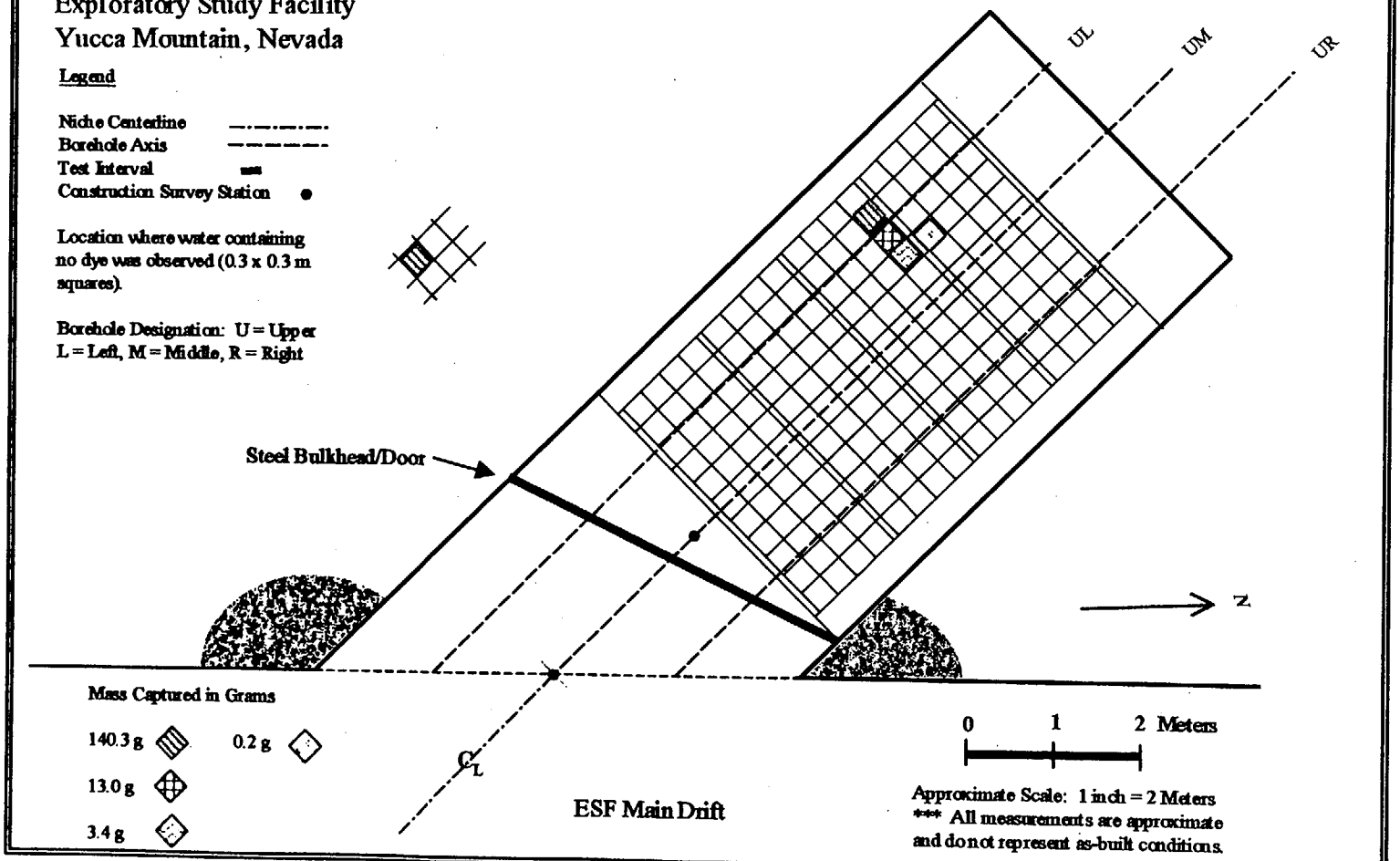

Figure A.9

LIQUID OUTFLOW DISTRIBUTION 3/4/98 - NICHE 3650
BOREHOLE UL: TEST INTERVAL 7.62 - 7.92 METERS

Lawrence Berkeley National Laboratory
Exploratory Study Facility
Yucca Mountain, Nevada

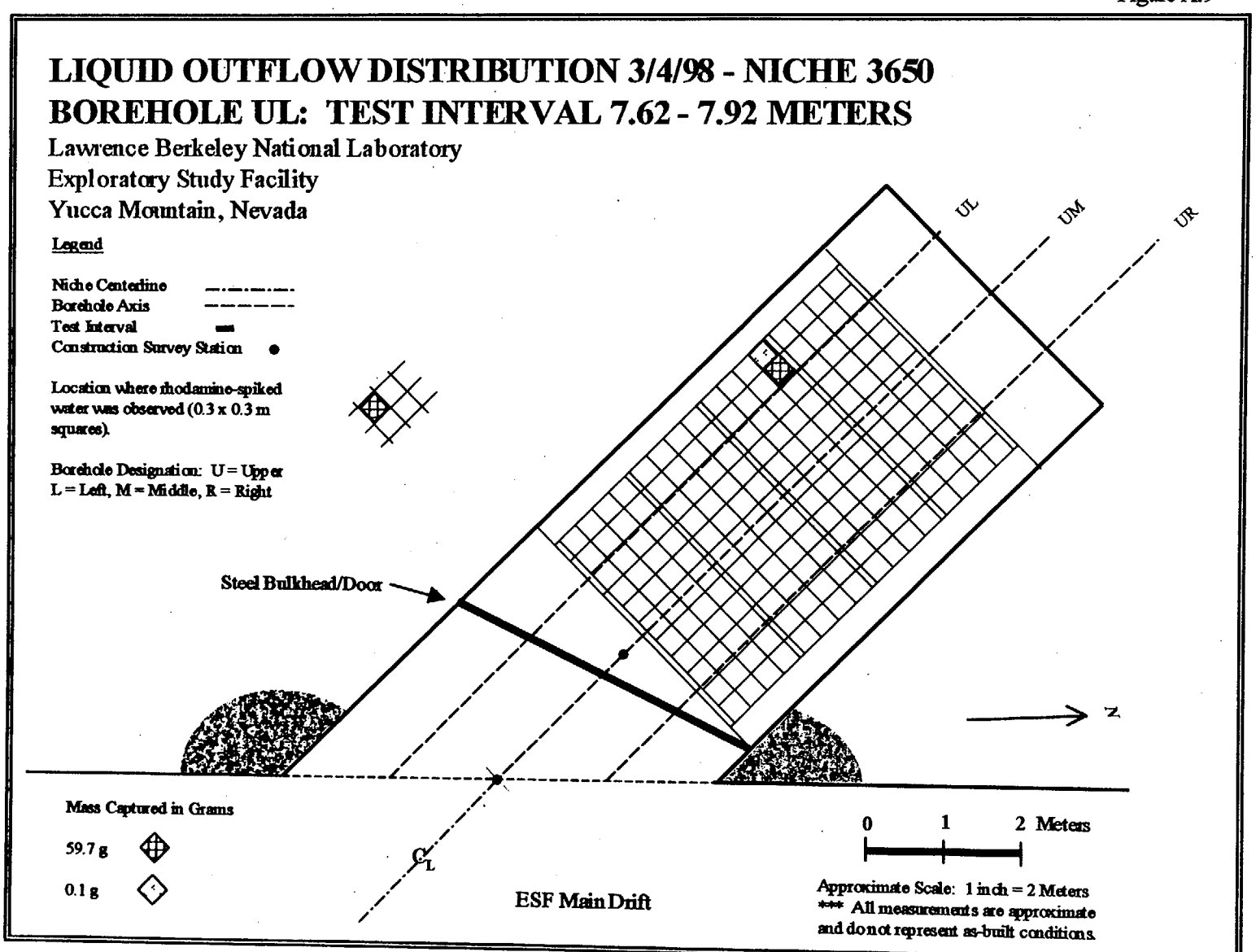

6/16/98
Version 1.0

Figure A.10

LIQUID OUTFLOW DISTRIBUTION 11/13/97 - NICHE 3650
BOREHOLE UM: TEST INTERVAL 4.27 - 4.57 METERS

Lawrence Berkeley National Laboratory
Exploratory Study Facility
Yucca Mountain, Nevada

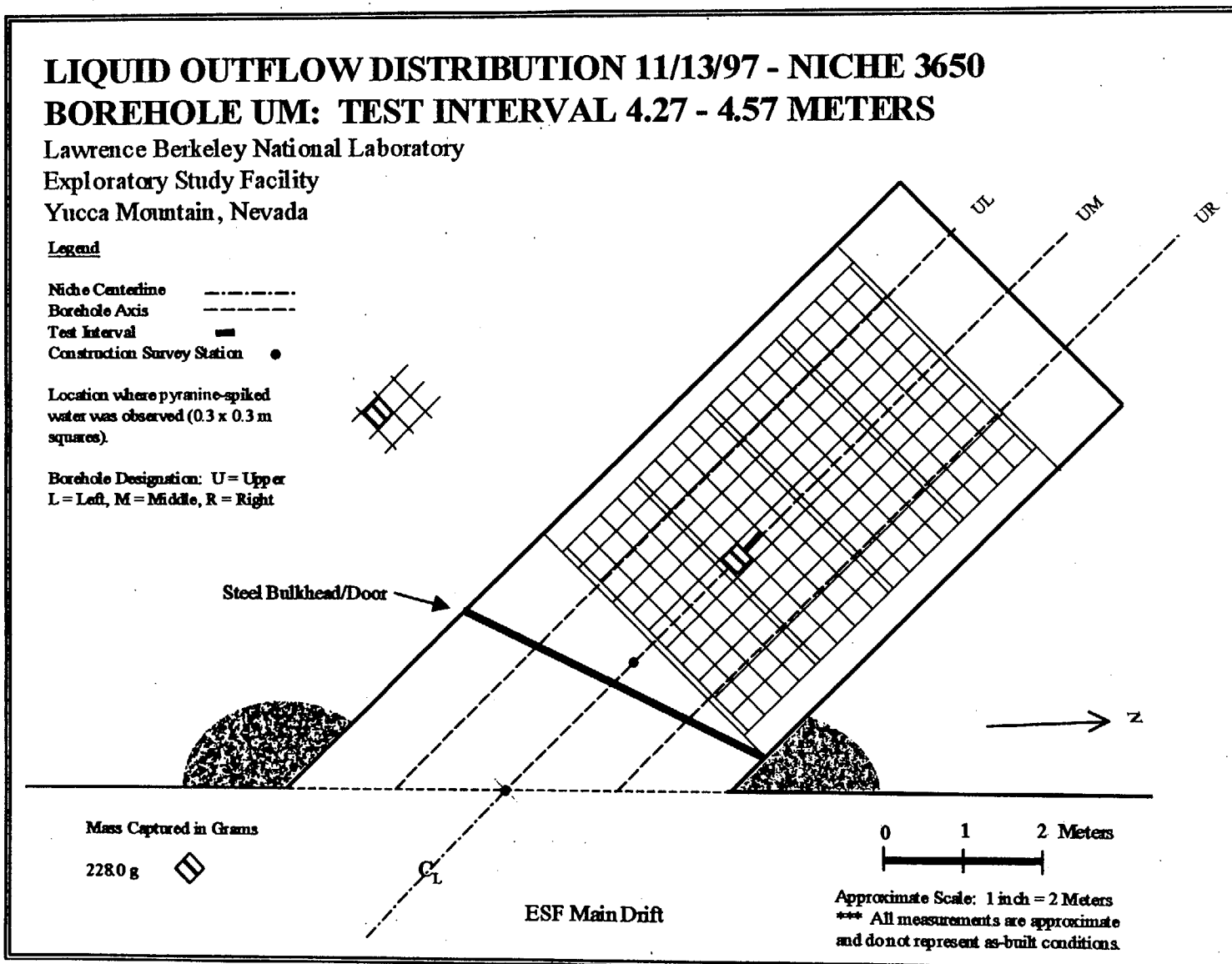

Figure A.11

LIQUID OUTFLOW DISTRIBUTION 12/3/97 (12:34 PM) - NICHE 3650
BOREHOLE UM: TEST INTERVAL 4.27 - 4.57 METERS

Lawrence Berkeley National Laboratory
Exploratory Study Facility
Yucca Mountain, Nevada

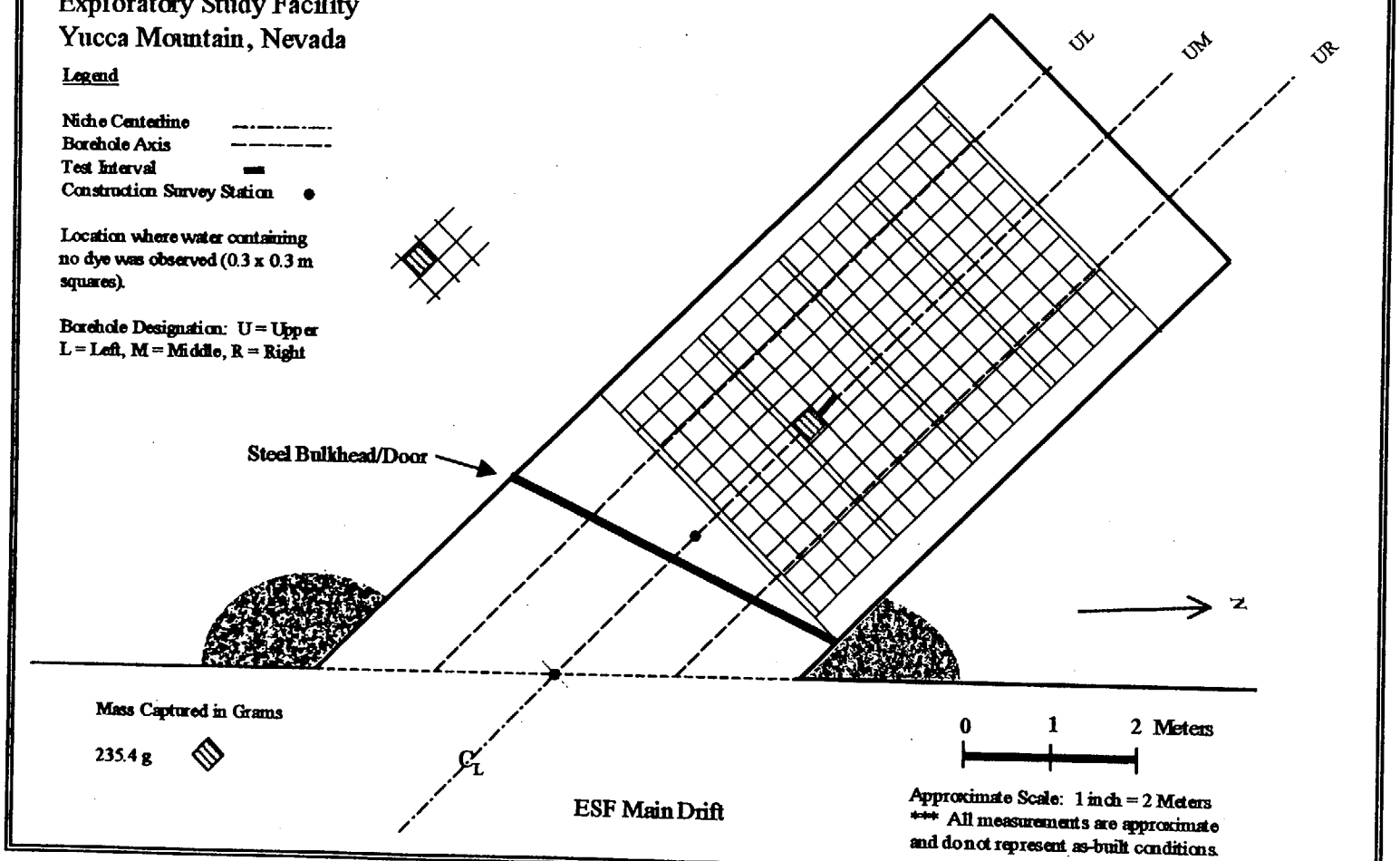

6/16/98
Version 1.0

Figure A.12

LIQUID OUTFLOW DISTRIBUTION 12/3/97 (14:30 PM) - NICHE 3650
BOREHOLE UM: TEST INTERVAL 4.27 - 4.57 METERS

Lawrence Berkeley National Laboratory
Exploratory Study Facility
Yucca Mountain, Nevada

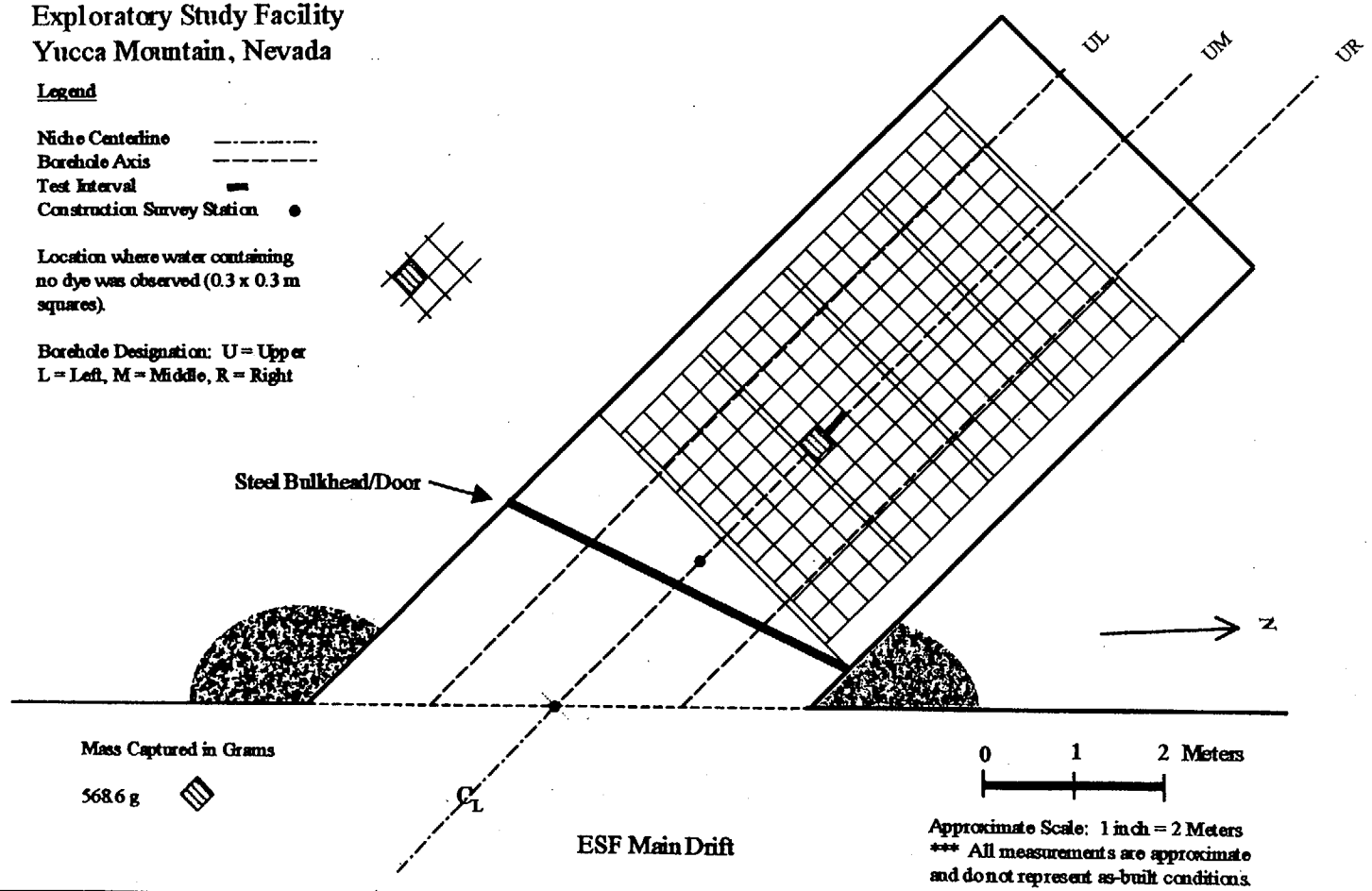

Figure A.13

LIQUID OUTFLOW DISTRIBUTION 1/7/98 - NICHE 3650
BOREHOLE UM: TEST INTERVAL 4.27 - 4.57 METERS

Lawrence Berkeley National Laboratory
Exploratory Study Facility
Yucca Mountain, Nevada

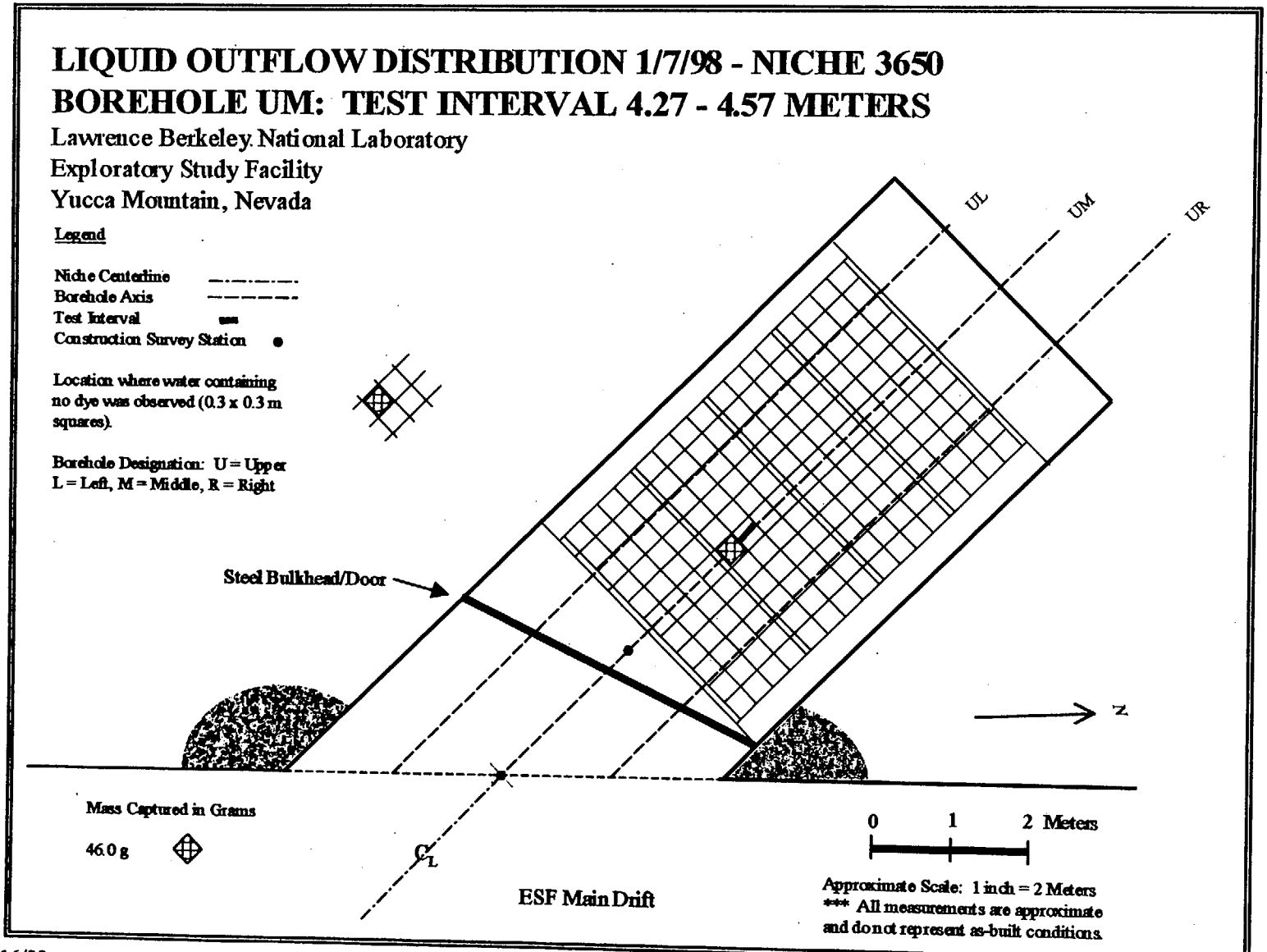

6/16/98
Version 1.0

LIQUID OUTFLOW DISTRIBUTION 2/10/98 - NICHE 3650
BOREHOLE UM: TEST INTERVAL 4.27 - 4.57 METERS

Lawrence Berkeley National Laboratory
Exploratory Study Facility
Yucca Mountain, Nevada

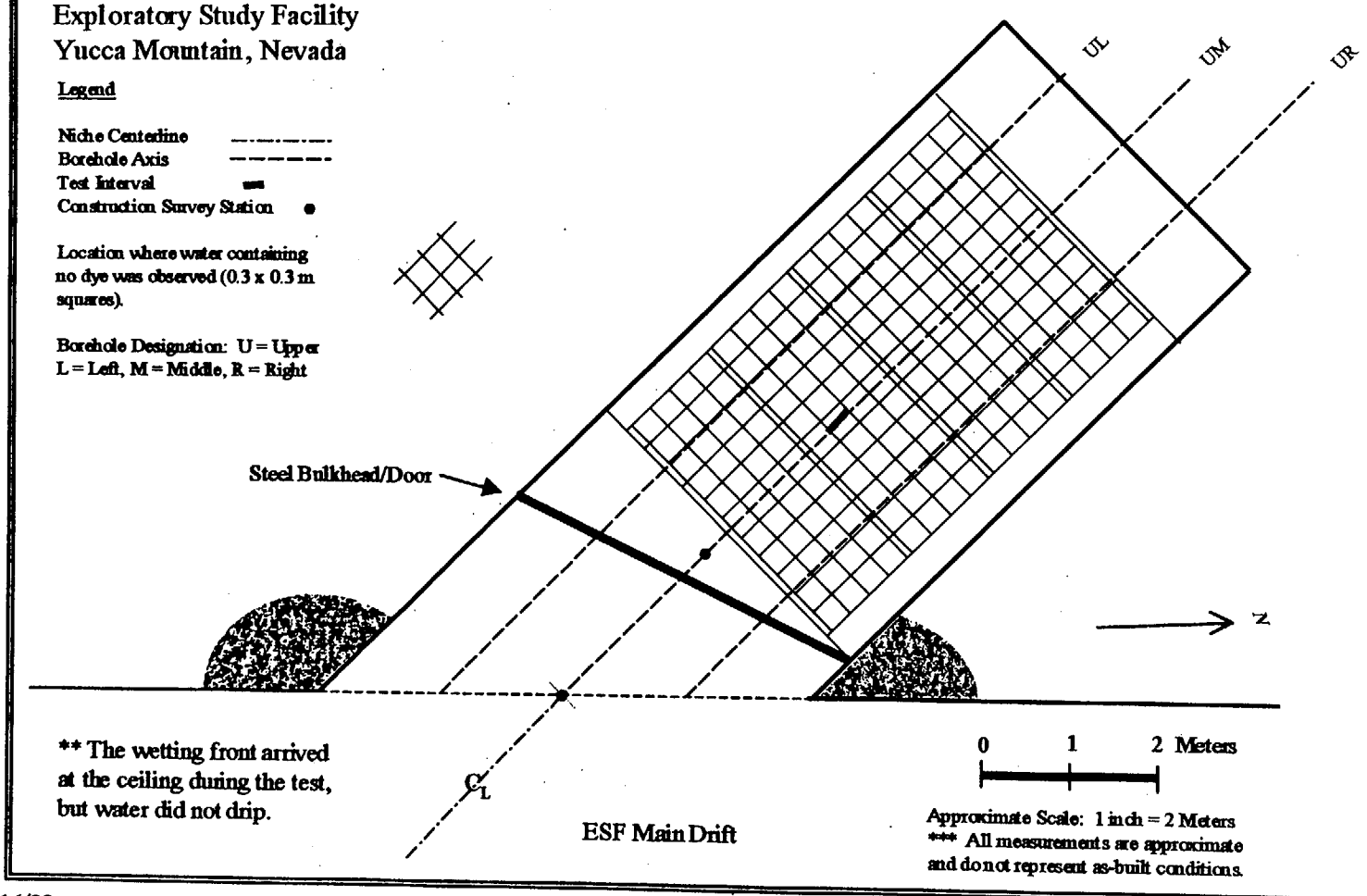

Figure A.15

LIQUID OUTFLOW DISTRIBUTION 11/12/97 - NICHE 3650
BOREHOLE UM: TEST INTERVAL 4.88 - 5.18 METERS

Lawrence Berkeley National Laboratory
Exploratory Study Facility
Yucca Mountain, Nevada

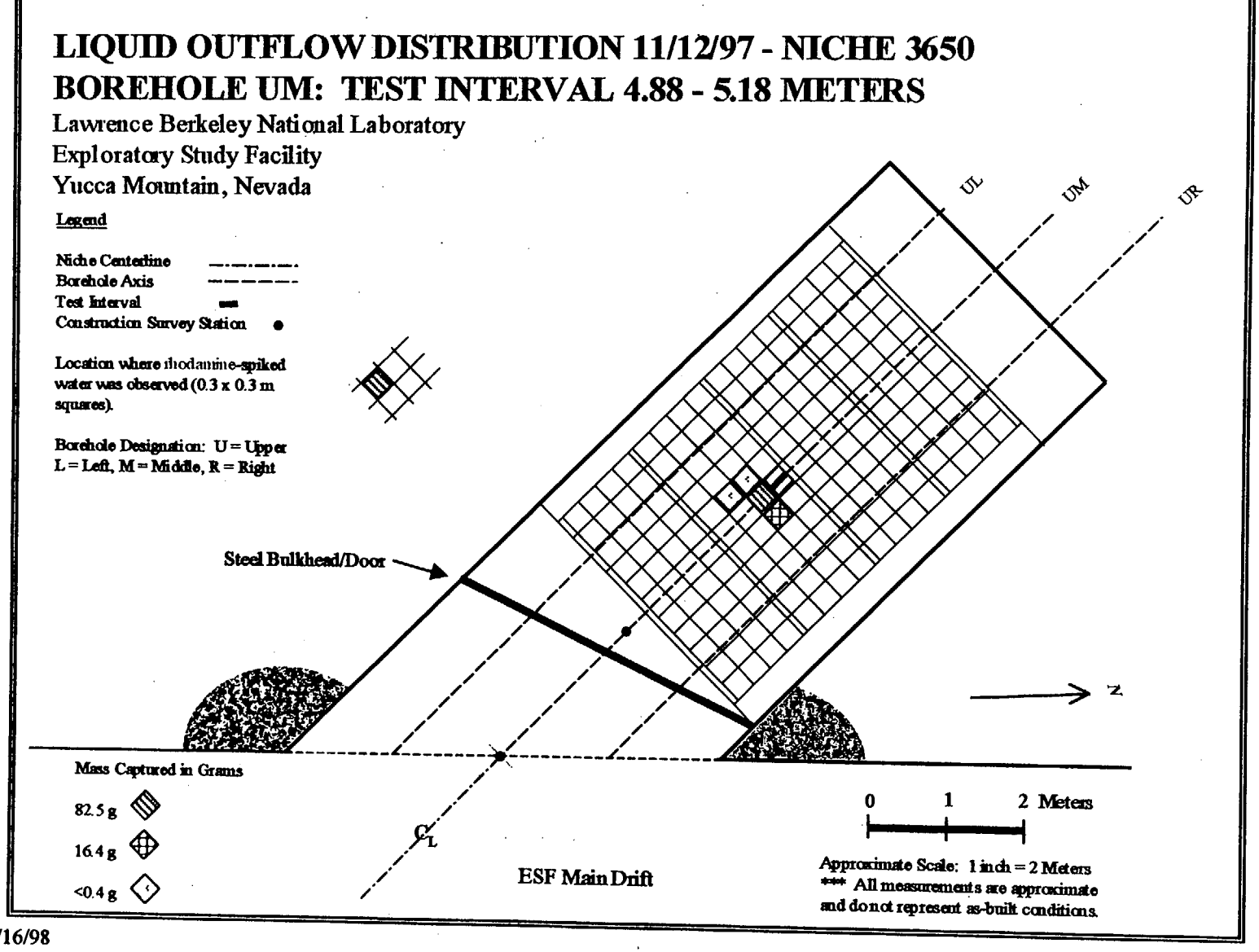

Figure A.16

LIQUID OUTFLOW DISTRIBUTION 12/4/97 - NICHE 3650
BOREHOLE UM: TEST INTERVAL 4.88 - 5.18 METERS

Lawrence Berkeley National Laboratory
Exploratory Study Facility
Yucca Mountain, Nevada

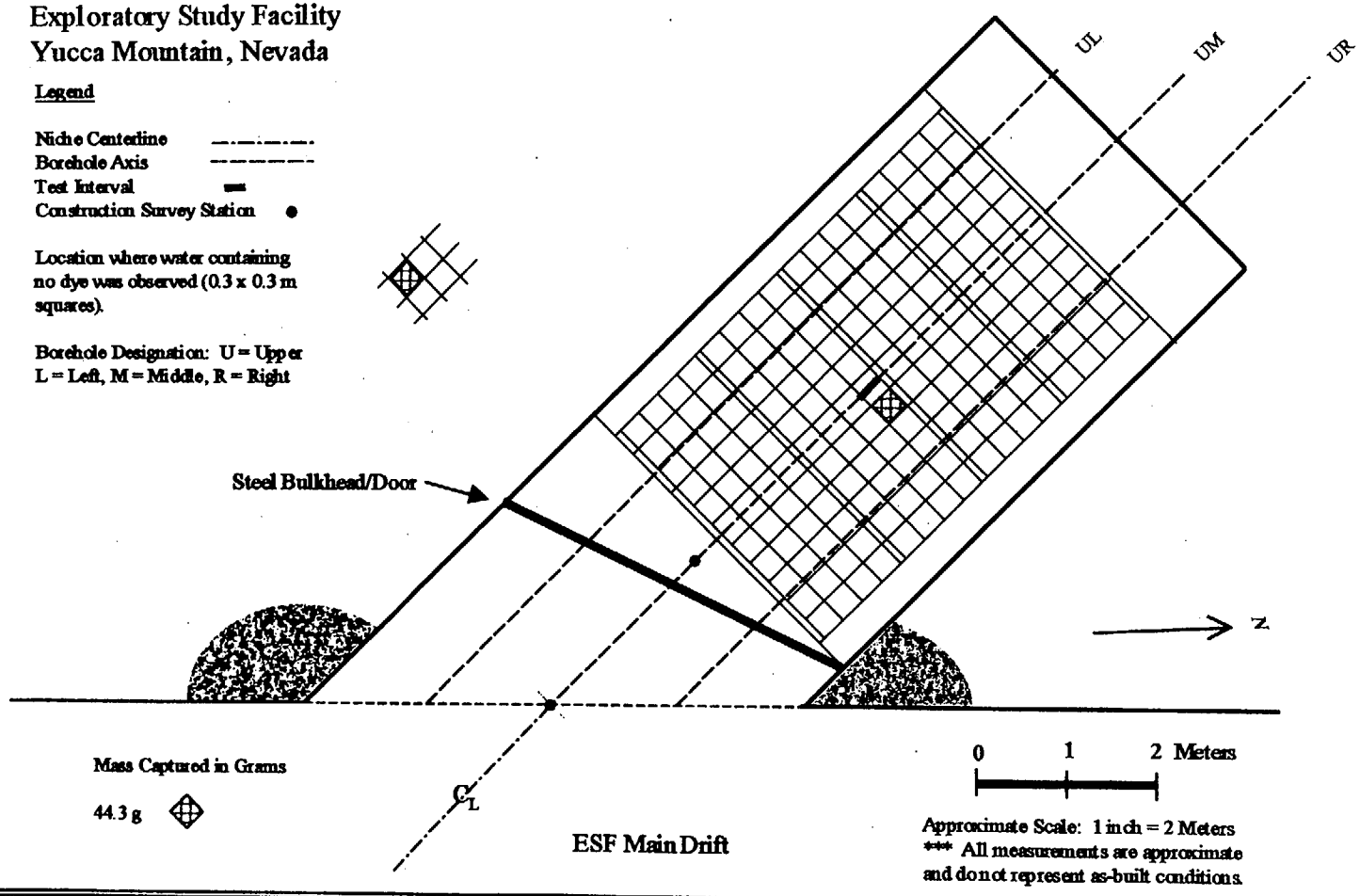

Figure A.17

LIQUID OUTFLOW DISTRIBUTION 12/5/97 - NICHE 3650
BOREHOLE UM: TEST INTERVAL 4.88 - 5.18 METERS

Lawrence Berkeley National Laboratory
Exploratory Study Facility
Yucca Mountain, Nevada

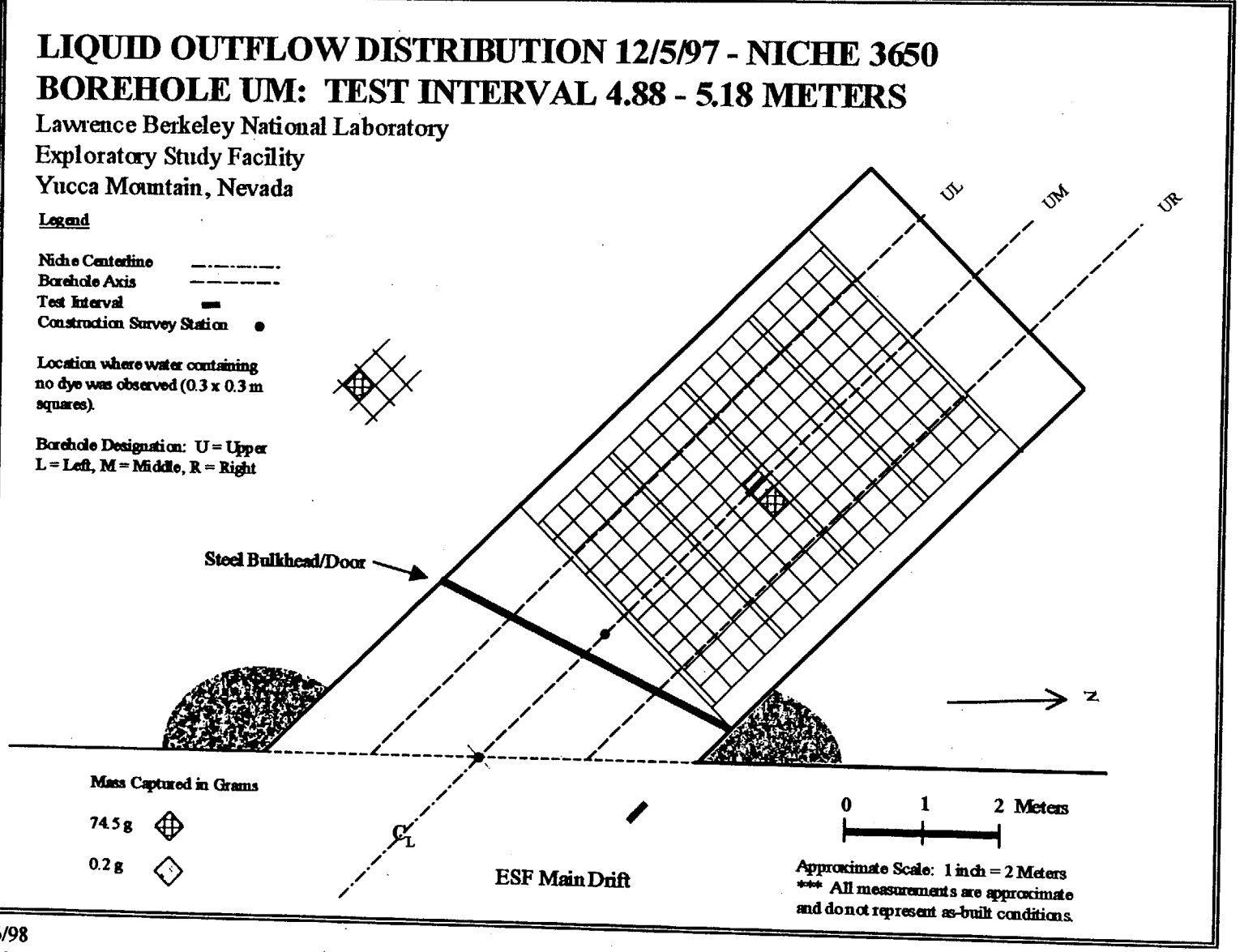

LIQUID OUTFLOW DISTRIBUTION 1/8/98 - NICHE 3650
BOREHOLE UM: TEST INTERVAL 4.88 - 5.18 METERS

Lawrence Berkeley National Laboratory
Exploratory Study Facility
Yucca Mountain, Nevada

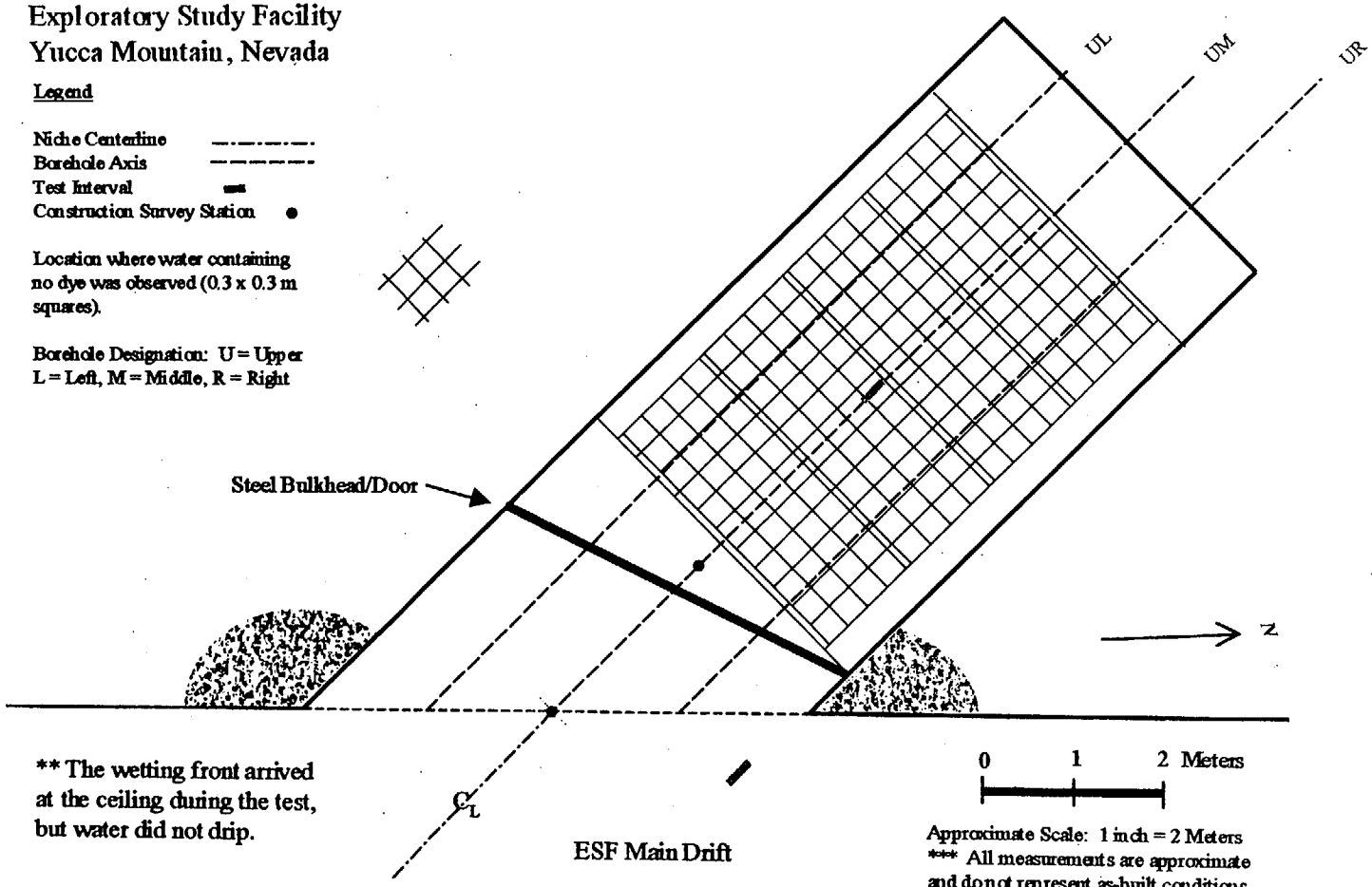

6/16/98
Version 1.0

LIQUID OUTFLOW DISTRIBUTION 3/6/98 - NICHE 3650
BOREHOLE UM: TEST INTERVAL 4.88 - 5.18 METERS

Lawrence Berkeley National Laboratory
Exploratory Study Facility
Yucca Mountain, Nevada

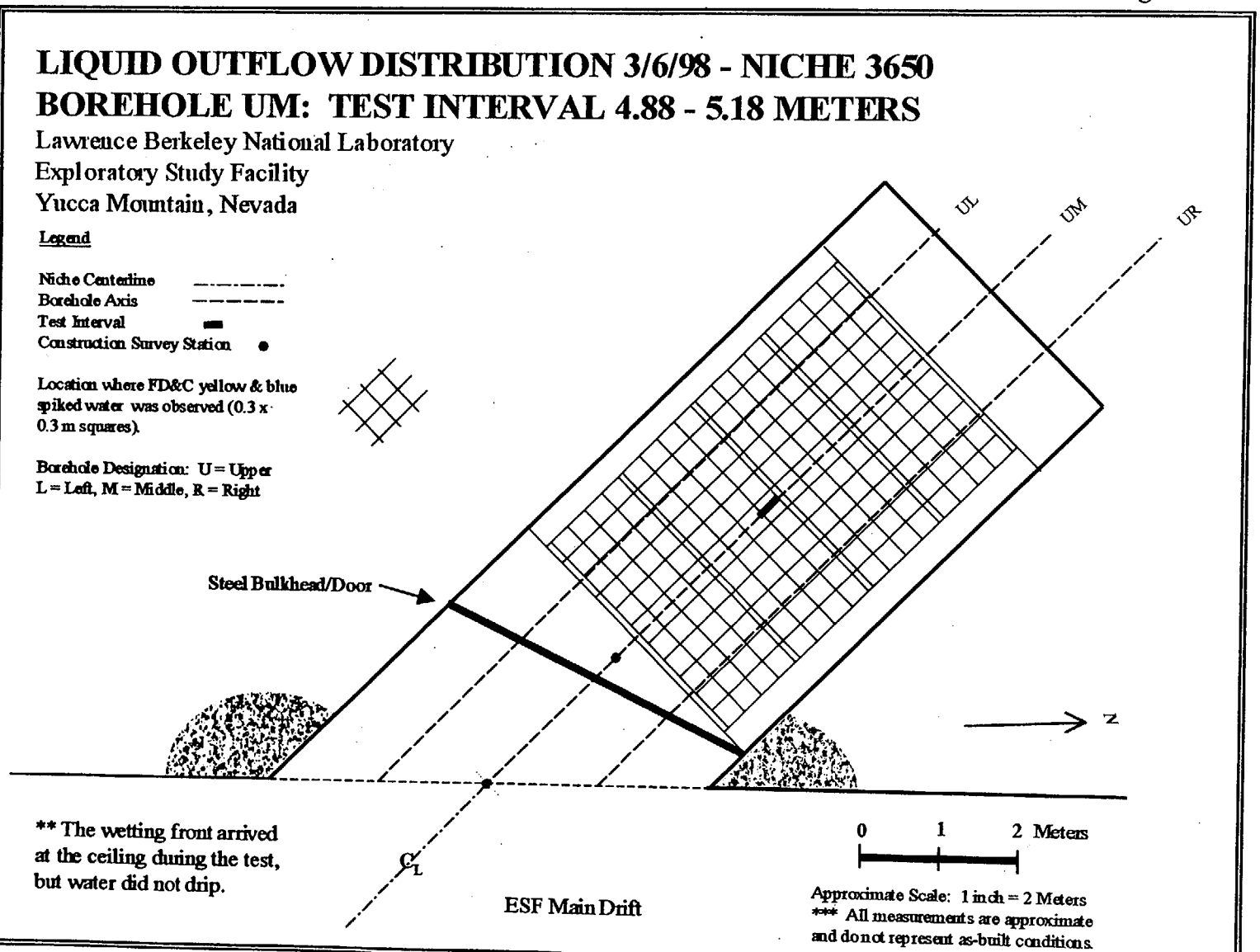

LIQUID OUTFLOW DISTRIBUTION 11/13/97 - NICHE 3650
BOREHOLE UM: TEST INTERVAL 5.49 - 5.79 METERS

Lawrence Berkeley National Laboratory
Exploratory Study Facility
Yucca Mountain, Nevada

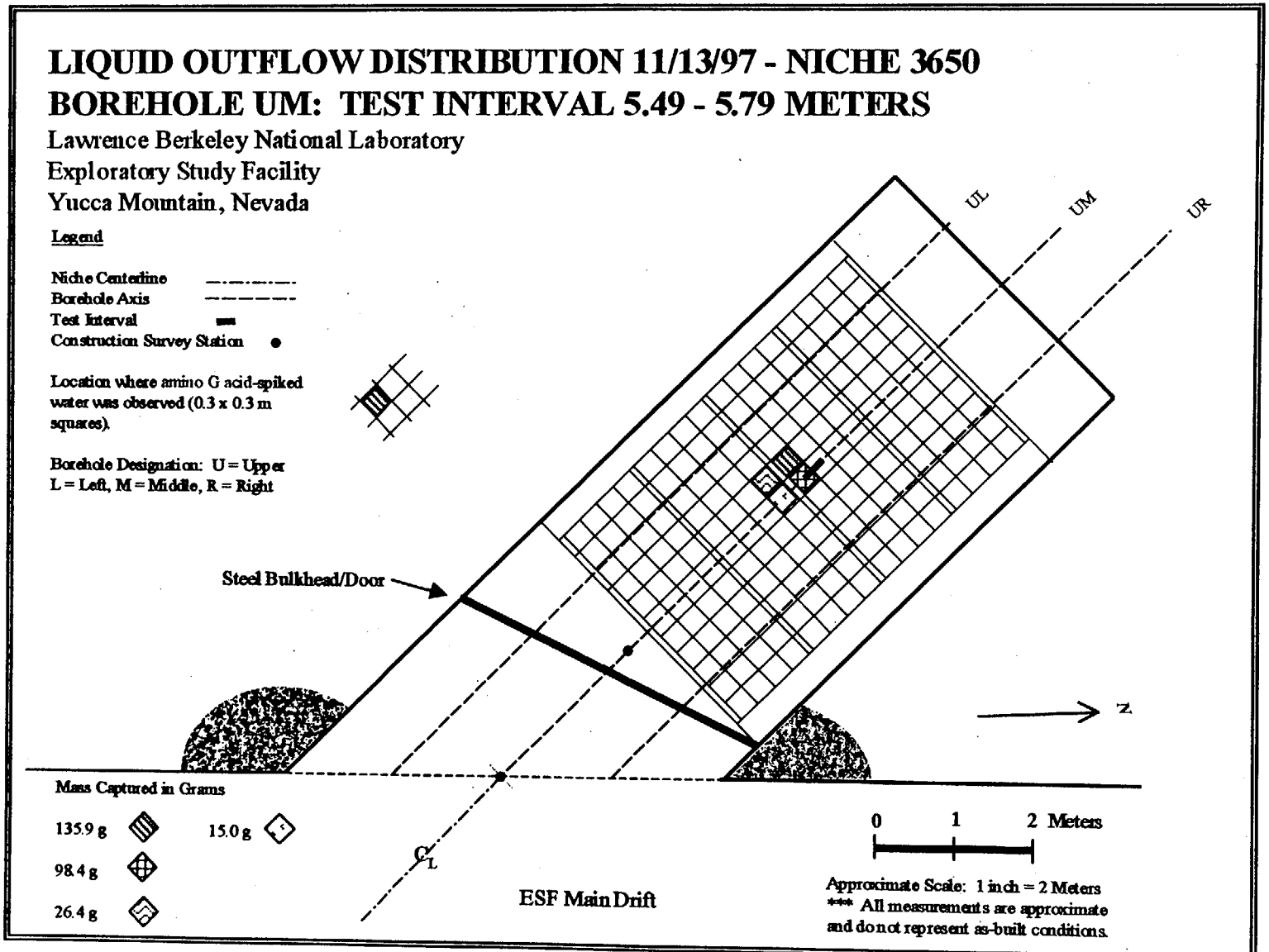

Figure A.21

LIQUID OUTFLOW DISTRIBUTION 12/4/97 - NICHE 3650
BOREHOLE UM: TEST INTERVAL 5.49 - 5.79 METERS

Lawrence Berkeley National Laboratory
Exploratory Study Facility
Yucca Mountain, Nevada

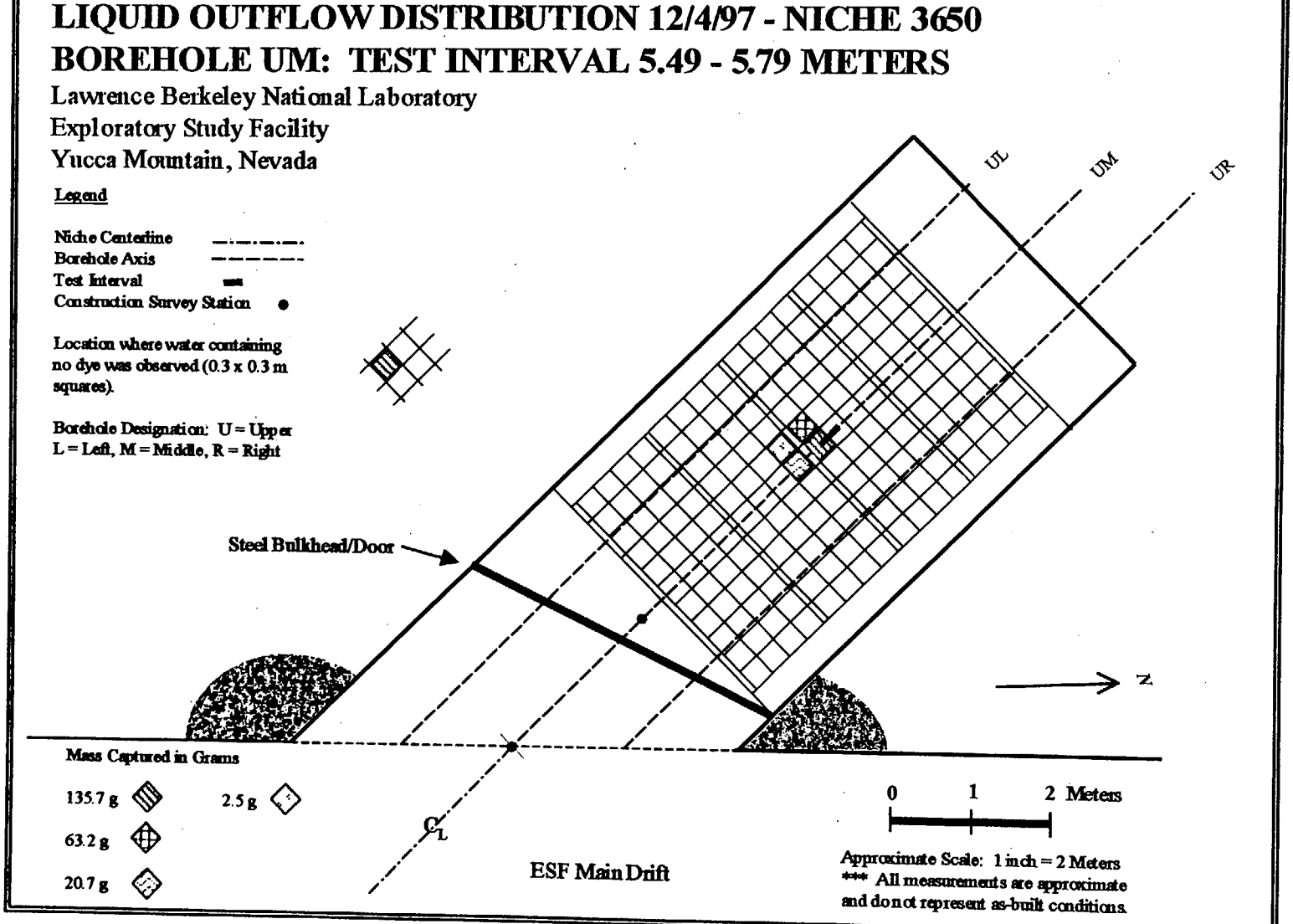

6/16/98
Version 1.0

Figure A.22

LIQUID OUTFLOW DISTRIBUTION 1/9/98 - NICHE 3650
BOREHOLE UM: TEST INTERVAL 5.49 - 5.79 METERS

Lawrence Berkeley National Laboratory
Exploratory Study Facility
Yucca Mountain, Nevada

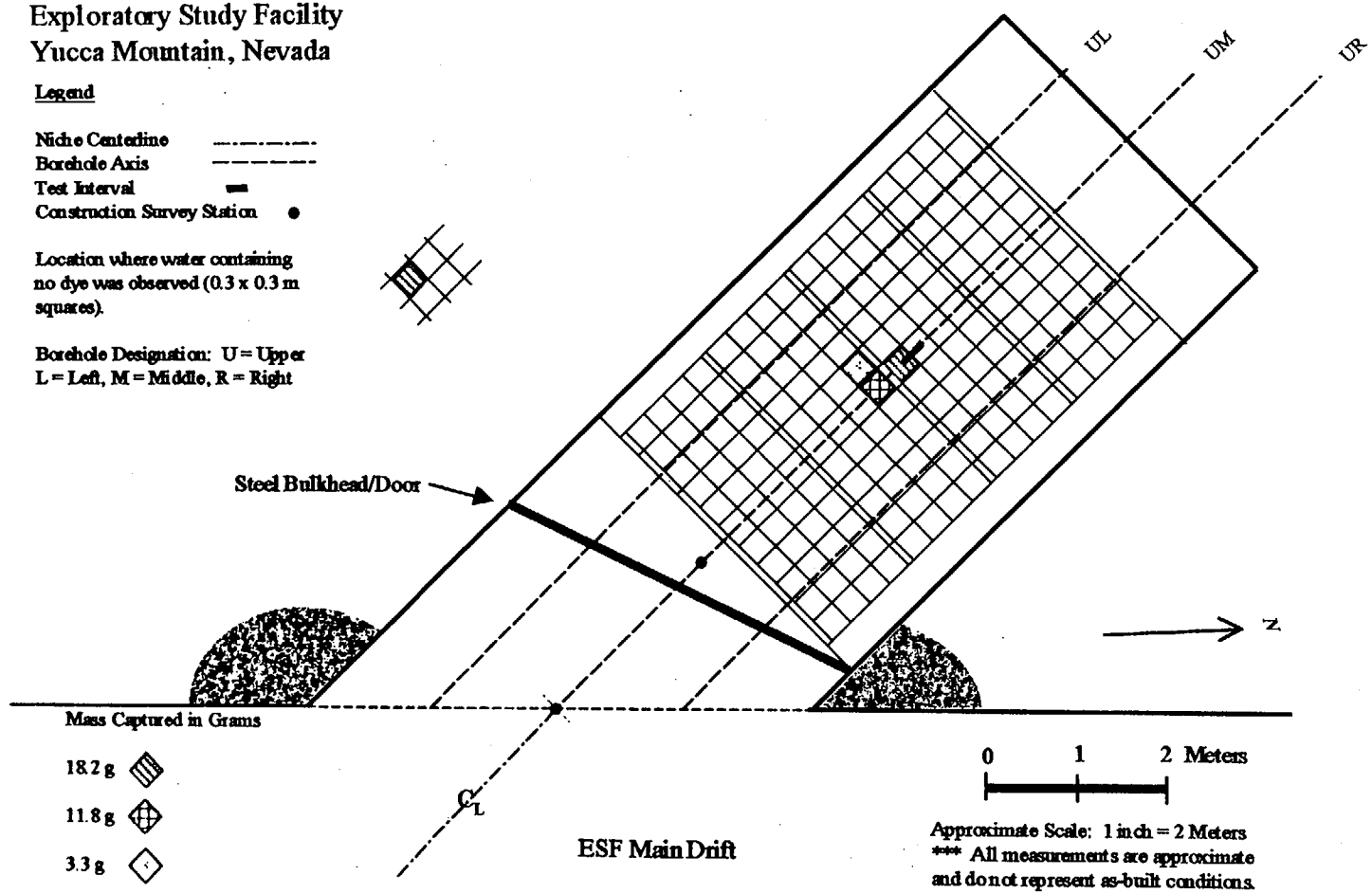

Figure A.23

LIQUID OUTFLOW DISTRIBUTION 2/11/98 - NICHE 3650
BOREHOLE UM: TEST INTERVAL 5.49 - 5.79 METERS

Lawrence Berkeley National Laboratory
Exploratory Study Facility
Yucca Mountain, Nevada

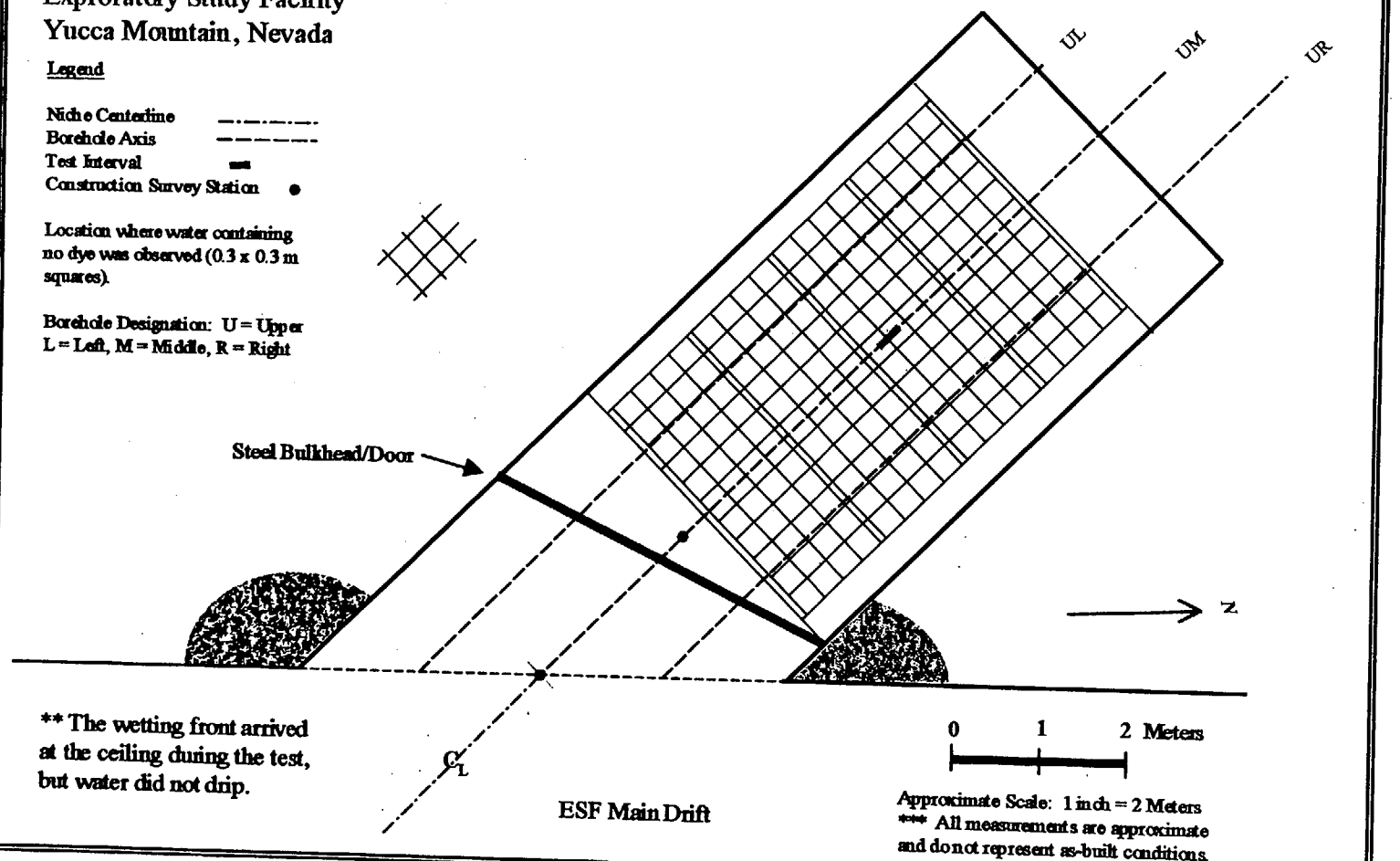

6/16/98
Version 1.0

Figure A.24

LIQUID OUTFLOW DISTRIBUTION 11/13/97 - NICHE 3650
BOREHOLE UM: TEST INTERVAL 6.10 - 6.40 METERS

Lawrence Berkeley National Laboratory
Exploratory Study Facility
Yucca Mountain, Nevada

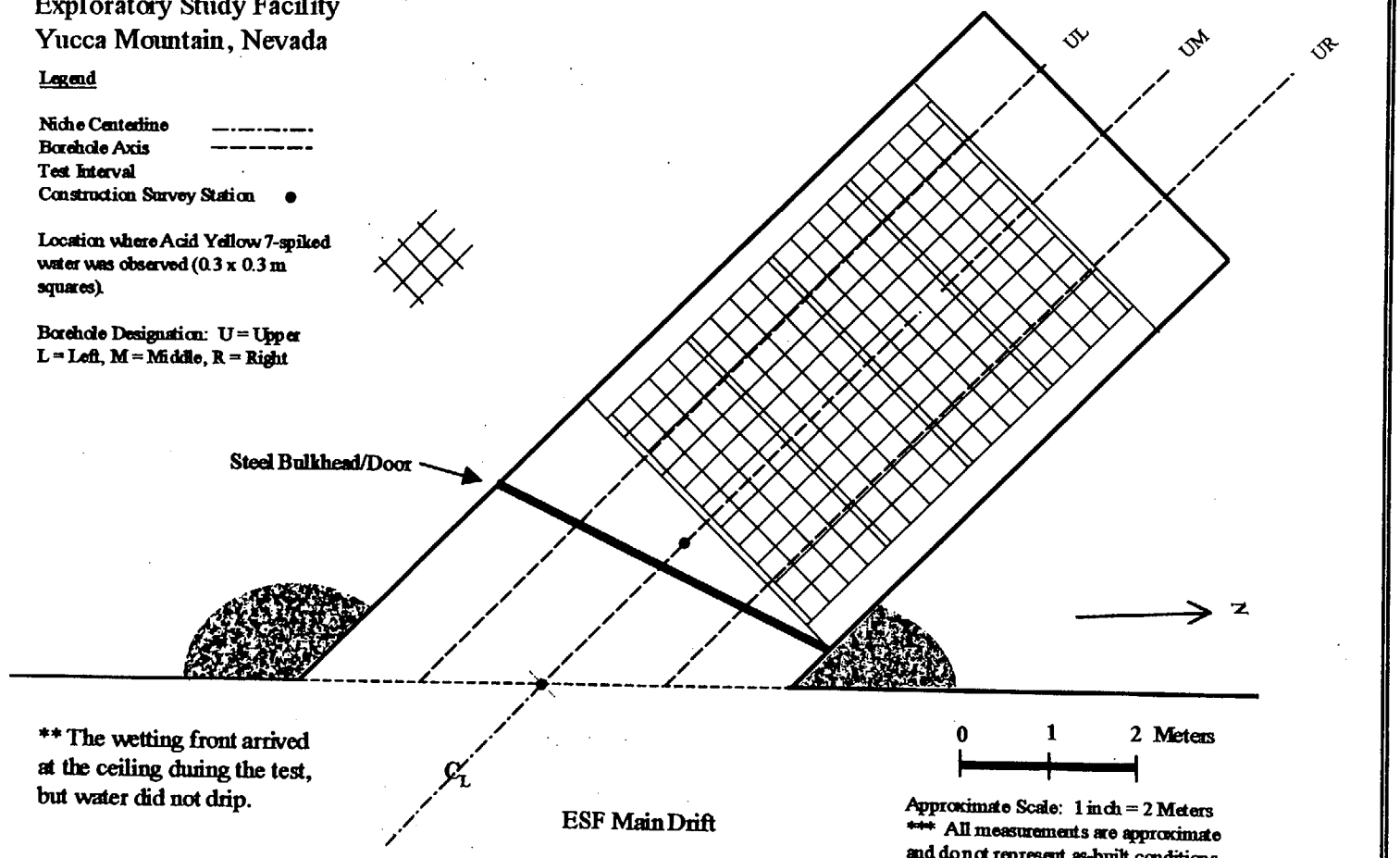

Figure A.25

LIQUID OUTFLOW DISTRIBUTION 12/4/97 - NICHE 3650
BOREHOLE UM: TEST INTERVAL 6.10 - 6.40 METERS

Lawrence Berkeley National Laboratory
Exploratory Study Facility
Yucca Mountain, Nevada

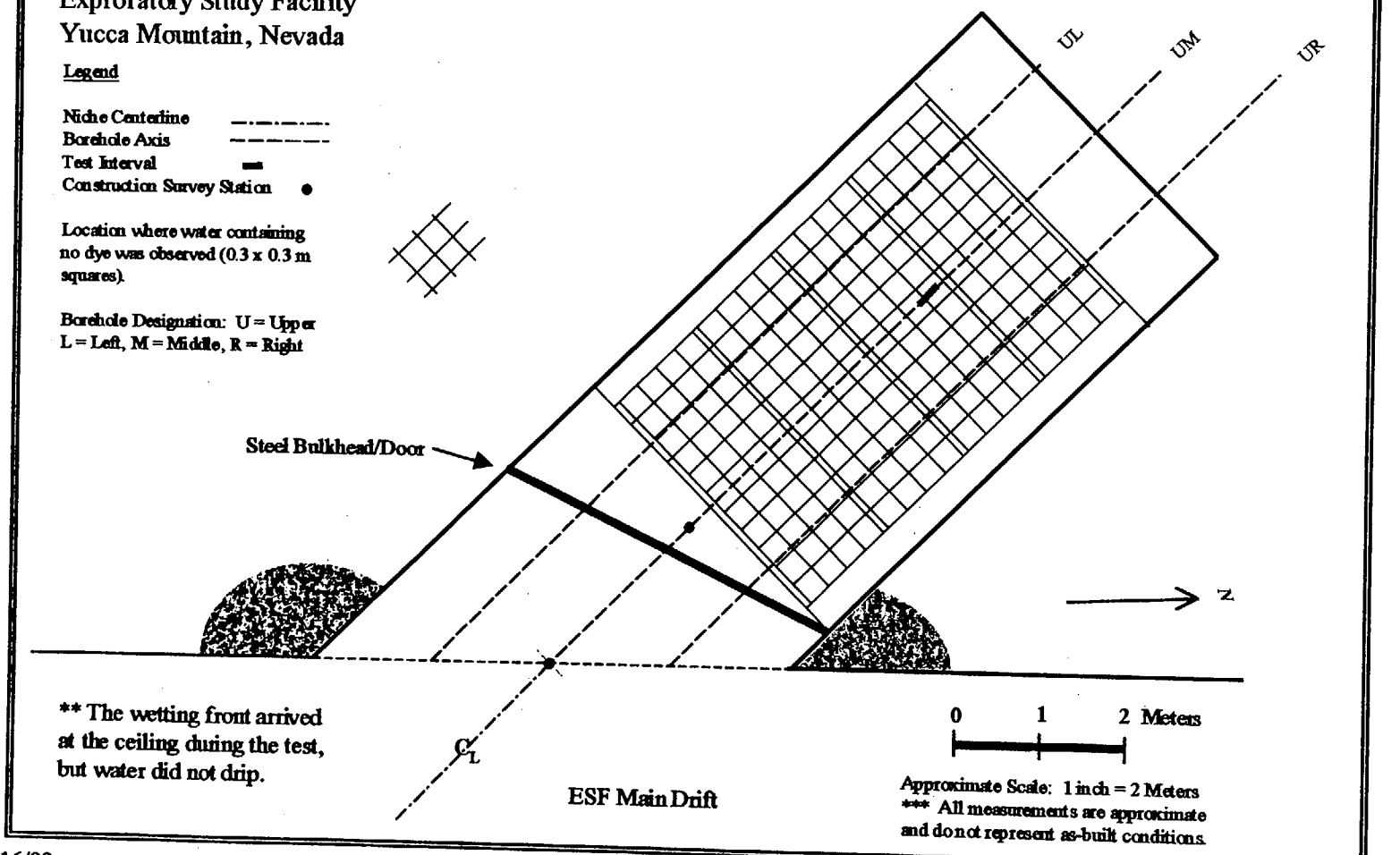

6/16/98
Version 1.0

Figure A.26

LIQUID OUTFLOW DISTRIBUTION 1/12/98 - NICHE 3650
BOREHOLE UM: TEST INTERVAL 6.10 - 6.40 METERS

Lawrence Berkeley National Laboratory
Exploratory Study Facility
Yucca Mountain, Nevada

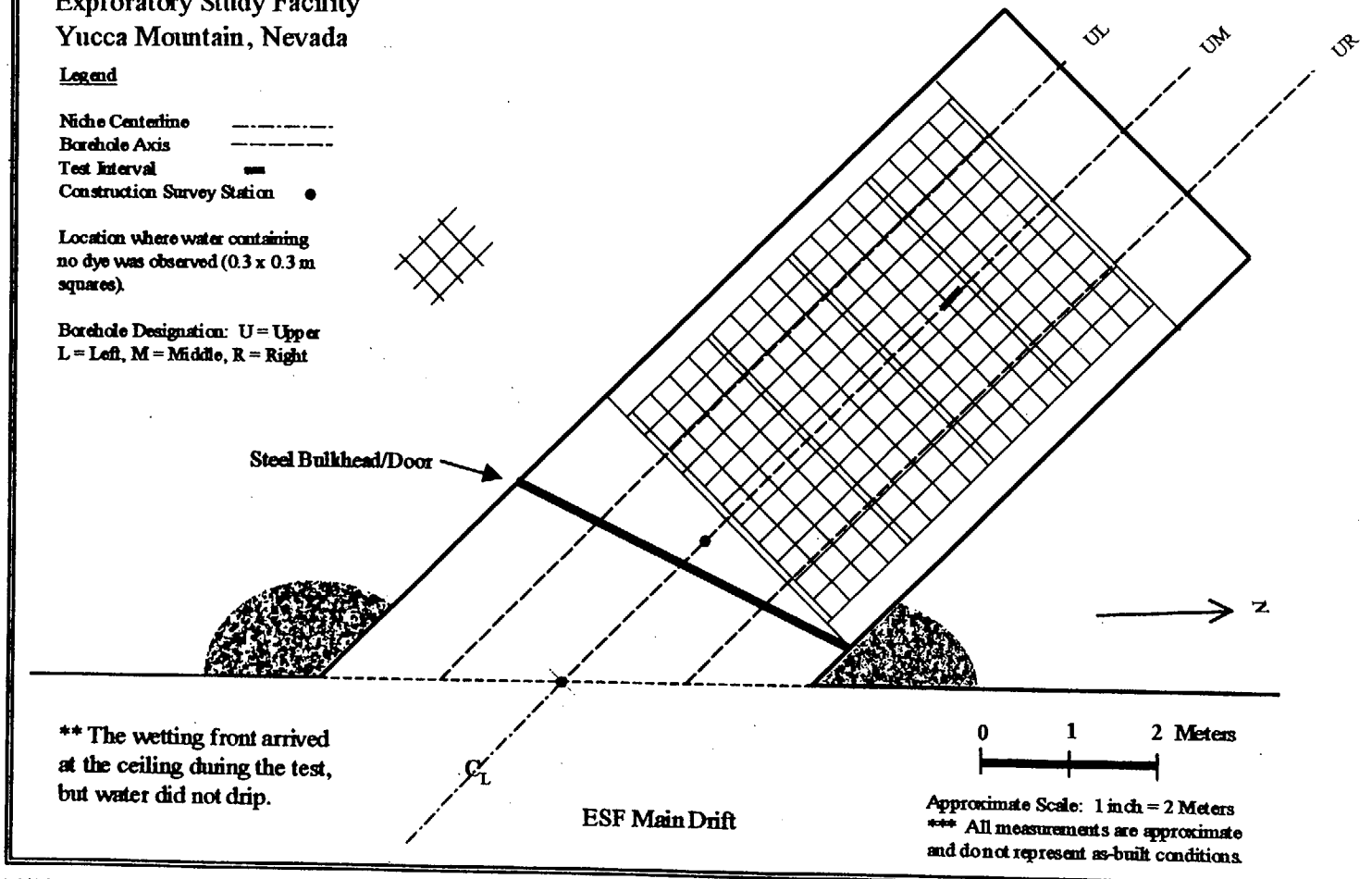

Figure A.27

LIQUID OUTFLOW DISTRIBUTION 11/12/97 - NICHE 3650
BOREHOLE UM: TEST INTERVAL 6.71 - 7.01 METERS

Lawrence Berkeley National Laboratory
Exploratory Study Facility
Yucca Mountain, Nevada

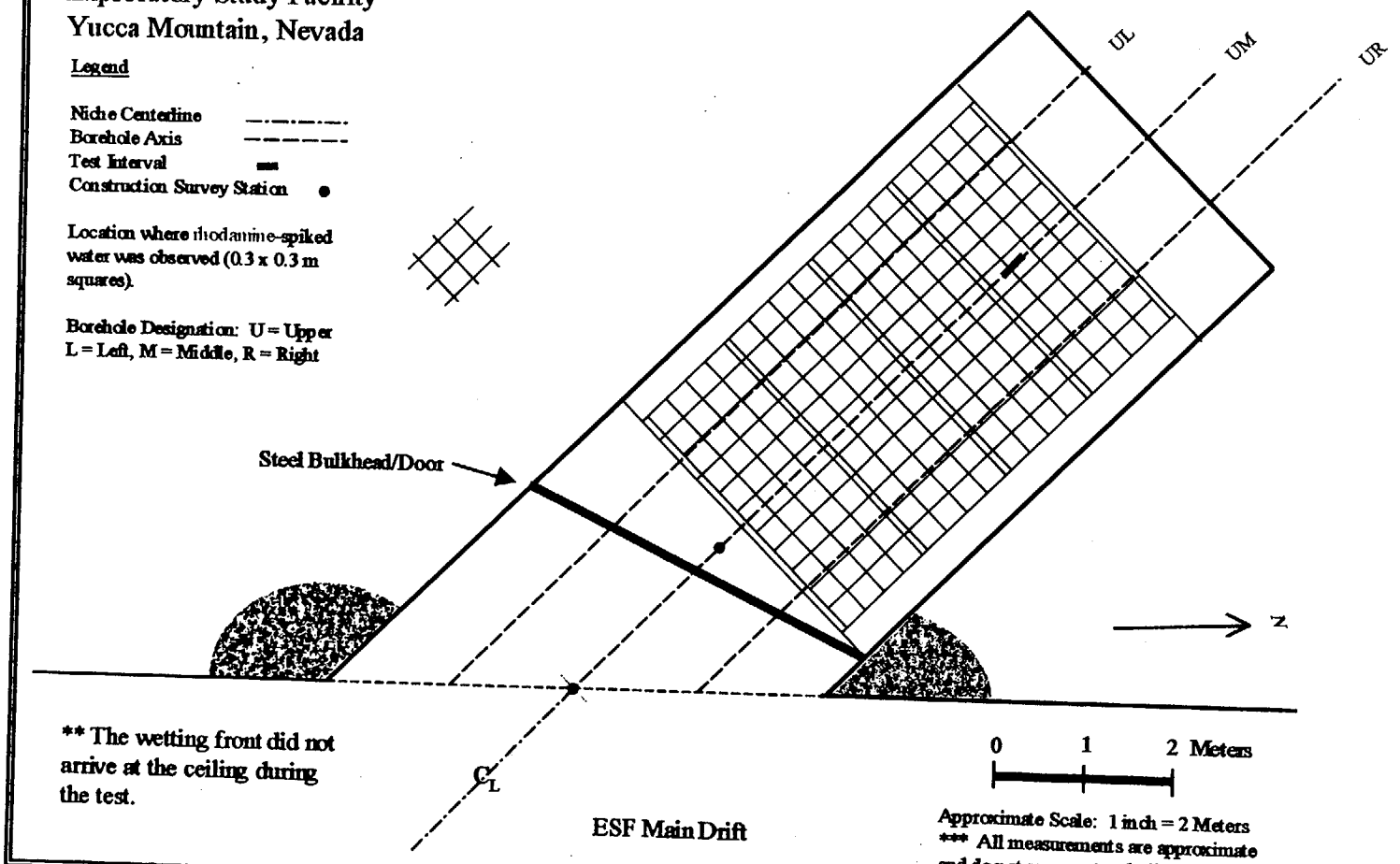

6/16/98
Version 1.0

Figure A.28

LIQUID OUTFLOW DISTRIBUTION 12/5/97 - NICHE 3650
BOREHOLE UM: TEST INTERVAL 6.71 - 7.01 METERS

Lawrence Berkeley National Laboratory
Exploratory Study Facility
Yucca Mountain, Nevada

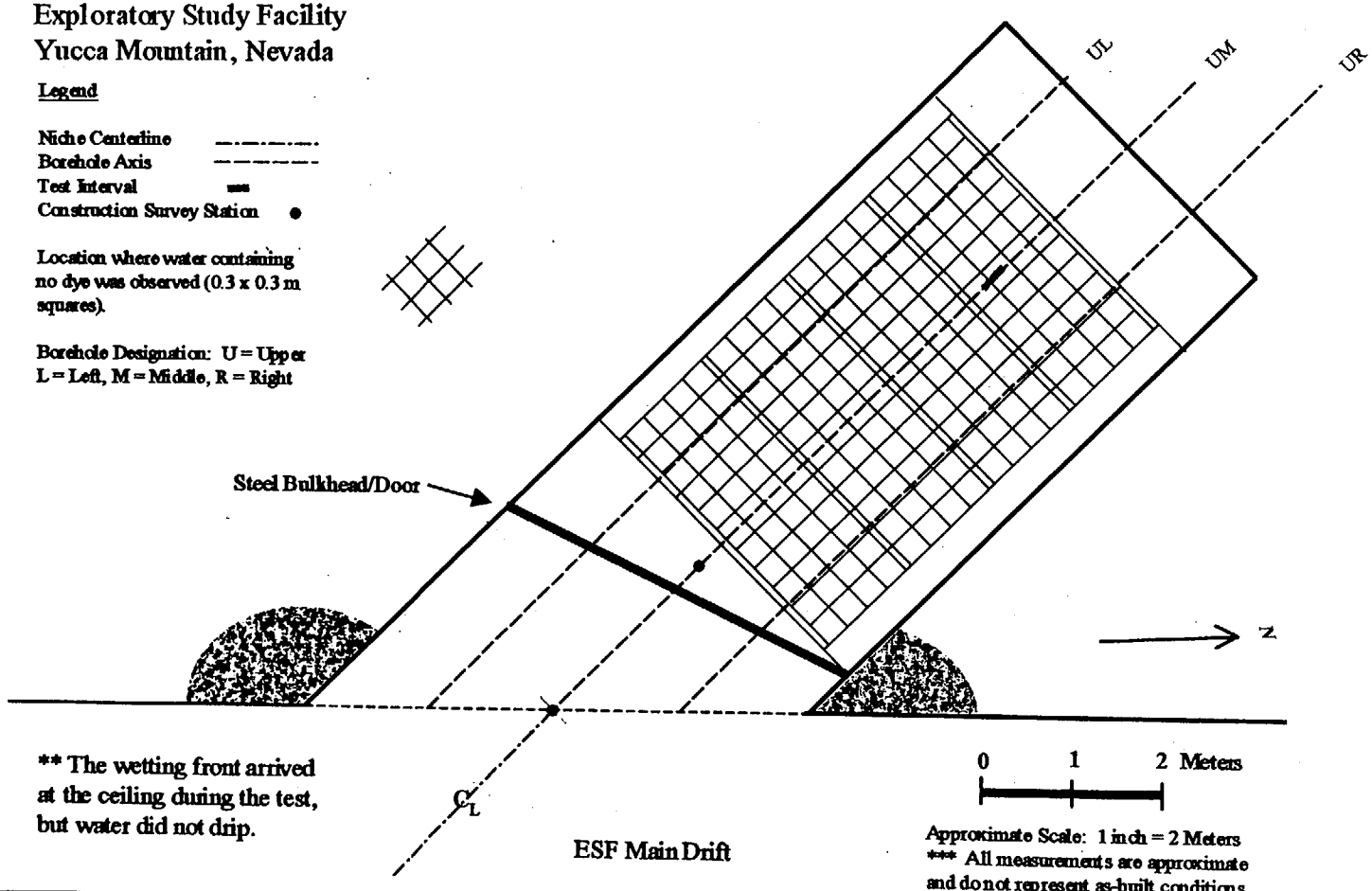

Figure A.29

LIQUID OUTFLOW DISTRIBUTION 1/14/98 - NICHE 3650
BOREHOLE UR: TEST INTERVAL 4.27 - 4.57 METERS

Lawrence Berkeley National Laboratory
Exploratory Study Facility
Yucca Mountain, Nevada

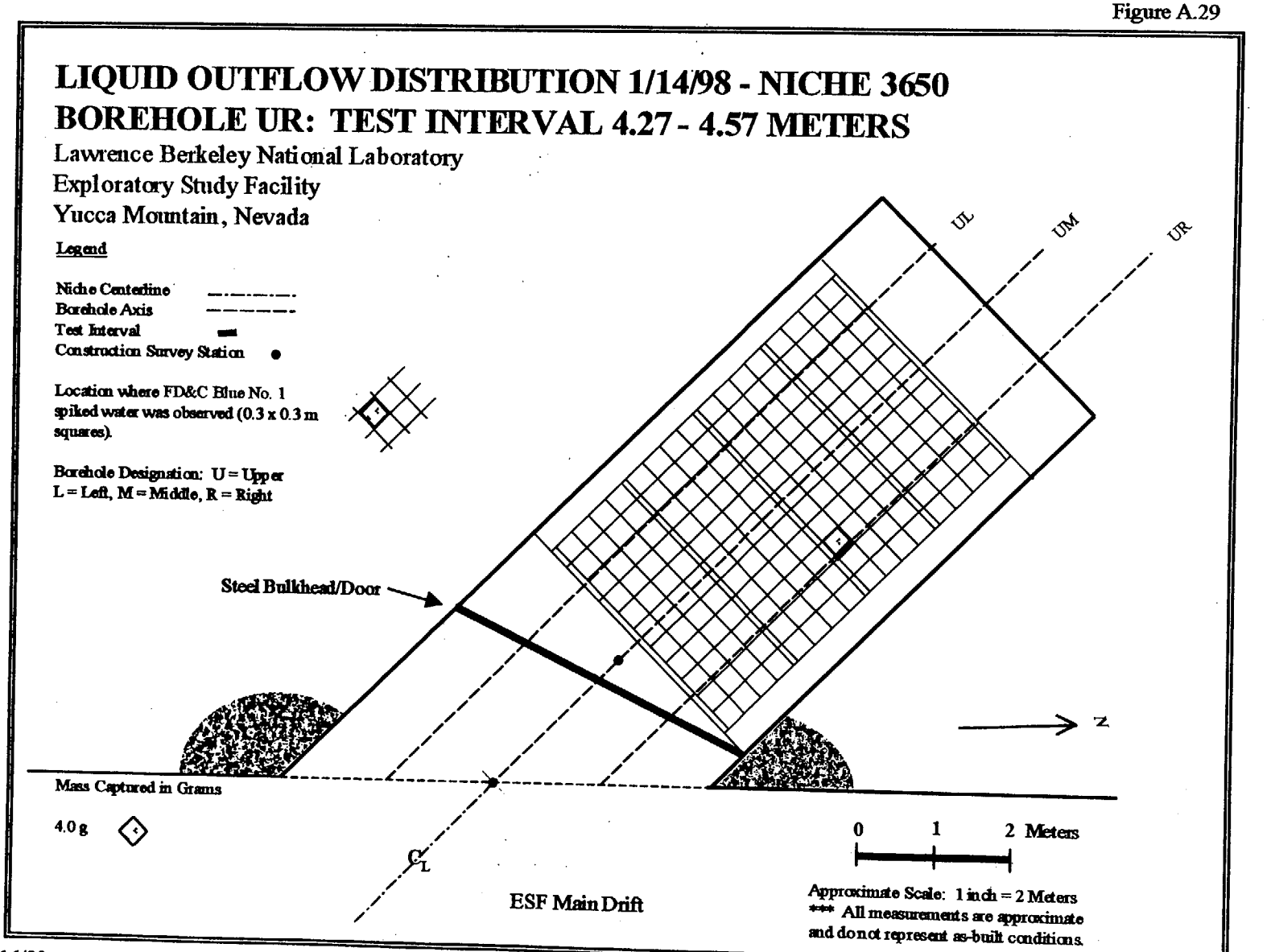

6/16/98
Version 1.0

LIQUID OUTFLOW DISTRIBUTION 2/5/98 - NICHE 3650
BOREHOLE UR: TEST INTERVAL 4.27 - 4.57 METERS

Lawrence Berkeley National Laboratory
Exploratory Study Facility
Yucca Mountain, Nevada

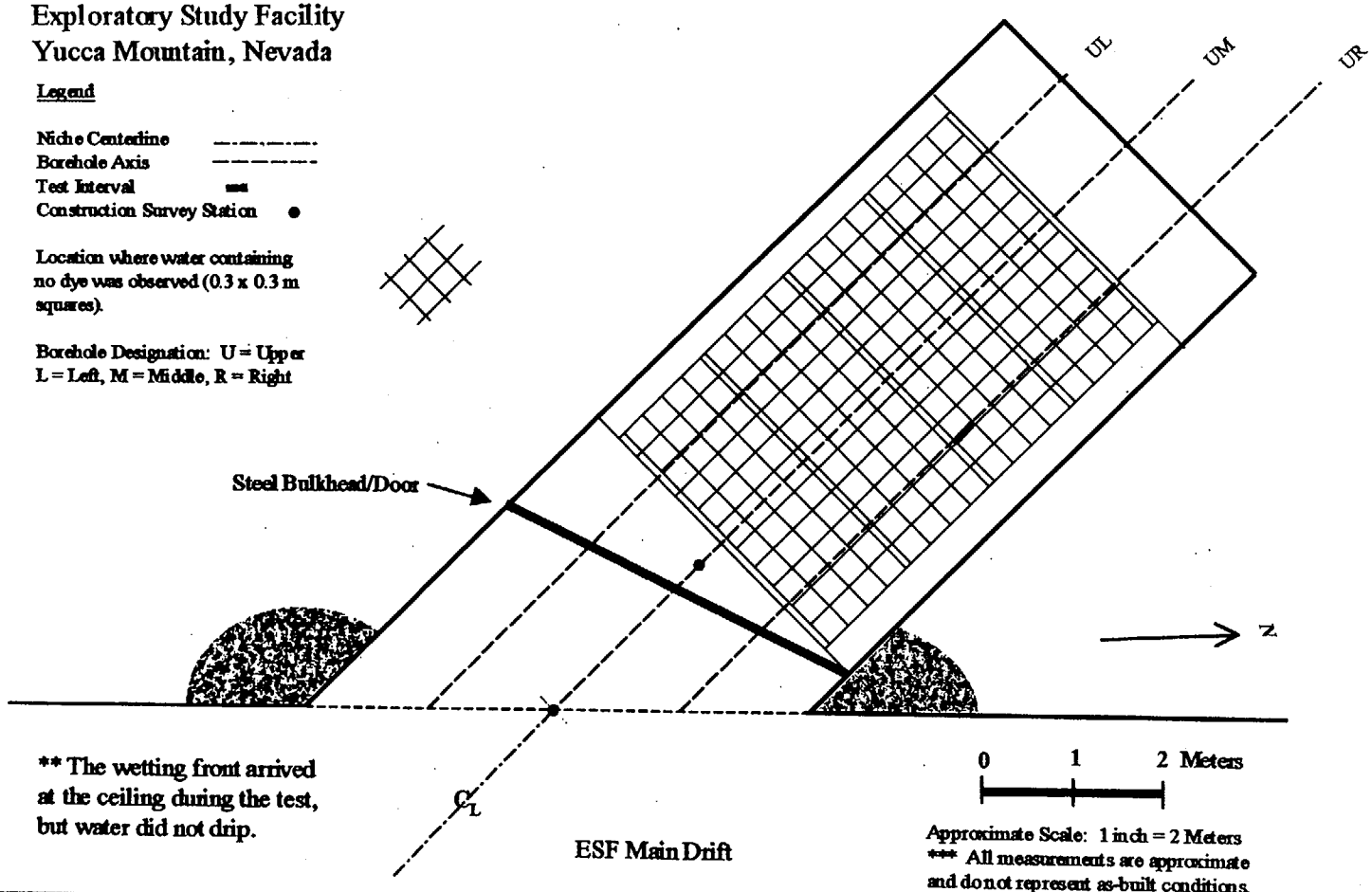

Figure A.31

LIQUID OUTFLOW DISTRIBUTION 1/15/98 - NICHE 3650
BOREHOLE UR: TEST INTERVAL 4.88 - 5.18 METERS

Lawrence Berkeley National Laboratory
Exploratory Study Facility
Yucca Mountain, Nevada

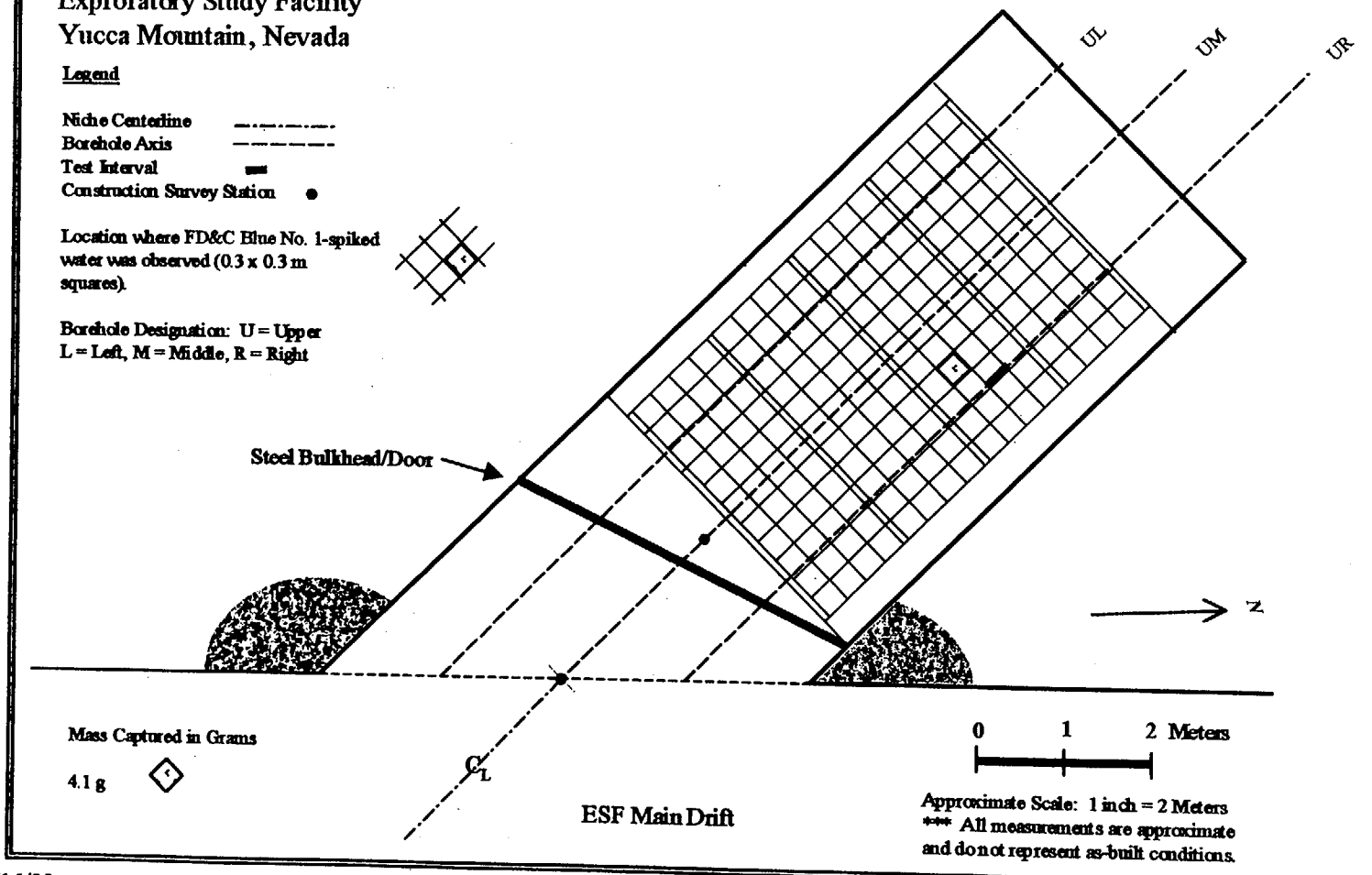

Figure A.32

LIQUID OUTFLOW DISTRIBUTION 2/6/98 - NICHE 3650
BOREHOLE UR: TEST INTERVAL 4.88 - 5.18 METERS

Lawrence Berkeley National Laboratory
Exploratory Study Facility
Yucca Mountain, Nevada

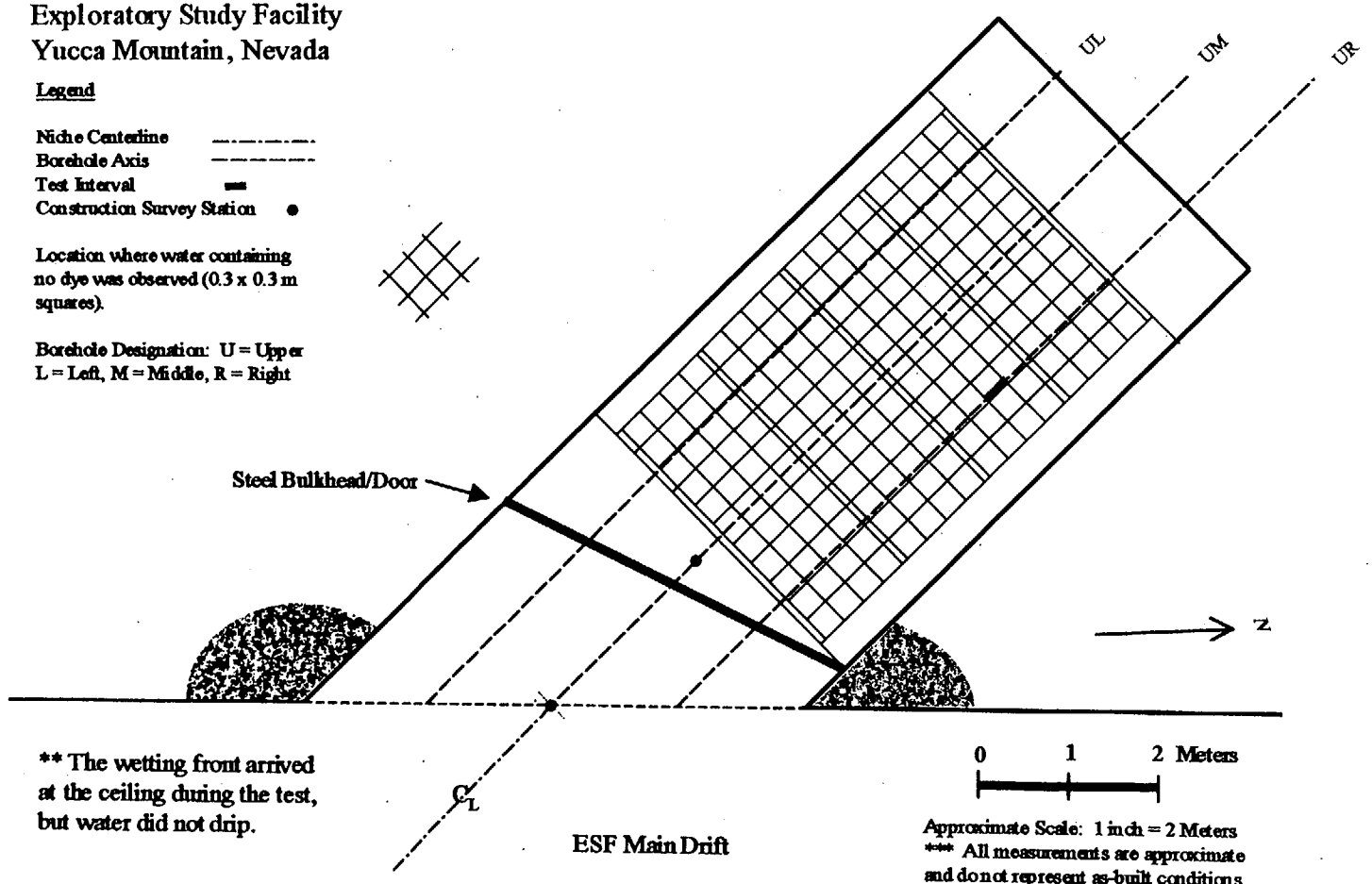

LIQUID OUTFLOW DISTRIBUTION 1/13/98 - NICHE 3650
BOREHOLE UR: TEST INTERVAL 5.49 - 5.79 METERS

Lawrence Berkeley National Laboratory
Exploratory Study Facility
Yucca Mountain, Nevada

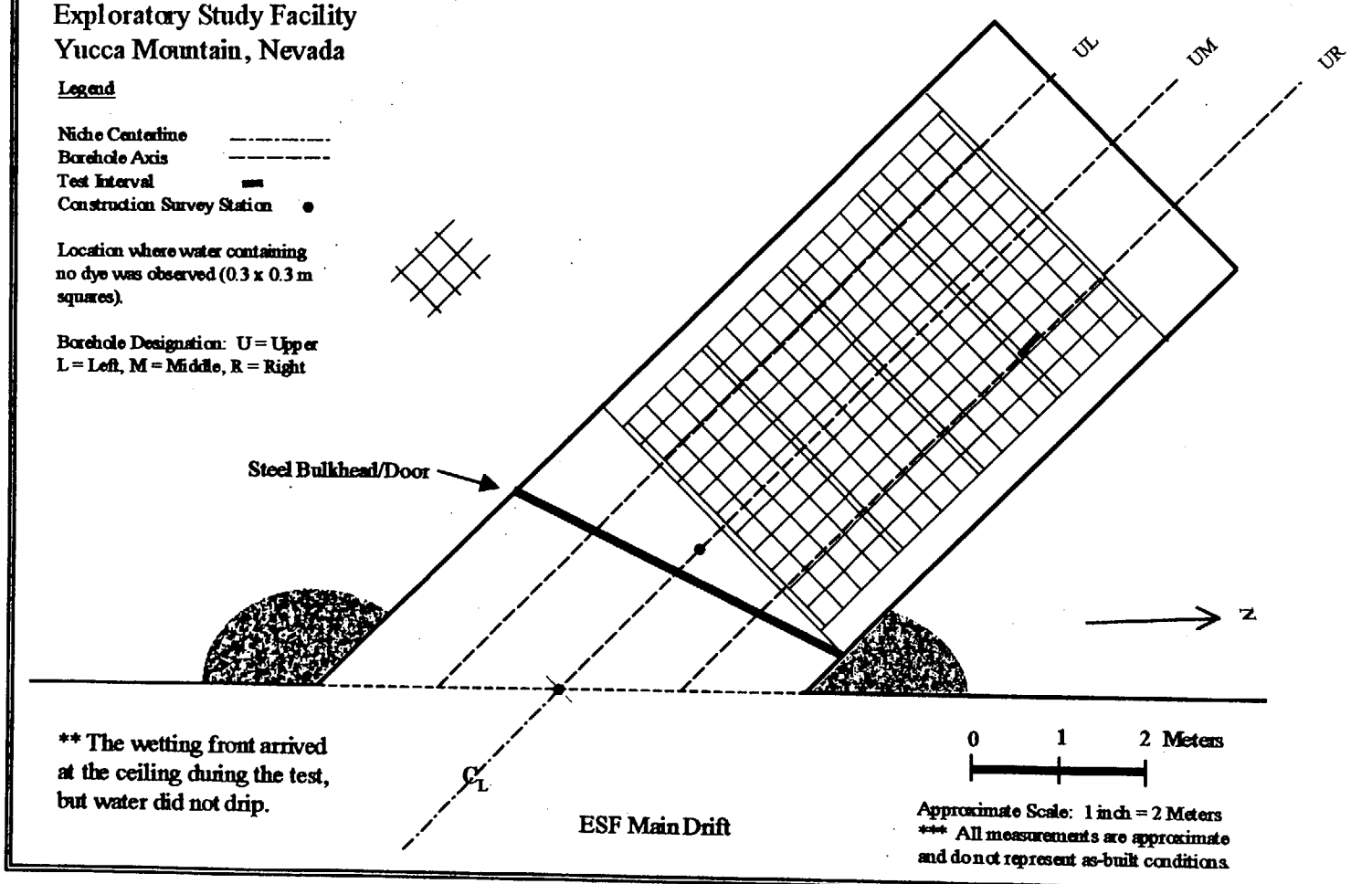

LIQUID OUTFLOW DISTRIBUTION 2/10/98 - NICHE 3650
BOREHOLE UR: TEST INTERVAL 5.49 - 5.79 METERS

Lawrence Berkeley National Laboratory
Exploratory Study Facility
Yucca Mountain, Nevada

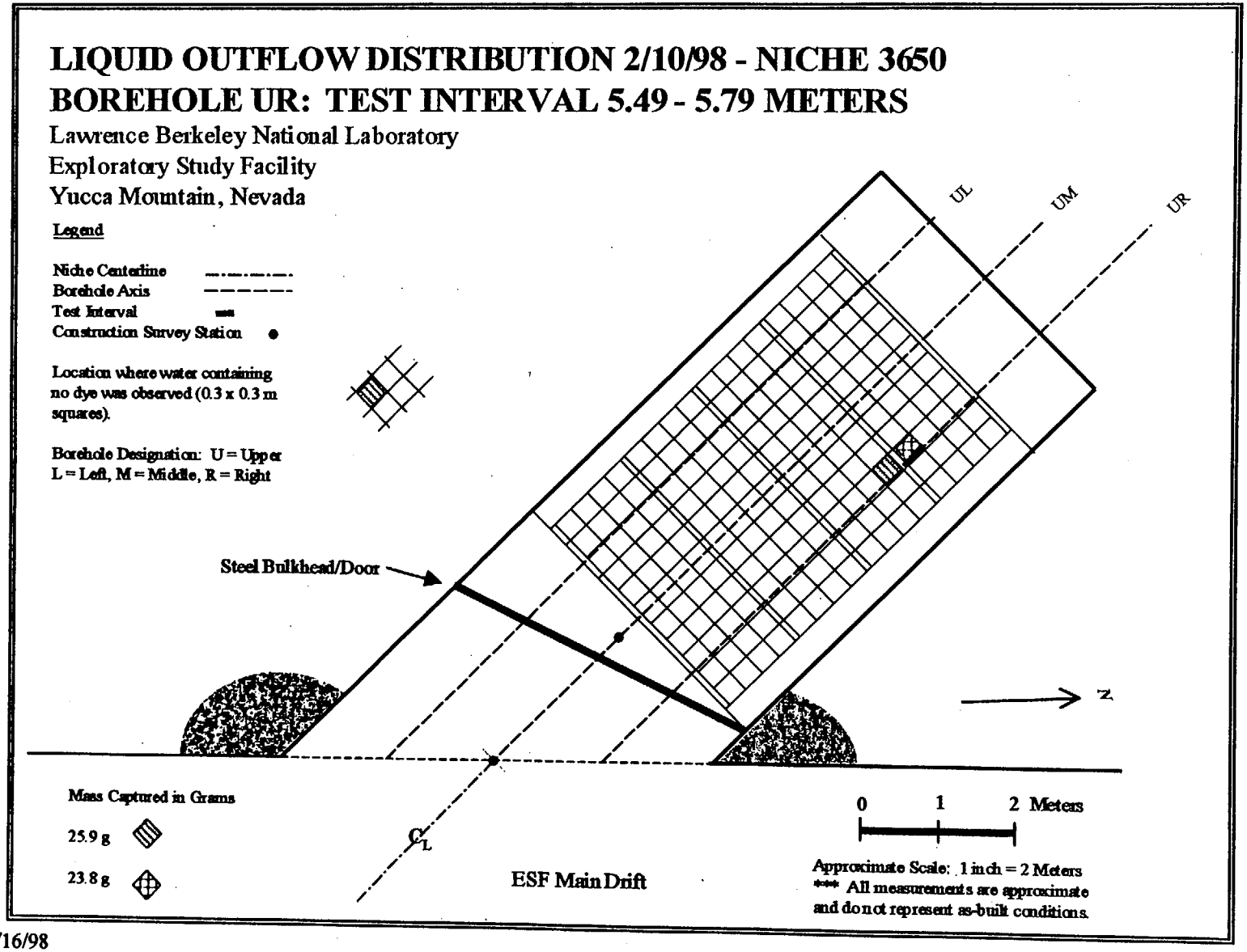

Figure A.35

LIQUID OUTFLOW DISTRIBUTION 1/14/98 - NICHE 3650
BOREHOLE UR: TEST INTERVAL 6.10 - 6.40 METERS

Lawrence Berkeley National Laboratory
Exploratory Study Facility
Yucca Mountain, Nevada

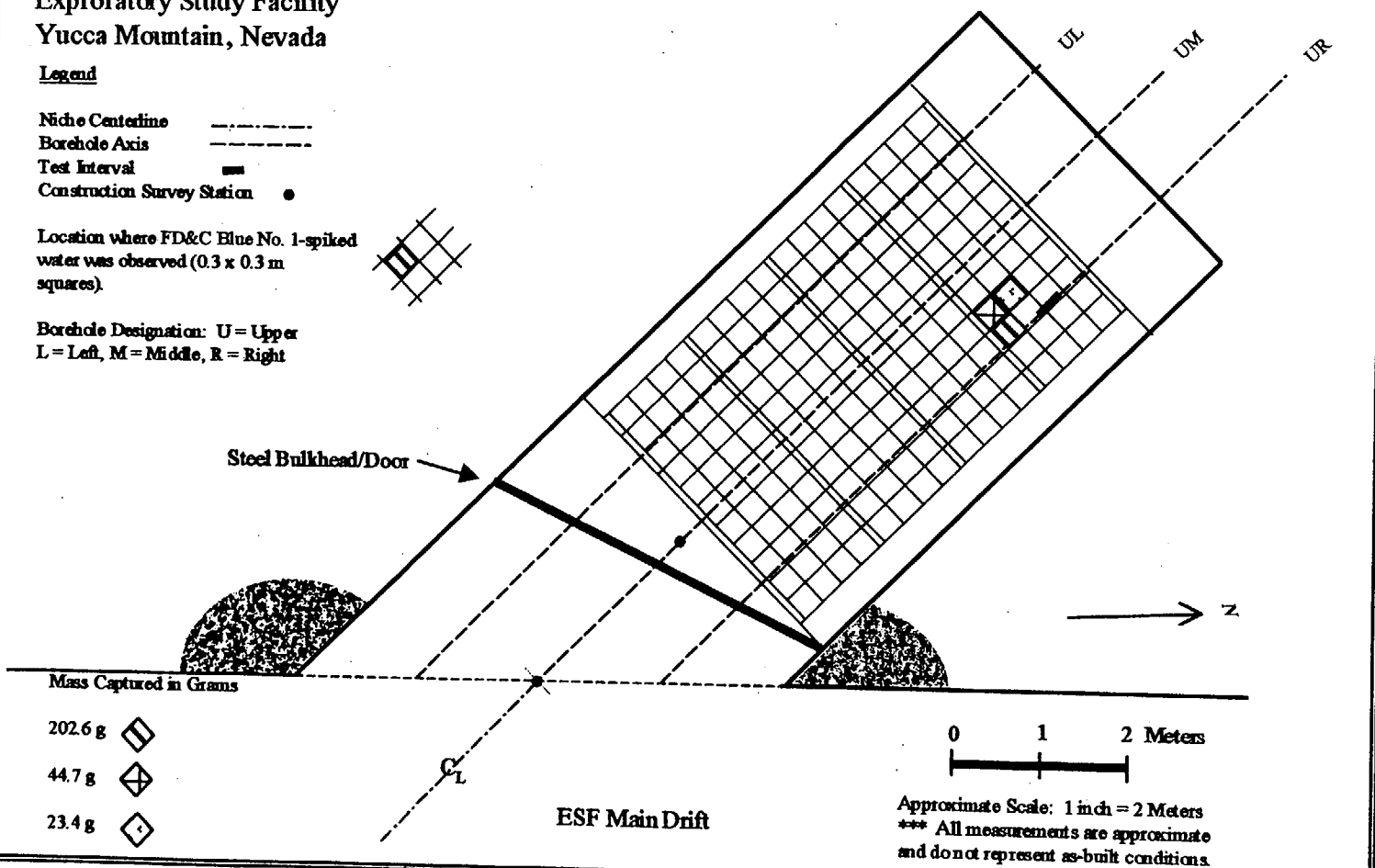

6/16/98
Version 1.0

Figure A.36

LIQUID OUTFLOW DISTRIBUTION 2/4/98 - NICHE 3650
BOREHOLE UR: TEST INTERVAL 6.10 - 6.40 METERS

Lawrence Berkeley National Laboratory
Exploratory Study Facility
Yucca Mountain, Nevada

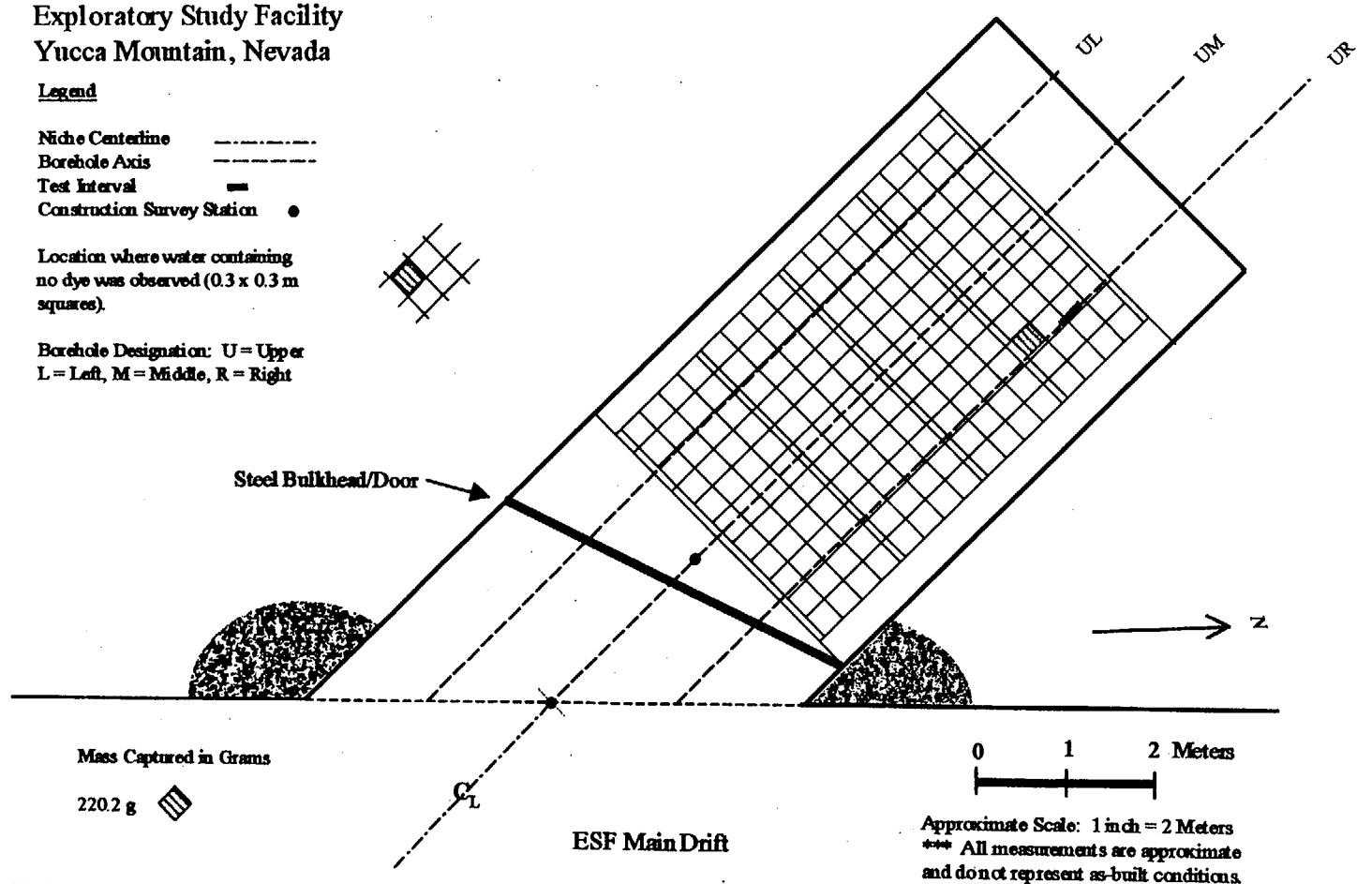

LIQUID OUTFLOW DISTRIBUTION 1/13/98 - NICHE 3650
BOREHOLE UR: TEST INTERVAL 6.71 - 7.01 METERS

Lawrence Berkeley National Laboratory
Exploratory Study Facility
Yucca Mountain, Nevada

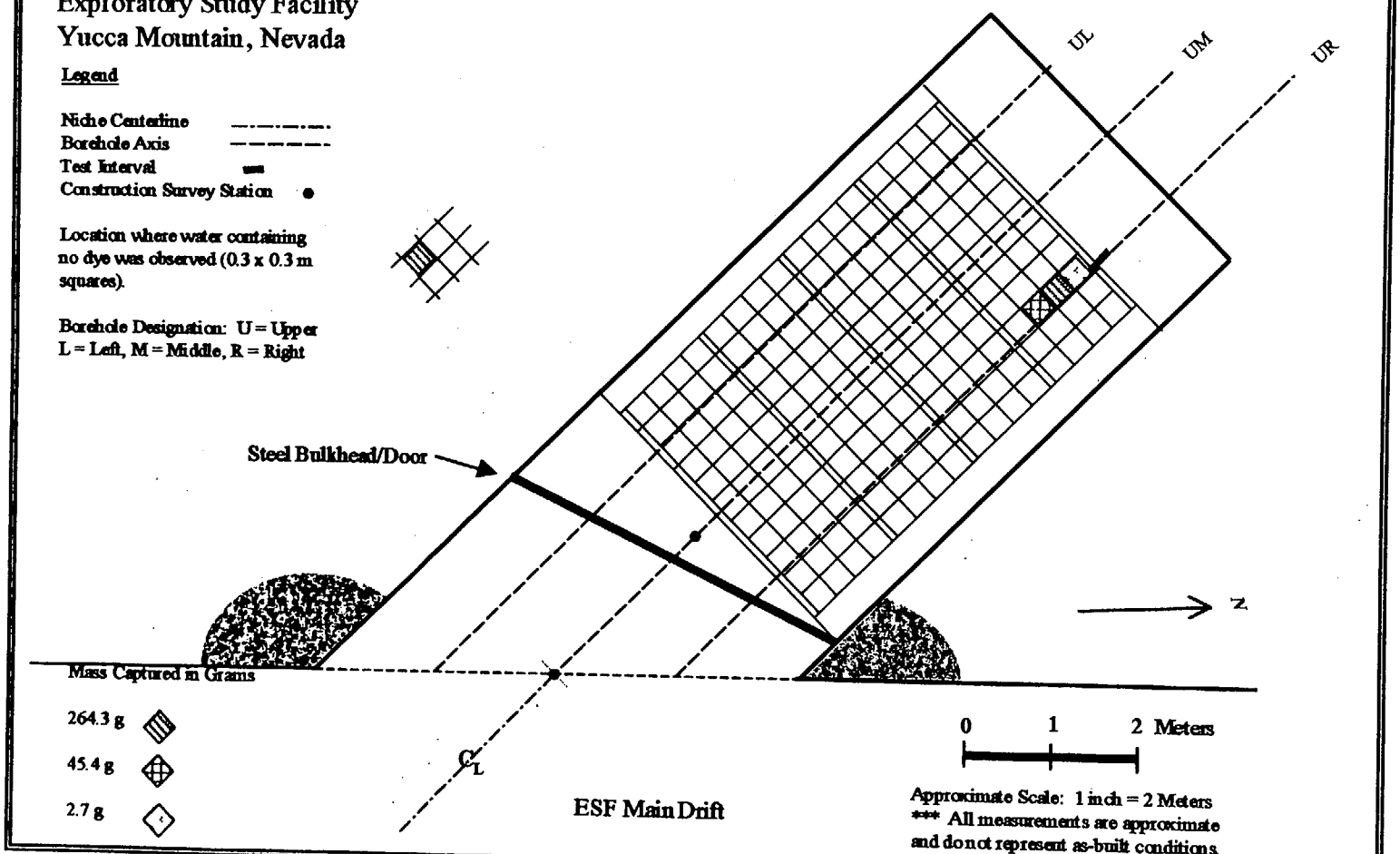

LIQUID OUTFLOW DISTRIBUTION 2/3/98 - NICHE 3650
BOREHOLE UR: TEST INTERVAL 6.71 - 7.01 METERS

Lawrence Berkeley National Laboratory
Exploratory Study Facility
Yucca Mountain, Nevada

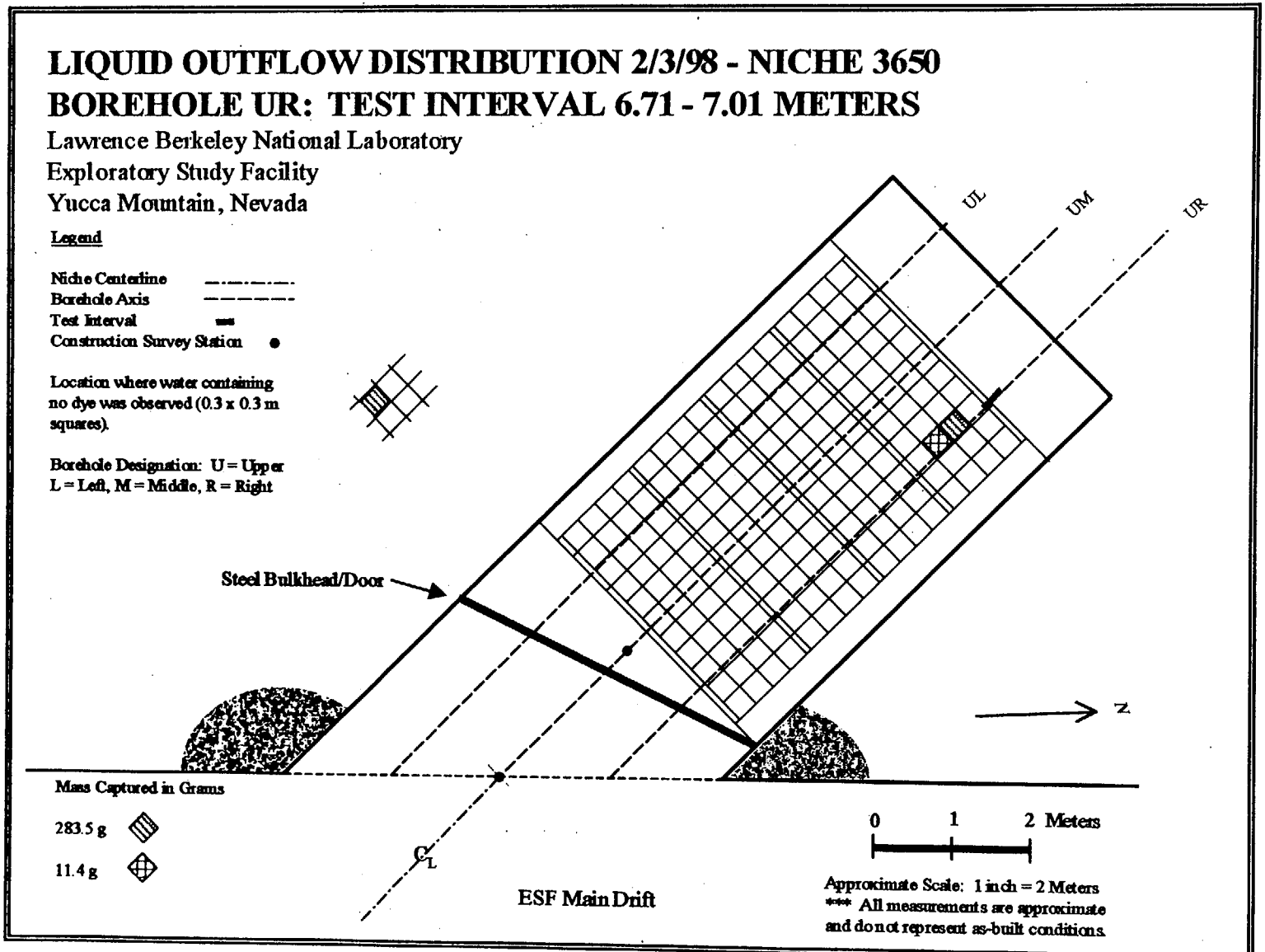

LIQUID OUTFLOW DISTRIBUTION 3/5/98 - NICHE 3650
BOREHOLE UR: TEST INTERVAL 6.71 - 7.01 METERS

Lawrence Berkeley National Laboratory
Exploratory Study Facility
Yucca Mountain, Nevada

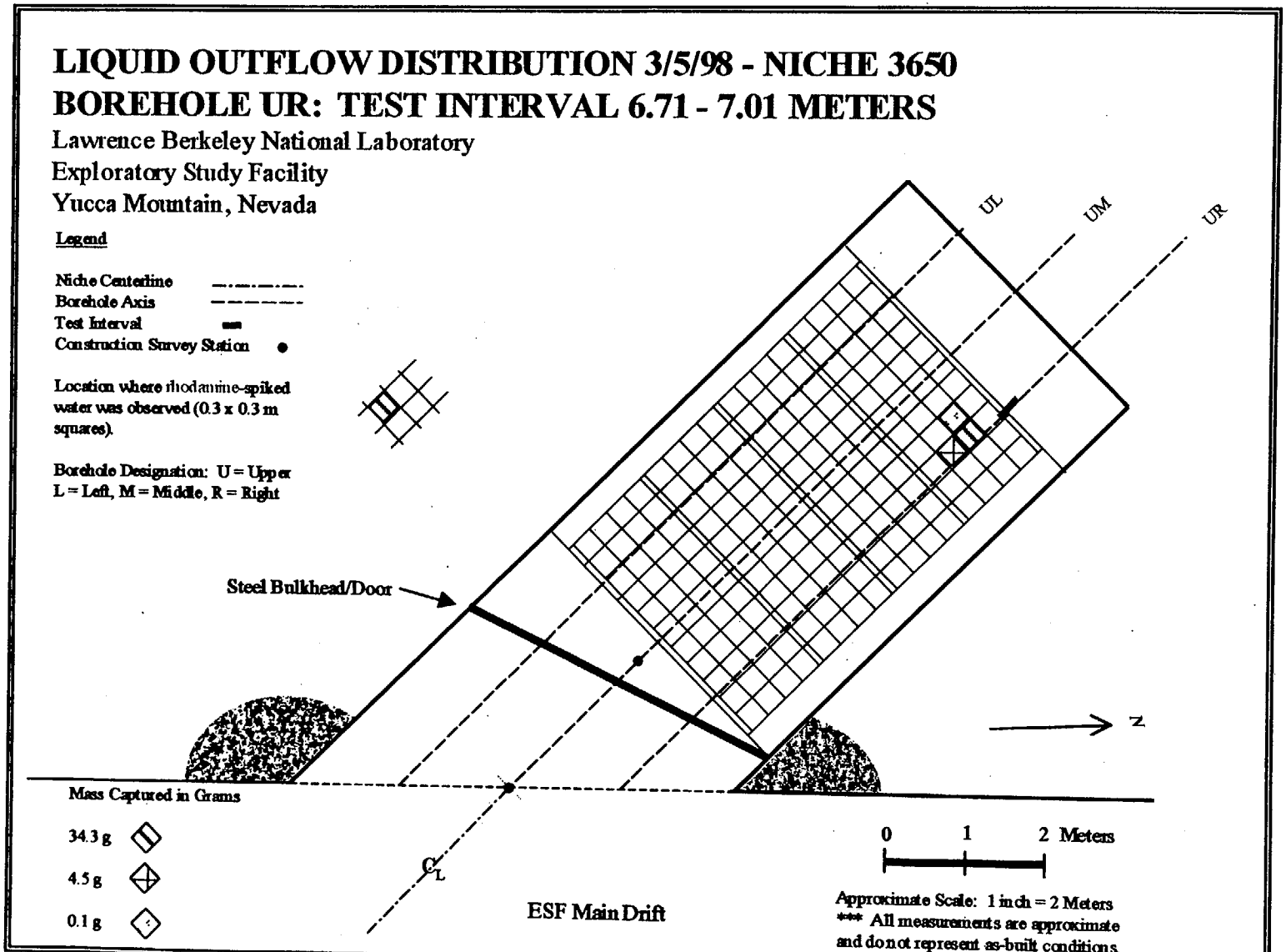

LIQUID OUTFLOW DISTRIBUTION 3/12/98 - NICHE 3650
BOREHOLE UR: TEST INTERVAL 7.62 - 7.92 METERS

Lawrence Berkeley National Laboratory
Exploratory Study Facility
Yucca Mountain, Nevada

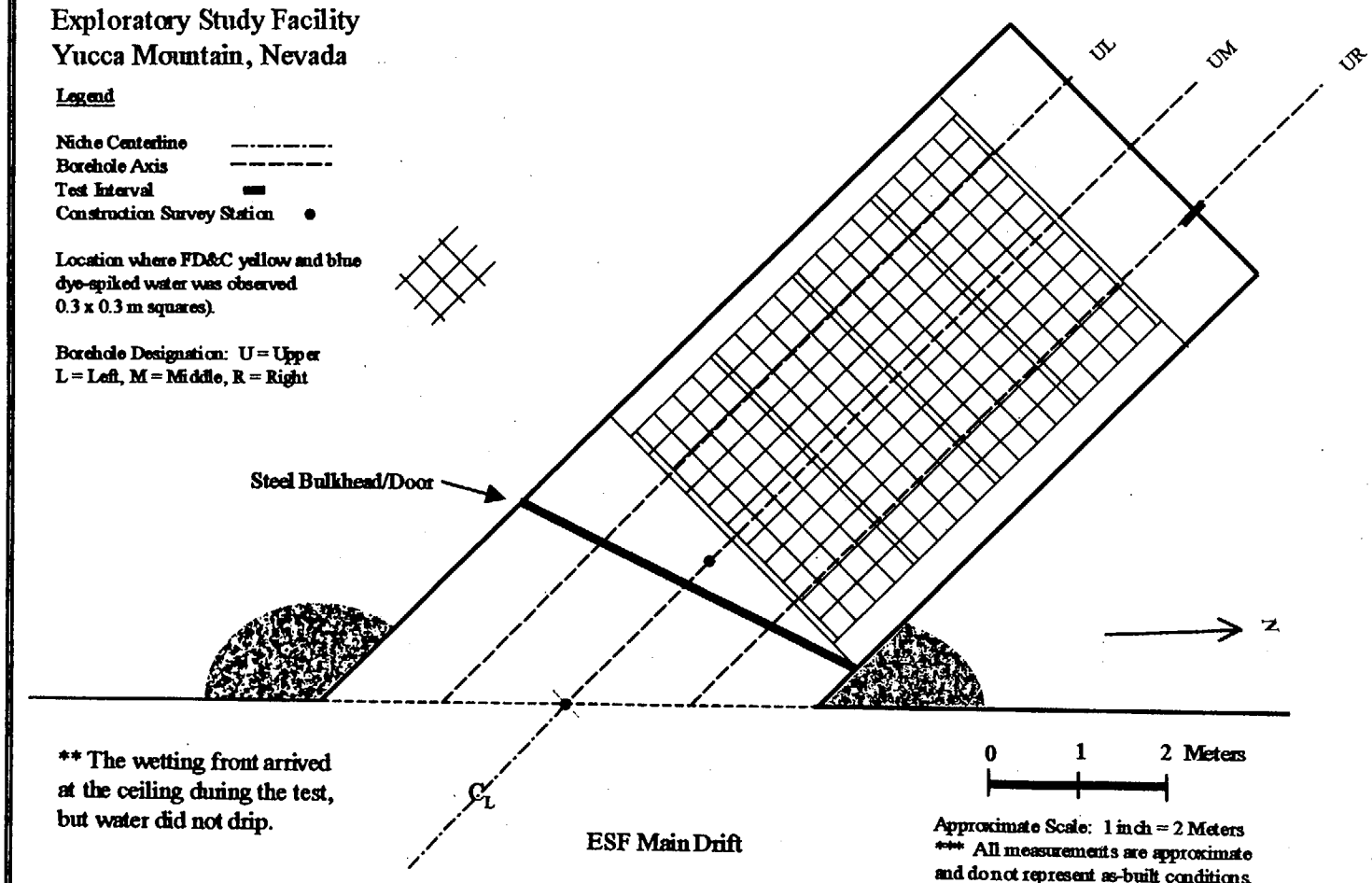

Appendix B

Plots Showing Seepage Percentage Versus Liquid-Release Rate

Liquid-Release Rate vs. Seepage Percentage Niche 3650 Borehole UR: 5.18 - 5.49 m

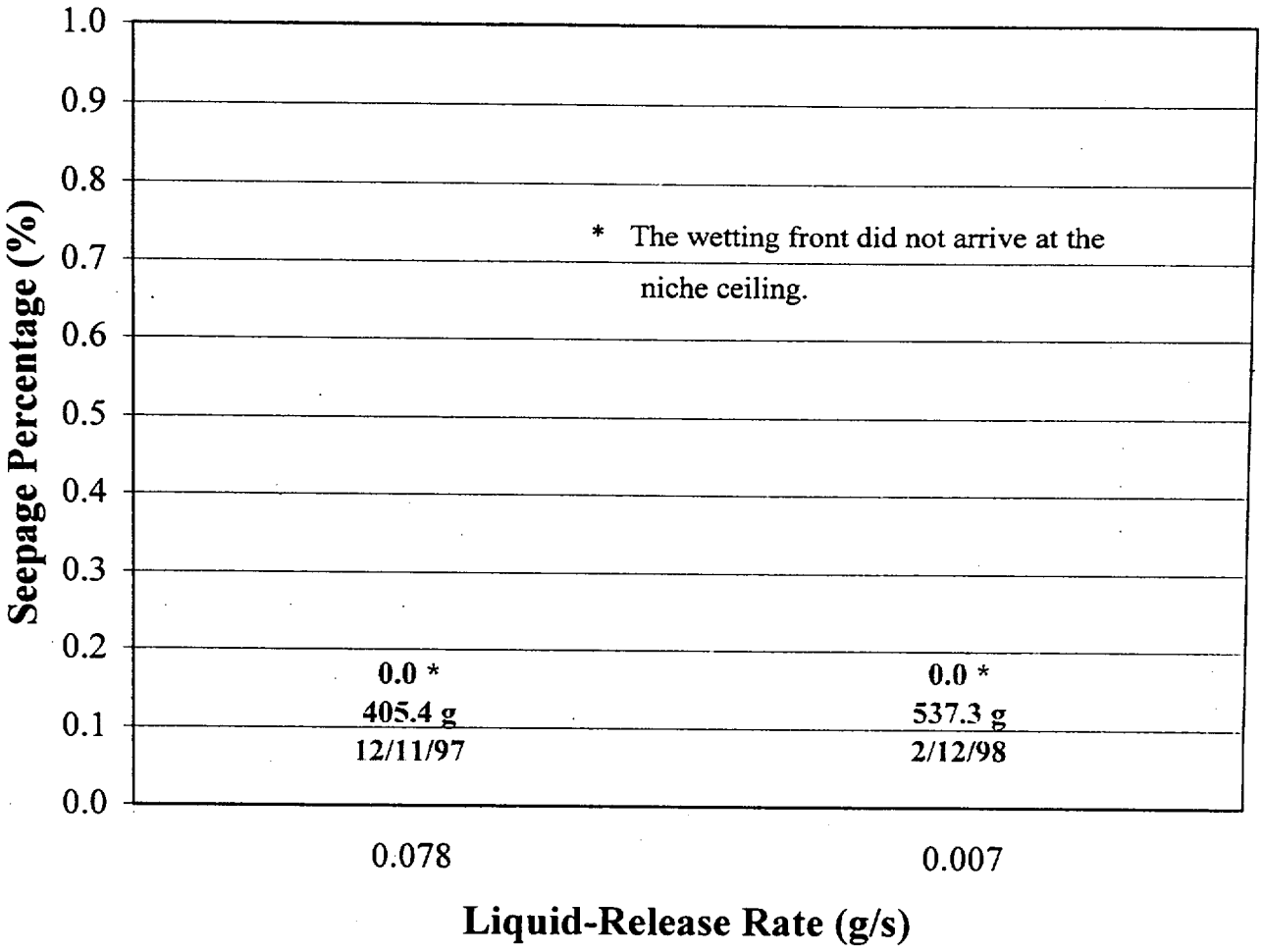

Liquid-Release Rate vs. Seepage Percentage
Niche 3650 Borehole UL: 5.79 - 6.10 m

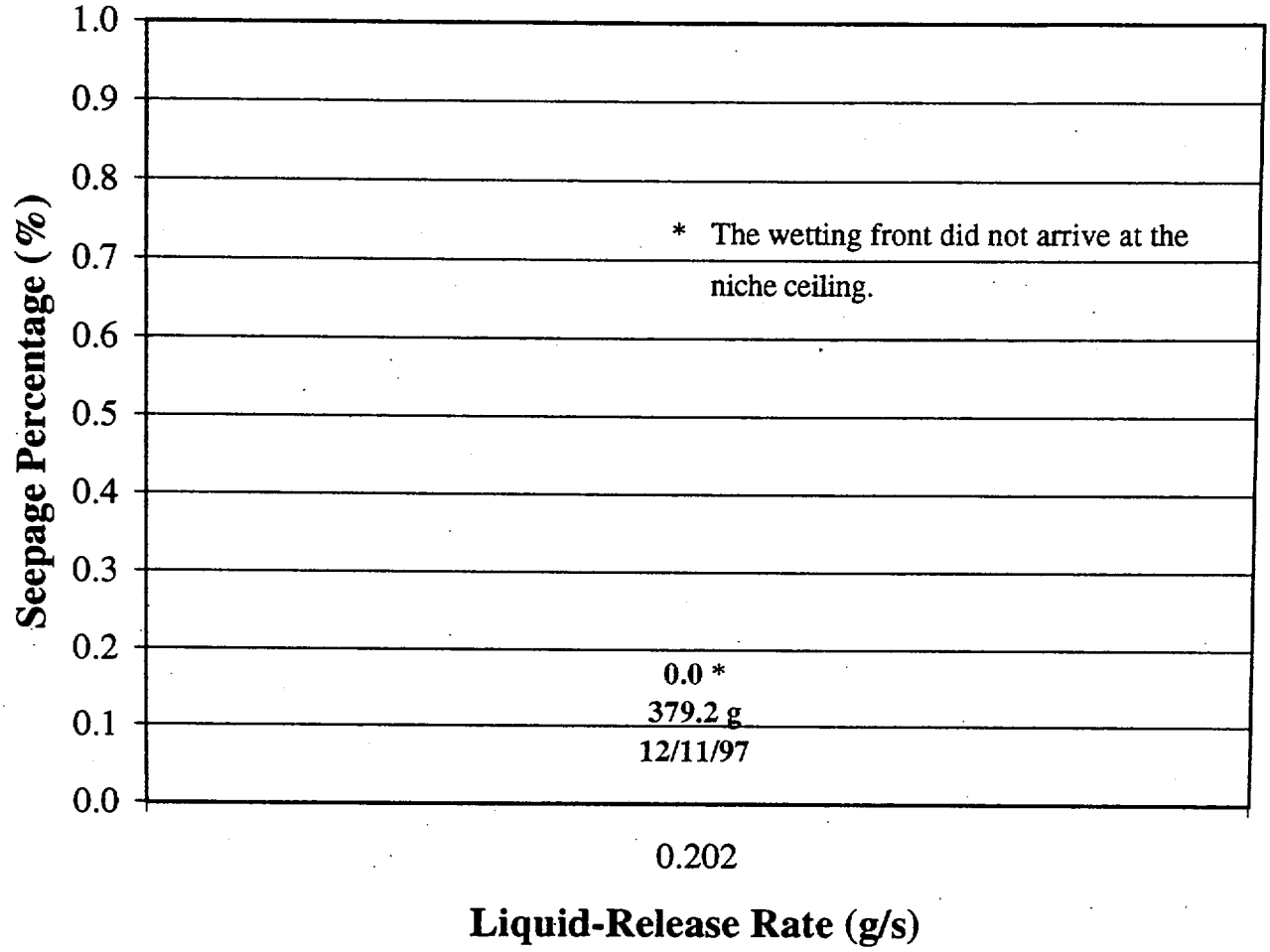

Liquid-Release Rate vs. Seepage Percentage
Niche 3650 Borehole UL: 6.40 - 6.71 m

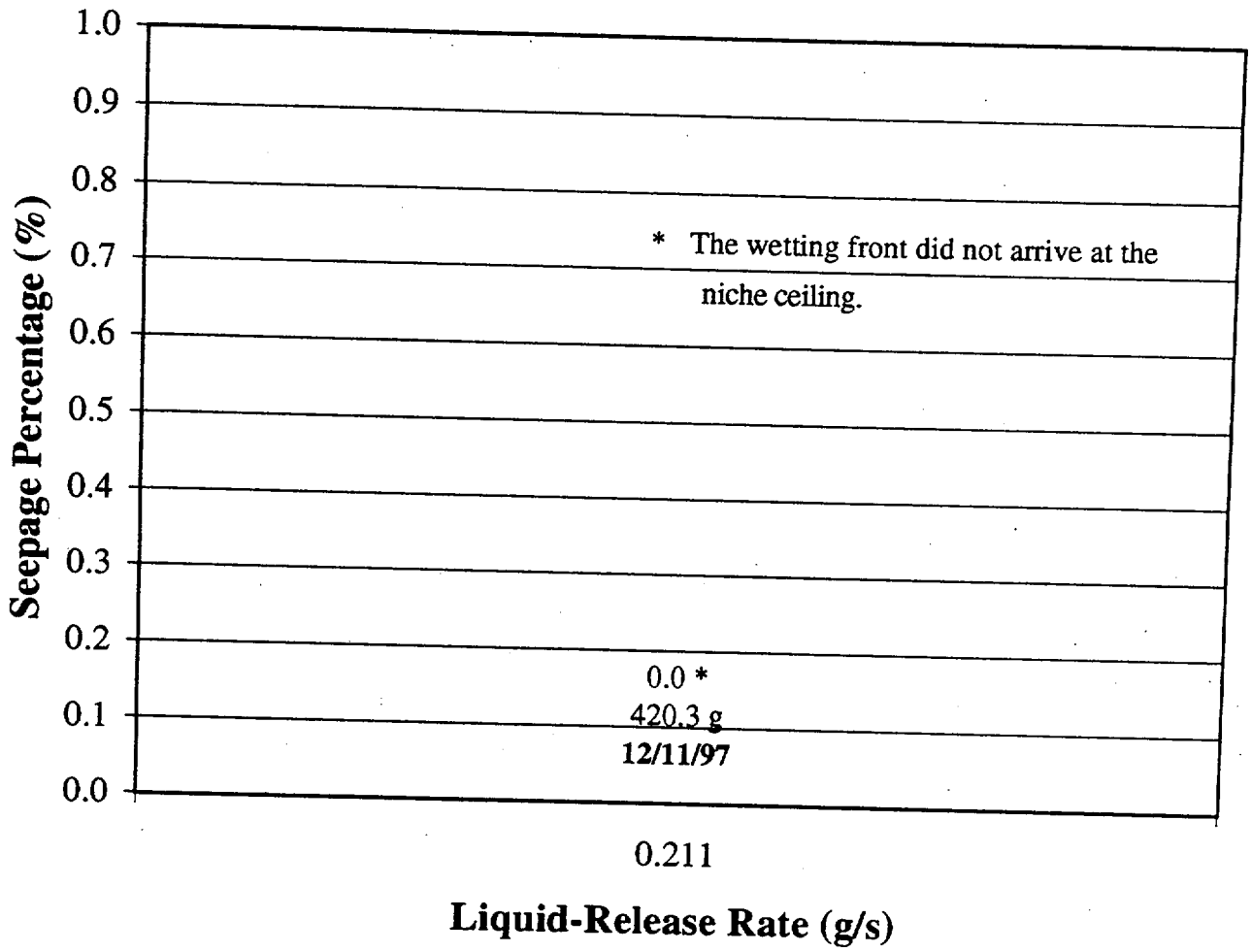

Liquid-Release Rate vs. Seepage Percentage
Niche 3650 Borehole UL: 7.01-7.32 m

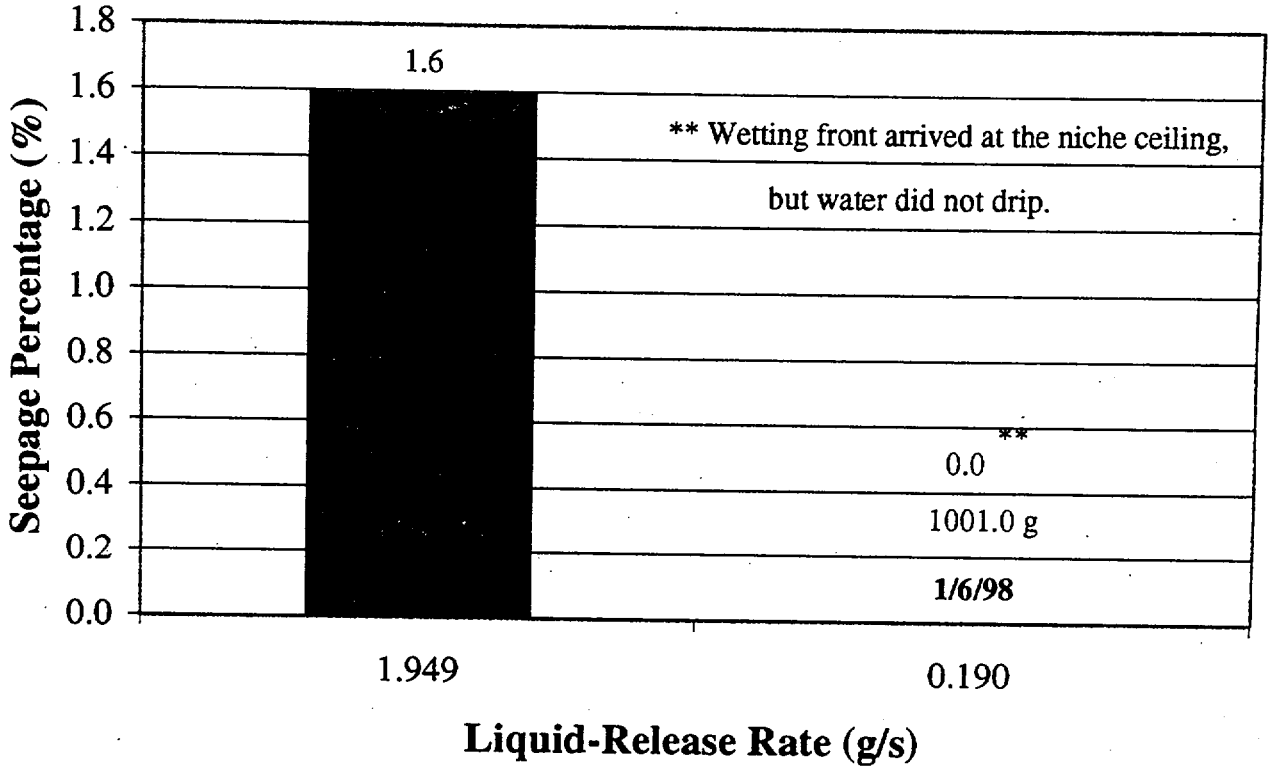

Liquid-Release Rate vs. Seepage Percentage
Niche 3650 Borehole UL: 7.62 - 7.92 m

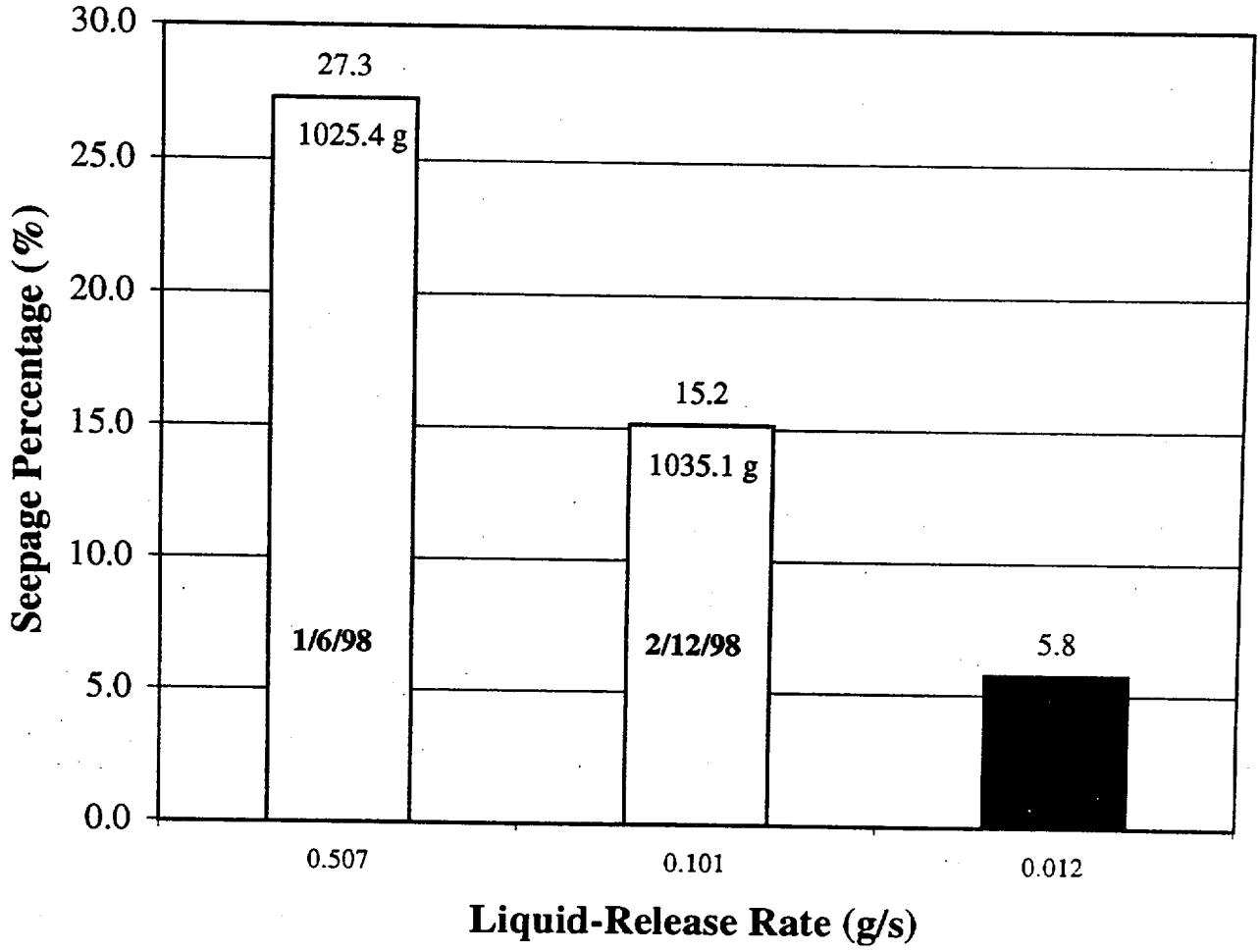

Liquid-Release Rate vs. Seepage Percentage
Niche 3650 Borehole UM: 4.27-4.57 m

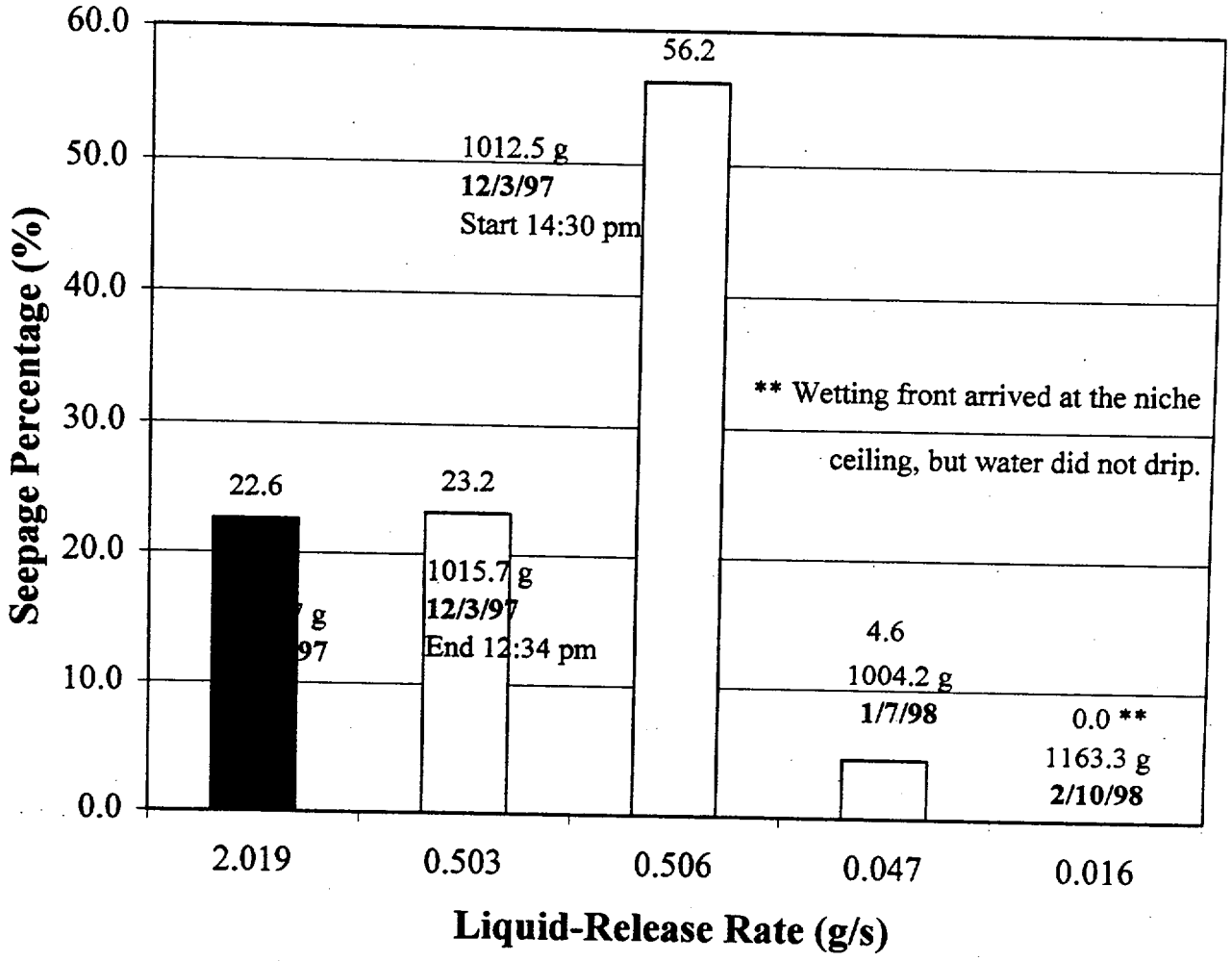

Liquid-Release Rate vs. Seepage Percentage
Niche 3650 Borehole UM: 5.49-5.79 m

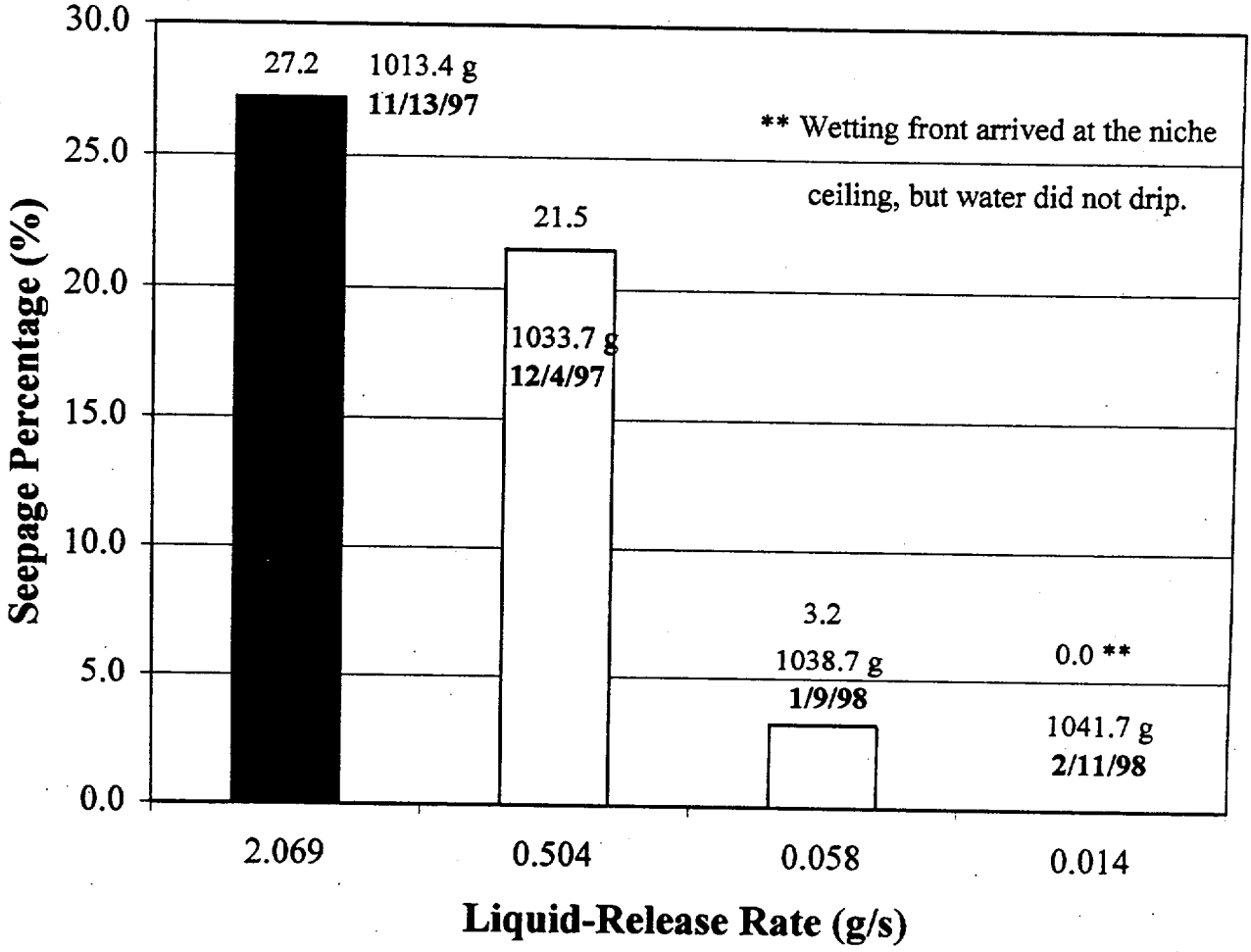

Liquid-Release Rate vs. Seepage Percentage Niche 3650 Borehole UM: 6.10 - 6.40 m

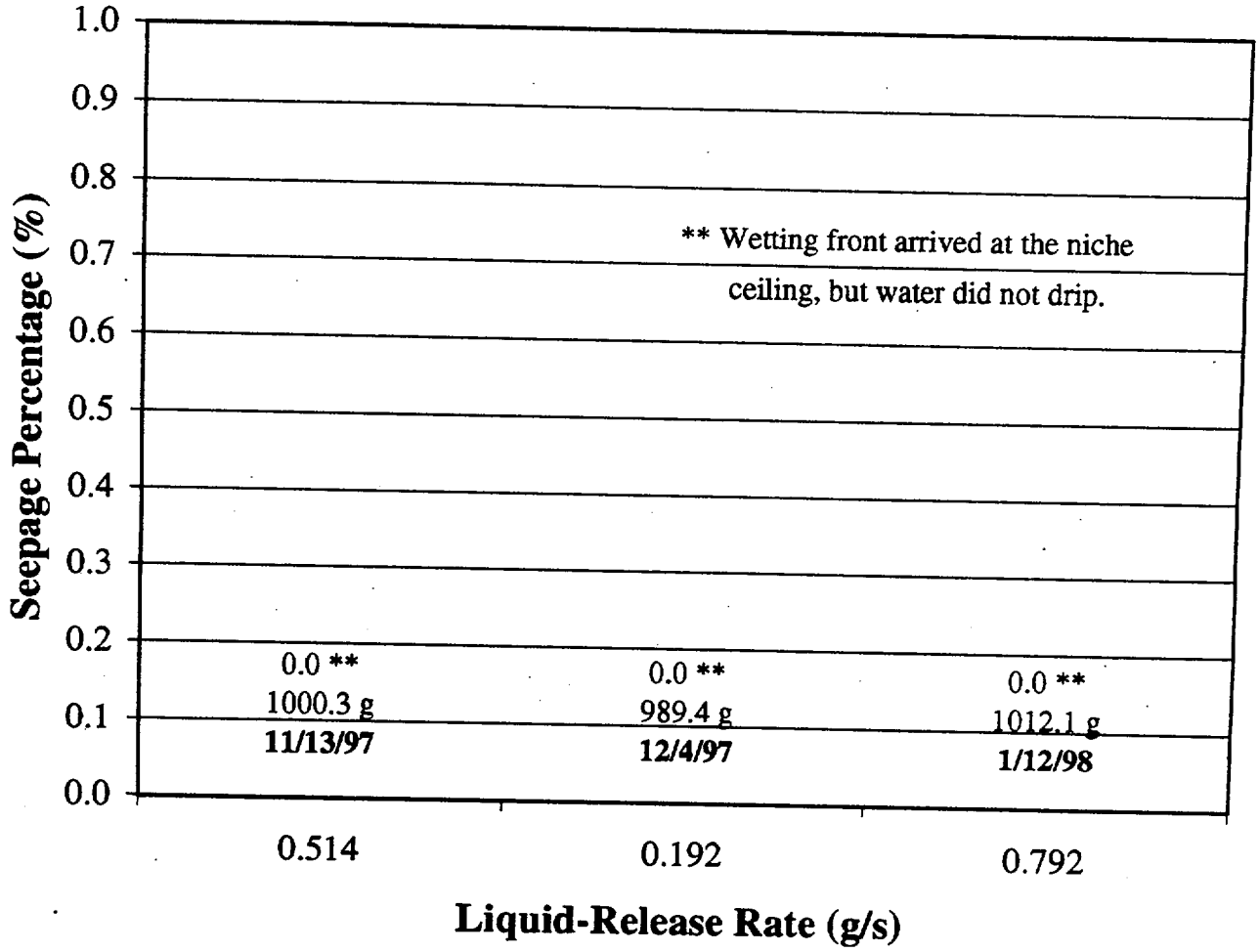

Liquid-Release Rate vs. Seepage Percentage
Niche 3650 Borehole UM: 6.71 - 7.01 m

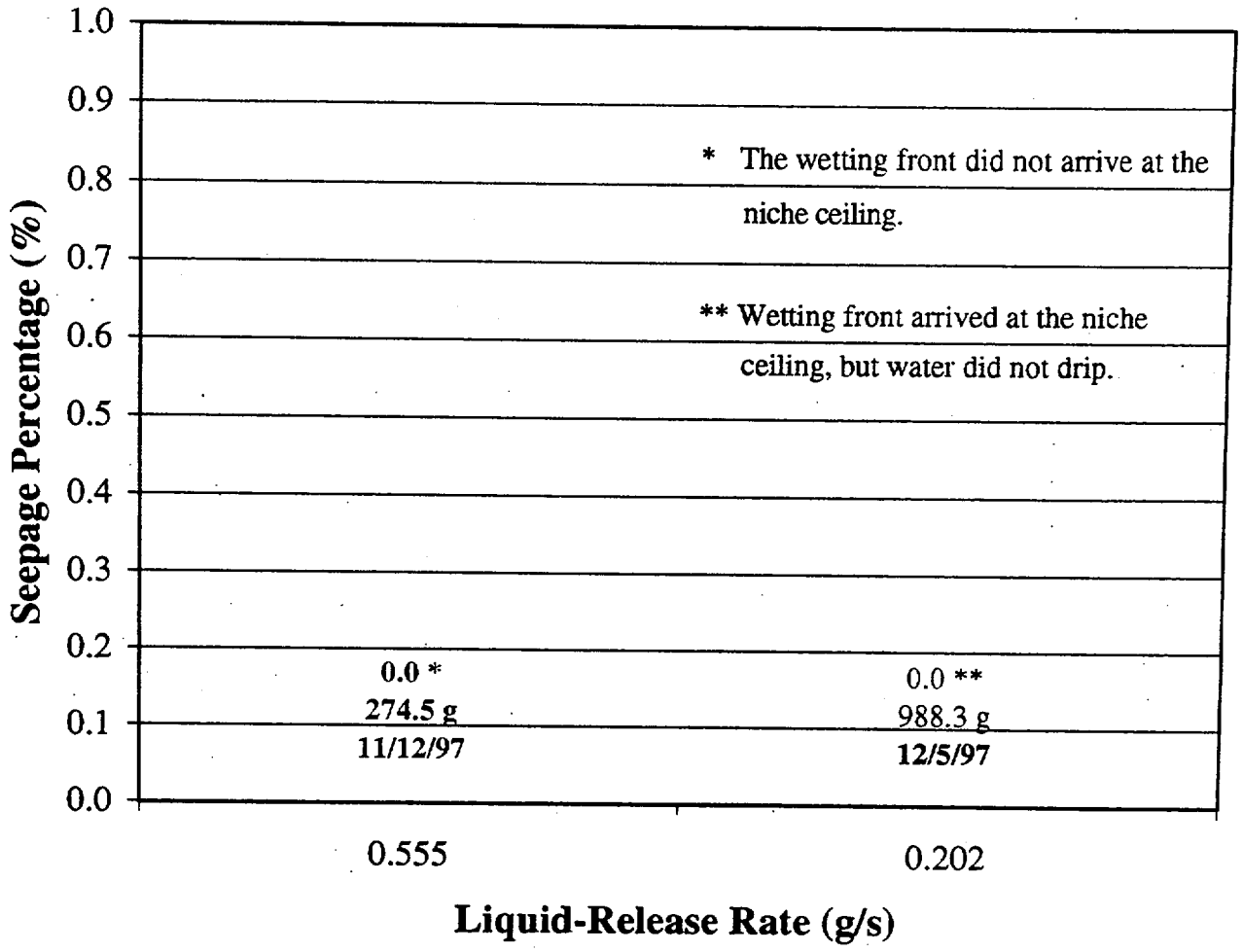

Liquid-Release Rate vs. Seepage Percentage
Niche 3650 Borehole UR: 4.27-4.57 m

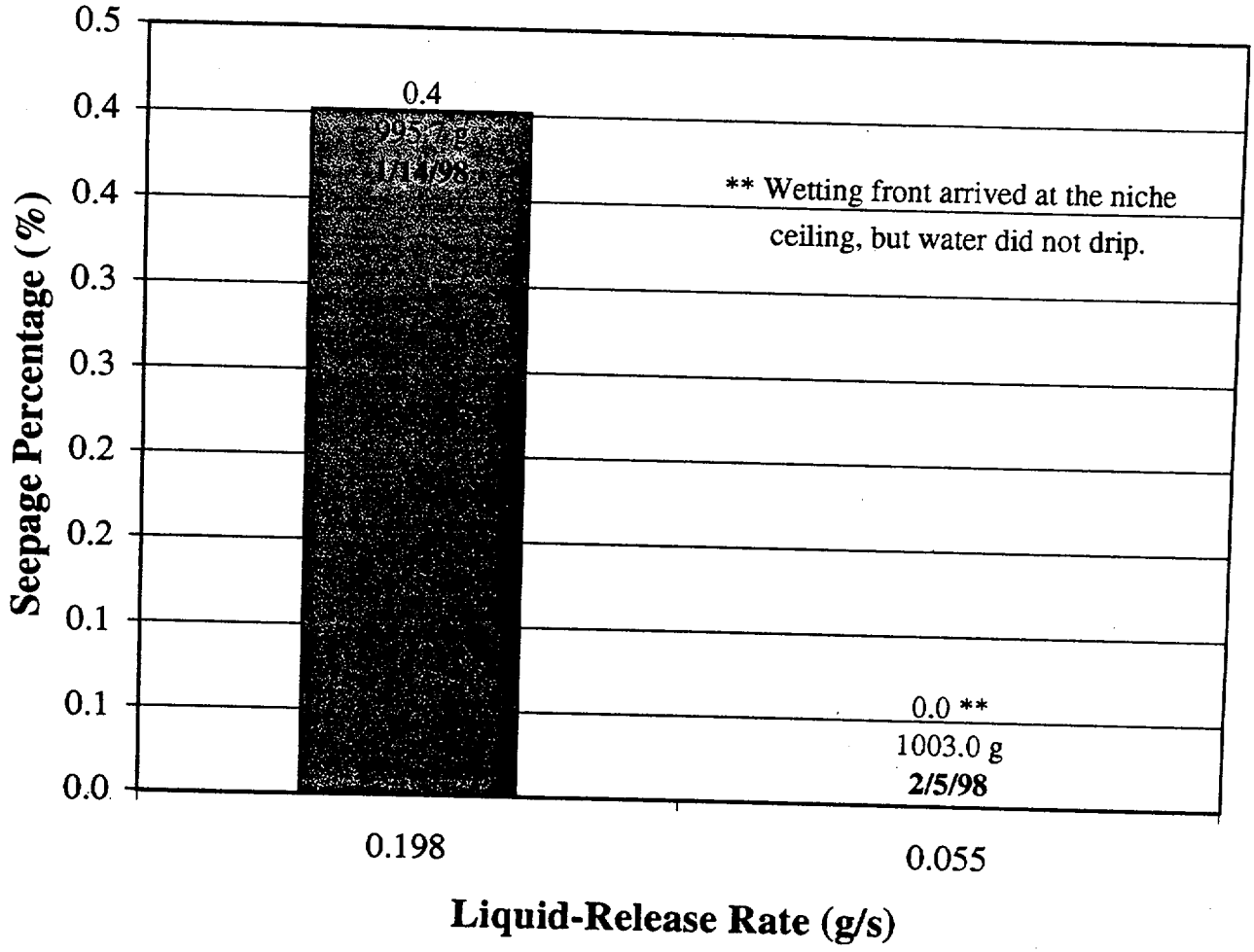

Liquid-Release Rate vs. Seepage Percentage
Niche 3650 Borehole UR: 4.88-5.18 m

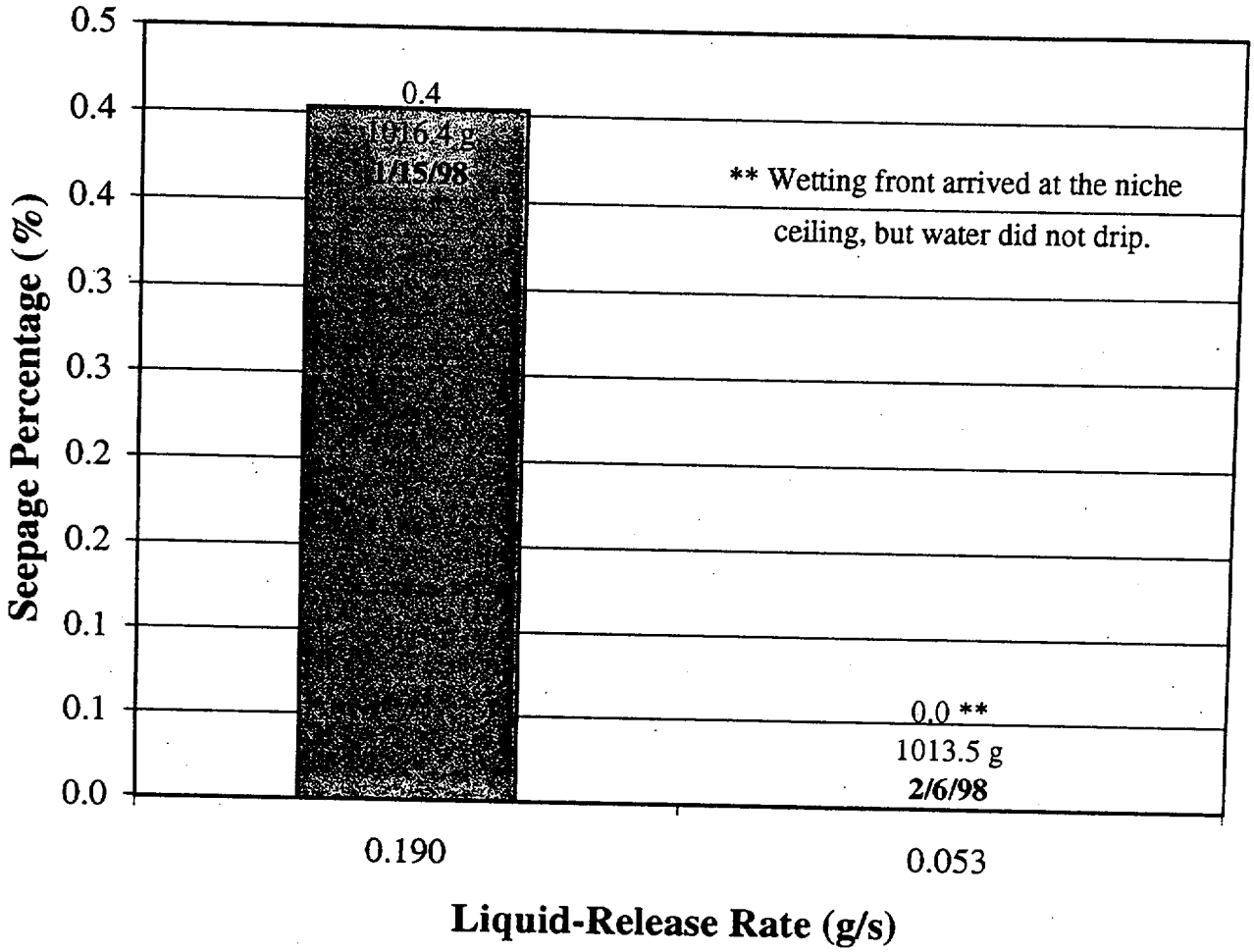

Liquid-Release Rate vs. Seepage Percentage
Niche 3650 Borehole UR: 5.49 - 5.79 m

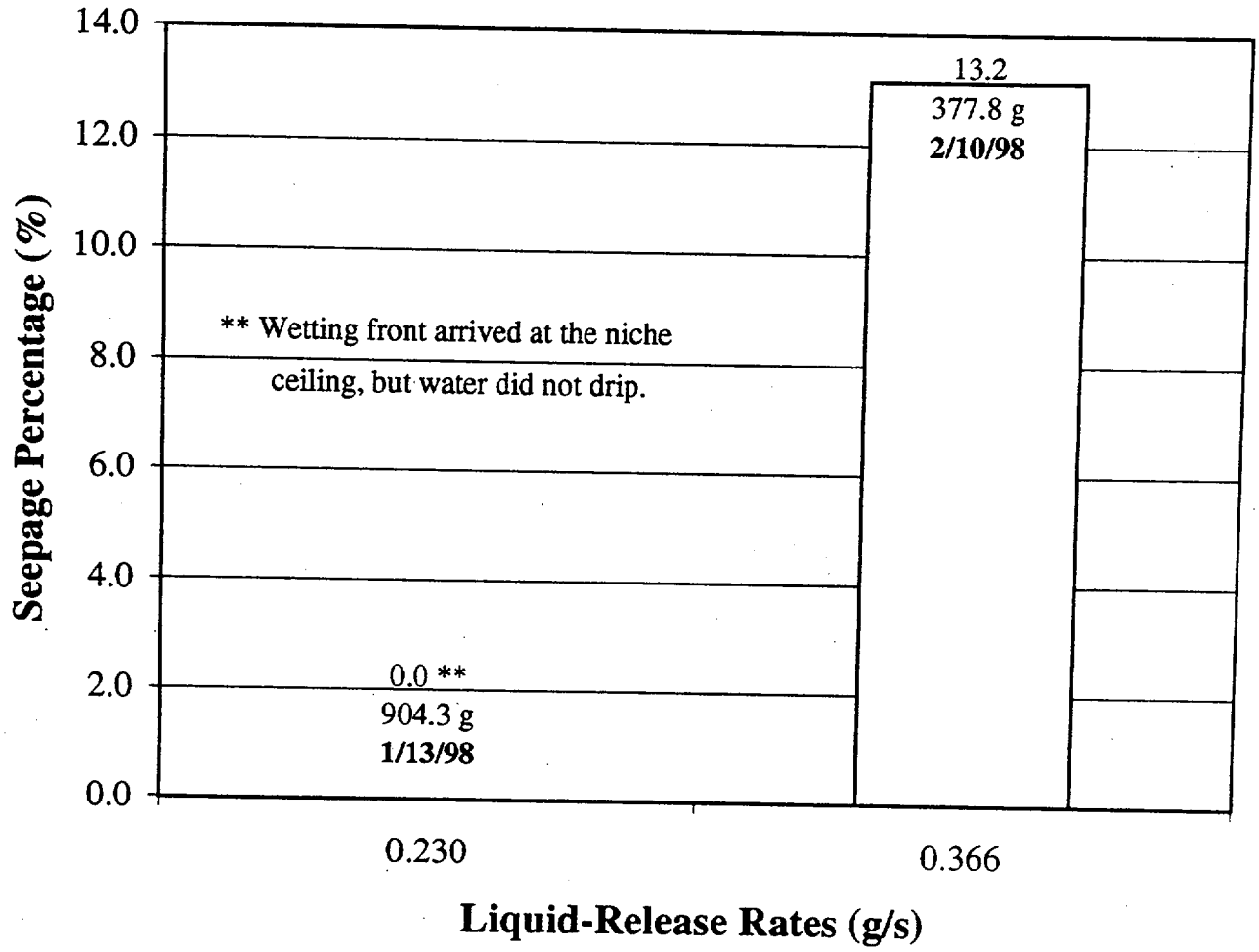

Liquid-Release Rate vs. Seepage Percentage
Niche 3650 Borehole UR: 6.10 - 6.40 m

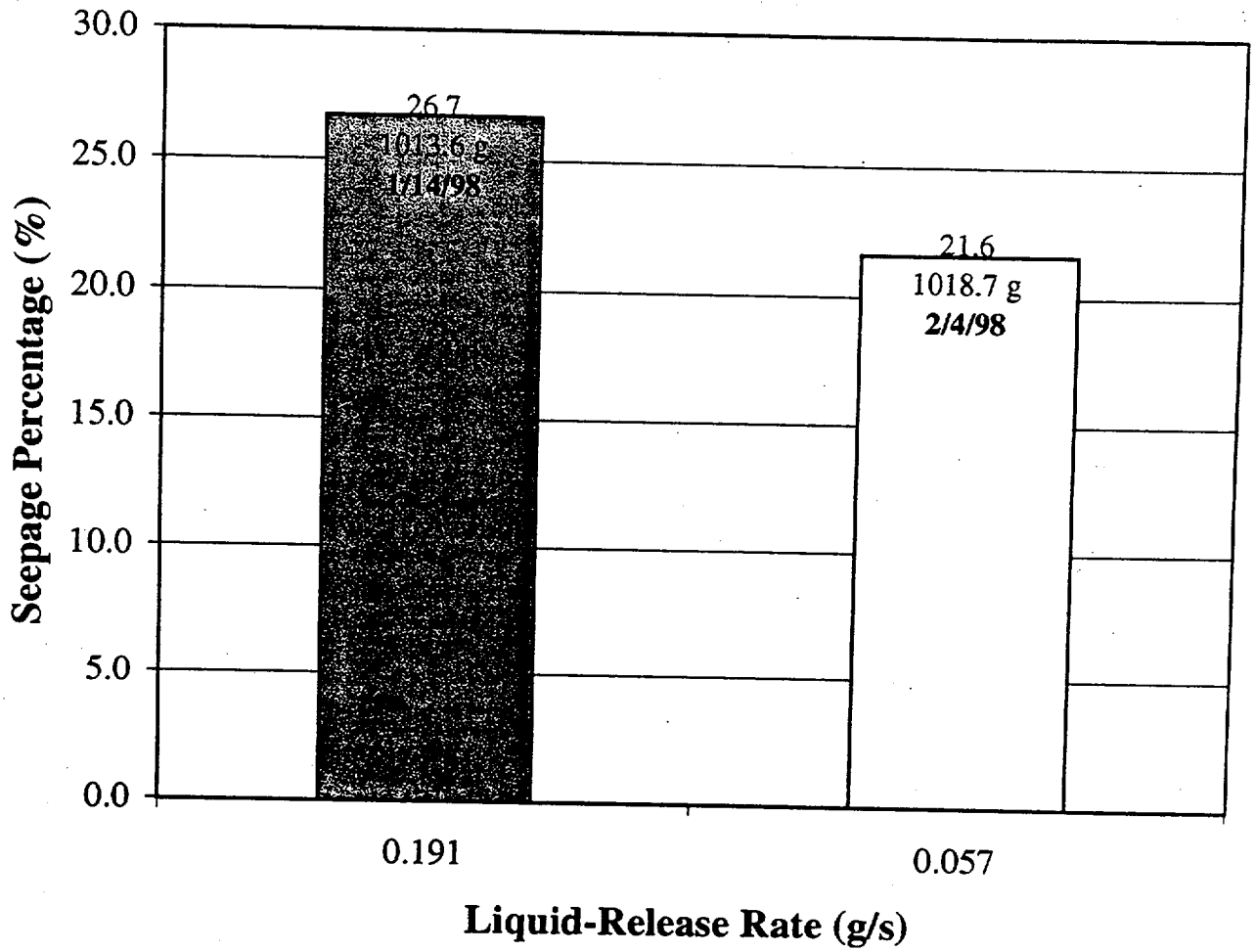

Liquid-Release Rate vs. Seepage Percentage
Niche 3650 Borehole UR: 6.71 - 7.01 m

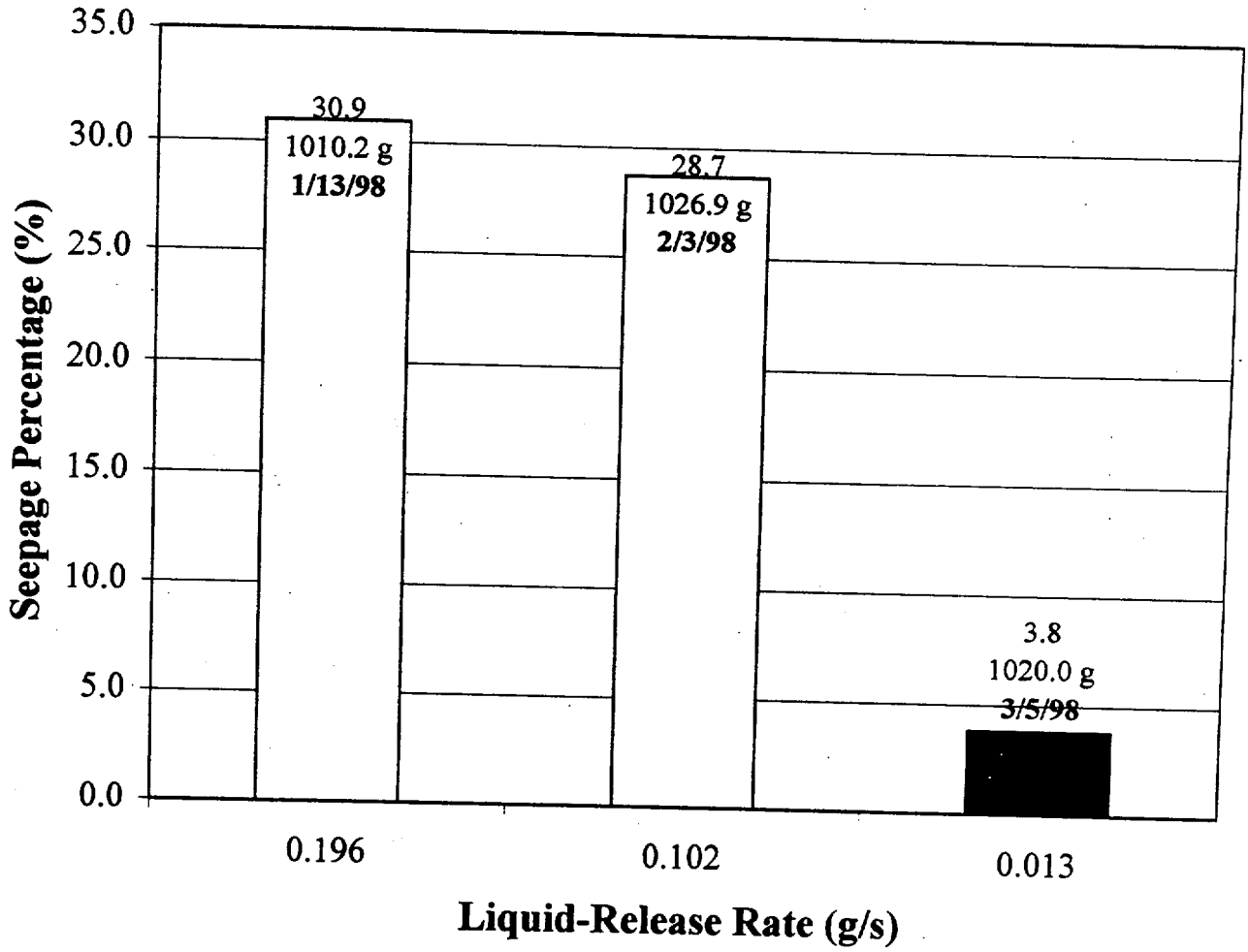

Liquid-Release Rage vs. Seepage Percentage
Niche 3650 Borehole UR: 7.62 - 7.92 m

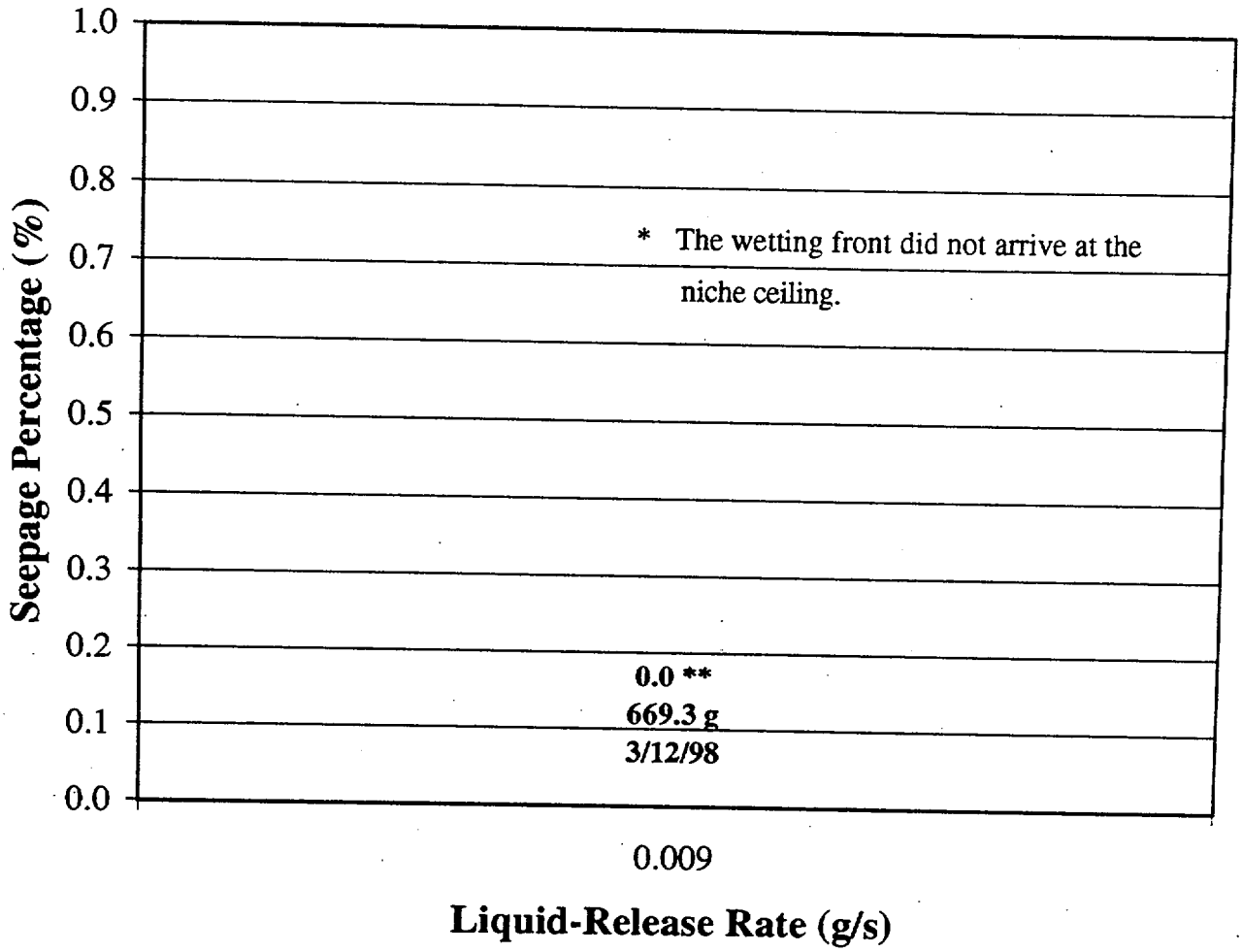

Appendix C

Plots Showing Seepage Percentage Versus Liquid-Release Flux

Liquid-Release Flux Versus Seepage Percentage
Niche 3650 Borehole UM: 4.27 - 4.57 m

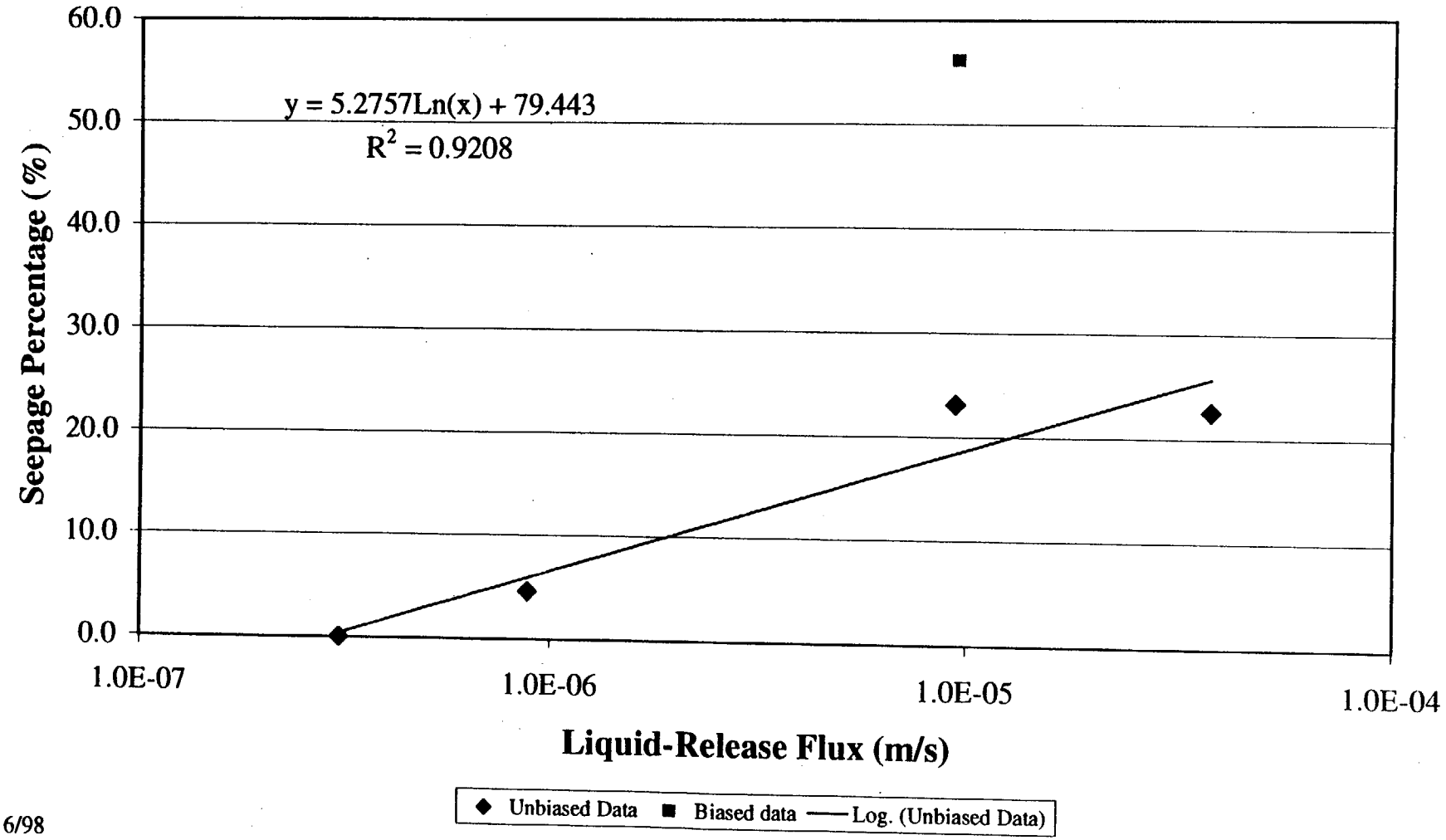

Liquid-Release Flux Versus Seepage Percentage
Niche 3650 Borehole UM: 4.88 - 5.18 m

Figure C.2

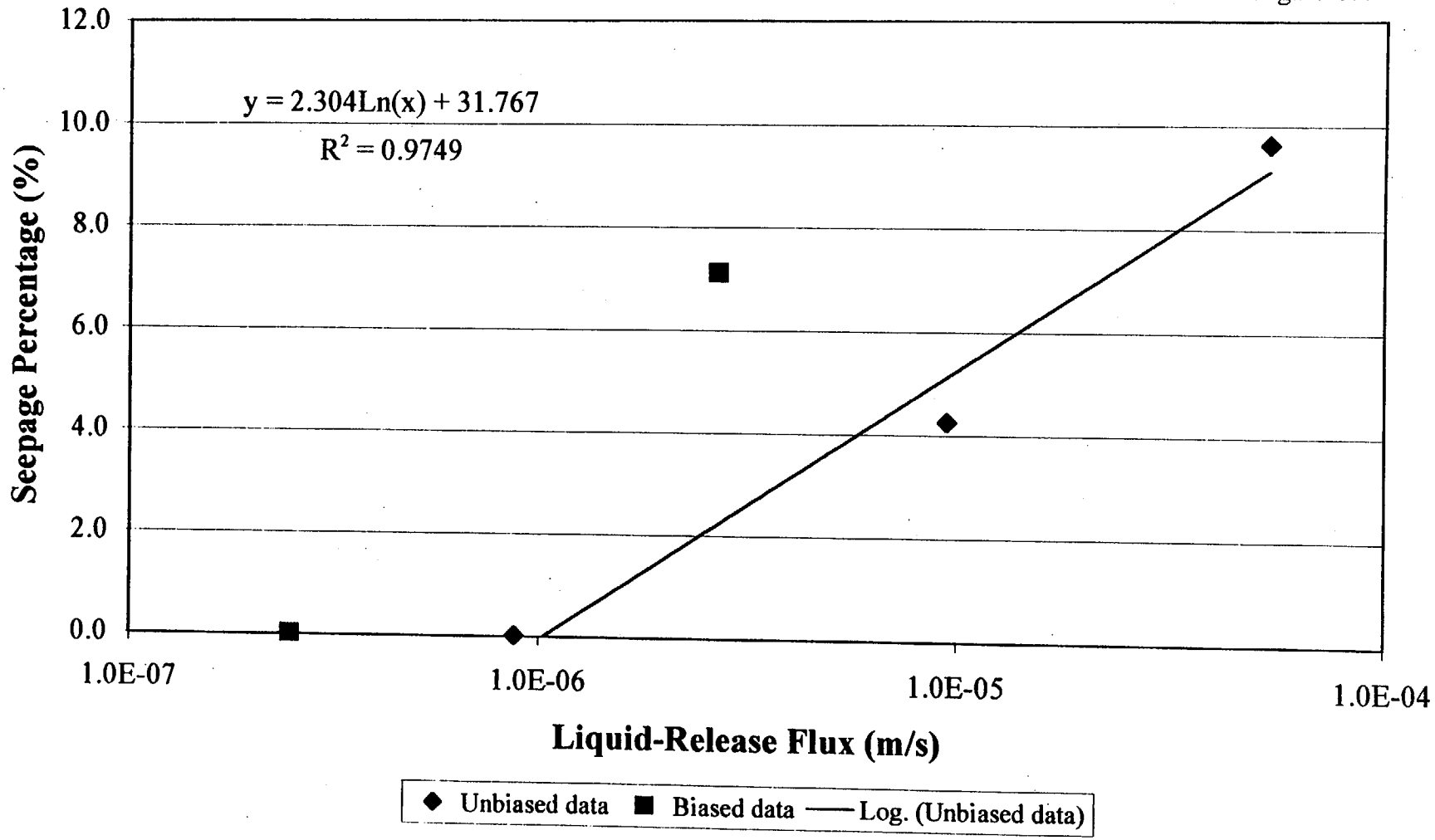

6/16/98
Version 1.0

Liquid-Release Flux Versus Seepage Percentage
Niche 3650 Borehole UM: 5.49 - 5.79 m

Figure C.3

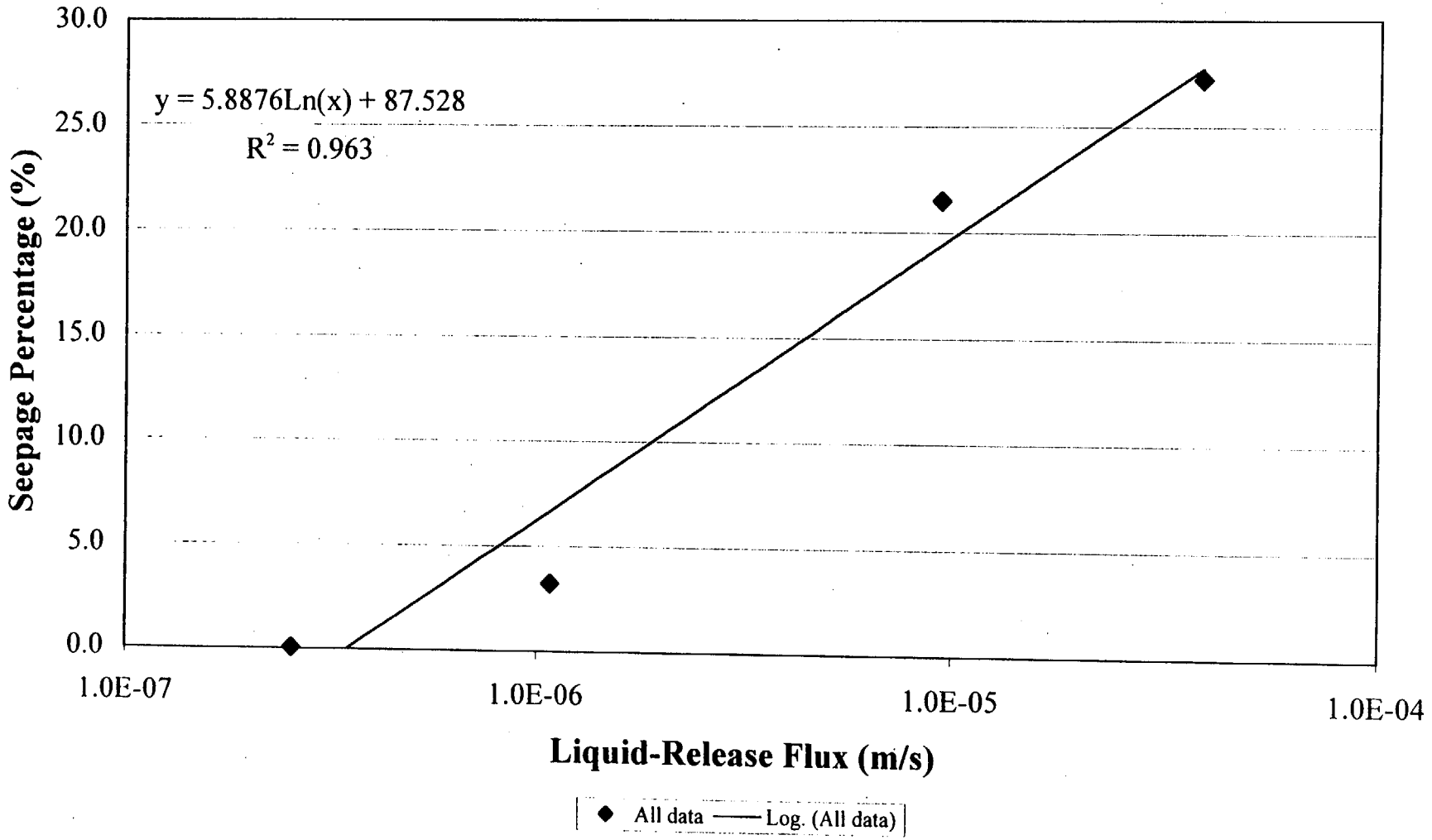

Liquid-Release Flux Versus Seepage Percentage
Niche 3650 Borehole UL: 7.01 - 7.32 m

Figure C.4

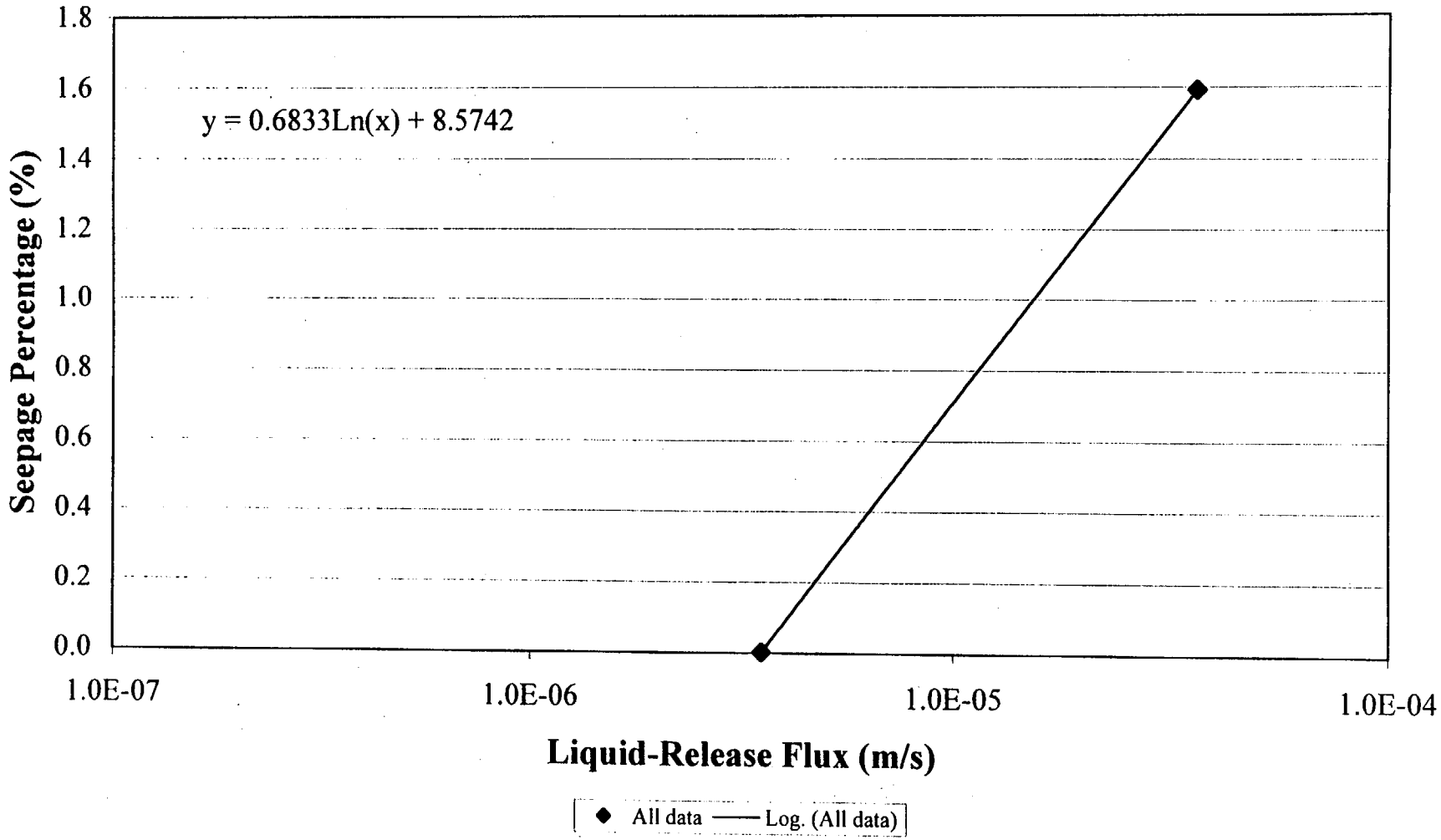

Liquid-Release Flux Versus Seepage Percentage
Niche 3650 Borehole UL: 7.62 - 7.92 m

Figure C.5

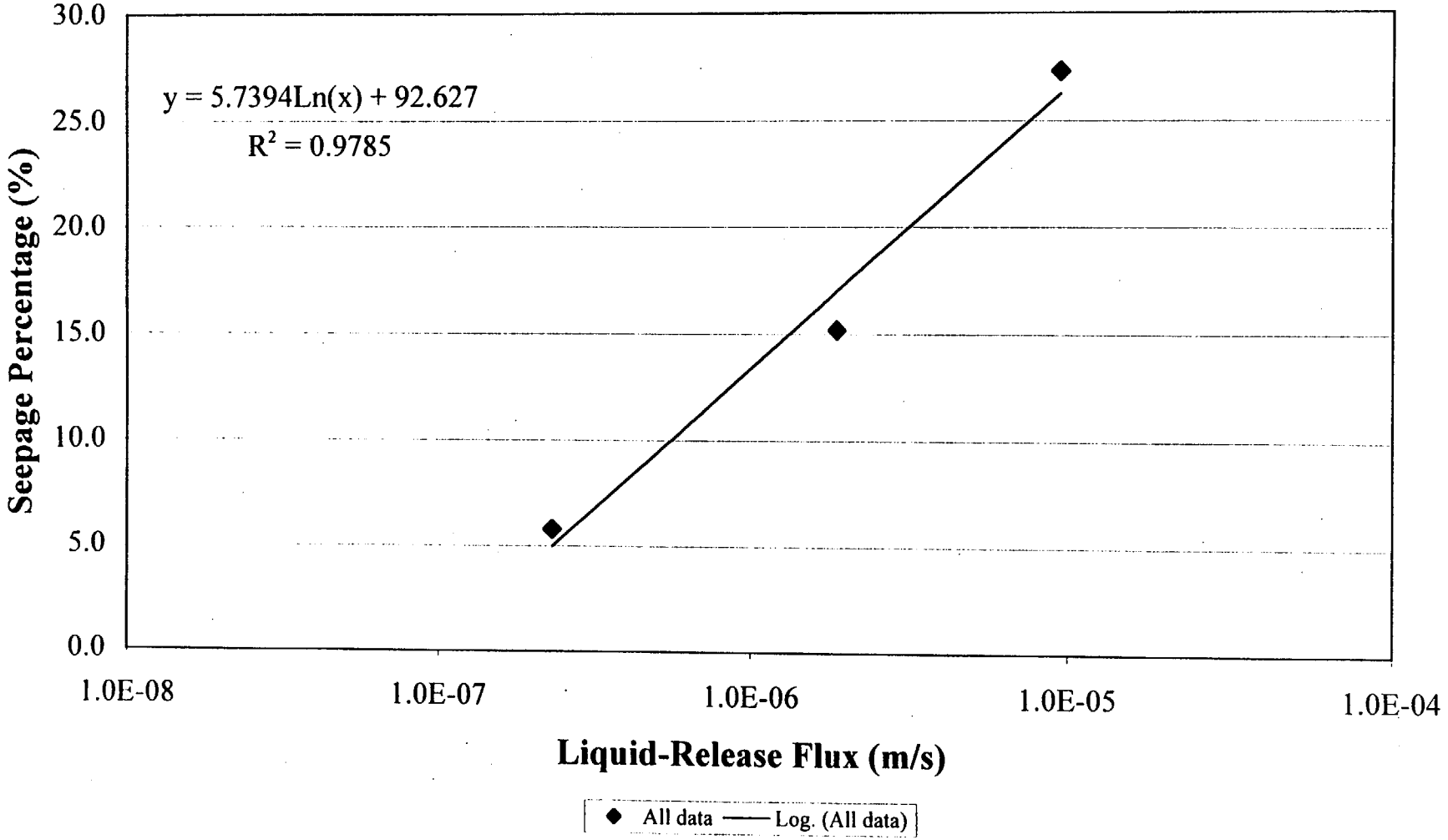

Liquid-Release Flux Versus Seepage Percentage
Niche 3650 Borehole UM: 4.27 - 4.57 m

Figure C.6

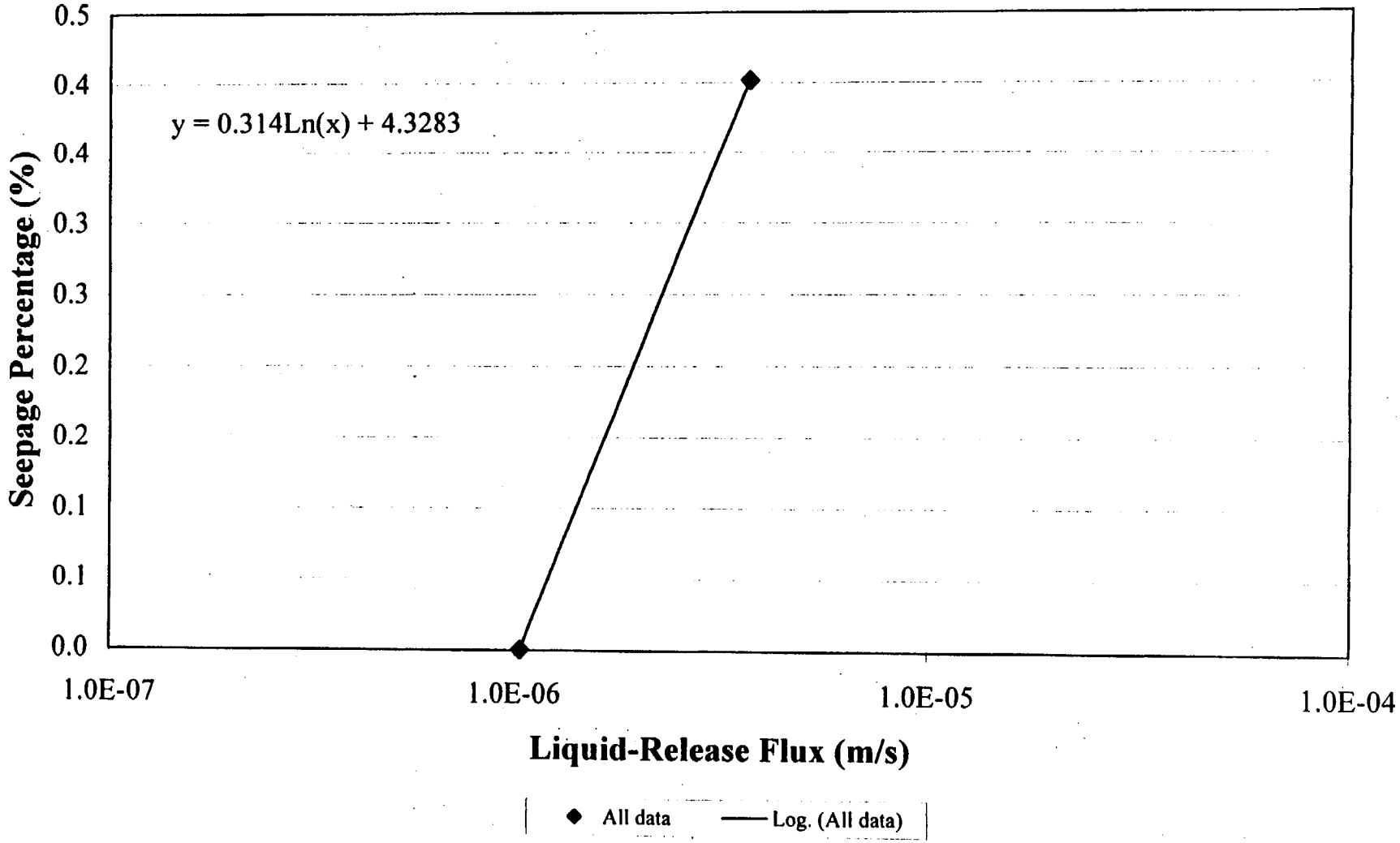

Liquid-Release Flux Versus Seepage Percentage
Niche 3650 Borehole UR: 4.88 - 5.18 m

Figure C.7

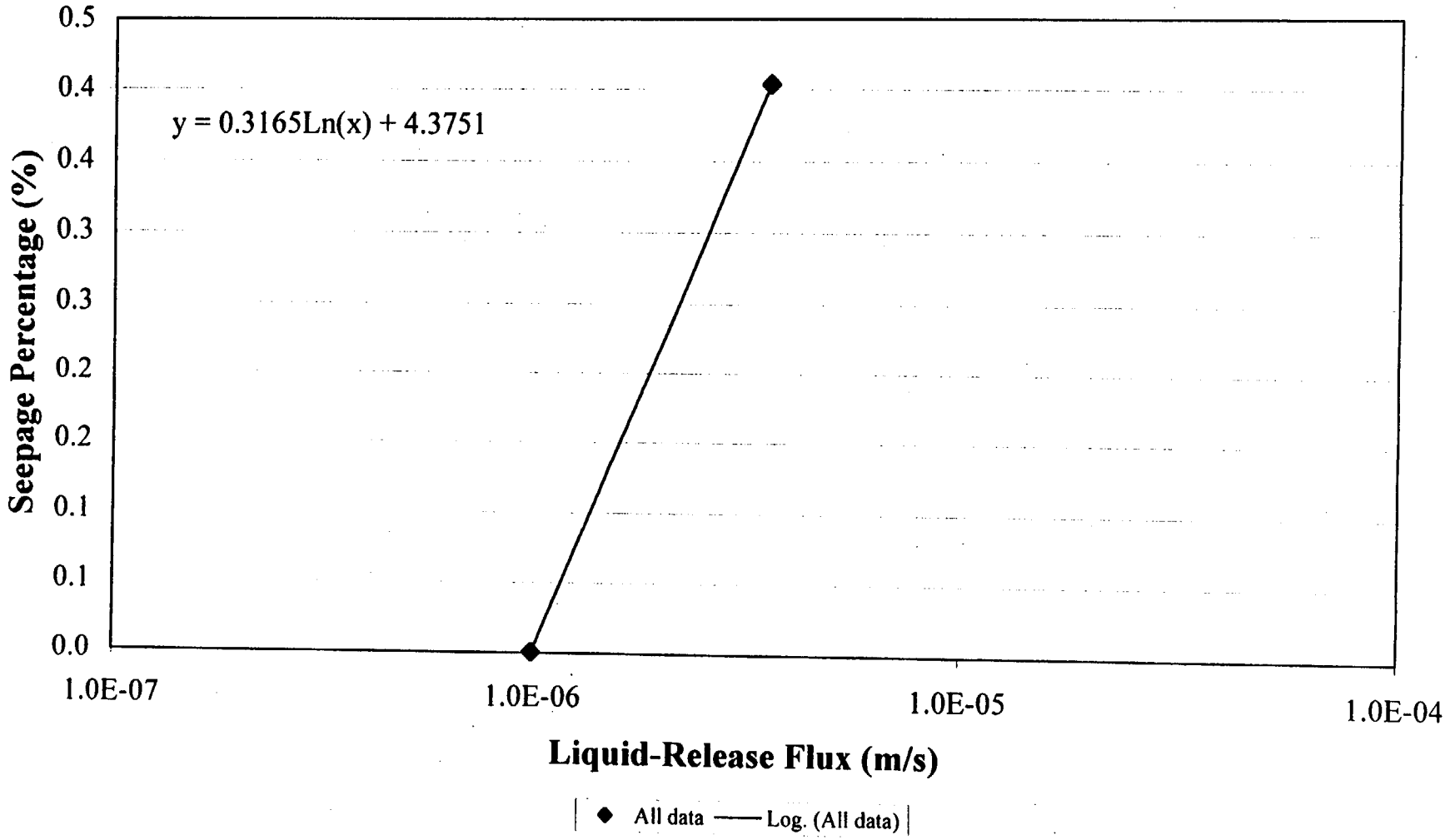

Liquid-Release Flux Versus Seepage Percentage
Niche 3650 Borehole UR: 5.49 - 5.79 m

Figure C.8

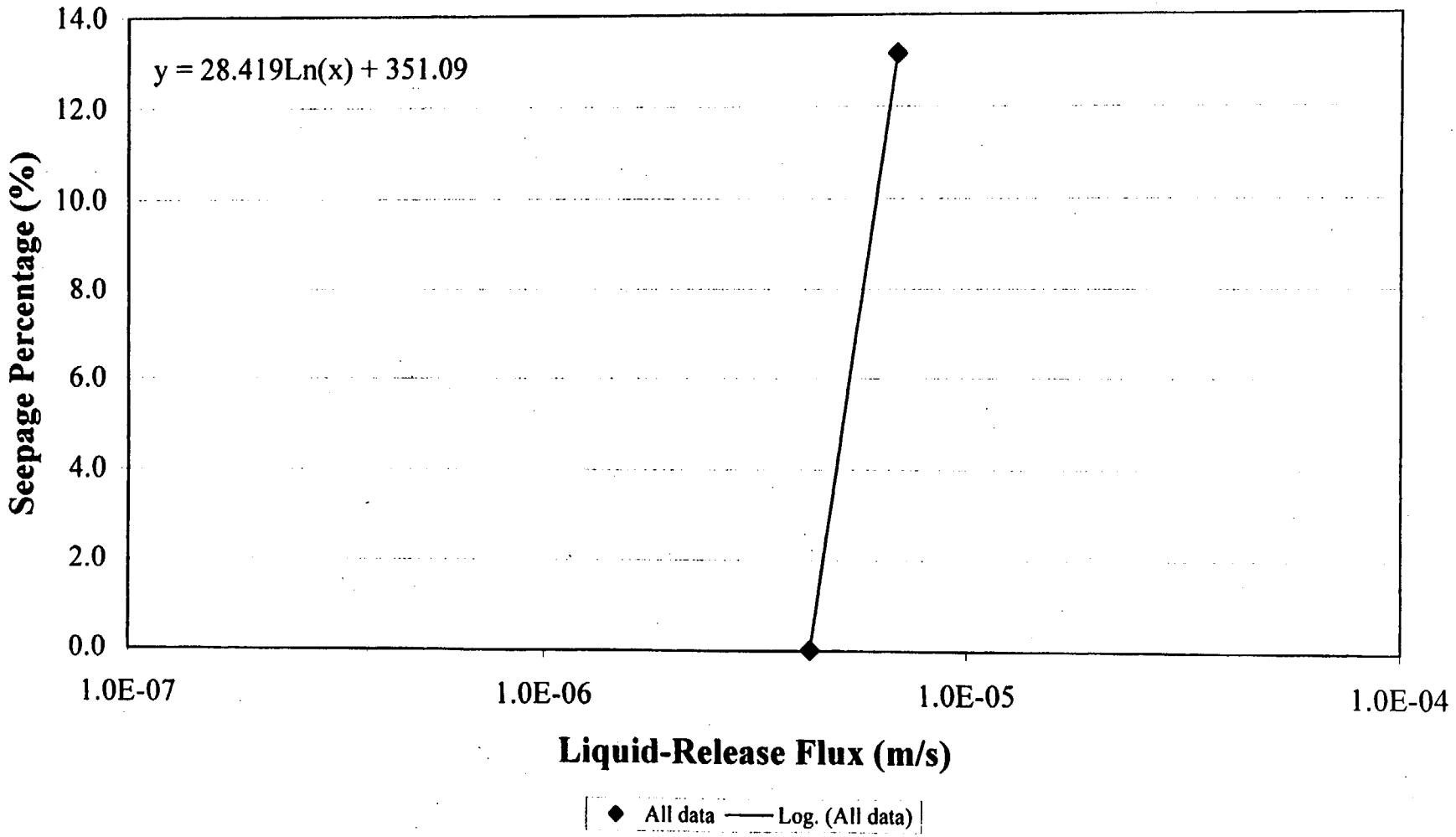

Liquid-Release Flux Versus Seepage Percentage
Niche 3650 Borehole UR: 6.10 - 6.40 m

Figure C.9

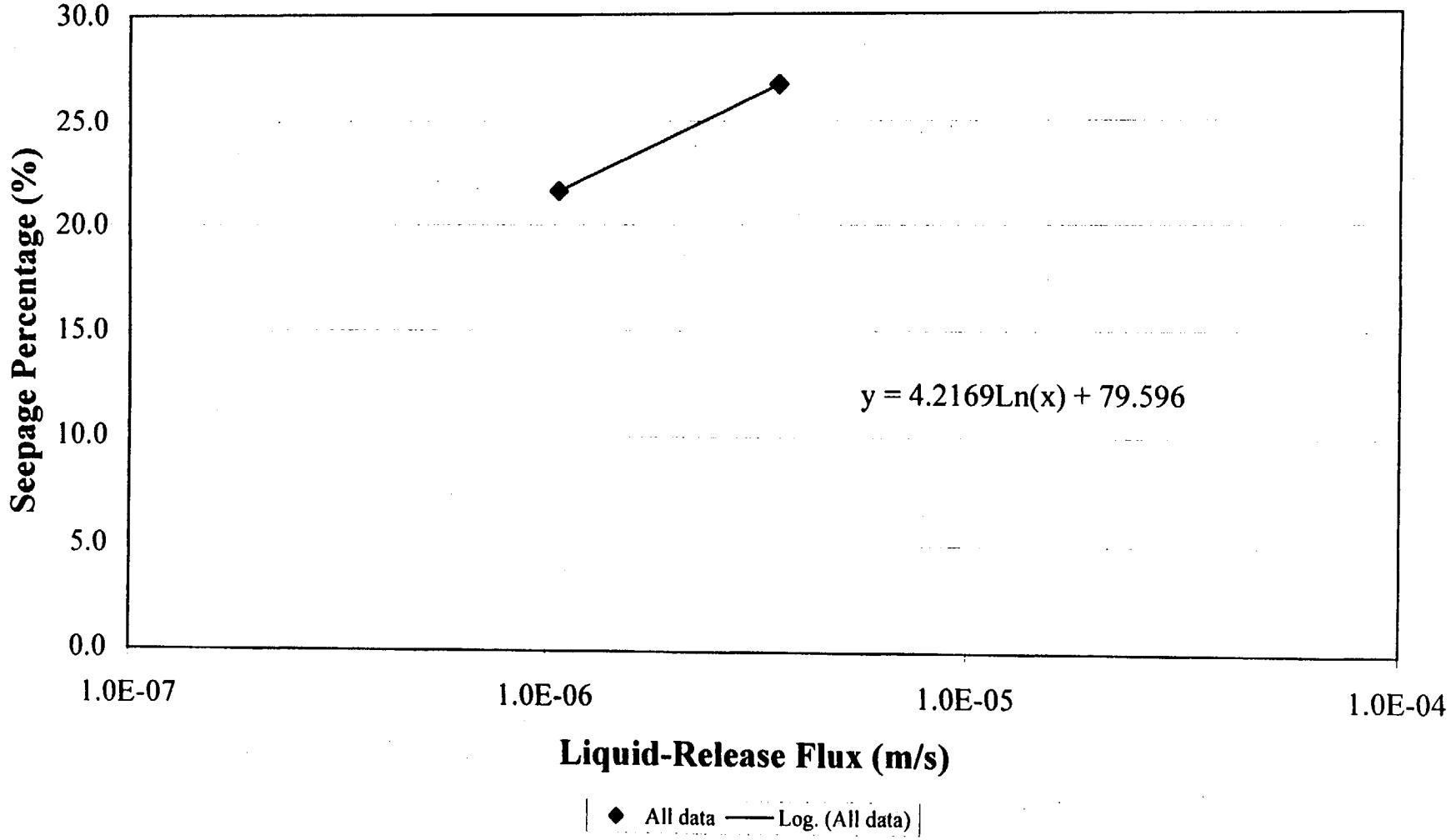

Liquid-Release Flux Versus Seepage Percentage
Niche 3650 Borehole UR: 6.71 - 7.01 m

Figure C.10

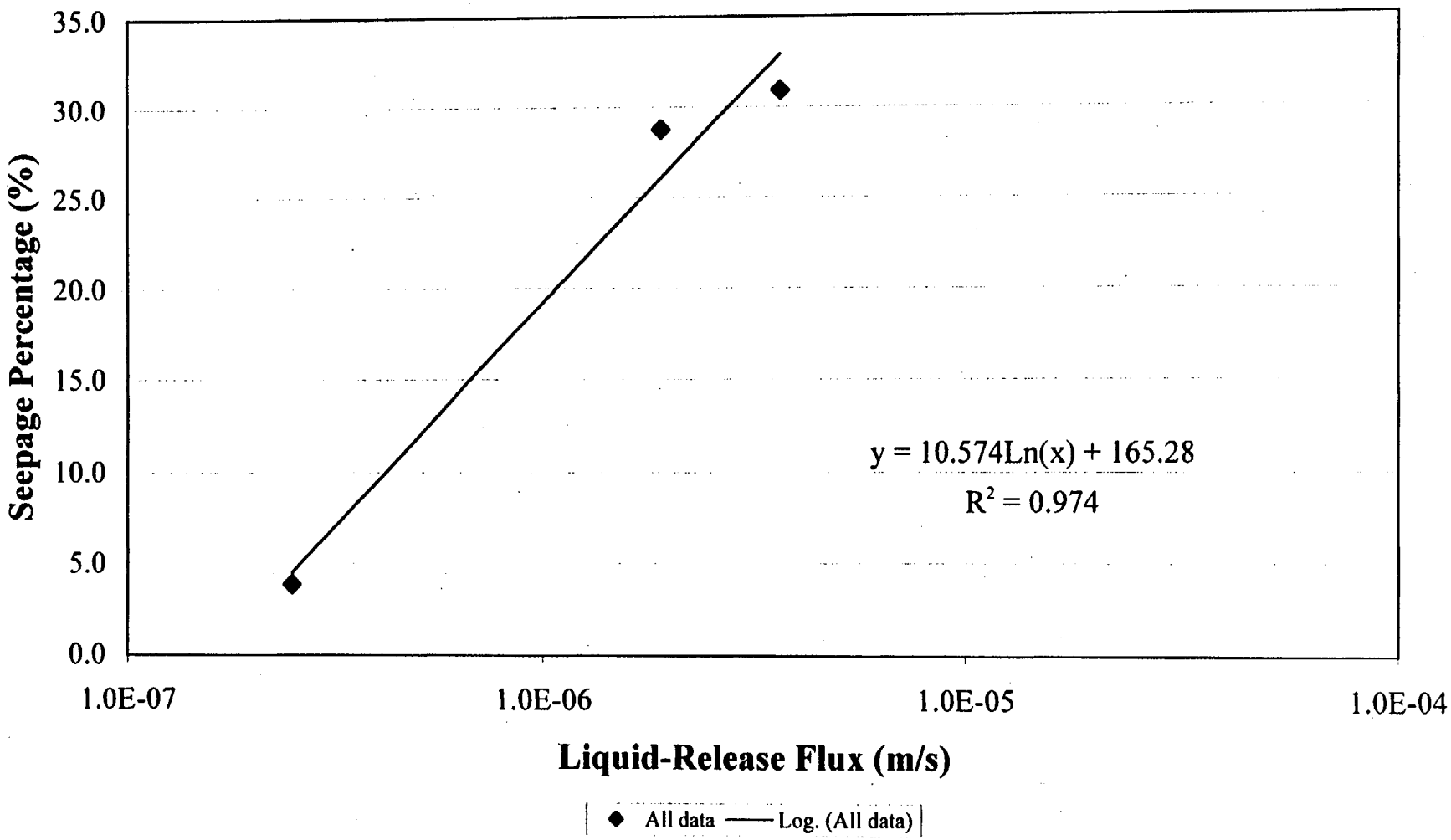

Appendix D

Dimensionless Moisture Potential, $\vartheta_{max} = Phi_{max}$

Table D.1 - s = 20

Computed Values of the Maximum Dimensionless Potential, Phi_{max}

Refer to Philip *et al.* , (1989) for an explanation of nomenclature.

K_I	s	2s	Phi_{max} 2s + s - 1/s	$[Phi_{max}]^{-1}$	Ko*
1.000E-09	20	40	41.95	2.38E-02	2.38E-11
1.500E-09			41.95	2.38E-02	3.58E-11
2.000E-09			41.95	2.38E-02	4.77E-11
3.000E-09			41.95	2.38E-02	7.15E-11
4.000E-09			41.95	2.38E-02	9.54E-11
5.000E-09			41.95	2.38E-02	1.19E-10
6.000E-09			41.95	2.38E-02	1.43E-10
7.000E-09			41.95	2.38E-02	1.67E-10
8.000E-09			41.95	2.38E-02	1.91E-10
9.000E-09			41.95	2.38E-02	2.15E-10
1.000E-08			41.95	2.38E-02	2.38E-10
1.500E-08			41.95	2.38E-02	3.58E-10
2.000E-08			41.95	2.38E-02	4.77E-10
3.000E-08			41.95	2.38E-02	7.15E-10
4.000E-08			41.95	2.38E-02	9.54E-10
5.000E-08			41.95	2.38E-02	1.19E-09
6.000E-08			41.95	2.38E-02	1.43E-09
7.000E-08			41.95	2.38E-02	1.67E-09
8.000E-08			41.95	2.38E-02	1.91E-09
9.000E-08			41.95	2.38E-02	2.15E-09
1.000E-07			41.95	2.38E-02	2.38E-09
1.500E-07			41.95	2.38E-02	3.58E-09
2.000E-07			41.95	2.38E-02	4.77E-09
3.000E-07			41.95	2.38E-02	7.15E-09
4.000E-07			41.95	2.38E-02	9.54E-09
5.000E-07			41.95	2.38E-02	1.19E-08
6.000E-07			41.95	2.38E-02	1.43E-08
7.000E-07			41.95	2.38E-02	1.67E-08
8.000E-07			41.95	2.38E-02	1.91E-08
9.000E-07			41.95	2.38E-02	2.15E-08
1.000E-06			41.95	2.38E-02	2.38E-08
1.500E-06			41.95	2.38E-02	3.58E-08
2.000E-06			41.95	2.38E-02	4.77E-08

K_l	s	2s	Phi_{max} 2s + s - 1/s	$[Phi_{max}]^{-1}$	Ko*
3.000E-06			41.95	2.38E-02	7.15E-08
4.000E-06			41.95	2.38E-02	9.54E-08
5.000E-06			41.95	2.38E-02	1.19E-07
6.000E-06			41.95	2.38E-02	1.43E-07
7.000E-06			41.95	2.38E-02	1.67E-07
8.000E-06			41.95	2.38E-02	1.91E-07
9.000E-06			41.95	2.38E-02	2.15E-07
1.000E-05			41.95	2.38E-02	2.38E-07
1.500E-05			41.95	2.38E-02	3.58E-07
2.000E-05			41.95	2.38E-02	4.77E-07
3.000E-05			41.95	2.38E-02	7.15E-07
4.000E-05			41.95	2.38E-02	9.54E-07
5.000E-05			41.95	2.38E-02	1.19E-06
6.000E-05			41.95	2.38E-02	1.43E-06
7.000E-05			41.95	2.38E-02	1.67E-06
8.000E-05			41.95	2.38E-02	1.91E-06
9.000E-05			41.95	2.38E-02	2.15E-06
1.000E-04			41.95	2.38E-02	2.38E-06
1.500E-04			41.95	2.38E-02	3.58E-06
2.000E-04			41.95	2.38E-02	4.77E-06
3.000E-04			41.95	2.38E-02	7.15E-06
4.000E-04			41.95	2.38E-02	9.54E-06
5.000E-04			41.95	2.38E-02	1.19E-05
6.000E-04			41.95	2.38E-02	1.43E-05
7.000E-04			41.95	2.38E-02	1.67E-05
8.000E-04			41.95	2.38E-02	1.91E-05
9.000E-04			41.95	2.38E-02	2.15E-05
1.000E-03			41.95	2.38E-02	2.38E-05
1.500E-03			41.95	2.38E-02	3.58E-05
2.000E-03			41.95	2.38E-02	4.77E-05
3.000E-03			41.95	2.38E-02	7.15E-05
4.000E-03			41.95	2.38E-02	9.54E-05
5.000E-03			41.95	2.38E-02	1.19E-04
6.000E-03			41.95	2.38E-02	1.43E-04
7.000E-03			41.95	2.38E-02	1.67E-04
8.000E-03			41.95	2.38E-02	1.91E-04
9.000E-03			41.95	2.38E-02	2.15E-04
1.000E-02			41.95	2.38E-02	2.38E-04

Table D.2 - s = 100

Computed Values of the Maximum Dimensionless Potential, Phi_{max}

Refer to Philip *et al.* , (1989) for an explanation of nomenclature.

K_I	s	2s	Phi_{max} 2s + s - 1/s	$[Phi_{max}]^{-1}$	Ko*
1.000E-09	100	200	201.99	4.95E-03	4.95E-12
1.500E-09			201.99	4.95E-03	7.43E-12
2.000E-09			201.99	4.95E-03	9.90E-12
3.000E-09			201.99	4.95E-03	1.49E-11
4.000E-09			201.99	4.95E-03	1.98E-11
5.000E-09			201.99	4.95E-03	2.48E-11
6.000E-09			201.99	4.95E-03	2.97E-11
7.000E-09			201.99	4.95E-03	3.47E-11
8.000E-09			201.99	4.95E-03	3.96E-11
9.000E-09			201.99	4.95E-03	4.46E-11
1.000E-08			201.99	4.95E-03	4.95E-11
1.500E-08			201.99	4.95E-03	7.43E-11
2.000E-08			201.99	4.95E-03	9.90E-11
3.000E-08			201.99	4.95E-03	1.49E-10
4.000E-08			201.99	4.95E-03	1.98E-10
5.000E-08			201.99	4.95E-03	2.48E-10
6.000E-08			201.99	4.95E-03	2.97E-10
7.000E-08			201.99	4.95E-03	3.47E-10
8.000E-08			201.99	4.95E-03	3.96E-10
9.000E-08			201.99	4.95E-03	4.46E-10
1.000E-07			201.99	4.95E-03	4.95E-10
1.500E-07			201.99	4.95E-03	7.43E-10
2.000E-07			201.99	4.95E-03	9.90E-10
3.000E-07			201.99	4.95E-03	1.49E-09
4.000E-07			201.99	4.95E-03	1.98E-09
5.000E-07			201.99	4.95E-03	2.48E-09
6.000E-07			201.99	4.95E-03	2.97E-09
7.000E-07			201.99	4.95E-03	3.47E-09
8.000E-07			201.99	4.95E-03	3.96E-09
9.000E-07			201.99	4.95E-03	4.46E-09
1.000E-06			201.99	4.95E-03	4.95E-09
1.500E-06			201.99	4.95E-03	7.43E-09
2.000E-06			201.99	4.95E-03	9.90E-09
3.000E-06			201.99	4.95E-03	1.49E-08

4.000E-06	201.99	4.95E-03	1.98E-08
5.000E-06	201.99	4.95E-03	2.48E-08
6.000E-06	201.99	4.95E-03	2.97E-08
7.000E-06	201.99	4.95E-03	3.47E-08
8.000E-06	201.99	4.95E-03	3.96E-08
9.000E-06	201.99	4.95E-03	4.46E-08
1.000E-05	201.99	4.95E-03	4.95E-08
1.500E-05	201.99	4.95E-03	7.43E-08
2.000E-05	201.99	4.95E-03	9.90E-08
3.000E-05	201.99	4.95E-03	1.49E-07
4.000E-05	201.99	4.95E-03	1.98E-07
5.000E-05	201.99	4.95E-03	2.48E-07
6.000E-05	201.99	4.95E-03	2.97E-07
7.000E-05	201.99	4.95E-03	3.47E-07
8.000E-05	201.99	4.95E-03	3.96E-07
9.000E-05	201.99	4.95E-03	4.46E-07
1.000E-04	201.99	4.95E-03	4.95E-07
1.500E-04	201.99	4.95E-03	7.43E-07
2.000E-04	201.99	4.95E-03	9.90E-07
3.000E-04	201.99	4.95E-03	1.49E-06
4.000E-04	201.99	4.95E-03	1.98E-06
5.000E-04	201.99	4.95E-03	2.48E-06
6.000E-04	201.99	4.95E-03	2.97E-06
7.000E-04	201.99	4.95E-03	3.47E-06
8.000E-04	201.99	4.95E-03	3.96E-06
9.000E-04	201.99	4.95E-03	4.46E-06
1.000E-03	201.99	4.95E-03	4.95E-06
1.500E-03	201.99	4.95E-03	7.43E-06
2.000E-03	201.99	4.95E-03	9.90E-06
3.000E-03	201.99	4.95E-03	1.49E-05
4.000E-03	201.99	4.95E-03	1.98E-05
5.000E-03	201.99	4.95E-03	2.48E-05
6.000E-03	201.99	4.95E-03	2.97E-05
7.000E-03	201.99	4.95E-03	3.47E-05
8.000E-03	201.99	4.95E-03	3.96E-05
9.000E-03	201.99	4.95E-03	4.46E-05
1.000E-02	201.99	4.95E-03	4.95E-05

Chapter 3 Compilation of Borehole Permeability Values from the Pre- and Post-Excavation Air Injection Tests

P. J. Cook, R. C. Trautz, and J. S. Y. Wang

3.0 Introduction

From May through October 1997, prior to dye release tests conducted at the niche sites at 3566 meters and 3650 meters (referred to henceforth as Niche 3566 and Niche 3650, respectively) in the ESF, extensive cross-hole air permeability measurements were made in the groups of 10-meter boreholes at the niches to facilitate selection of the dye release locations and to compare the effects of niche excavation on permeability. Cross-hole pressure response data will enable characterization of potential flow paths. Single-hole pressure response data were used for the dye release point determination. Single-hole data set is a subset of the cross-hole testing program. Information from both types of measurements will be used as input to the modeling programs. In this chapter we focus on the single-hole data.

Air permeability tests have been used extensively at various locations at the ESF to characterize the potential fluid flow paths (e.g., Tsang et al. 1996 and 1997, and Wang et al. 1997). Once a correlation between dye tests and air permeability tests has been made, it can help to extend knowledge of seepage distribution to other locations in which air permeability has been measured. Comparisons between the air permeability at different general locations, such as between one niche and another, from tests of similar scale can be made. Comparisons of tests performed before and after niche excavation can provide information on the effects of mining on the characteristics of the rock. Also, an examination can be made of the scale effects associated with different test interval lengths.

3.1 Air Permeability Testing

3.1.1 Test Location

Niche 3566 is located in a brecciated zone between the Sundance Fault and a cooling joint where samples containing elevated concentrations of ^{36}Cl were collected. The detection of elevated ^{36}Cl concentrations implies that relatively young groundwater is present at Niche 3566 and that a

preferential-flow pathway, perhaps associated with the Sundance Fault, may be present. In contrast, Niche 3650 is located in a competent rock mass with lower fracture density. The isotopic signature of samples collected in the vicinity of Niche 3650 suggests that a preferential-flow pathway is not present at this location. Three boreholes for air permeability and dye release studies were initially drilled at Niche 3566, and seven boreholes were drilled at Niche 3650. The niches were eventually mined back into the tunnel wall, leaving some of the boreholes intact. These remaining boreholes were then retested.

3.1.2 Testing Configuration

One goal of the multi-zone air permeability testing at the niches is to gain an understanding of the flow patterns within the formations by comparing tests of zones over the whole volume of interest. In heterogeneous rock, such as at the niches, it is difficult to later normalize or subtract out variations in results caused by varying parameters such as scale or flow rate. It is therefore important to keep the testing as self-consistent as possible in order to vary only one parameter when performing the tests, that of location of the zones. Zone lengths were therefore kept the same throughout testing, and tests with at least one common flow rate were performed at all the zones. All the boreholes were drilled to nominally 7.6-cm diameter, parallel to each other, and at Niche 3650, all nearly one meter apart so that there would be little variation in distance between laterally adjacent zones. To ensure that the air permeability of unaltered rock could be measured, the boreholes were drilled dry and at low RPM, using a diamond core bit. All the borings contained very little damage so that the packer systems could be placed at any location with the exception of the last 3 meters of each of the three boreholes at Niche 3566, which were blocked with obstructions. The boreholes in each niche were drilled horizontally and at 45° with respect to the ESF tunnel wall. Figure 3.1 depicts the configuration of the boreholes at each niche. Niche 3566 had three boreholes in a vertical arrangement, and the uppermost was left intact subsequent to excavation. Niche 3650 had seven boreholes, four of which were mined out. After the excavation of Niche 3566, a set of horizontal boreholes was drilled in a radial pattern from a central location within the niche into its walls. The configurations for these boreholes are shown in Figure 3.2. The niche locations with respect to the ESF are shown in Figure 3.3.

3.1.3 Test Equipment

Two types of specially designed packer systems, one for observation and one for injection, were installed simultaneously in the three holes at Niche 3566 and again in the seven holes at Niche 3650. All packers used multiple inflatable rubber glands to seal alternate 0.3048-meter sections of a borehole, thereby leaving a series of 0.3048 meter open zones in which to perform tests. The 6.096-meter-long observation-type packers were capable of sealing 10 zones (nine straddle and one end zone) at a time, and contained ports to each of these zones from which to monitor zone

pressure. The single 3.35-meter injection packer sealed six zones (five straddle and one end zone) at a time and contained two ports to each zone, one small diameter port for pressure measurement and one large diameter port for injecting air into the zone. Packer design was such that the sealed zones had minimal enclosed volume. This low storage design ensured that the tests responded to the properties of the rock as opposed to the properties of the borehole volume. With this design, properties such as storativity, should they be needed, would make themselves evident in the transient regions of the pressure response curves. To ensure packer integrity and durability throughout testing, the packers were constructed of welded stainless steel. The long packers were jointed with specially designed o-ring seals to minimize transportation stresses and ease installation.

Pressure monitoring was accomplished using either Setra® 4-20 mA or Kavlico® voltage-output pressure transducers. These transducers were connected to injection and monitoring zones using 1/8-inch plastic tubing. Sierra Instruments® mass flow controllers (MFC's) with voltage control and output were used to obtain a constant mass rate of air injected for each permeability test. Four sizes of these controllers (from 1 to 500 standard liters per minute or SLPM) were employed to span the anticipated flow rate ranges. On the MFC's the set point and the indicated flow rate were continually monitored to assure adequate performance. Voltages and currents from all types of transducers were recorded digitally using a Keithley® model 2001 multimeter and an accompanying computer.

3.1.4 Testing Methodology

In operation, the packer system enabled testing of every other 0.3048 of a meter for a particular set of installations. Moving the packers in or out by 0.3048 meter and performing another set of injections allowed complete coverage of the borehole. Almost all permutations of injection and observation positions were used. The observation packers themselves were moved in unison because it was not desired to observe the second-order effect of moving them individually. In addition, since the packers did not run the entire length of the boreholes, large relocations of 3.048 meters at a time enabled coverage of almost the whole of each 10-meter borehole. In practice, the observation packers were positioned near the collars of the observation boreholes while the injections were performed in the first two-thirds of the injected borehole. For testing of the last third of the injected borehole, the observation packers were moved in 3.048 meters from the collars so as to position them to provide good lateral coverage of potential flow paths from the far end of the injection hole.

During an injection test, permeability measurements were made possible by taking pressure readings in the injection zone while flowing air into the zone at constant mass-flow rate. Pressures were monitored to a resolution of 0.3 kPa in all the observation zones, the injected

zone, and also the non-injected zones of the injection packer. This last type of monitoring was useful to determine if air were leaking by the packer or if there were a genuine connection axial to the injected hole caused by a flow feature. These noninjected zones were therefore shut in for pressure monitoring when not used for injection.

Flow into each injection zone was controlled by the MFC's to within 10% of the desired value. A common flow rate of 5 SLPM was used for all tests. After flowing once at the common flow rate, a second injection was performed, the rate of which was determined by observing the pressure developed in the injected zone. If the pressure came close to the packer leak-by pressure (about 138 kPa pressure differential), then the test was repeated with a lower flow rate of 1 SLPM. If the pressure response was instead low enough to indicate that a higher value could be tolerated by the packers, or as in the cases of very permeable zones, if a response was not observable, then the test was repeated at a higher flow rate. By using two rates of flow, sensitivity to flow rate of any formula to be used for calculating permeability could later be characterized. The same permeability should result, independent of the flow rate used. This two-rate strategy also ensured that very permeable zones would obtain enough pressure utilizing a higher flow rate to generate observable responses in at least the well-connected observation zones. The low flow rate allowed the very tight zones to be measured without the interference of packer leak-by caused by the common flow rate.

Roughly 50,000 curves of pressure response and flow rate for Niche 3650, and a smaller number for Niche 3566 were generated in this fashion. Data were taken at 5-second intervals from up to 70 pressure channels and eight flow channels. Injection tests each lasted about three minutes, long enough to ensure a steady-state response in all the measured zones. Determination of steady state was made by the operator, assisted by real-time graphs of the injection pressure. One- to two-minute pauses between tests left time to monitor recovery pressure. If an injection zone was still recovering during this pause, the excess pressure was bled off before shutting-in the zone and switching the injection to a new zone.

3.2 Quality Status of Data

All equipment used to obtain the permeability measurements was calibrated and operated by qualified personnel in accordance with the LBNL-QA program. Data for the single-hole permeabilities for this milestone are quality assured. Digitization in the field is performed using averaging and bit lengths that easily accommodate the precision of the instruments. Data storage and all subsequent conversions are performed using double-precision floating-point numbers so

that there is no loss of accuracy. The data are qualified. The steady state single-hole data is the focus of this report and is submitted concurrently.

3.3 Results

3.3.1 Single-hole Data Management

Field testing, although mechanized, involves direct operator control. The acquired data therefore also requires a direct involvement for the purposes of sorting and reporting because it is not recorded in a manner amenable to full automation of reportage. However, specific criterion are used for retrieval and reportage. The data in the field are acquired in the form of voltage output from the various instruments and converted in real time or post-test time to engineering units using each instrument's calibration data. The time, date, and location at the start of each individual permeability test are recorded by hand in the scientific notebook by the test operator. These time, date, and location notes are correlated by hand to the time and date stamps on each data point in the acquired data file, so as to extract the information from the file needed to report the relevant data and make the permeability calculations.

Reported data consists of the acquisition filename, test location, time, date, channel number, flow rate, start pressure, steady-state pressure, and steady-state pressure run time. The derived steady-state single-hole permeability is also included. There are instances of multiple tests at the same conditions and location, which creates a choice as to which of the data to include for the report, a choice made mainly for convenience since there is no technical preference. There is also a choice of different flow rates for any given test location. A 5-SLPM flow rate was attempted at all test locations, and so this flow rate was then the desired one to use for reportage. If, however, the zone response was below the accuracy level or beyond the range of the instruments for this rate, then a higher or lower rate respectively was chosen for the report. A cursory look at permeability values obtained from locations that supported more than one flow rate confirmed that the choice of an alternate flow rate for reporting was reasonable. A steady state pressure response was usually ensured after two minutes of testing. For consistency, this two-minute time interval is the default choice. At certain test locations, however, due to time constraints, a test ran shorter than two minutes; in other cases, two minutes was not enough to ensure a steady-state response and the test instead ran two to three times longer. In both these cases, the longest available time was used to obtain the steady-state response.

3.3.2 Permeability Calculation

The values for single-hole permeability were obtained using the following technique (as used by LeCain 1995):

$$k = \frac{P_{sc} Q_{sc} \mu \ln\left(\frac{L}{r_w}\right) T_f}{\pi L \left(P_2^2 - P_1^2\right) T_{sc}} \qquad (3.1)$$

k	permeability, m^2
P_{sc}	standard pressure, Pa
Q_{sc}	flow rate, m^3/s
μ	dynamic viscosity of air, Pa*s
L	length of zone, m
r_w	radius of bore, m
T_f	temperature of formation, K
P_2	steady state pressure, Pa
P_1	ambient pressure, Pa
T_{sc}	standard temperature

Equation (3.1) assumes that the air behaves as an ideal gas and is derived for homogeneous porous medium. The geometry is assumed to be that of a line source in an infinite medium with a zone of influence equal to the zone length. While the fractured tuff of Niches 3566 and 3650 is not a homogenous or infinite medium, the equation provides a consistent method of obtaining a permeability value for an equivalent homogeneous case and enables comparison of the various test results. A comparison of the different zones and locations is, after all, the focus of these tests.

For the Sierra MFC's and for the purposes of calculation, standard pressure is 1 atmosphere, and standard temperature is 21.1 °C . The dynamic viscosity of air used is 1.78E-5 Pa·S. Formation temperature is known to be close the standard temperature, and so is chosen to be the same.

3.3.3 Single-hole Permeability and Permeability Distribution

Permeabilities for single-holes from Niche 3566 and 3650 are plotted in Figures 3.4 through 3.13. It appears that the overall permeability of Niche 3566 is higher than that of Niche 3650. Niche 3650 has some discrete high-permeability features in the first few zones of Borehole UL. Zones at the far ends of the boreholes in Niche 3650 are less permeable than those at the ends of the boreholes in Niche 3566, which intersect a rubble zone. The last value on each of the graphs of permeability for Niche 3566 is actually for the whole of the last third of each borehole, because

the packers could not be placed any further in than this location, and the length in Equation (3.1) is used to compensate accordingly. The effect of excavation of Niche 3650 is evident from the comparison plots of Boreholes UL, UM and UR in Figures 3.14 through 3.16. This effect might result partially from the exposure of a free surface near the boreholes altering the apparent permeability, but it is probable that the rock has been altered enough mechanically to change its actual permeability. Results from the radial holes tested inside Niche 3566 are shown in Figures 3.17 and 3.18. These holes have significantly higher permeability throughout their length than the previously tested holes at Niche 3566. As can be seen in Figure 3.2, Radial Holes 1 and 6 each go through general areas that are known to have characteristically high permeability. Also presented are the distributions of permeability for the pre-excavation zones at both niches in Figures 3.19 through 3.28. Comparisons of pre- and post-excavation distributions are shown in Figures 3.29 through 3.31; distributions for the radial holes are shown in Figures 3.32 through 3.33. Lastly, the distribution for all pre-excavation tests is compared to that for all post-excavation tests in Figure 3.34. Also included on this figure is the distribution for all pre-excavation zones at Niche 3566 and for all the radial hole zones at Niche 3566.

An important observation can be made after comparing frequency distributions niche to niche for all tested zones pre and post-excavation, as shown in the plots in Figure 3.34. When considering the distribution plots of permeability for all pre-excavation zones in Niche 3566 versus all pre-excavation zones in Niche 3650, it appears that both share a similar distribution from 10^{-15} to 10^{-12} m^2 but with slightly more emphasis at the higher permeabilities for Niche 3566. The distributions share a peak, but the shoulders are somewhat offset, with Niche 3566 having a higher overall average permeability. After excavation of the niches, the remaining holes at Niche 3650 and the radial holes tested in Niche 3566 show almost identical distributions, both markedly modified from the pre-excavation values. The peaks from pre- to post-excavation change by about two orders of magnitude. This observation may indicate that induced permeability due to the effects of excavation overrides the intrinsic permeability of the rock formation, and that the readings are independent of the orientation of introduced constant pressure boundaries such as the niche walls. Any introduction of higher permeability features in locations of previously low permeability will reduce the number of low permeability readings obtained. The only low permeability readings subsequently obtained will be from areas of undisturbed rock. The shift of the whole distribution for post-excavation indicates that the permeability structure in most of the tested rock was altered. Table 3.1 lists the peak values and the minimum and maximum permeability found at the niches for pre- and post-excavation. The highest and lowest values are both obtained from the pre-excavation data from Niche 3650. This was the largest sample of points, from seven boreholes as compared to three and two boreholes in the other three data sets.

The permeabilities of zones in the single-holes were used in determine at which locations and at what rates the dye release should take place. Both high permeability and low permeability zones were chosen for the release.

3.4 Summary

From the extensive cross-hole air-permeability testing conducted at Niches 3566 and 3650, the subset of single-hole permeability tests provides some insight into the variations from hole to hole and from niche to niche. In addition to aiding in the selection of dye release rates and locations, single-hole permeability measurements from pre- and post-excavation testing of remaining and new holes allows the investigation of the effect of excavation on the permeability of the rock surrounding the niches. There is a marked difference between the pre- and post-excavation permeability in remaining holes at Niche 3650 and also between permeability from holes drilled before after and Niche 3566 excavation. As more niches are tested and constructed, similar testing techniques will allow a broader understanding of the permeability structure at different phases of excavation, at various scales, and in different lithologies along the entire ESF.

References

LeCain, G. D. 1995. *Pneumatic Testing in 45-Degree-Inclined Boreholes in Ash-Flow Tuff near Superior, Arizona.* U.S. Geol. Surv. Water Resour. Invest. Rep. 95-4073. Denver, Colorado: U.S. Geological Survey. MOL.19960416.0160, GS940912331210.005 (Non-Q).

Tsang Y. W., Wang, J.; Freifeld, B.; Cook, P.; Suarez-Rivera, R.; and Tokunaga, T. 1996. *Letter Report on Hydrological Characterization of the Single Heater Test Area in the ESF.* Yucca Mountain Project Level 4 Milestone OS327322D1. Berkeley, California: Lawrence Berkeley National Laboratory. MOY-970512-07-B. DTN: LB960500834244.001 (Q).

Tsang, Y.W. and Cook, P. 1997. *Ambient Characterization of the ESF Drift Scale Test Area by Field Air Permeability Measurements.* Yucca Mountain Project Level 4 Milestone SP9512M4. Berkeley, California: Lawrence Berkeley National Laboratory. LB970600123142.001 (Q).

Wang, J.S.Y., Cook, P.J.; Trautz, R.C.; Salve, R.; James, A.L.; Finsterle, S.; Tokunaga, T.K.; Solbau, R.; and Clyde, J. 1997. *Field Testing and Observation of Flow Paths in Niches, Phase 1 Status Report of the Drift Seepage Test and Niche Moisture Study.* Yucca Mountain Project Level 4 Milestone SPC31DM4. Berkeley, California: Lawrence Berkeley National Laboratory. LB970601233124.001 (Q).

Table 3.1 Maximum, Minimum and Peak Permeabilities by Group.

	Niche 3650		*Niche 3566*	
	pre	*post*	*pre*	*radial holes*
max K m^2	1.27E-10	1.01E-10	2.48E-11	4.38E-11
min	1.53E-15	3.02E-15	4.29E-15	1.11E-14
peak	1.E-14	1.E-12	1.E-14	1.E-12

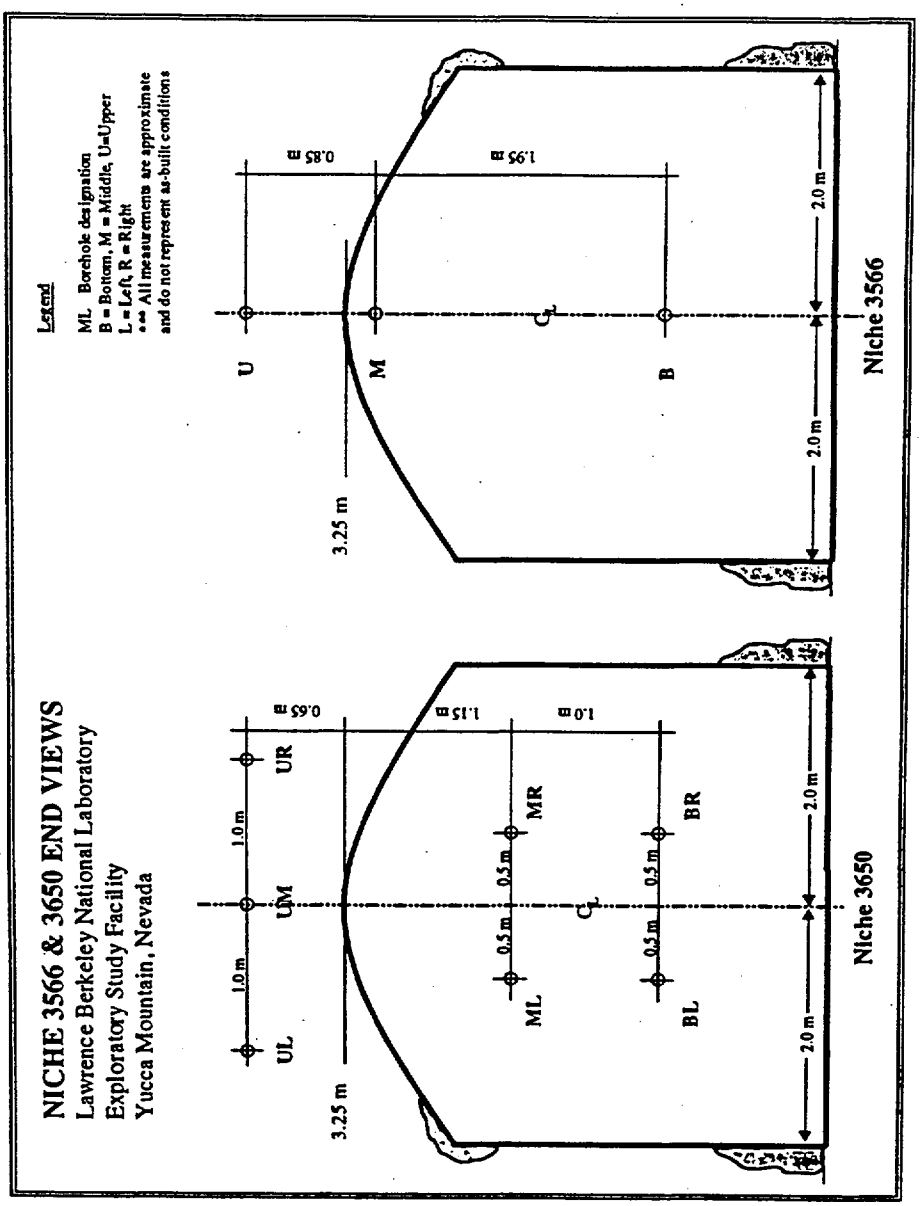
NICHE 3566 & 3650 END VIEWS
Lawrence Berkeley National Laboratory
Exploratory Study Facility
Yucca Mountain, Nevada
Legend
ML Borehole designation
B = Bottom, M = Middle, U=Upper
L = Left, R = Right
** All measurements are approximate and do not represent as-built conditions
Niche 3566
Niche 3650
U
M
B
UR
UM
UL
MR
ML
BR
BL
0.85 m
1.95 m
0.65 m
1.15 m
1.0 m
3.25 m
2.0 m
1.0 m
0.5 m

Figure 3.1

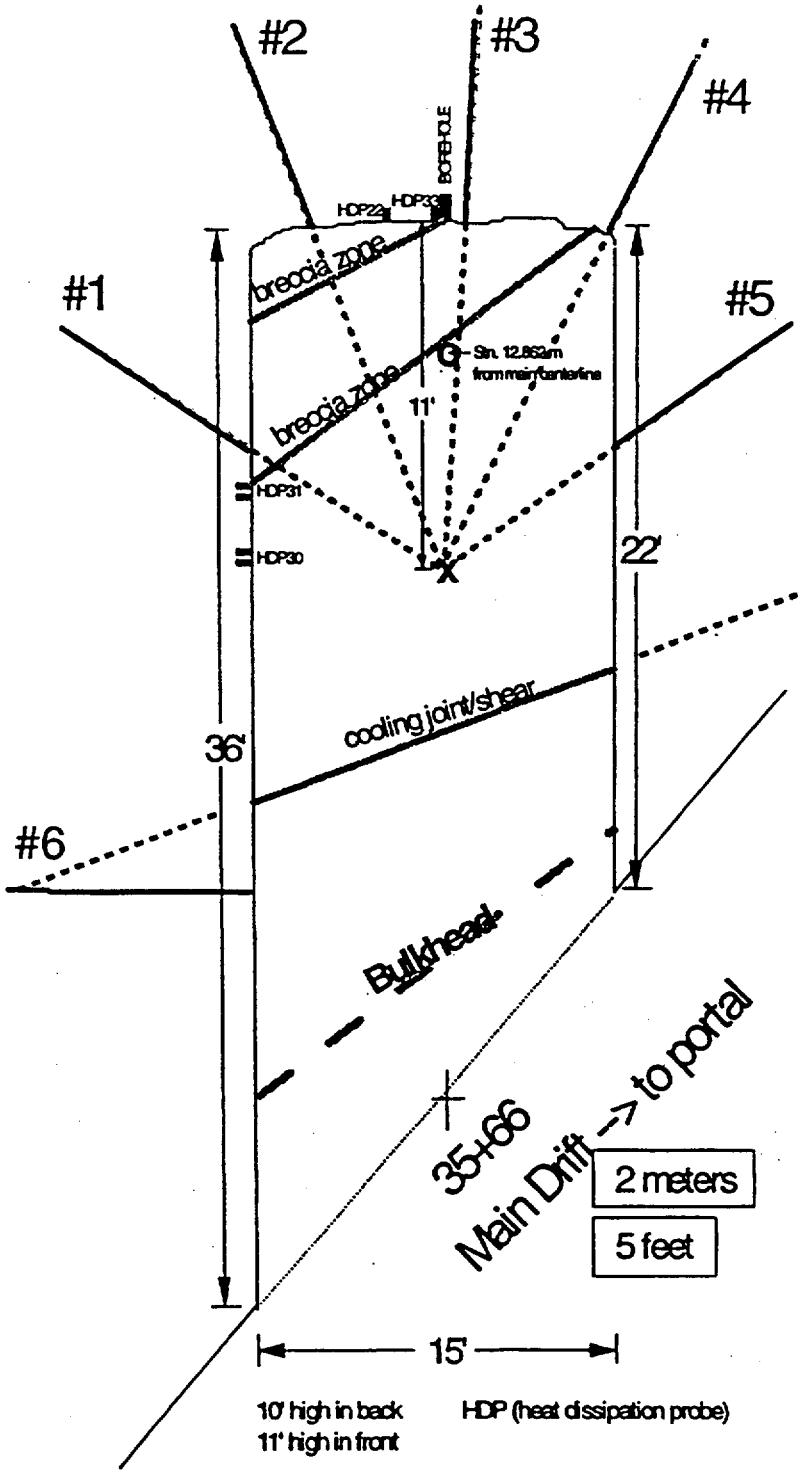

Figure 3.2 Schematic of Niche 3566 with locations of niche based boreholes #1, #2, #3, #4, #5, and #6 and locations of heat dissipation probes (HDP) used to measure rock water potential.

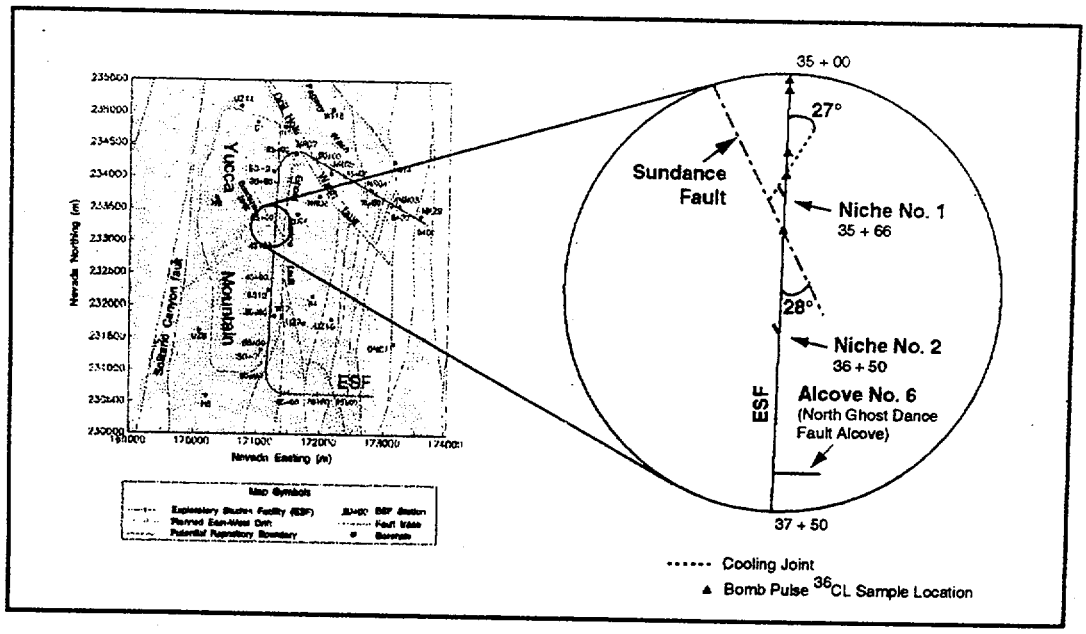

Figure 3.3 Location map of the niche at CS 3566 site near the Sundance Fault and the niche at CS 3650 site between Sundance Fault and Alcove 6.

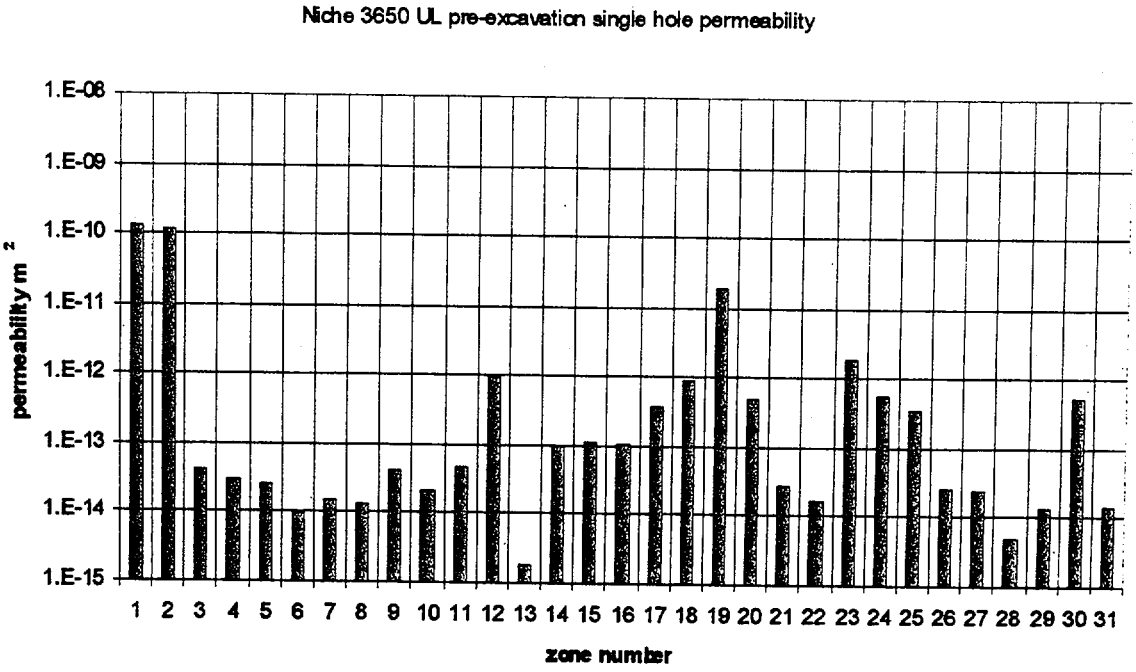

Figure 3.4

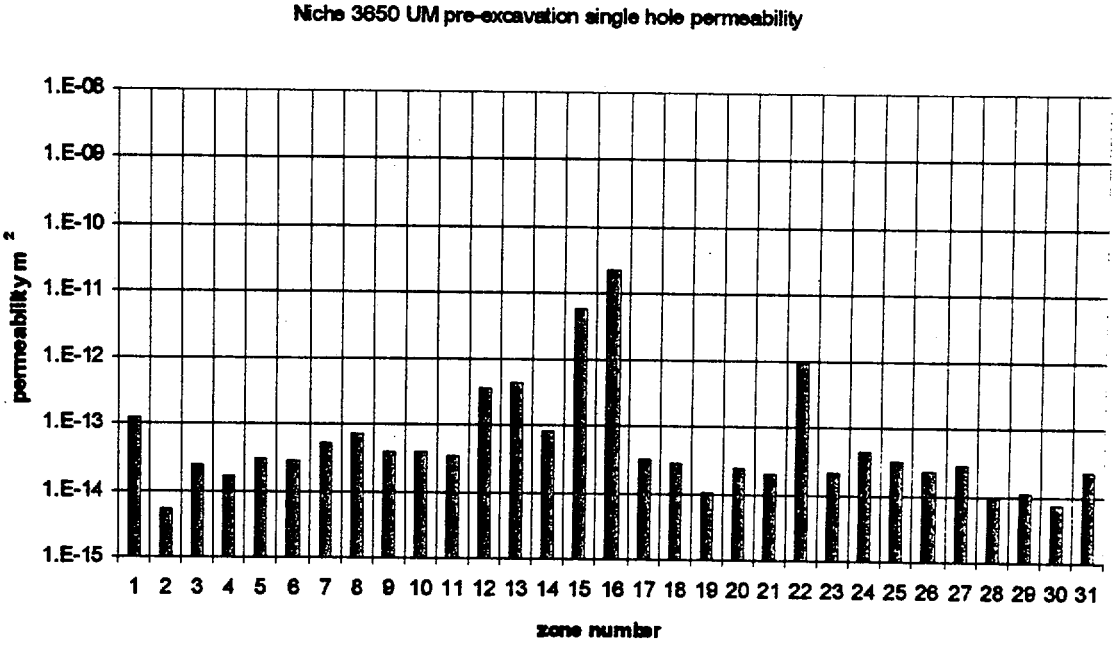

Figure 3.5

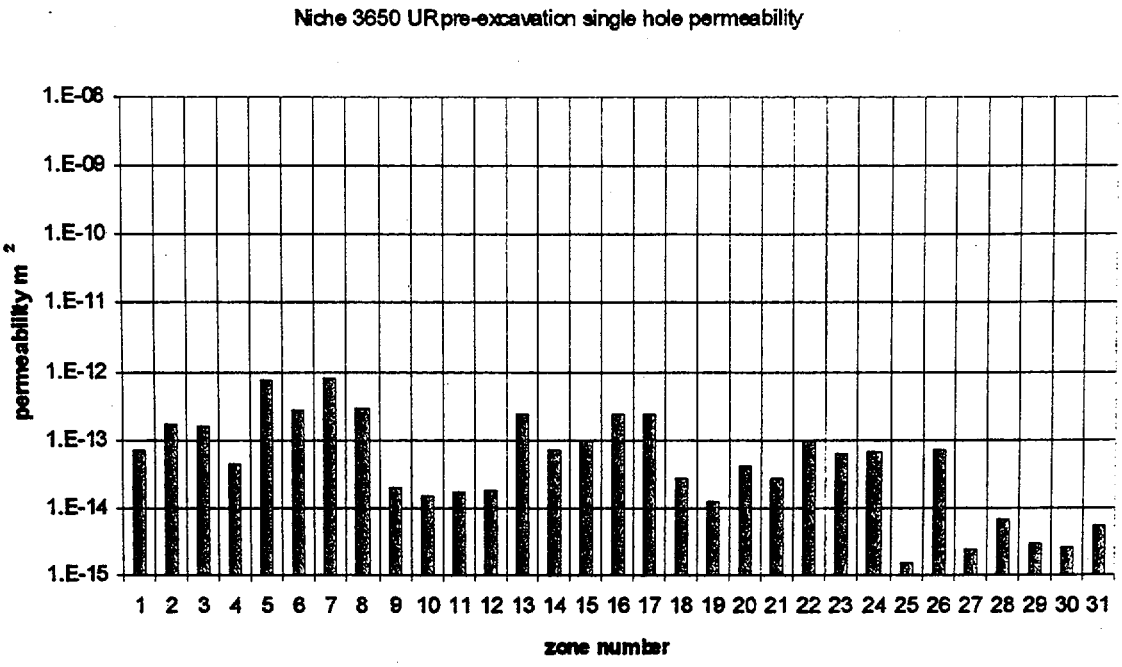

Figure 3.6

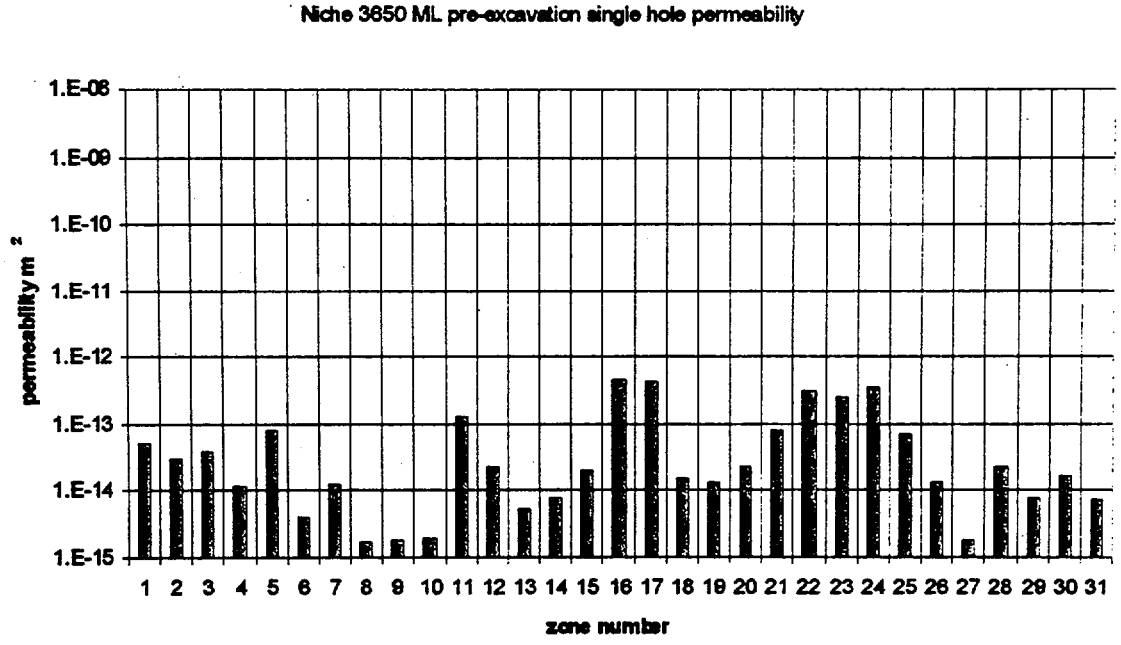

Figure 3.7

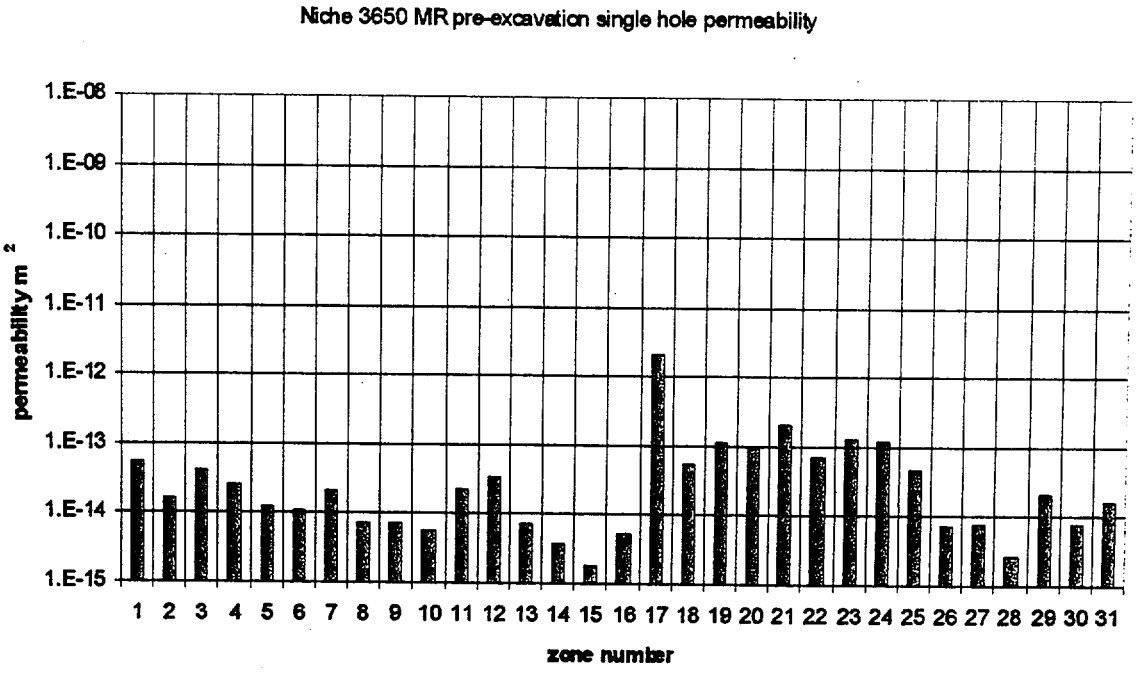

Figure 3.8

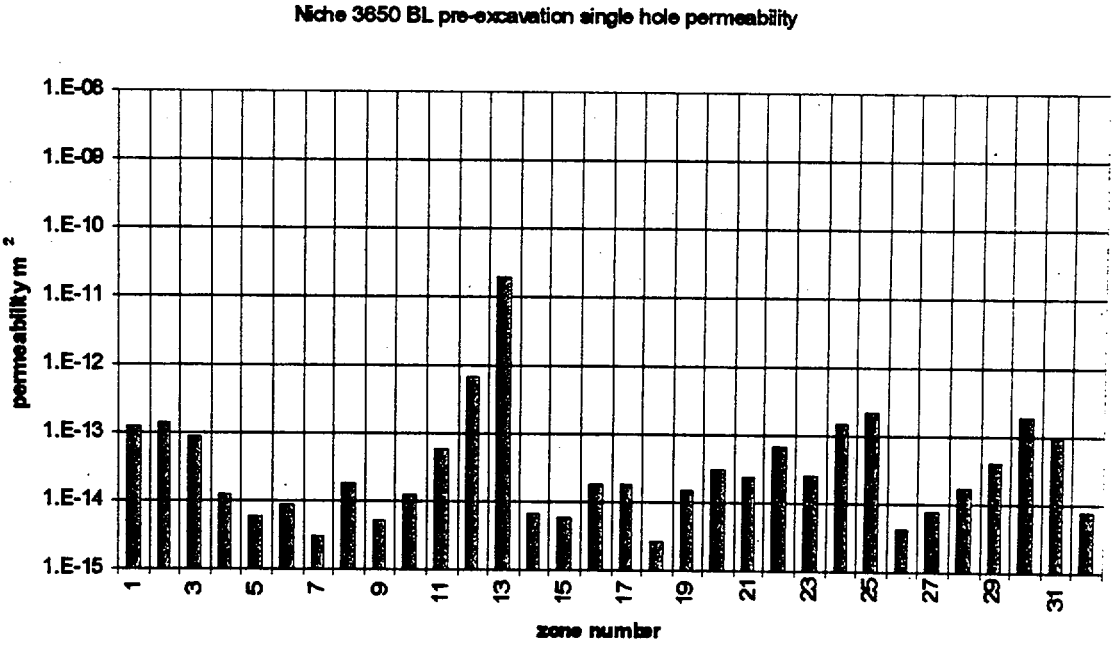

Figure 3.9

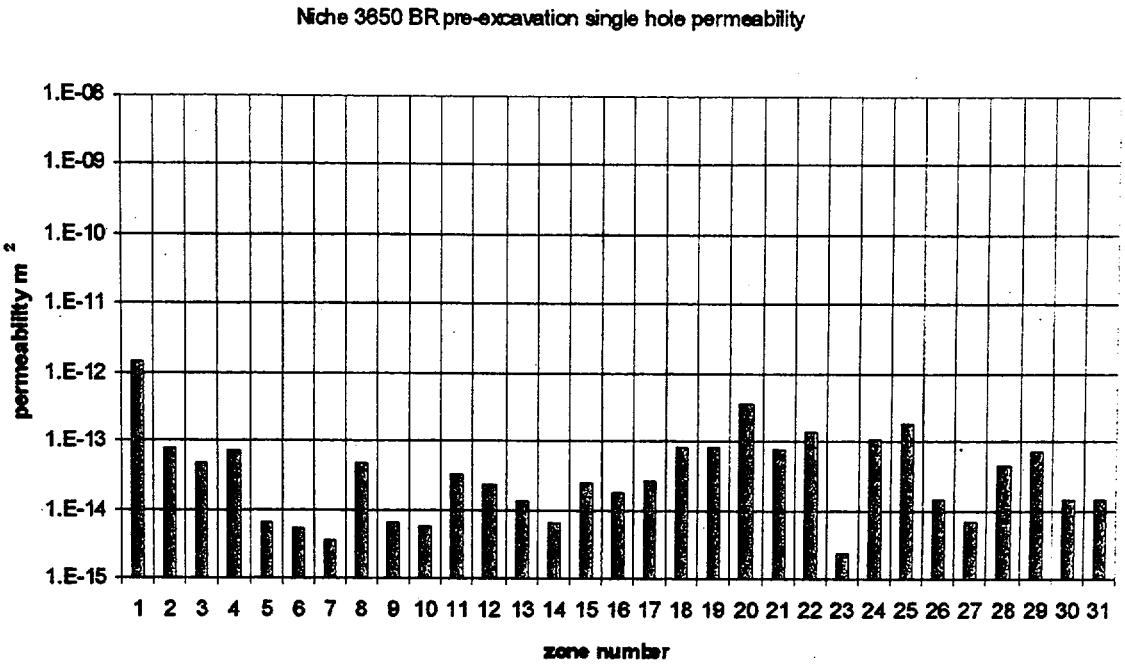

Figure 3.10

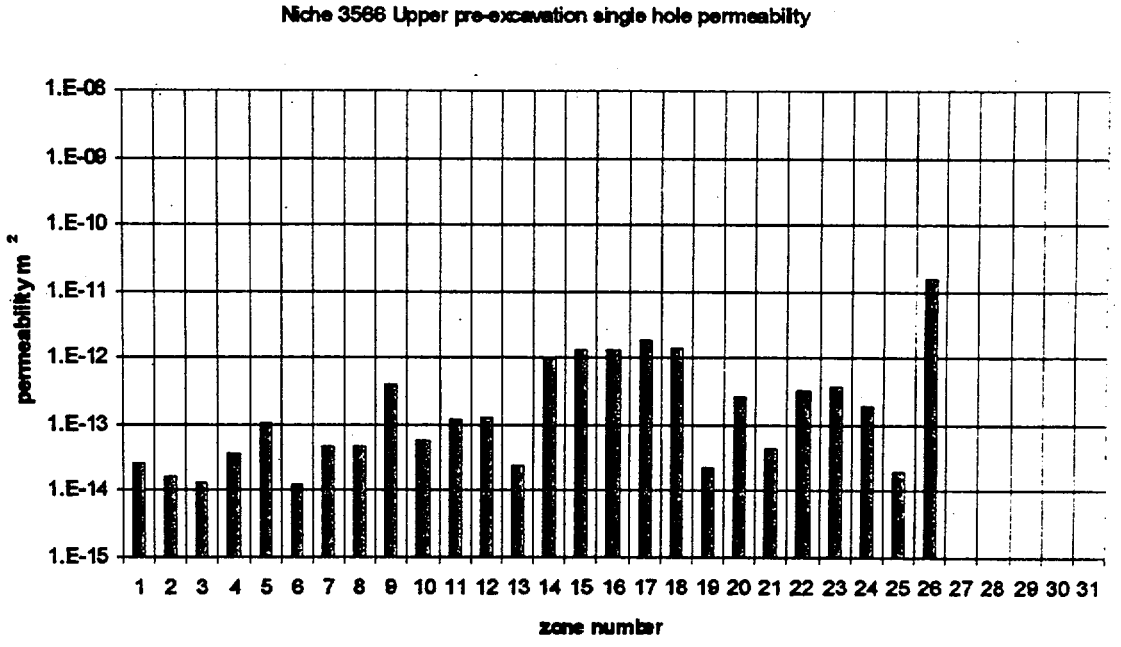

Figure 3.11

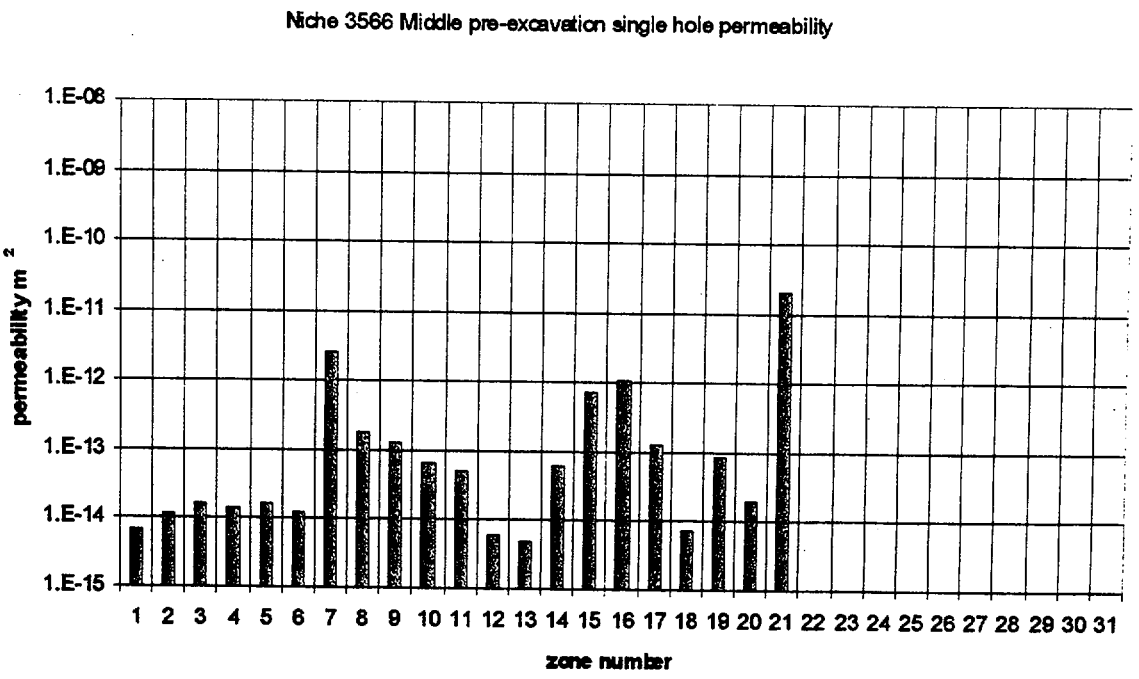

Figure 3.12

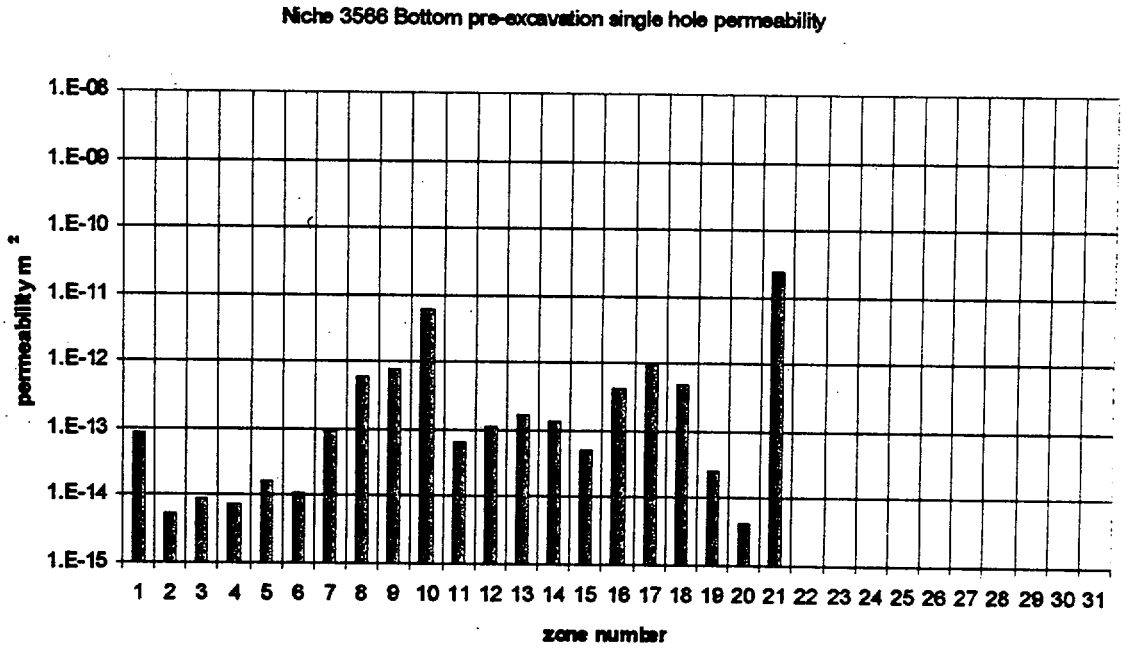

Figure 3.13

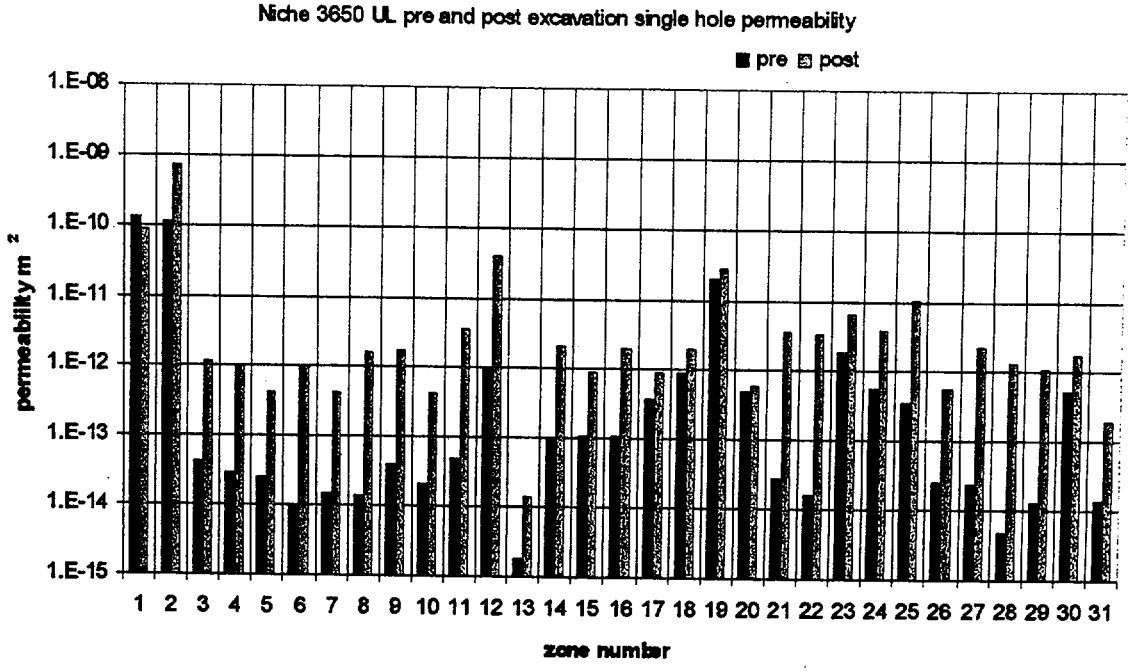

Figure 3.14

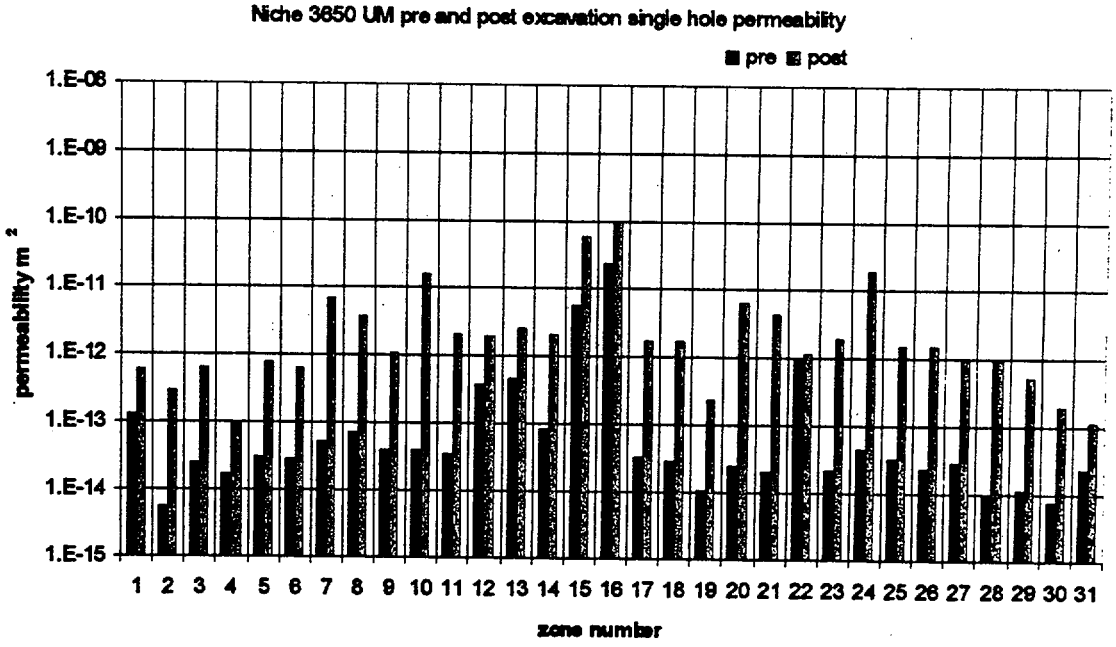

Figure 3.15

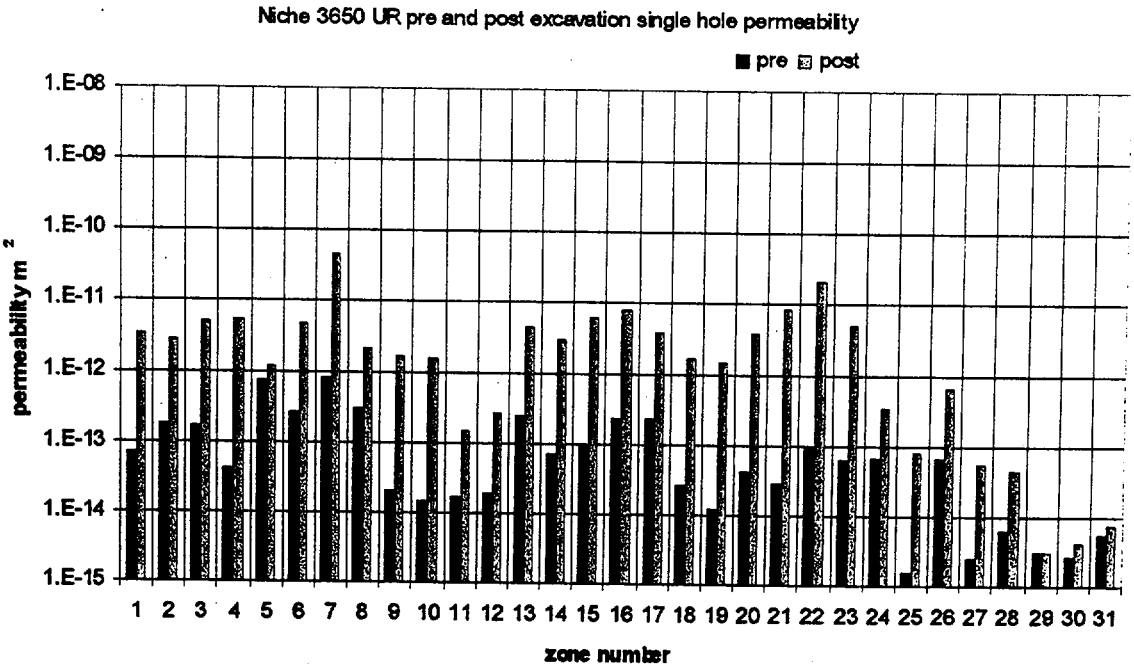

Figure 3.16

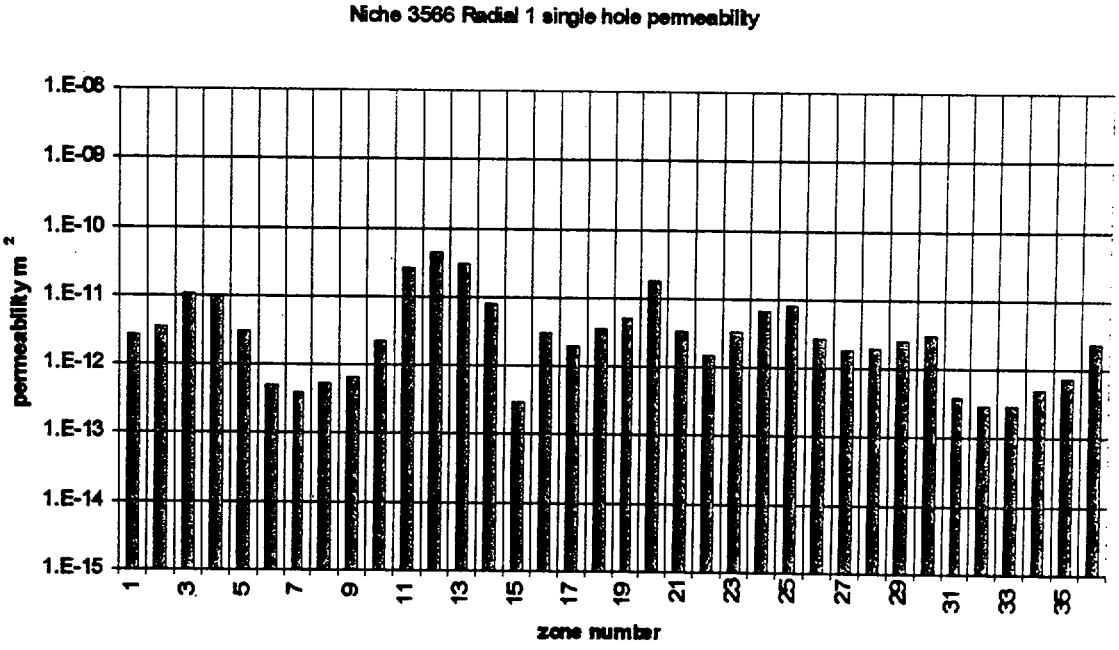

Figure 3.17

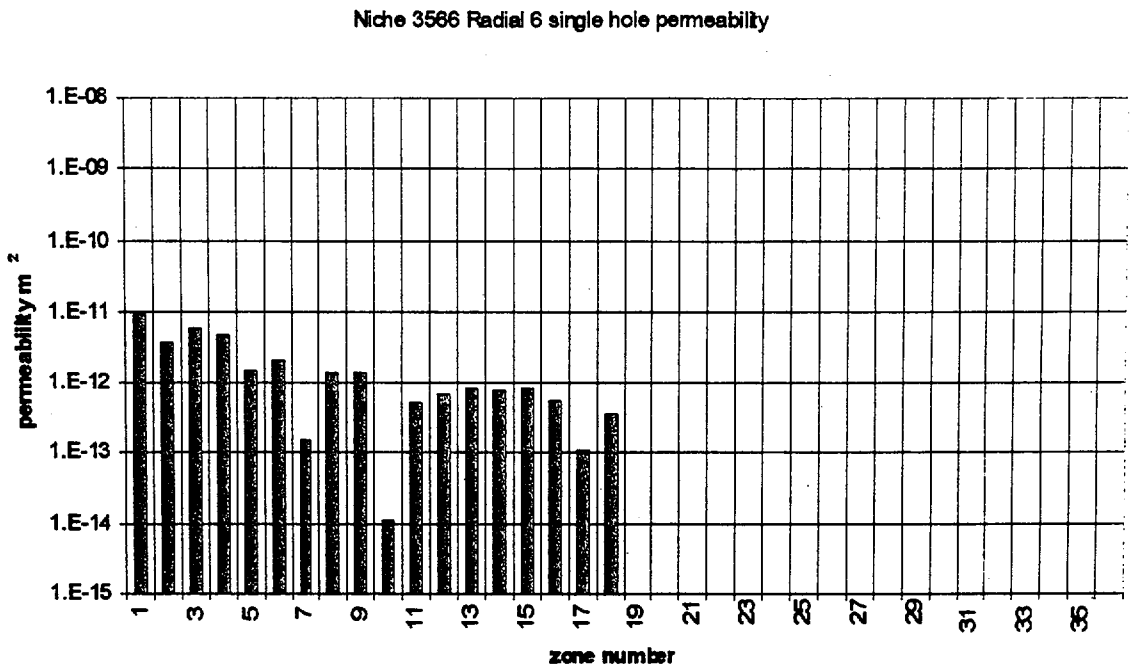

Figure 3.18

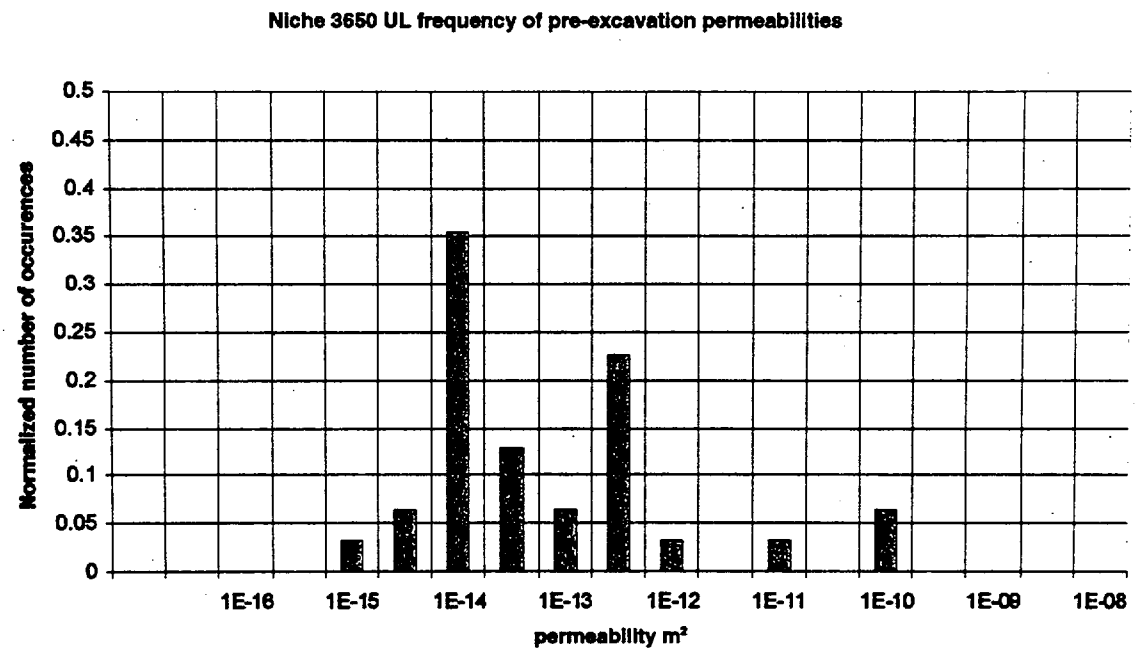

Figure 3.19

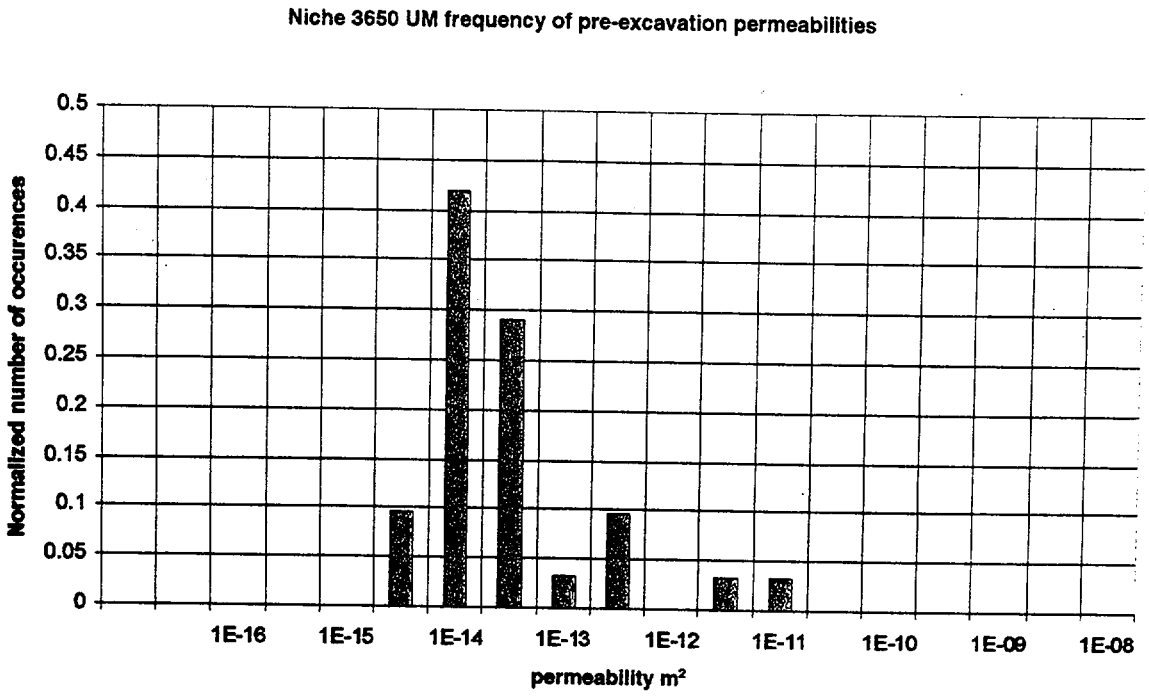

Figure 3.20

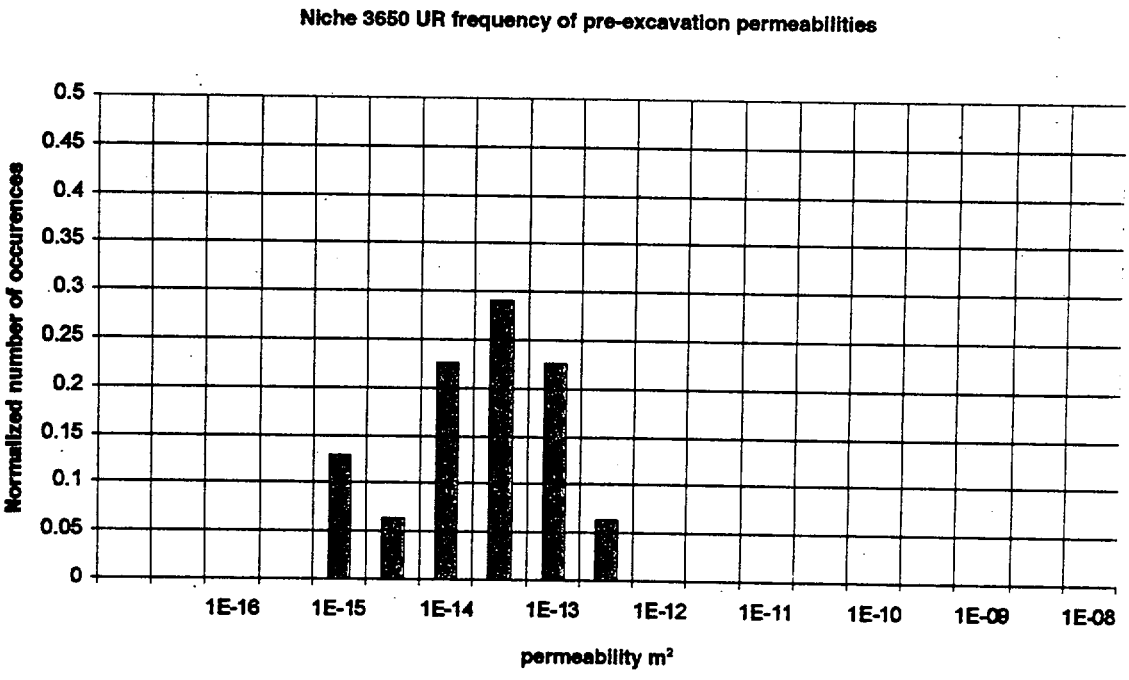

Figure 3.21

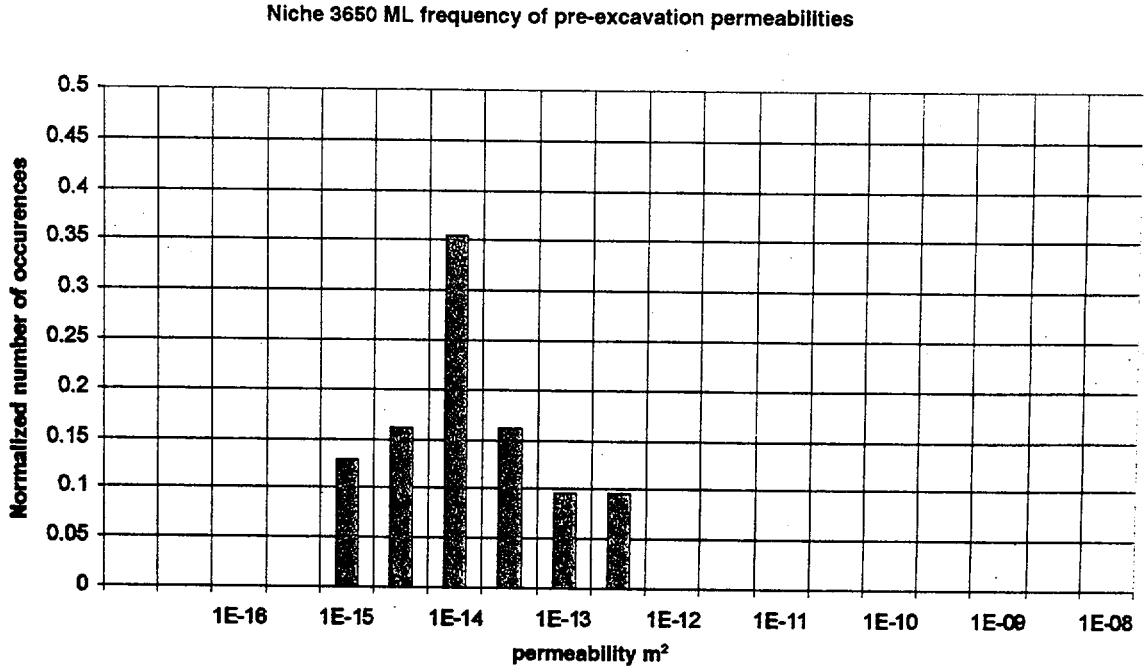

Figure 3.22

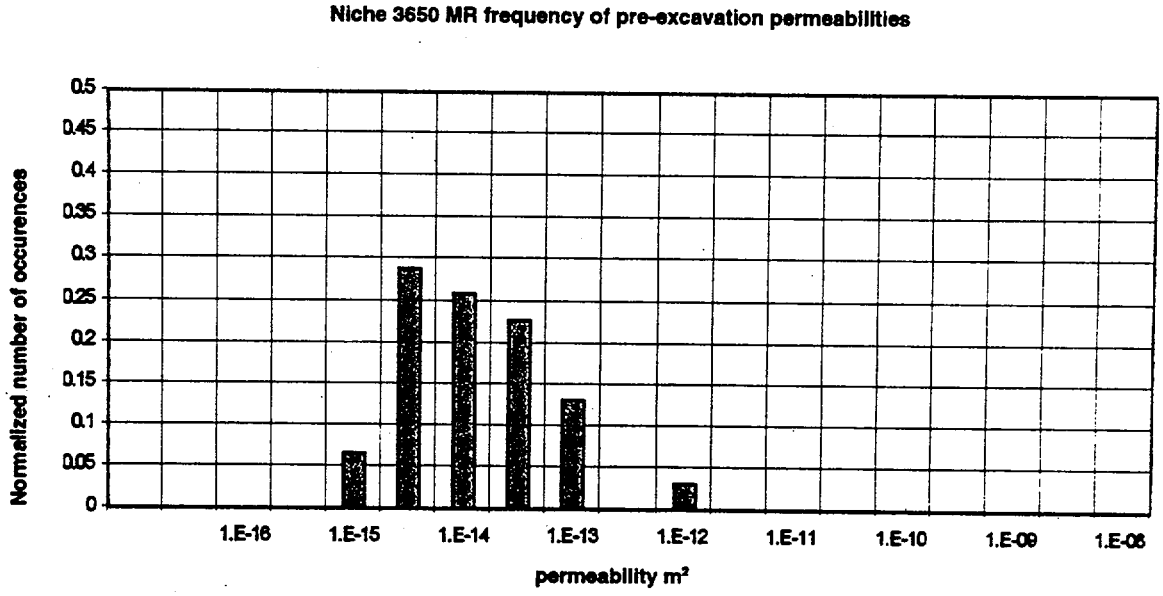

Figure 3.23

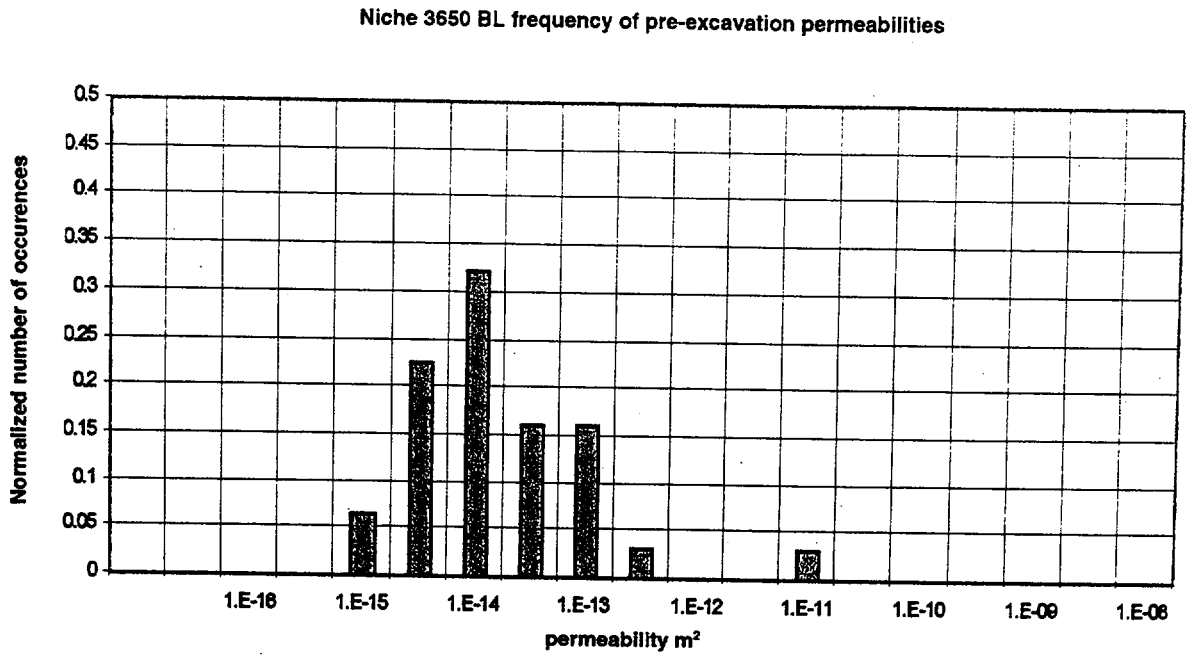

Figure 3.24

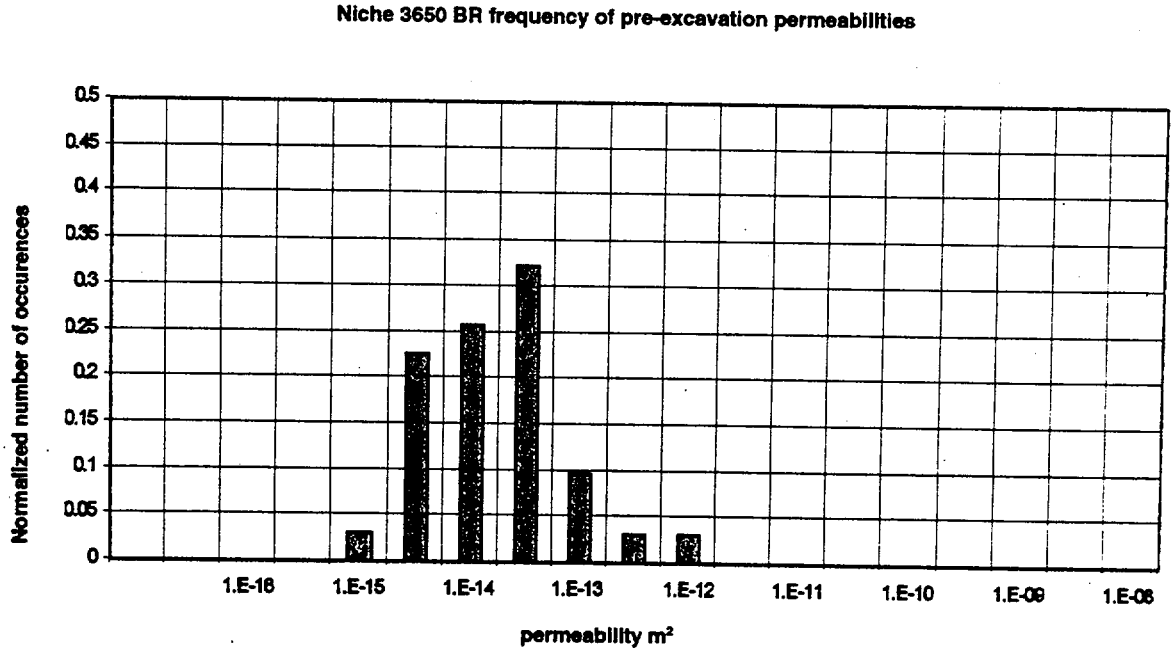

Figure 3.25

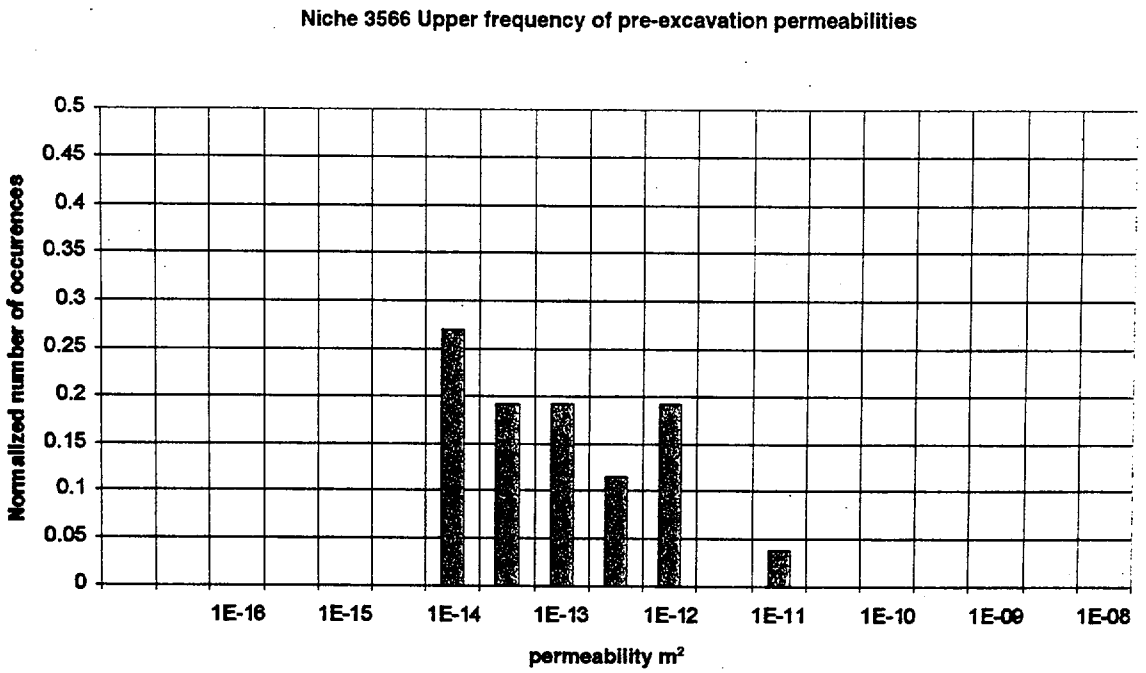

Figure 3.26

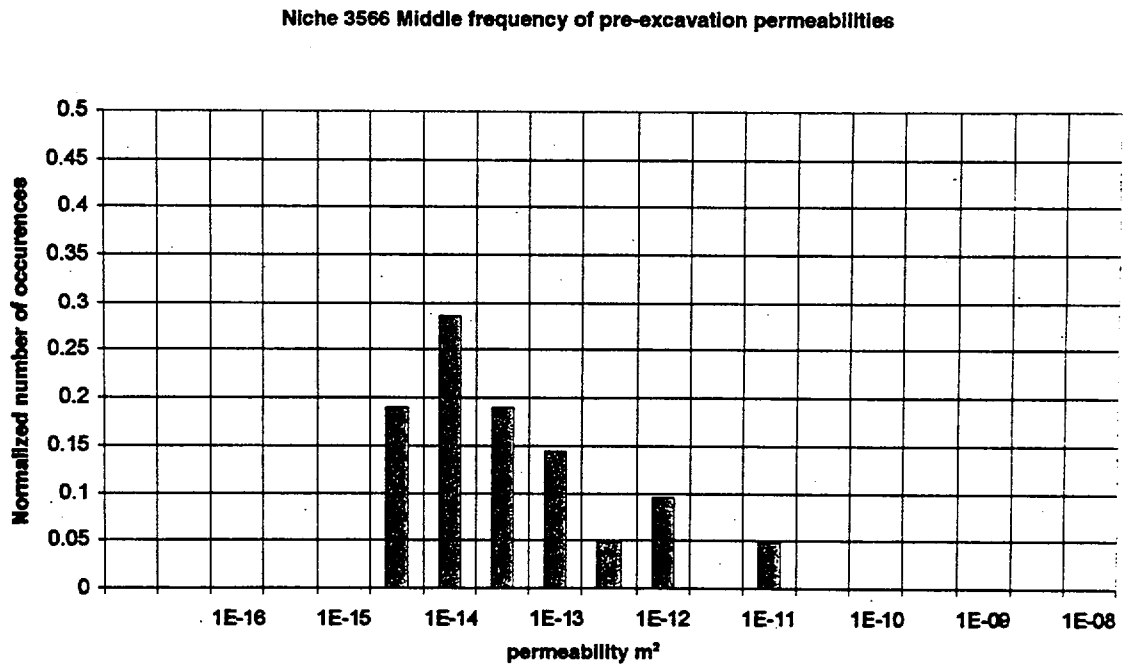

Figure 3.27

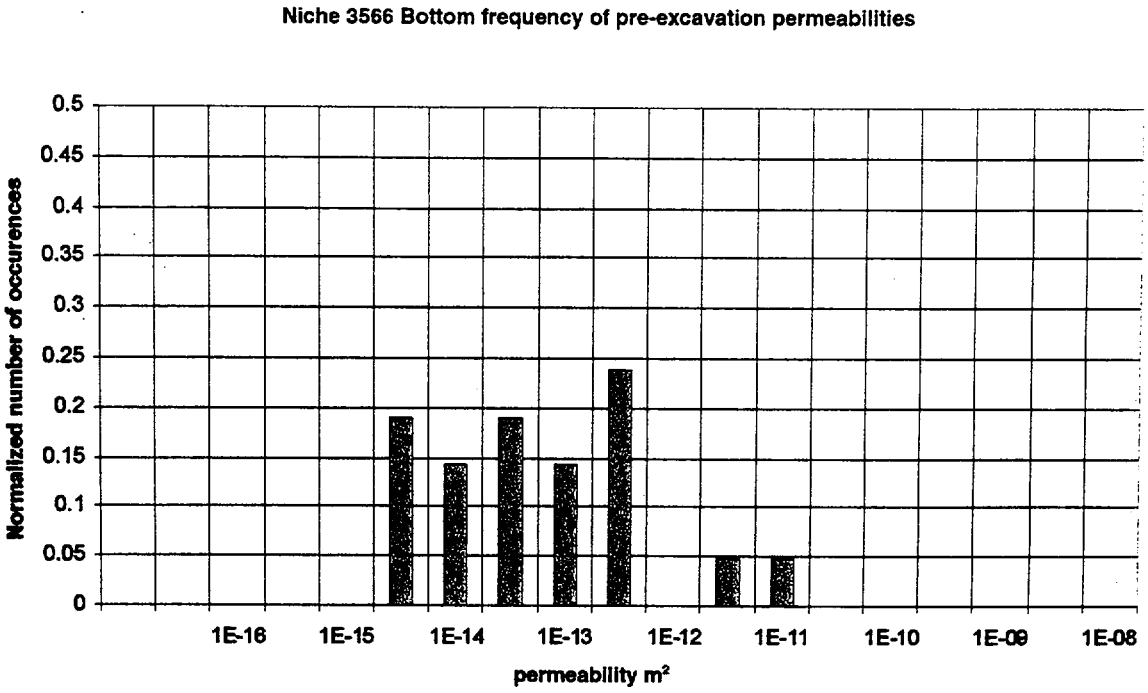

Figure 3.28

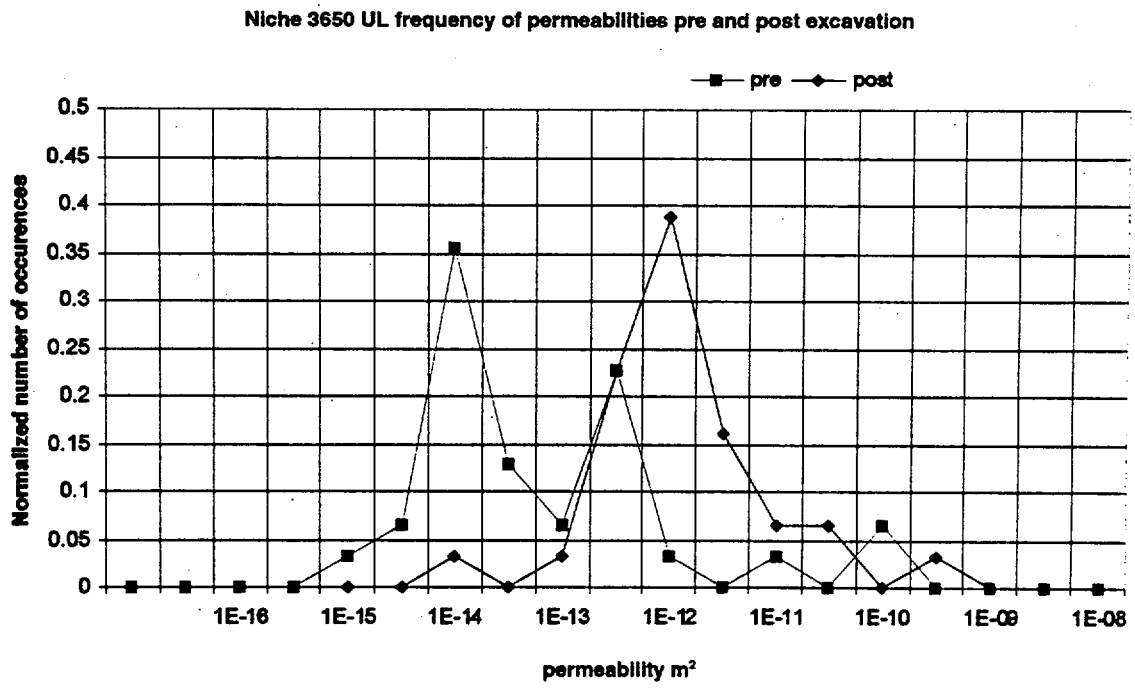

Figure 3.29

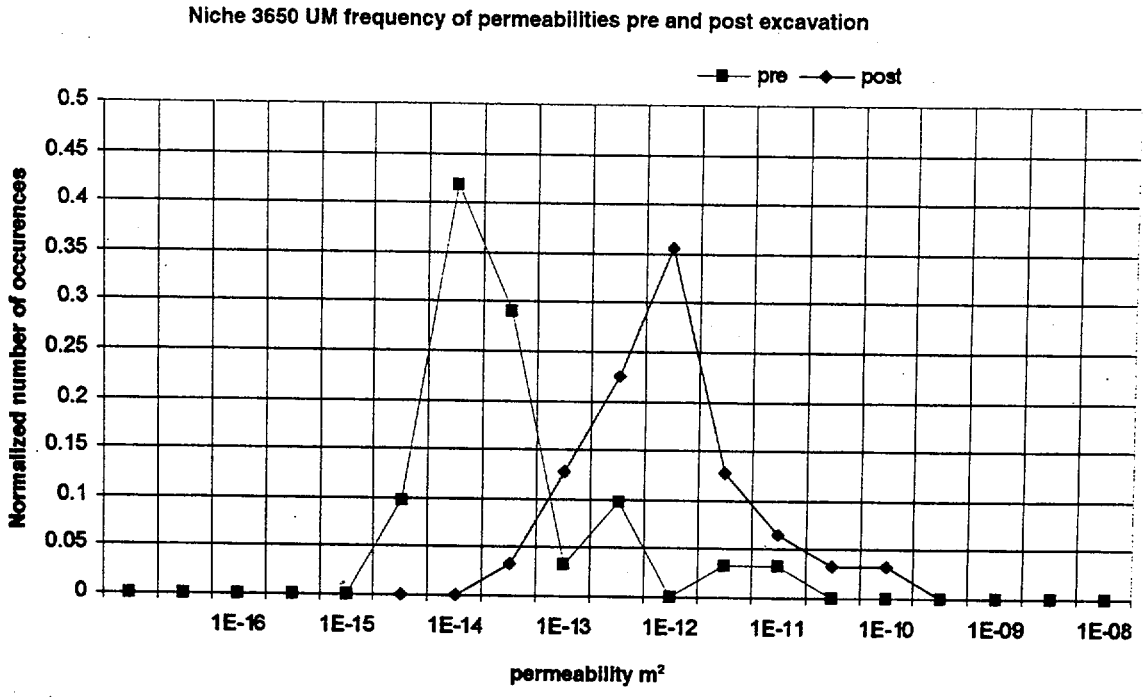

Figure 3.30

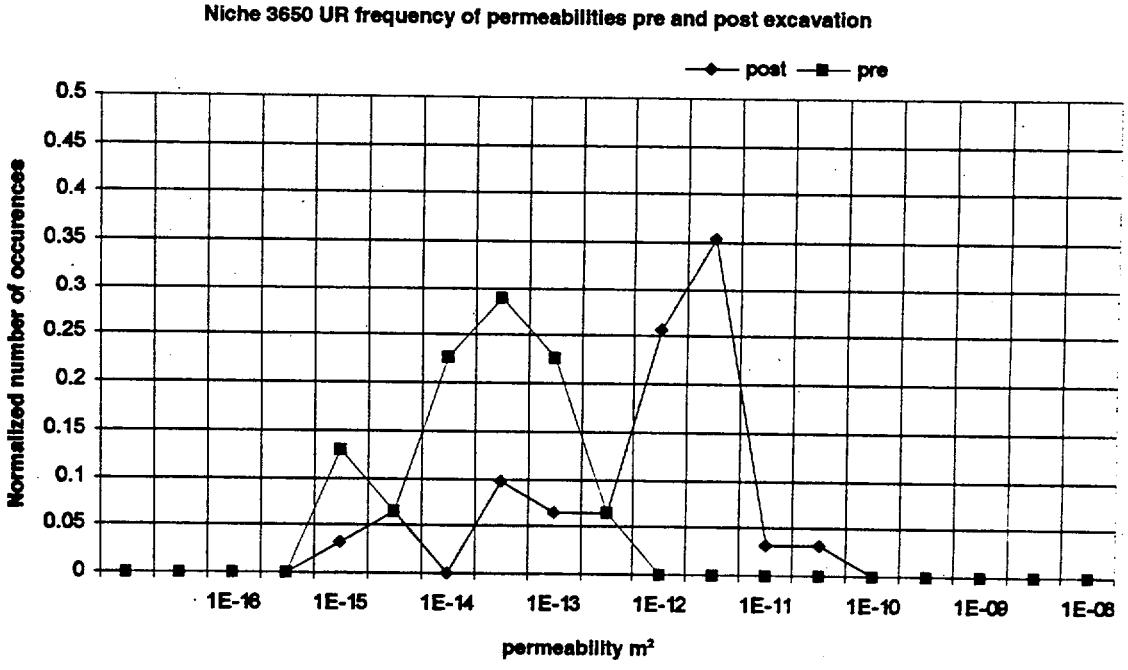

Figure 3.31

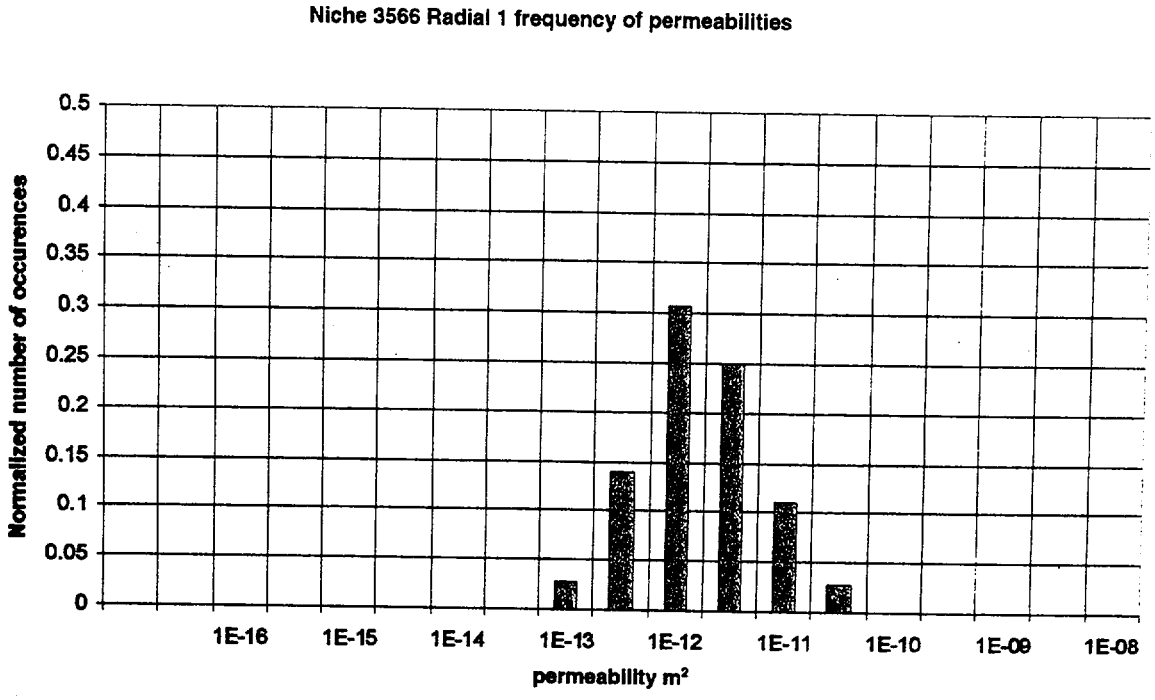

Figure 3.32

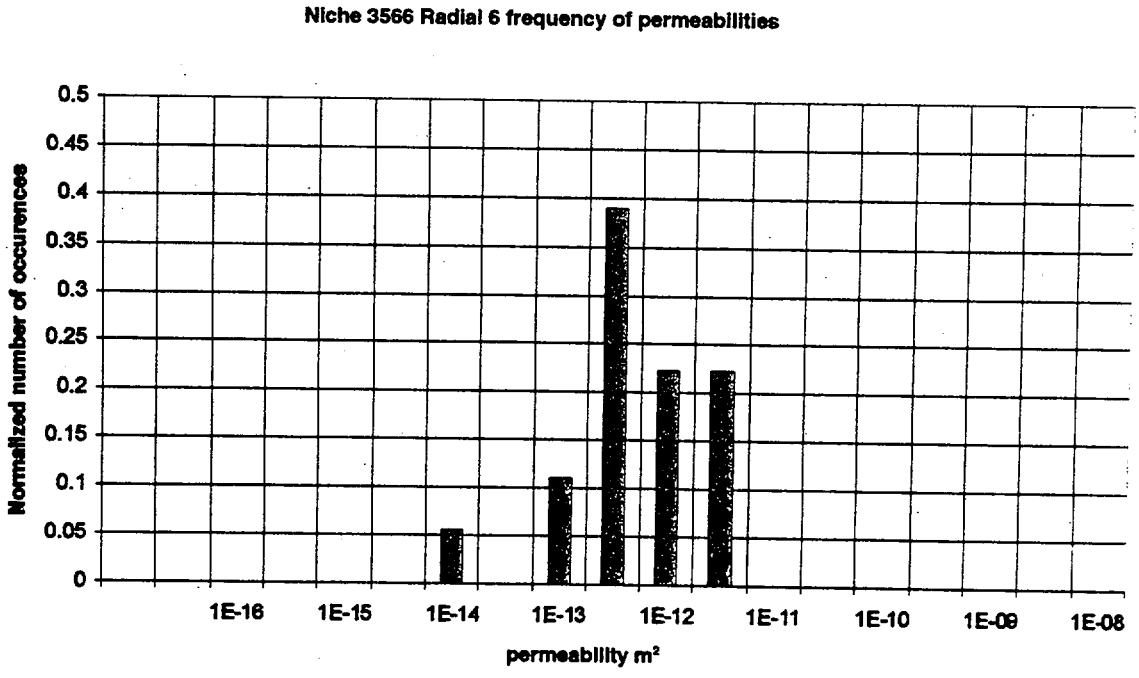

Figure 3.33

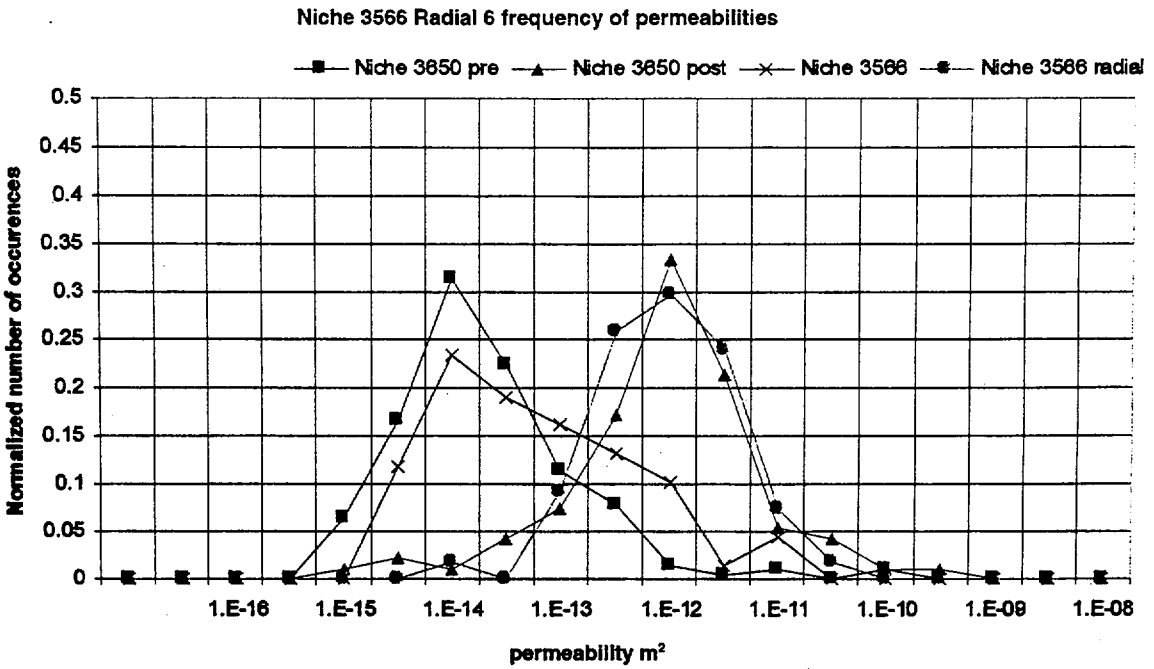

Figure 3.34 Permeability distributions for pre and post niche excavation, grouped.

Chapter 4 Compilation of Water Potentials Measured in the Niches

R. Salve and J. S. Y. Wang

4.0 Introduction

Borehole clusters and niches provide a framework for studies investigating drift-scale seepage and testing in the ESF. These studies have been designed to measure *in-situ* permeability and other hydrologic parameters of repository level rock, while attempting to identify drift-scale seepage processes. Typically, a cluster of boreholes installed along the right rib of the main drift of the ESF is monitored to determine water content and potentials. This is followed by a series of tests in which air and water permeabilities are determined at various locations within the cluster of boreholes. A niche is then excavated and a second cluster of boreholes is cored into the niche wall. *In situ* measurements of water content and potential in these new boreholes are followed by measurements of air permeability and liquid release.

In this chapter measurements of water potentials from three niche sites in the ESF are presented. These sites are located on the west side of the main drift 3566, 3650 and 3107 m from the north portal of the ESF. Two faults (the Ghost Dance and Sundance Faults) lie within the immediate vicinity of the niches, with Niche 3566 lying on a cooling joint intercepting the Sundance Fault. The criteria and rationale for the selection of these niches is described elsewhere (Wang et al. 1997).

4.1 Potential Measurements

The primary objective of this effort was to determine the water potential at various points within the three niche sites. To meet this objective a common method to measure water potential, the use of psychrometers, was adapted for borehole application.

4.1.1 Measurement of water potential with psychrometers

Water potential measurements were made with Wescor Inc. psychrometers (model PST-55) connected to a Campbell Scientific data logger (model CR7). Using the multiplexing capabilities of the data logger, hourly measurements of up to 20 psychrometers were automated. All readings of water potential were made using the psychometric method. In this method, the chromel-

constantan junction in the PST-55 psychrometer is cooled with an electric current to a temperature below dew point, after which the condensed water is allowed to evaporate. The temperature depression resulting from evaporation is then monitored and used to determine water potentials in the vicinity of the psychrometers.

Prior to field use, all psychrometers were calibrated in the laboratory, using potassium chloride solutions (0.1-1.0 molal). A second calibration was done in the laboratory after psychrometers had been used for field measurements. During the calibration procedure, psychrometers were isolated in an insulated box to minimize temperature fluctuations. Automated measurements were then made using the multiplexing capabilities of the CR7 data logger. When the psychrometers were observed to have reached equilibrium, they were removed from the calibration solution, washed in distilled water, air-dried and immersed in the next solution. After calibrations were completed, all psychrometers were washed before installation in the field.

During laboratory calibrations and preliminary field measurements, we noticed that the shape of the psychrometer output curve was significantly influenced by the size of the cooling voltage and cooling duration, for a given water potential (Figure 4.1). This curve was also dramatically altered when the psychrometers became contaminated with dust particles (Figure 4.2). Given the high rate of failure of psychrometers in the field, it was therefore important to optimize both the cooling voltage and duration for a given water potential, to help identify psychrometers that were contaminated or otherwise malfunctioning. Data from contaminated or malfunctioned psychrometers will not be used for interpretation and will be labeled in the scientific notebook. Attempts are made to repeat the tests if feasible.

4.1.2 Location of water potential measurements in the niches

Water potentials were measured either along the length, or at the ends of 3-inch-diameter boreholes. Three different types of housing units were used to locate psychrometers in the boreholes. The main feature of the housings was the creation of a small air chamber, which allowed for quick equilibration and measurements of humidity close to the borehole wall (Salve et al. 1997).

At Niche 3566, two separate sets of measurements were made; i.e., before and after niche excavation. Pre-excavation measurements were made in May 1997 in three holes at a distance of 10 m from the borehole collar (Figure 4.3a). Between July and September 1997, two sets of measurements were made along the upper borehole (U–see Figure 4.3a) at distances between 3.5 and 8.0 m from the collar. Post-excavation measurements of water potential were made in October 1997 in five boreholes extending radially along a horizontal plain from the niche cavity (Figure 4.3b).

At Niche 3650, two separate sets of water potential measurements were made in July 1997, before and after air-permeability tests were conducted in the boreholes. In three boreholes at this location (ML, BR and BL), water potentials were measured at the end of the boreholes (10 m), and in a single borehole (UM) measurements were made close to the borehole collar, i.e., between 0.6 and 1.2 m (Figure 4.4).

In Niche 3107, four boreholes were instrumented with psychrometers (Figure 4.5). In the upper middle (UM) borehole, multiple measurements were made along the first 3.0 m, while in the remaining three (ML, UL, UR), single measurements were made using different lengths of borehole cavity. In the upper-right borehole (UR), sensors were located at the back of the borehole and sealed off with inflation packers such that the borehole cavity was less than 0.04-m long. In the upper-left (UL) borehole, sensors were located 5.0 m from the borehole collar, with the cavity sealed off with inflation packers. In this case, the sensing cavity extended over 5.0 m of borehole. In the middle left borehole (ML), sensors were located 0.30 m from the borehole collar, with an inflation packer installed to isolate the entire 10.0-m length of borehole from the ESF main drift of the tunnel.

4.2 Observations

Water potential measurements obtained from the three niches are summarized in Tables 4.1 to 4.3. Included in these tables are calibration coefficients and raw voltage and temperature readings obtained in the field. Also included are the time and duration of measurements at each location.

4.2.1 Niche 3566 (Pre-excavation):

The water potentials measured at the ends of the three pre-excavation boreholes (U, B, and M) in Niche 3566 were close to saturation values, indicating that approximately 10 m from the ESF, the formation is relatively wet. Of the three, the end of the middle borehole appeared to be wettest, with water potentials between 0 and –1 bar. Measurements made along the profile of the upper borehole (between 3.7 and 7.9 m from the collar) ranged between –3.3 and –6.9 bars. (Figure 4.6).

4.2.2 Niche 3566 (Post-excavation):

In the excavated niche cavity, water potentials were monitored in five boreholes. The monitored locations in Borehole A (Figure 4.3b) were selected to be 6.25 and 6.75 m from the collar

following observations of high neutron counts (i.e., suggesting a moist zone) made by Flint and Flint (1997). The high water potentials measured at these points (i.e. –0.2 and –2.9 bars respectively) support these observations. In three of the remaining boreholes (B, D, and E) water potentials measured at depths of 6.0 m varied significantly between boreholes. Here, Borehole D (–2.1 to –3.1 bars) was wettest, followed by B (–4.2 bars) and then E (–7.3 to –7.9 bars). These observations appear to be consistent with those made in the pre-excavation holes that indicated that the formation tended to get wetter with increasing distance from the main drift.

Measurements made close to the collar in Borehole C suggest that there was significant dry-out in the rock surrounding the niches up to a depth of at least 0.15 m, extending possibly to 2.6 m.

4.2.3 Niche 3650

Measurements were made at the end of three boreholes BR, BL, ML, (Figure 4.4), each 10 m long, before and after a series of air-permeability tests. Pre-test water potential values ranged between –0.1 and –3.8 bars. However, following the test, water potentials in borehole BR dropped to between –4.7 and –5.7 bars, in borehole ML dropped to between –2.9 and –3.8 bars, while in borehole BL the measurements did not show significant changes.

Closer to the borehole collar, readings made between 0.6 and 1.2 m indicate a relatively dry zone, with water potentials between –12.5 and –16.2 bars.

4.2.4 Niche 3107

The three sets of observations made in Niche 3107 show significant variability within the boreholes in the niche. Measurements made at the ends of Boreholes UL (–1.5 bars) and ML (–8.2 bars) indicate that at a depth of 10 m within a horizontal distance of 1 m, there is a steep potential gradient. Further, from observations within Borehole UM, it is clear that there is a prominent dry-out zone (Figure 4.7) associated with the main drift of the ESF.

4.3 Discussion

Psychrometer measurements in the ESF suggest that there is significant variability in water potentials between and within the three niches. One source of the variability can be attributed to the possible drying out of the matrix resulting from ventilation effects along the main drift of the ESF. This is evident from multiple measurements made close to the borehole collars, which show increasing water potentials with increasing distances from the collar. A similar dry-out

observed close to the collar in Borehole C in the Niche 3566 cavity indicates that ventilation effects are also prominent in enclaves along the main drift. Our data suggests that the extent to which ventilation effects may have penetrated the matrix is possibly greater than 3.0 m.

The second source of variability is formation heterogeneities, which allow zones with high moisture content to develop (i.e. fast flow paths). Our data points to two possible zones that have significantly high water potentials. The first was observed at the end of the middle borehole in Niche 3566 (pre-excavation) while the second was detected 6.25 m along Borehole A in Niche 3566 (post-excavation).

In the zone beyond where ventilation effects of the ESF are felt (i.e. at 10-m depths), Niche 3566 appears to be wetter than Niche 3650. The data from Niche 3107 is inadequate to draw any such conclusions. The two measurements made in Niche 3107 suggest that there is large variability (-1.5 and -8.5 bars) in the short distance (0.75 m) between the two boreholes.

4.3.1 Suggestions for future niche moisture measurements:

Our preliminary observations of variability in water potentials between and within niches raise questions about:

1. The extent and rate of dry-out associated with ventilation along the main drift,

2. The spatial gradients in water potentials associated with features such as the Sundance fault, and

3. The effect of air permeability tests in moisture redistribution within the formation being investigated.

To address the first question, it is recommended that moisture potentials be monitored in a cluster of boreholes, installed immediately following the creation of a ventilated drift. This is possible in the cross-drift currently being excavated. A suitable approach would be to install a series of psychrometers along the length of 10-15-m-long boreholes. These could then be monitored over an extended period.

Niche 3566 appears to be a suitable site for determining spatial gradients associated with geological features. The single borehole above the niche, along with the six boreholes stemming from the niche, provide enough spatial coverage to include variability introduced by the fault and shear zone. Of particular interest is the moist zones observed at the end of the 10-m boreholes (middle borehole, pre-excavation), and along Borehole A (post-excavation). It is recommended

here that these seven boreholes be monitored with psychrometers and probes to detect changes in moisture content over a period of at least one year. Here the probes should be spaced 0.25-1.0 m apart within the boreholes to capture spatial gradients.

The drop in water potentials in the BR hole in Niche 3650 following air-permeability tests suggests the possibility of formation dry-out associated with the test. Since these tests are an integral part of the investigations pertaining to drift-scale seepage processes, it is important to determine the extent and magnitude (spatial and temporal) of this type of disturbance on the formation. This can be addressed by pre-test measurements of water potential followed by long term monitoring until the formation recovers.

References

Flint, A. L., and L. E. Flint, 1997. "Niche Moisture Analysis" *in* Wang, J. S. Y (Ed.) *Field Testing and Observation of Flow Paths in Niches: Phase 1 Status Report of the Drift Seepage Test and Niche Moisture Study,* edited by J.S.Y. Wang. Milestone SPC314M4,

Salve, R., T. K. Tokunaga, J. S. Y. Wang, R. Solbau, and J. Clyde 1997. "Hydrologic Monitoring in Unsaturated Fractured Tuff Boreholes: Some Preliminary Results." *Field Testing and Observation of Flow Paths in Niches: Phase 1 Status Report of the Drift Seepage Test and Niche Moisture Study,* edited by J.S.Y. Wang. Yucca Mountain Project Level 4 Milestone SPC314M4. Berkeley, California: Lawrence Berkeley National Laboratory.

Trautz, R.C.; Cook, P.J.; and Wang, J.S.Y. 1997. "Liquid Migration Along Fracture Flow Paths." Chapter 3 of *Field Testing and Observation of Flow Paths in Niches,* edited by J.S.Y. Wang. Yucca Mountain Project Level 4 Milestone. Berkeley, California: Lawrence Berkeley National Laboratory. MOY 971226.01

Wang, J.S.Y, Cook, P.; Trautz, R.; James, A.; Finsterle, S. Sonnenthal, E.; Salve, R.; Hesler, G.; and Flint, A. 1997. *Drift Seepage Test and Niche Moisture Study: Phase 1 Progress Report on Data Interpretation and Model Prediction.* Yucca Mountain Project Level 4 Milestone SPC31DM4. Berkeley, California: Lawrence Berkeley National Laboratory. LB970601233124.001 (Q).

Table 4.1. WATER POTENTIAL MEASUREMENTS IN NICHE 3566

Borehole ID	Dist. from collar (m)	Duration of measurement	Psych #	Calibration coeff. Slope	Calibration coeff. intercept	Temp.	Reading (mV)	Corrected R.	Pressure (m)	Pressure (bars)
Pre-excavation Measurements										
U	10.0	5/9-16/97	Psy -51	-24.59	12.55	23.33	0.977	1.02	-13	-1.2
U	10.0	5/9-16/97	Psy -52	-26.83	14.66	23.32	0.992	1.04	-13	-1.3
M	10.0	5/9-16/97	Psy -53	-24.43	13.45	23.29	0.803	0.84	-7	-0.7
M	10.0	5/9-16/97	Psy -54	-24.41	11.86	23.27	0.449	0.47	0.4	0.04
B	10.0	5/9-16/97	Psy -55	-26.56	9.51	23.23	0.783	0.82	-12	-1.2
U	6.1	7/8-14/97	Psy -42	-24.17	0.60	24.76	2.019	2.03	-49	-4.8
U	5.5	7/8-14/97	Psy -43	-26.97	-2.92	25.31	1.62	1.61	-46	-4.5
U	5.5	7/8-14/97	Psy -44	-38.62	35.98	24.93	1.81	1.81	-34	-3.3
U	4.9	7/8-14/97	Psy -45	-25.33	3.89	24.97	1.95	1.95	-46	-4.5
U	4.3	7/8-14/97	Psy -48	-24.51	-3.67	25.31	2.628	2.61	-68	-6.6
U	3.7	7/8-14/97	Psy -50	-25.48	14.66	25.51	3.066	3.02	-62	-6.1
U	7.9	9/16-24/97	Psy -42	-24.17	0.60	24.28	2	2.04	-49	-4.8
U	7.3	9/16-24/97	Psy -60	-25.19	3.44	24.45	1.935	1.96	-46	-4.5
U	6.7	9/16-24/97	Psy -45	-25.33	3.89	25.33	2.972	2.95	-71	-6.9
U	6.1	9/16-24/97	Psy -48	-24.51	-3.67	24.75	2.553	2.57	-67	-6.5
U	5.5	9/16-24/97	Psy -50	-25.48	14.66	24.9	1.98	1.99	-36	-3.5
Post-excavation Measurements										
A	6.25	10/18-21/97	Psy-43a	-30.32	14.15	22.91	0.504	0.53	-2	-0.2
A	6.75	10/18-21/97	Psy-60	-25.19	3.44	22.99	1.247	1.32	-30	-2.9
B	6.00	10/18-21/97	Psy-51	-24.27	9.59	22.72	2.04	2.17	-43	-4.2
C	0.15	10/18-21/97	Psy-49	-24.66	2.93	25.82	5.595	5.47	-132	-12.9
C	0.76	10/18-21/97	Psy-42	-24.17	0.60	25.12	1.401	1.40	-33	-3.2
C	1.98	10/18-21/97	Psy-45	-25.33	3.89	24.07	1.007	1.03	-22	-2.2
C	1.98	10/18-21/97	Psy-47	-25.37	8.65	24.07	2.149	2.20	-47	-4.6
C	1.37	10/18-21/97	Psy-48	-24.51	-3.67	24.53	1.476	1.49	-40	-4.0
C	2.60	10/18-21/97	Psy-43	-26.97	-2.92	23.81	1.94	2.00	-57	-5.6
D	6.00	10/18-21/97	Psy-54	-24.71	8.18	23.89	1.177	1.21	-22	-2.1
D	6.00	10/18-21/97	Psy-56	-25.88	-4.66	23.84	1.017	1.05	-32	-3.1
E	6.00	10/18-21/97	Psy-57	-25.17	-10.00	28.88	2.848	2.58	-75	-7.3
E	6.00	10/18-21/97	Psy-59	-26.65	-3.82	28.88	3.202	2.90	-81	-7.9

Table 4.2. WATER POTENTIAL MEASUREMENTS IN NICHE 3650

			Calibration coeff.							
Borehole ID	Dist. from collar (m)	Duration of measurement	Psych #	Slope	intercept	Temp.	Reading (mV)	Corrected R.	Pressure (m)	Pressure (bars)
Pre-excavated Measurements										
UM	1.2	7/1-8/97	Psy -48	-24.51	-3.67	26.53	5.26	5.05	-127	-12.5
UM	0.6	7/1-8/97	Psy -49	-24.66	2.93	26.87	6.06	5.77	-139	-13.7
UM	0.6	7/1-8/97	Psy -50	-25.48	14.66	26.86	7.40	7.05	-165	-16.2
BR	10.0	7/1-8/97	Psy -51	-24.27	9.59	23.24	1.82	1.91	-37	-3.6
BR	10.0	7/1-8/97	Psy -52	-28.49	-3.50	23.23	1.18	1.24	-39	-3.8
BR	10.0	7/1-8/97	Psy -53	-25.36	-1.51	23.23	1.15	1.21	-32	-3.2
BL	10.0	7/1-8/97	Psy -54	-24.71	8.18	23.24	1.25	1.31	-24	-2.4
BL	10.0	7/1-8/97	Psy -55	-26.32	9.67	23.24	1.64	1.72	-36	-3.5
ML	10.0	7/1-8/97	Psy -57	-25.17	-10.00	23.15	-0.33	-0.35	-1	-0.1
Post-excavation Measurements										
ML	10.0	7/24-28/97	Psy -51	-24.27	9.59	23.27	1.521	1.60	-29	-2.9
ML	10.0	7/24-28/97	Psy -52	-28.49	-3.50	23.27	1.142	1.20	-38	-3.7
ML	10.0	7/24-28/97	Psy -53	-25.36	-1.51	23.26	1.406	1.48	-39	-3.8
BR	10.0	7/24-28/97	Psy -54	-24.71	8.18	23.29	2.548	2.67	-58	-5.7
BR	10.0	7/24-28/97	Psy -55	-26.32	9.67	23.31	2.119	2.22	-49	-4.8
BR	10.0	7/24-28/97	Psy -56	-25.88	-4.66	23.28	1.605	1.68	-48	-4.7
BL	10.0	7/24-28/97	Psy -57	-25.17	-10.00	23.25	0.419	0.44	-21	-2.1
BL	10.0	7/24-28/97	Psy -58	-25.67	7.66	23.25	0.838	0.88	-15	-1.5
BL	10.0	7/24-28/97	Psy -59	-26.65	-3.82	23.26	0.872	0.91	-28	-2.8

Table 4.3. WATER POTENTIAL MEASUREMENTS IN NICHE 3107

			Calibration coeff.							
Borehole ID	Dist. from collar (m)	Duration of measurement	Psych #	Slope	intercept	Temp.	Reading (mV)	Corrected R.	Pressure (m)	Pressure (bars)
UM	0.5	12/22/97-1/8/98	Psy-86	-31.31	8.55	22.32	8.35	9.00	-273	-26.8
UM	1.1	12/22/97-1/8/98	Psy-83	-28.17	15.19	24.32	5.892	6.00	-154	-15.1
UM	1.7	12/22/97-1/8/98	Psy-75	-26.56	13.46	24.92	3.625	3.63	-83	-8.1
UM	2.9	12/22/97-1/8/98	Psy-68	-26.11	1.32	25.69	1.151	1.13	-28	-2.8
UL	10.0	12/22/97-1/8/98	Psy-64	-26.51	17.67	25.69	1.249	1.23	-15	-1.5
ML	10.0	12/22/97-1/8/98	Psy-66	-27.87	16.74	23.7	3.491	3.62	-84	-8.2

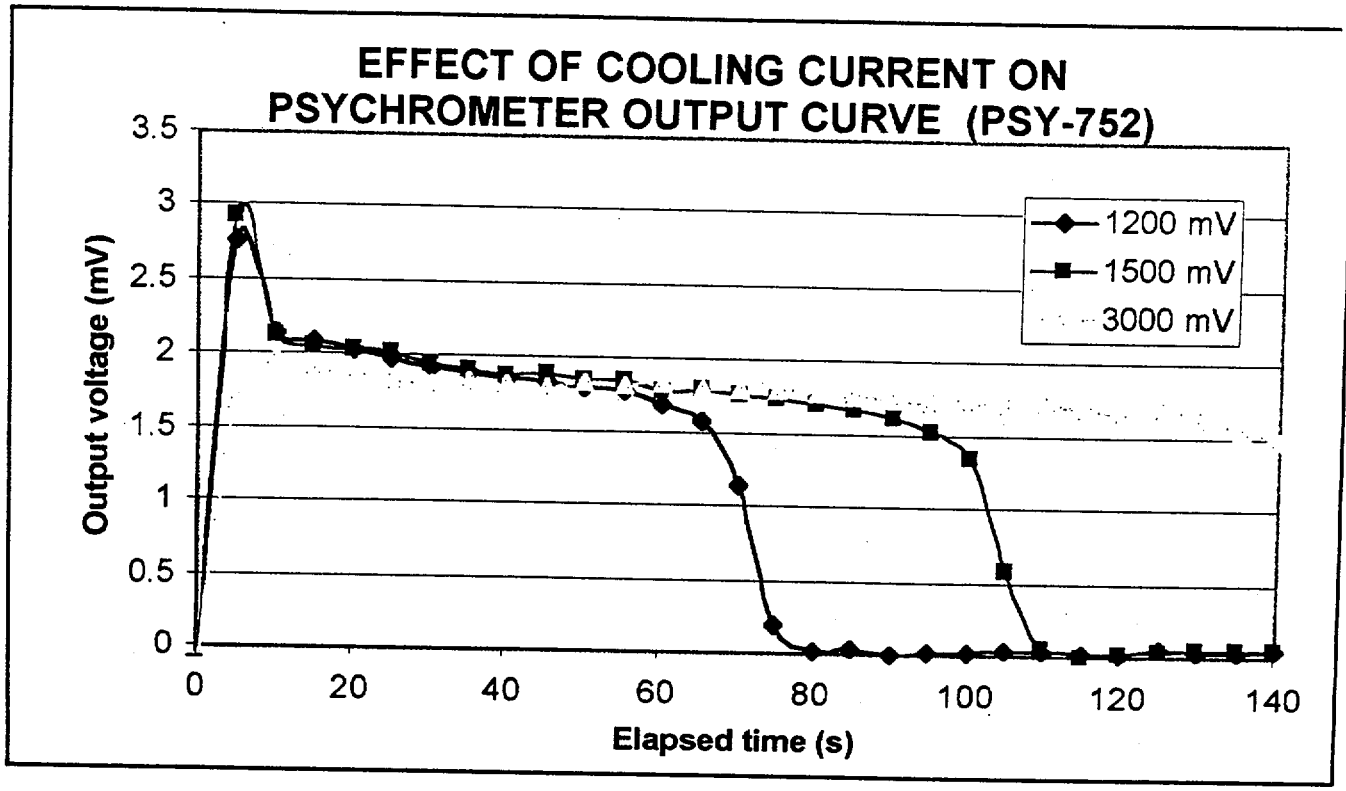
EFFECT OF COOLING CURRENT ON
PSYCHROMETER OUTPUT CURVE (PSY-752)
Output voltage (mV)
3.5
3
2.5
2
1.5
1
0.5
0
0
20
40
60
80
100
120
140
Elapsed time (s)
1200 mV
1500 mV
3000 mV

Figure 4.1

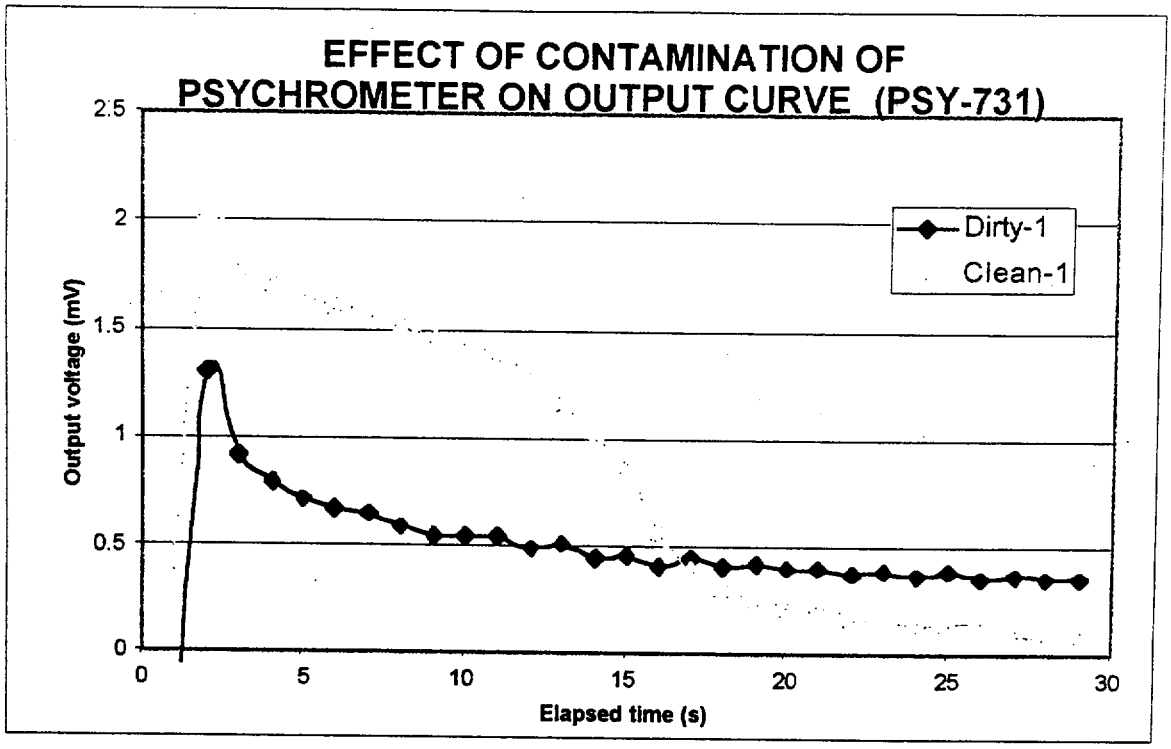
EFFECT OF CONTAMINATION OF PSYCHROMETER ON OUTPUT CURVE (PSY-731)
Output voltage (mV)
2.5
2
1.5
1
0.5
0
0
5
10
15
20
25
30
Elapsed time (s)
Dirty-1
Clean-1

Figure 4.2

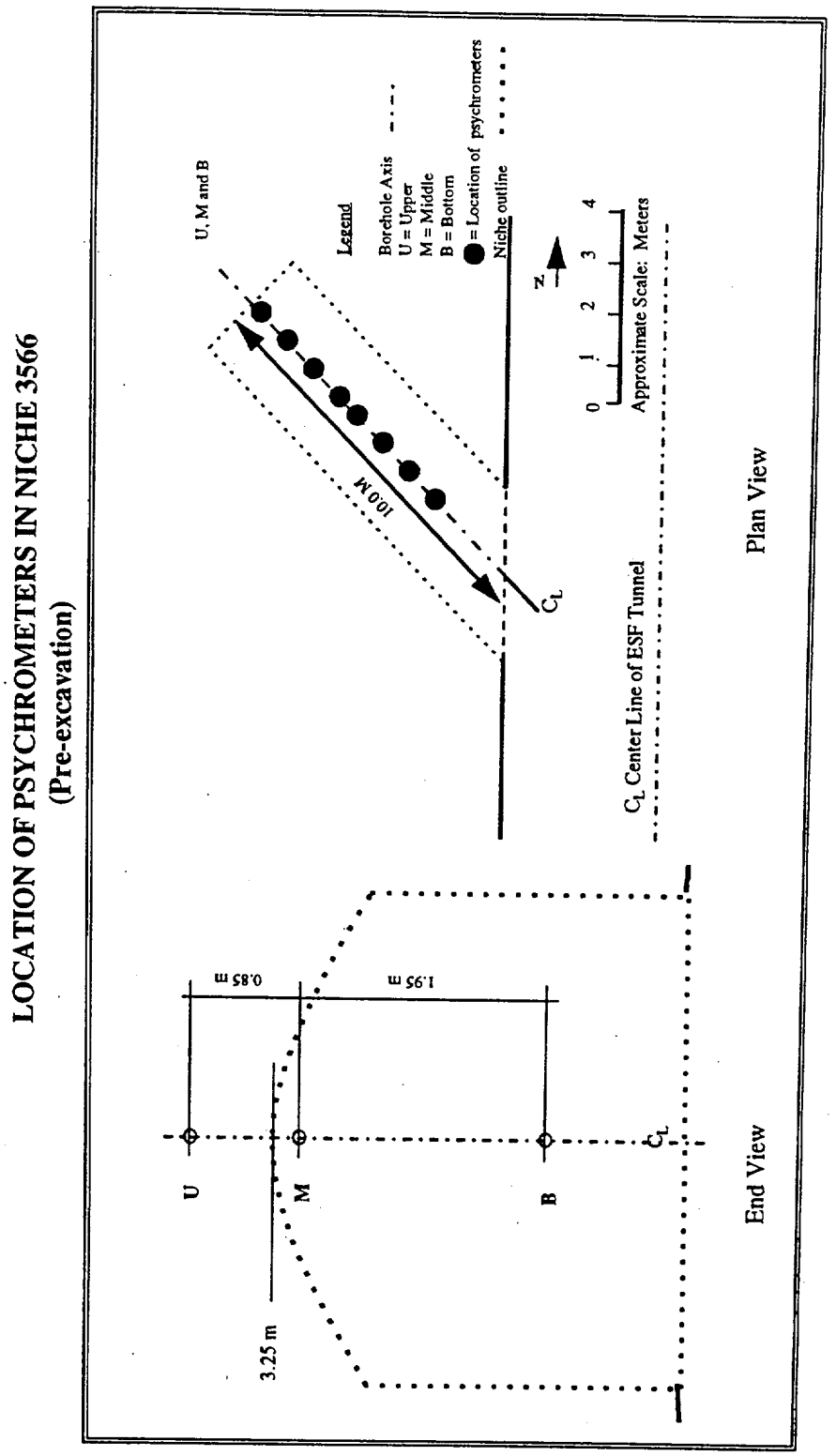
LOCATION OF PSYCHROMETERS IN NICHE 3566
(Pre-excavation)
U, M and B
Legend
Borehole Axis
U = Upper
M = Middle
B = Bottom
= Location of psychrometers
Niche outline
N
0 1 2 3 4
Approximate Scale: Meters
10.0 M
C_L
C_L Center Line of ESF Tunnel
Plan View
0.85 m
1.95 m
U
M
B
C_L
3.25 m
End View
(Adapted from Trautz et al, 1997)

Figure 4.3a

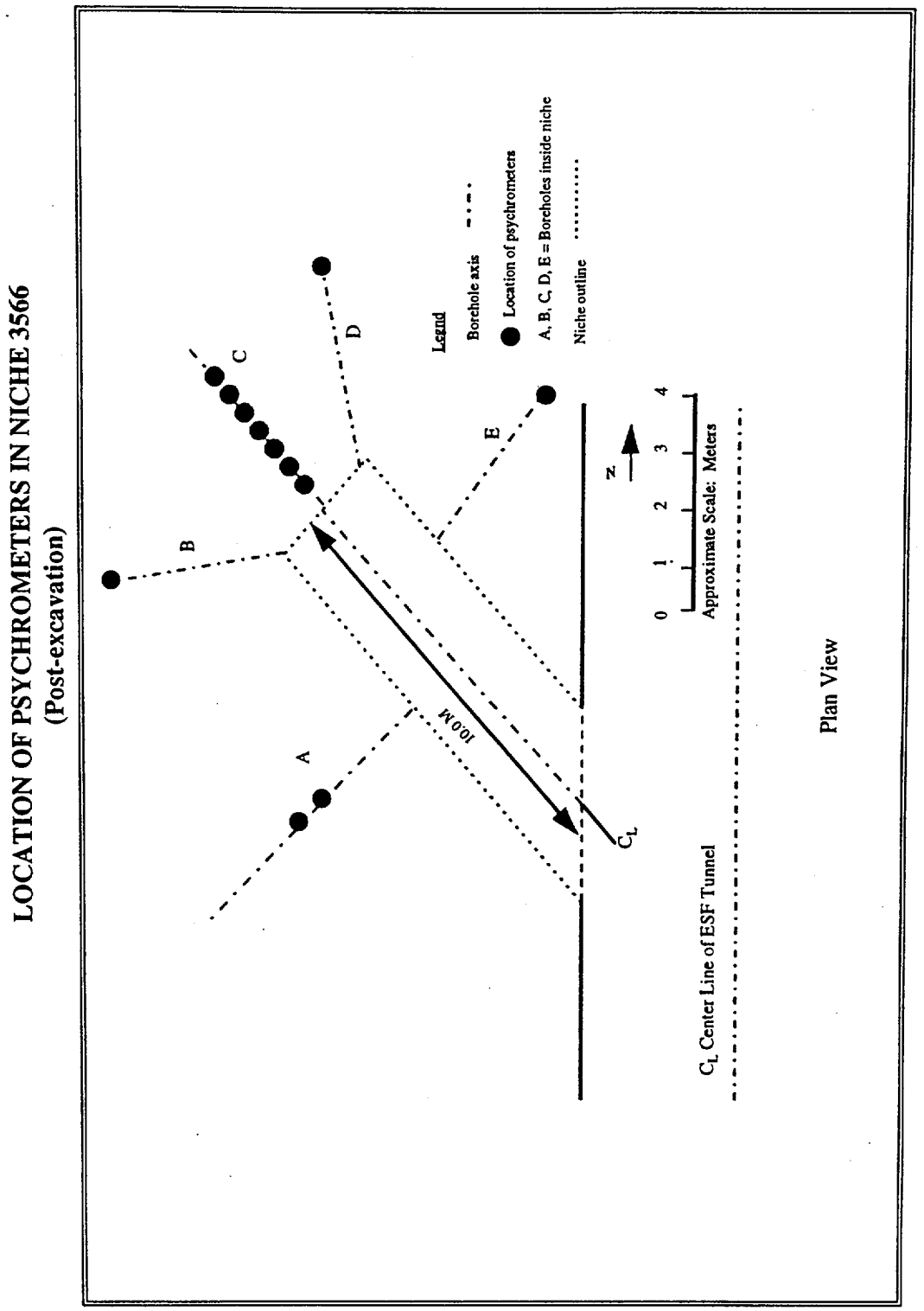
LOCATION OF PSYCHROMETERS IN NICHE 3566
(Post-excavation)
Legend
Borehole axis
Location of psychrometers
A, B, C, D, E = Boreholes inside niche
Niche outline
A
B
C
D
E
10.0 M
N
0 1 2 3 4
Approximate Scale: Meters
C_L
C_L Center Line of ESF Tunnel
Plan View

Figure 4.3b

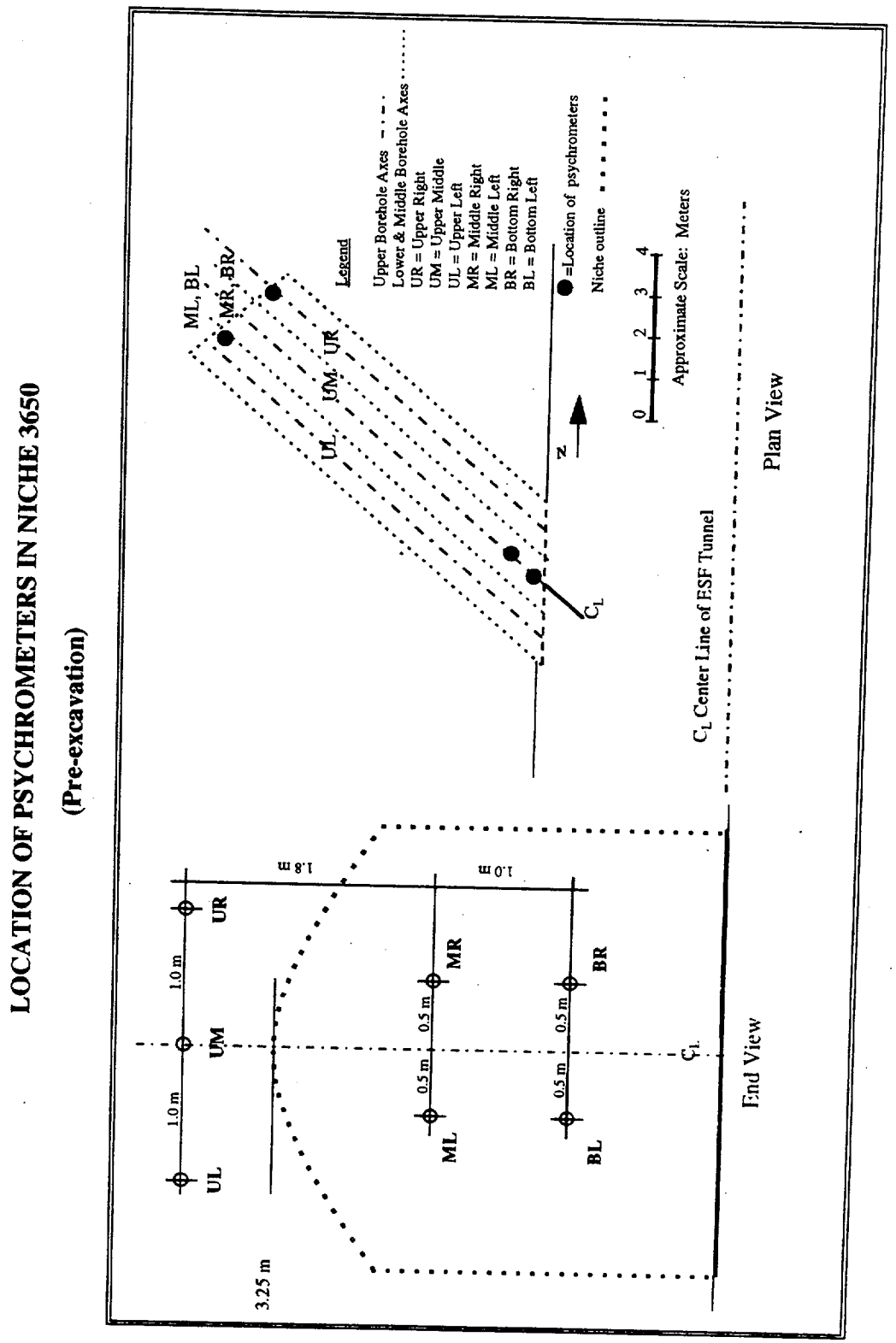
LOCATION OF PSYCHROMETERS IN NICHE 3650
(Pre-excavation)
Plan View
End View
Legend
Upper Borehole Axes
Lower & Middle Borehole Axes
UR = Upper Right
UM = Upper Middle
UL = Upper Left
MR = Middle Right
ML = Middle Left
BR = Bottom Right
BL = Bottom Left
=Location of psychrometers
Niche outline
Approximate Scale: Meters
0 1 2 3 4
N
ML, BL
MR, BR
UL
UM
UR
C_L
C_L Center Line of ESF Tunnel
1.8 m
1.0 m
1.0 m
1.0 m
0.5 m
0.5 m
0.5 m
0.5 m
3.25 m

Figure 4.4

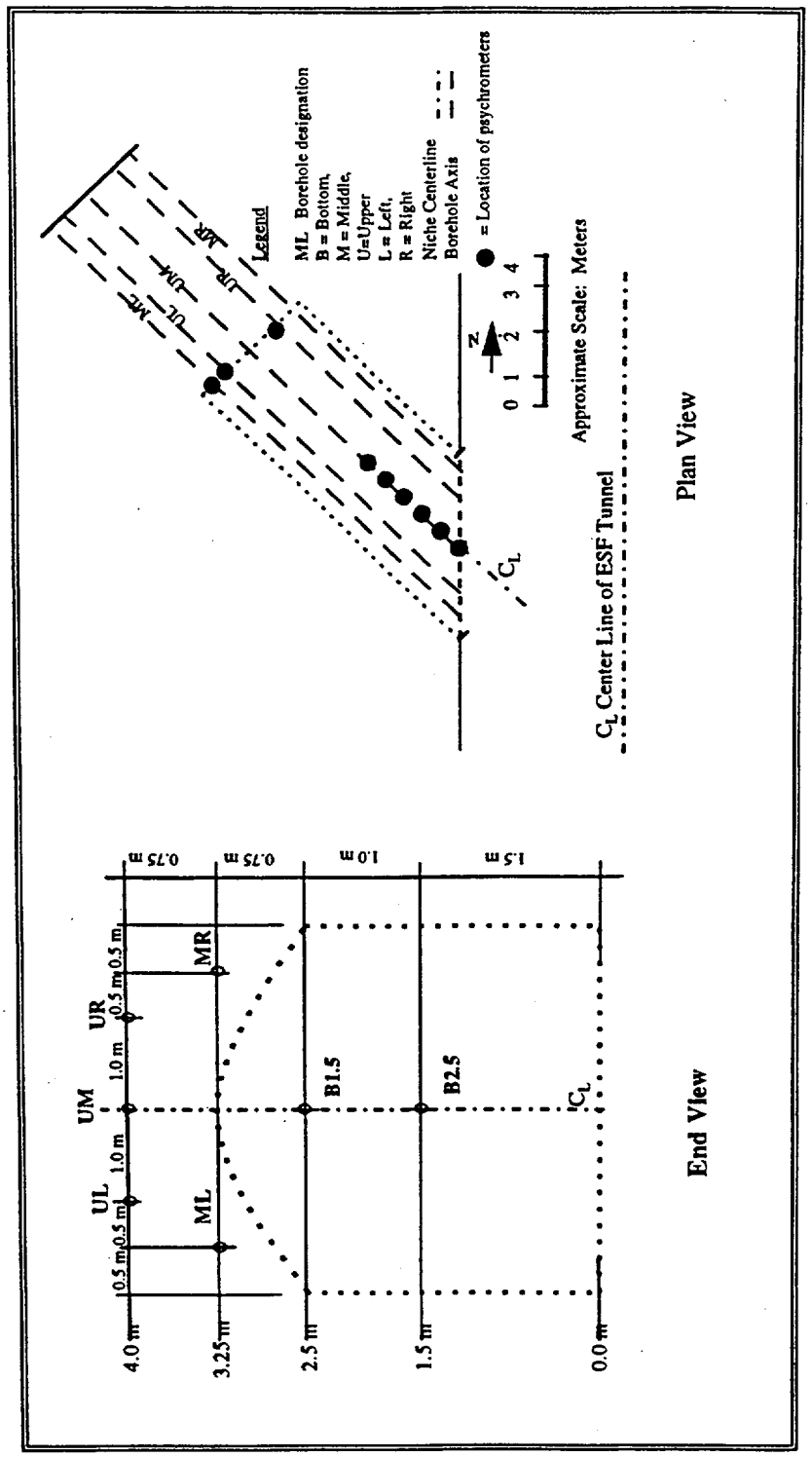
LOCATION OF PSYCHROMETERS IN NICHE 3107
(Pre-excavation)
Legend
ML Borehole designation
B = Bottom,
M = Middle,
U=Upper
L = Left,
R = Right
Niche Centerline
Borehole Axis
= Location of psychrometers
Approximate Scale: Meters
C_L Center Line of ESF Tunnel
Plan View
End View
UR
UM
UL
MR
ML
B1.5
B2.5
0.5 m
1.0 m
0.75 m
1.0 m
1.5 m
4.0 m
3.25 m
2.5 m
1.5 m
0.0 m

Figure 4.5

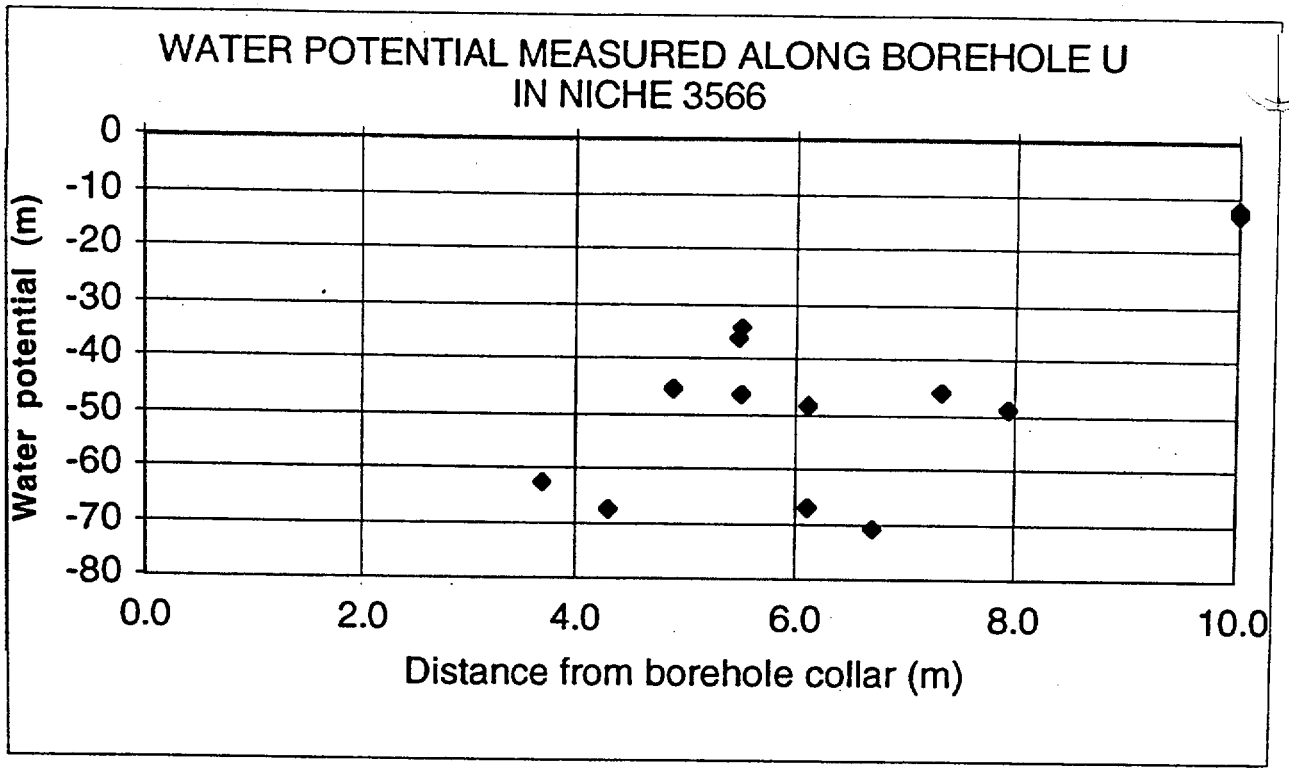

Figure 4.6

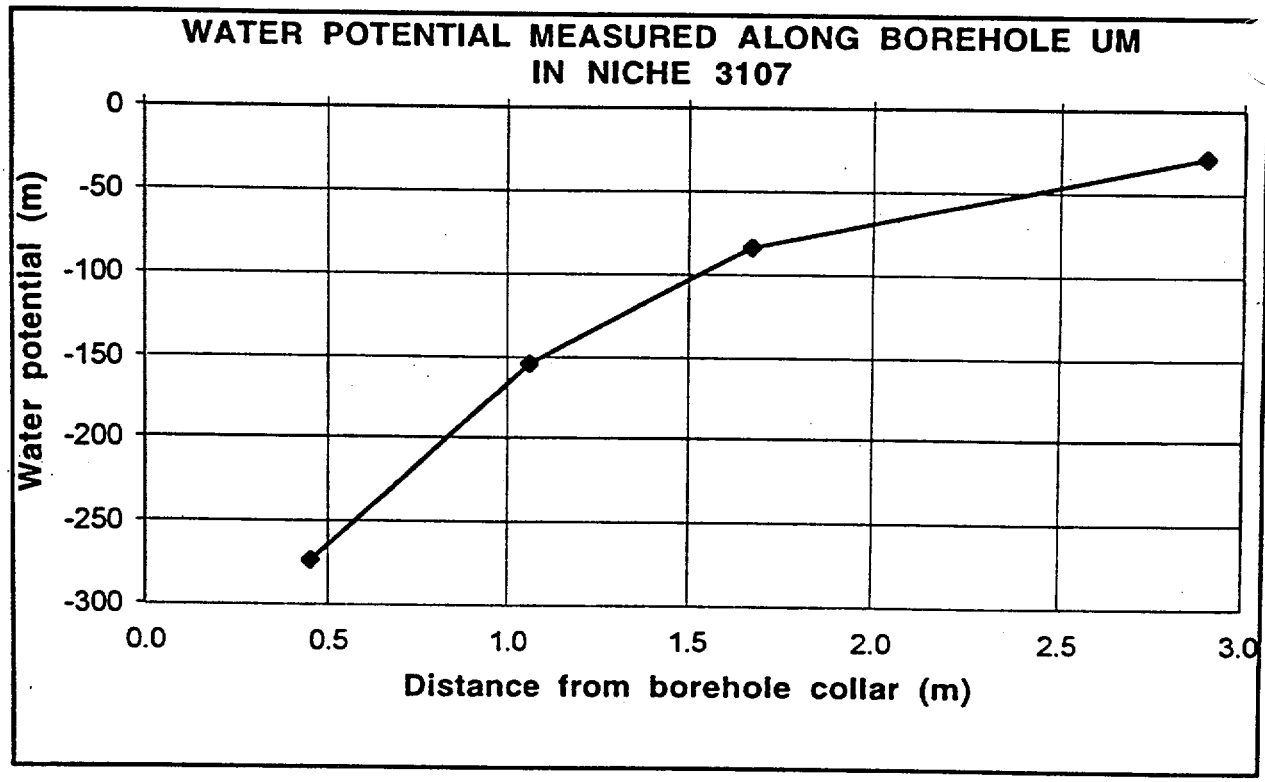

Figure 4.7